TECHNICAL REPORT STANDARD TITLE PAGE

1. Report No.	2. Government Accession No.	3. Recipient's Catalog No.

4. Title and Subtitle	5. Report Date
Moisture Movement Under the Pavement Structure	November 1989
	6. Performing Organization Code

7. Author(s)	8. Performing Organization Report No
Mohd Asri Bin Abd Rahim and Miguel Picornell	1165-1

9. Performing Organization Name and Address	10. Work Unit No
Center for Geotechnical & Highway Materials Research University of Texas at El Paso El Paso, Texas 79968-0516	11. Contract or Grant No 10--8-88-1165
	13. Type of Report and Period Covered Final September 1988 August 1989
12. Sponsoring Agency Name and Address State Department of Highways & Public Transportation P.O. Box 5051 Austin, Texas 78763	14. Sponsoring Agency Code

15. Supplementary Notes

Volume 1 of 2

16. Abstract

One of the measures being tried in Texas to stabilize the development of roughness of pavements on expansive soils is the installation of vertical moisture barriers. The purpose of the barrier is to prevent subsurface water from accessing into the crack fabric within the subgrade soils. Several sites throughout Texas have been already monitored and some conflicting results have been observed. In some cases, the moisture barrier seems to reduce considerably the rate at which roughness develops but, in other cases, the barrier has somewhat increased the rate of roughness development.

The moisture barrier can prevent the horizontal flow of rain water from the side to the soils underneath the pavement. The pavement surface is normally considered an impermeable surface; however, there is evidence that cracks in the pavement result in large flows of the rain water through the pavement surface especially during low-intensity, long duration rainfall events. This vertical flow of rain water can explain some of the conflicting field behaviors observed.

The main purpose of this study was to assemble a computer program that would predict the behavior of different barrier alternatives. These predictions could then allow a reduction in the number of trial sections to be monitored. Furthermore, it would help explain observed field behavior and to identify controlling parameters. Expansive soils have extremely low pemeabilities, and thus the absorption of water by soil clods is a very slow process. By way of contrast, water flow within the crack fabric is a much faster process, by several order of magnitude. The main feature of

(continued on back of page)

17. Key Words	18. Distribution Statement
Expansive Clay Soils Shrinkage Cracking Pavement Roughness Water Flow	No Restrictions. This document is available to the public through National Technical Information Service, Springfield, Virginia 22161

19. Security Classif. (of this report)	20. Security Classif. (of this page)	21. No. of Pages	22. Price
Unclassified	Unclassified	494	

Form DOT F 1700.7 (8-69)

this program is to consider the subsurface soil divided into parallelepipeds of different sizes. The water is considered to move through the cracks under positive pressures and from there is absorbed by the soil blocks. A master curve is developed for each block size to estimate the volume of water absorbed by the block for every day that the block is submerged under water.

The program performs a water balance for the unpaved soils on the side of the pavement and a second water balance for the soils underneath the pavement. The transfer of moisture between the two soil regions is through the cracks underneath the barrier. The period of each water balance ranges from a maximum of one day to a minimum of one minute. The length of the period is selected based on the head difference between the water in the crack fabric of the subbase soils.

At every time step, the volume of water absorbed by the blocks is used to reconsider the block and crack fabric geometry. From this point of view, three different regions are included. The first region corresponds to the soil on the side of the pavement, the second region includes the soil underneath the barrier and the edge of the pavement, and the third region are the subbase soils beyond the edge of the pavement.

The evapotranspiration removes soil water from the cracks within the soil on the side of the pavement. The actual evapotranspiration is estimated with a published simplified method developed for the climatic conditions of Texas.

The computer model predicts a steady closing of the crack fabric under the pavement structure. The rate of this phenomena is dependent of the water availability. The cracks under the edge of the pavement or those within the soil on the side of the pavement, close during wet periods and reopen under persistent dry conditions.

MOISTURE MOVEMENT UNDER THE PAVEMENT STRUCTURE

by

Mohd Asri B. Abd Rahim and Miguel Picornell

Research Report 1165-1

Volume I

Research Study 10-8-88-1165

for

The Texas State Department of Highways and Public Transportation

in cooperation with

The U.S. Department of Transportation Federal Highway Administration

Center for Geotechnical & Highway Materials Research

November 1989

ABSTRACT

One of the measures being tried in Texas to stabilize the development of roughness of pavements on expansive soils is the installation of vertical moisture barriers. The purpose of the barrier is to prevent rain water from accessing into the crack fabric within the subgrade soils. Several sites throughout Texas have already been monitored and some conflicting results have been observed. In some cases, the moisture barrier seems to reduce considerably the rate at which roughness develops but, in other cases, the barrier has somewhat increased the rate of roughness development.

The moisture barrier can prevent the horizontal flow of rain water from the side to the soils underneath the pavement. The pavement surface is normally considered an impermeable surface; however, there is evidence that cracks in the pavement result in large flows of rain water through the pavement surface especially during low-intensity, long-duration rainfall events. This vertical flow of rain water can explain some of the conflicting field behavior observed.

The main purpose of this study was to assemble a computer program that would predict the behavior of different barrier alternatives. These predictions could then allow a reduction in the number of trial sections to be monitored. Furthermore, it would help explain observed field behavior and in identifying controlling parameters.

Expansive soils have extremely low permeabilities, and thus the absorption of water by soil clods is a very slow process. By way of contrast, water flow within the crack fabric is a much faster process, by several orders of magnitude. The main feature of this program is to consider the subsurface soil divided into parallelepipeds of different sizes. The water is considered to move through the cracks under positive pressures and from there is absorbed by the soil blocks. A master curve is developed for each block size to estimate the volume of water absorbed by the block for every day that the block is submerged under water.

The program performs a water balance for the unpaved soils on the side of the pavement and a second water balance for the soils underneath the pavement. The transfer of moisture between the two soil regions is through the cracks underneath the barrier. The period of each water balance ranges from a maximum of one day to a minimum of one minute. The length of the period is selected based on the head difference between the water in the crack fabric within the soils on the side of the pavement and the water in the crack fabric of the subbase soils.

At every time step, the volume of water absorbed by the blocks is used to reconsider the block and crack fabric geometry. From this point of view, three different regions are included. The first region corresponds to the soil on the side of the pavement, the second region includes the soil underneath the barrier and the edge of the pavement, and the third region are the subbase soils beyond the edge of the pavement.

The evapotranspiration removes soil water from the cracks within the soil on the side of the pavement and from the soil blocks in thisregion and those under the edge of the pavement. The actual evapotranspiration is estimated with a published simplified method developed for the climatic conditions of Texas.

The computer model predicts a steady closing of the crack fabric under the pavement structure. The rate of this phenomena is dependent on the water availability. The cracks under the edge of the pavement, or those within the soil on the side of the pavement, close during wet periods and reopen under persistent dry conditions.

IMPLEMENTATION STATEMENT

This computer program can be used to predict the rate of moisture uptake by an expansive soil subbase based on the climatic conditions of the regional area and some characteristics and properties of the soil deposit. Nevertheless, some of the information required is not common knowledge for the expansive soils of Texas. Most specifically this includes the geometric definition of crack fabric in the expansive soil deposits of Texas. Specific information regarding this aspect for the Texas conditions would greatly enhance the usefulness of this computer program. The State Department of Highways and Public Transportation should consider acquiring this type of information for each climatic region and major expansive soil deposit.

DISCLAIMER

TABLE OF CONTENTS

TABLE OF CONTENTS (Continued)

TABLE OF CONTENTS (Continued)

LIST OF TABLES

LIST OF FIGURES

LIST OF FIGURES (Continued)

LIST OF FIGURES (Continued)

LIST OF FIGURES (Continued)

LIST OF FIGURES (Continued)

LIST OF FIGURES (Continued)

LIST OF FIGURES (Continued)

LIST OF FIGURES (Continued)

LIST OF FIGURES (Continued)

LIST OF FIGURES (Continued)

LIST OF FIGURES (Continued)

LIST OF FIGURES (Continued)

LIST OF FIGURES (Continued)

LIST OF FIGURES (Continued)

LIST OF FIGURES (Continued)

LIST OF FIGURES (Continued)

INTRODUCTION

Pavements built on expansive soils are known to develop roughness not associated with traffic. This type of pavement roughness has been attributed [1] to the presence of shrinkage cracks in the subbase soils. Rainfall can penetrate very fast through the crack fabric. The water moves impelled by gravity and under positive pressures and goes where the crack directs it. The water in the cracks has very little exposure to the atmosphere and, thus, ponds in the cracks allowing time for the water to be absorbed into the crack walls. This absorption causes surface heaving along the trace of the crack that is responsible for the development of roughness.

The pavement roughness reduces significantly the serviceability index and thus, requires periodic maintenance, such as releveling and overlays, to restore the riding quality. The Texas State Department of Highways and Public Transportation has been trying for some time to reduce the expenses associated with this periodic maintenance by the installation of vertical moisture barriers. Field test sections have, been implemented in San Antonio, Texas, on IH-37 [2], and along IH-30 in Greenville, Texas [3].

The purpose of the moisture barrier is to isolate the subbase soil from seasonal climatic changes. In the first trials [2], the moisture barrier was placed to a depth of 8 ft, because field monitoring data of soil moisture variations in the area indicated that the shallower 8 ft of soil had experienced some moisture changes. Later on, it was recognized [4] that one of the main functions to be performed by a vertical moisture barrier was to prevent rainwater from accessing the

crack fabric within the subbase soils. This consideration suggested that the depth of a moisture barrier should be chosen based on the expected maximum depth of shrinkage cracks possible at the site.

The results of field monitoring several test sections appear to indicate that the role of the vertical moisture barrier is quite different at different sites. In the test sections of IH-37 in San Antonio, Texas, suction measurements on both sides of the barrier indicated [5] that the soils enclosed by the barrier remained at a nearly constant suction during more than two years. Meanwhile, the soils on the side of the pavement were experiencing significant suction changes. In this case, the moisture barrier had protected the soils under the pavement of the moisture changes observed in the soils on the side of the pavement.

By way of contrast, the results of monitoring the performance of several trial barriers on IH-30 has shown [3] that the sections with the barrier experienced a higher rate of roughness development than adjacent control sections. At this site, it looked like that barrier would actually retain moisture inside rather than keep it outside. The performance of a moisture barrier is influenced by a number of parameters. In the most influential category are the climatic conditions of the site and perhaps the initial state of the subbase soils, and the depth and characteristics of the moisture barrier. The location of the site such as on a hill, on a slope, in a low area, or in a cut will also affect the performance of a barrier.

This incomplete list of parameters illustrates the large matrix of field trial tests that would be needed to observe all possible cases of moisture barrier performance. This monitoring program would imply large installation and monitoring costs. Additionally, these results

would only be known after a number of year have elapsed.

Considerable savings in funding and time could be realized if a computer model could appropriately simulate the moisture transfer through the pavement surface and around an impermeable moisture barrier. This computer program would allow a reduction in the number of field trials necessary to verify the simulation capabilities of the computer program. Then the computer program would be used to simulate the barrier performance for the array of most influential parameters. These considerations lead to project 1165. This report is concerned with the basis on which the computer program simulates the moisture movement under the pavement. It also includes a description of the capabilities of the program, a user's guide, and preliminary results of the simulations performed for several regional climatic conditions within the state of Texas.

REVIEW OF EXISTING LITERATURE

The flow of water into expansive soils has long been considered to be a non-Darcy flow. There is ample evidence [6, & 7] in the literature that rainfall percolates through cracks into the soil and then is slowly absorbed by the soil peds. As the soil absorbs water, it swells and progressively closes cracks.

The presence of shrinkage cracks in expansive soil deposits is very apparent. In very dry soils, profuse surface cracks form on the ground surface. Cracks with openings on the ground surface up to about one inch and several feet deep [8] have been reported. Furthermore, the crack patterns and frequency were observed [8] to depend on the vegetative cover. The crack opening progressively decreases from a

maximum on the soil surface to zero at the crack tip. The variation of the crack opening with depth has been described with linear shrinkage curves with depth [9]. Morphological studies have revealed [10] the presence of approximately squared blocks of soil formed by aggregation of soil peds.

The infiltration of rain water into the crack fabric has been observed to be determined by the soil surface micro-relief [10]. Water is directed towards the cracks through surface depressions. Then the water runs down the crack faces, wetting only a small fraction of the exposed crack surface. This effect causes [10] the bulk of rain water penetration into cracks to move directly to the tip of cracks rather than being absorbed on the crack walls.

The presence of cracks in aquifer bearing formations results in two distinctive flows taking place one through the cracks and the other through the porous medium between cracks. The water within the cracks is mobile and the water within the porous medium is stagnant. Traditionally, the modelling of this flow has been approached with Barenblatt's [11] double porosity concept. However, the usefulness of this concept is quite limited in the present application under unsaturated conditions. An additional complication is the fact that the cracks in the expansive soil deposit close as the water is absorbed into the crack walls; thus, the porosities do not remain constant through the process.

The first attempt, known to the authors, to include the effect of shrinkage cracks on the infiltration is due to Richards [12]. In this attempt the subsoil was considered divided into blocks and two different permeability coefficients were considered along the cracks and through the blocks. This model did not account for changes caused

by the swelling/shrinking of the soil. In actuality, when the soil blocks absorb water the mobile water mass is reduced by the same amount that the stagnant water is increased.

The water accumulated inside the crack fabric and the water trapped inside the soil blocks can be depleted as a result of evaporation at the soil surface and plant transpiration. Soil evaporation has been proved to be a very ineffective mechanism of moisture removal from the soil by a number of investigators [13,14,&15]. The consensus is that even small amounts of soil evaporation forms a dry soil crust at the soil surface that prevents any further evaporation from taking place. Existing field monitoring data [15] suggest that soil evaporation might affect only the soil within the upper foot of the soil deposit.

Plant transpiration, by way of contrast, is a much more effective mechanism. The native vegetation, such as roadside grasses, removes water from the soil through the root system. Nevertheless, when the soil suction reaches the wilting point of the vegetation all transpiration ceases. Due to the extremely small permeabilities of expansive soils, the removal of water by the root systems is confined to the rooting depth of the vegetation [16]. A consequence of this fact is that by preventing the root system of the vegetation from reaching the soils under the pavement, any possibility of moisture losses from these soils is eliminated. Thus a possible role for a moisture barrier would be to act as a root barrier.

The climatic conditions at a site determine the Potential Evapotranspiration. This parameter has been traditionally estimated based on average monthly temperatures according to Thornthwaite [17]. However, this approach neglects the influence of the relative humidity

in the environment. This parameter is known to affect, noticeably, the potential evapotranspiration and more recent approaches have been proposed to [18] to include its effect. Due to the large variations of the climate in the state of Texas, the second approach can yield more reliable estimates.

The actual evapotranspiration is only a fraction of the potential. The size of the fraction depends on water availability. The actual evapotranspiration ranges from a maximum equal to the potential under very wet conditions to nearly zero at the wilting point of the vegetation. The estimation of actual evapotranspiration for the typical Central Texas conditions can be accomplished with well established procedures tested for this area [19].

These considerations suggest that a model that could approximate the field behavior would have to consider the following:

1) The infiltration of rainfall into an expansive soil deposit takes place primarily through the crack fabric
2) The shrinkage cracks have divided the soil mass in approximately squared blocks
3) The transfer of water from the cracks to the soil blocks takes place by absorption
4) The absorption of water causes swelling of the soil blocks and thus modifies the crack fabric
5) The removal of water from the soil mass is primarily determined by the transpiration of the native vegetative cover. Thus soil water is only removed from the soil mass inside the rooting depth of the vegetation.

PURPOSE AND SCOPE OF THE STUDY

The overall goal of this study was to assemble a computer program to simulate the infiltration of rainfall, the losses due to evapotranspiration and the movement of moisture under a pavement resting on an expansive soil subbase. Specifically, it was desired that the program could account for the water flowing under the pavement from the sides and the percolation through cracks and fissures on the pavement surface.

One advantage desired to be gained with this program is the possibility of simulating the behavior through a large number of years. This need imposed the necessity of having to simulate stochastically the regional climatic conditions for the site in question.

Thus the computer program would have to handle the stochastic simulation of the climatic conditions in one part and in the second part would proceed to the simulation of moisture movement. The first part of the program would offer the possibility to start from raw meteorological data and form the distributions of rainfall depth and of potential evapotranspiration. These frequency distributions would be selected to simulate the variation of the relevant parameters with seasonal changes.

The second part of the program would handle the actual moisture movement under the pavement for any desired number of years. This required that the program keeps track of the following parameters:

1) Volume of water stored in the crack fabric underneath the pavement and outside the pavement,

2) Size and moisture conditions of the soil blocks, and

3) Size and shape of shrinkage crack fabric

The remaining sections of this report describe the basis on which the program has been assembled, and the results of several simulations implemented for regional areas of Texas.

REGIONAL CLIMATIC CONDITIONS

General

The climatic conditions are reduced to two daily parameters: rainfall depth and Potential Evapotranspiration. On rainy days, a third parameter is needed: the rainfall duration. The computer program accepts raw meteorological data and reduces it to rainfall depth and potential evapotranspiration for every day of the historical record. At the same time that the program reduces the data, it forms a histogram of the relative frequency for different magnitudes of events for each of the two daily variables.

After the program has scanned through the record of historical data, a theoretical distribution is fitted to each histogram. These theoretical distributions are then used in the stochastic simulation of the climatic conditions for the site. The remaining sections of this chapter discuss these steps in more detail.

Daily Rainfall

When the program scans through the historical data, it divides the days into dry days (without rainfall) and wet days (with rainfall). The program keeps track of the total number of days recorded and the total number of dry days preceded by a wet day and the total number of dry days preceded by a dry day. At the end, the program calculates the

transition probabilities.

The program divides the wet days into two groups: days with trace of rainfall (rainfall depth smaller than 0.005 in) and days with more than trace of rainfall. At the end of scanning through the historical data, the program calculates the probability of having traces of rainfall in wet days.

The rainfall depths registered during wet days with more than trace of rainfall are used to form a histogram with the relative frequence of occurrence. A gamma distribution with an exponent smaller than one (a distribution asymptotic to both axes in the first quadrant) is fitted to the formed histogram. The parameters of the distribution are calculated from the mean and standard deviation of the histogram using the maximum likelihood estimators of Greenwood et al. [20].

Rainfall Intensity/Duration

The rainfall depth versus duration for rainstorms is known to depend on the return period and geographical location. The rainfall intensity is commonly approximated by the following relationships:

$$i = \frac{a}{t+b} \quad \text{for } t < 120 \text{ minutes}$$

Where: t is the rainstorm duration,
i is the rainfall intensity, and
a & b are constants that depend on the return period and geographical location.

Values for the parameters a & b have been published [21] for some regions of the United States. To extend the values of the parameters a

& b to the State of Texas, published maps [22] of rainfall intensities have been used; specifically the one hour and two hours rainfall depths for each return period were used to solve for a and b. The resulting contour maps of these parameters throughout the State of Texas are shown in Figures 1 through 10. These figures include contour lines through the State of Texas for return periods of 1,2,5,10 and 25 years.

The rainfall intensity for rainstorms longer than 120 minutes has been represented [21] by the following relationship:

$$i = \frac{KT^x}{t^n} \qquad \text{for } t > 120 \text{ minutes}$$

Where: t is the rainstorm duration,

i is the rainfall intensity,

T is the return period, and

K, x & n are constants depending of geographical location

Values of the parameters K, x, and n have been published [21] for the Eastern half, of the State of Texas. The extension of these contour lines to the western half of the State of Texas has been accomplished based on published maps [22] of rainfall frequency and following a procedure that could reproduce the published contours in reference [21].

The complete set of all contour lines for the State of Texas is presented in Figure 11 for parameter K, in Figure 12 for parameter n, and in Figure 13 for parameter x. The published contour lines are shown as dotted lines and the extension to the western half of the State of Texas developed in this study are shown as solid lines.

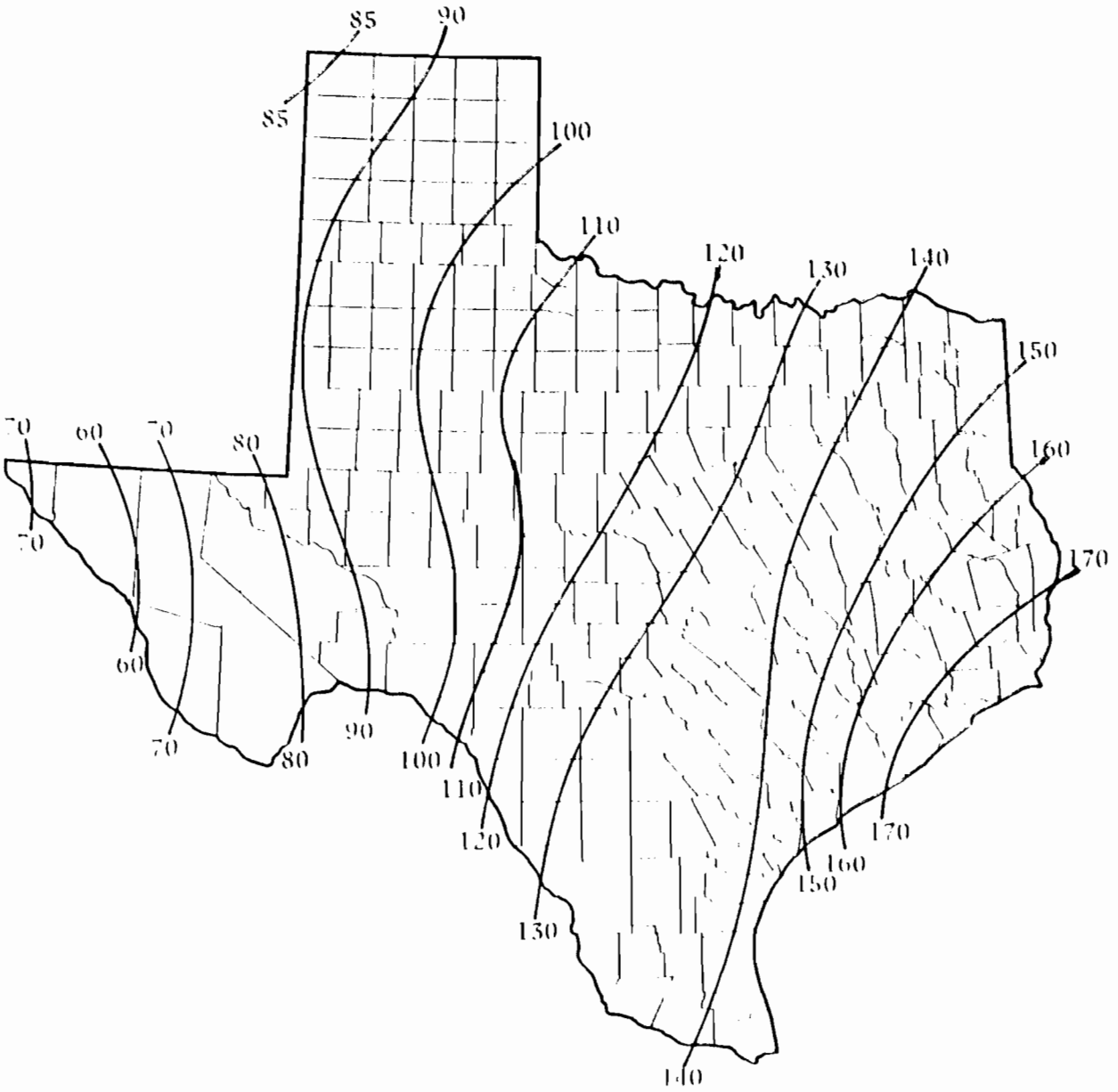

FIGURE 1 CONTOUR LINES THROUGHOUT TEXAS OF THE VALUES OF PARAMETER "a" IN THE INTENSITY - DEPTH - DURATION EQUATION FOR RAINSTORM EVENTS SHORTER THAN 120 MINUTES AND A RETURN PERIOD OF 1 YEAR

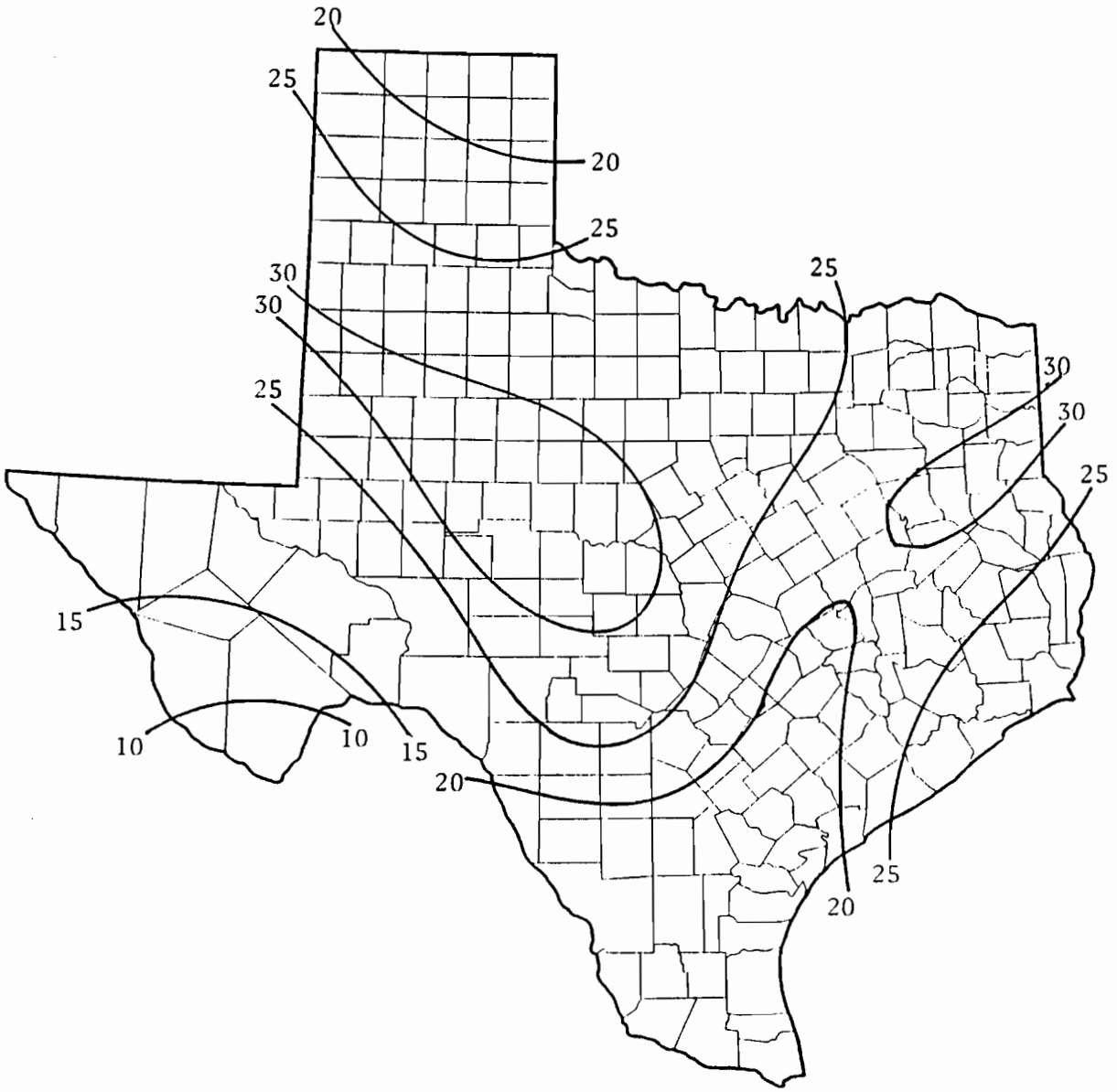

FIGURE 2 CONTOUR LINES THROUGHOUT TEXAS OF THE VALUES OF PARAMETER "b" IN THE INTENSITY - DEPTH - DURATION EQUATION FOR RAINSTORM EVENTS SHORTER THAN 120 MINUTES AND A RETURN PERIOD OF 1 YEAR

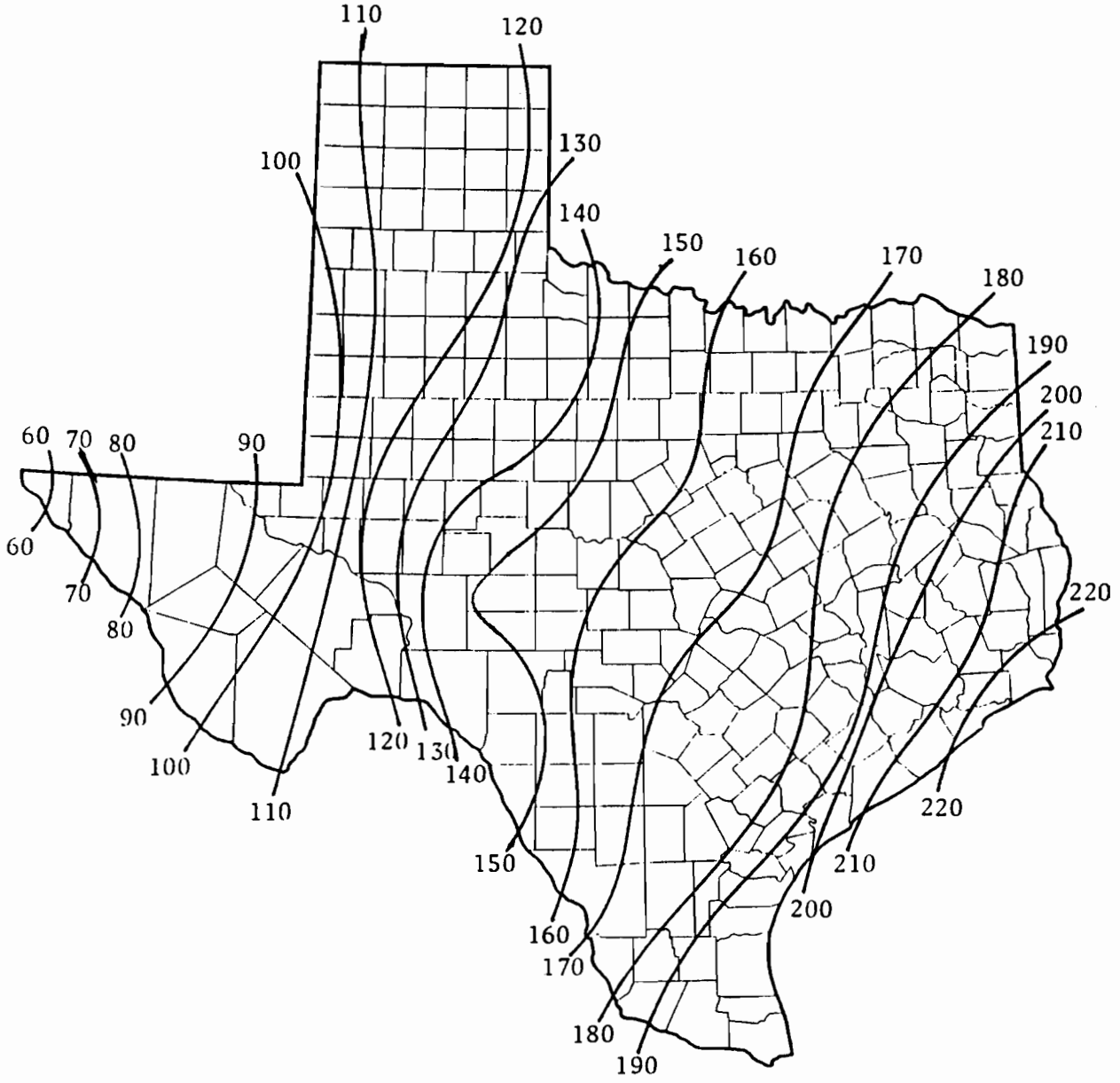

FIGURE 3 CONTOUR LINES THROUGHOUT TEXAS OF THE VALUES OF PARAMETER "a" IN THE INTENSITY - DEPTH - DURATION EQUATION FOR RAINSTORM EVENTS SHORTER THAN 120 MINUTES AND A RETURN PERIOD OF 2 YEAR

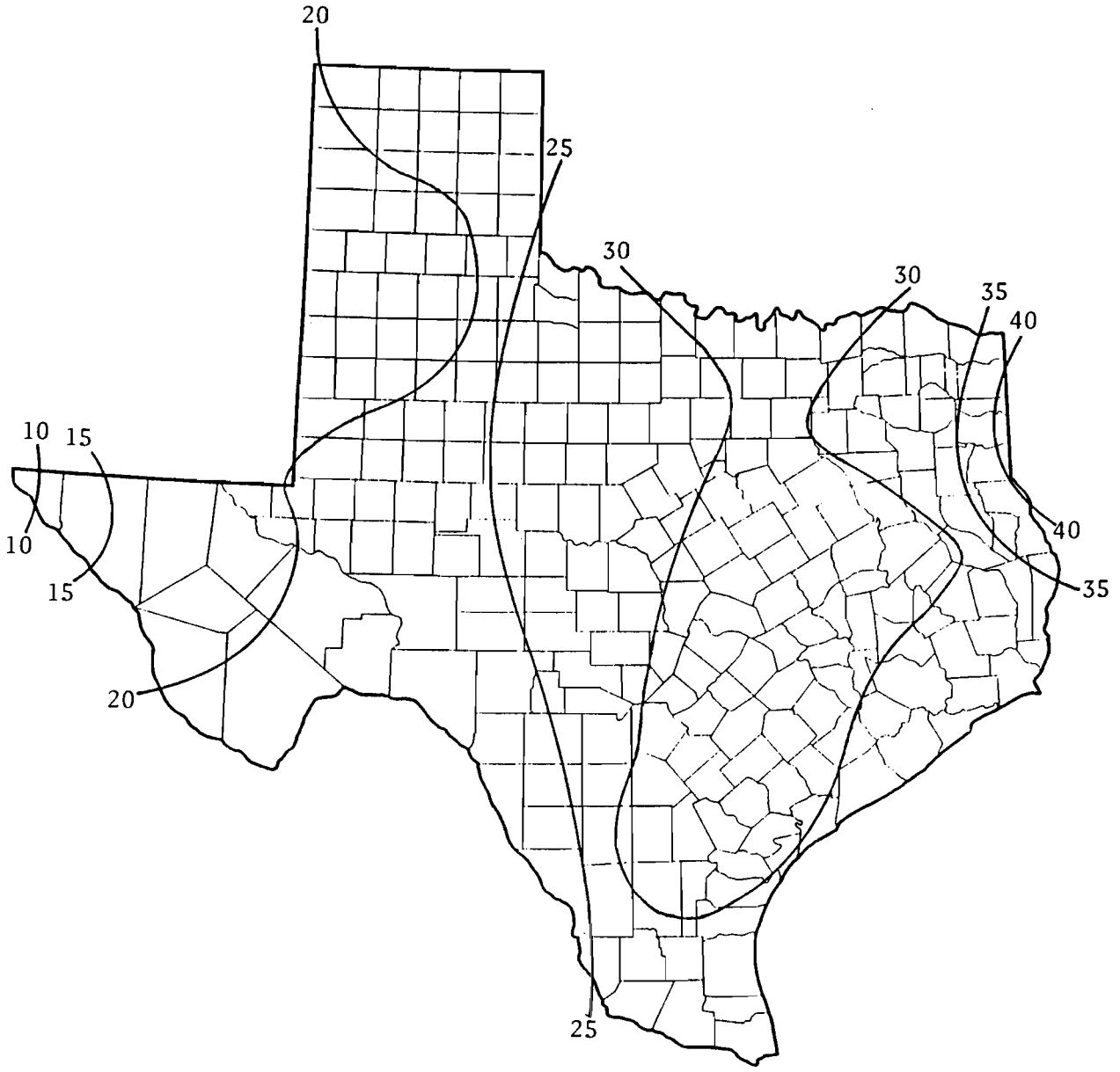

FIGURE 4 CONTOUR LINES THROUGHOUT TEXAS OF THE VALUES OF PARAMETER "b" IN THE INTENSITY - DEPTH - DURATION EQUATION FOR RAINSTORM EVENTS SHORTER THAN 120 MINUTES AND A RETURN PERIOD OF 2 YEAR

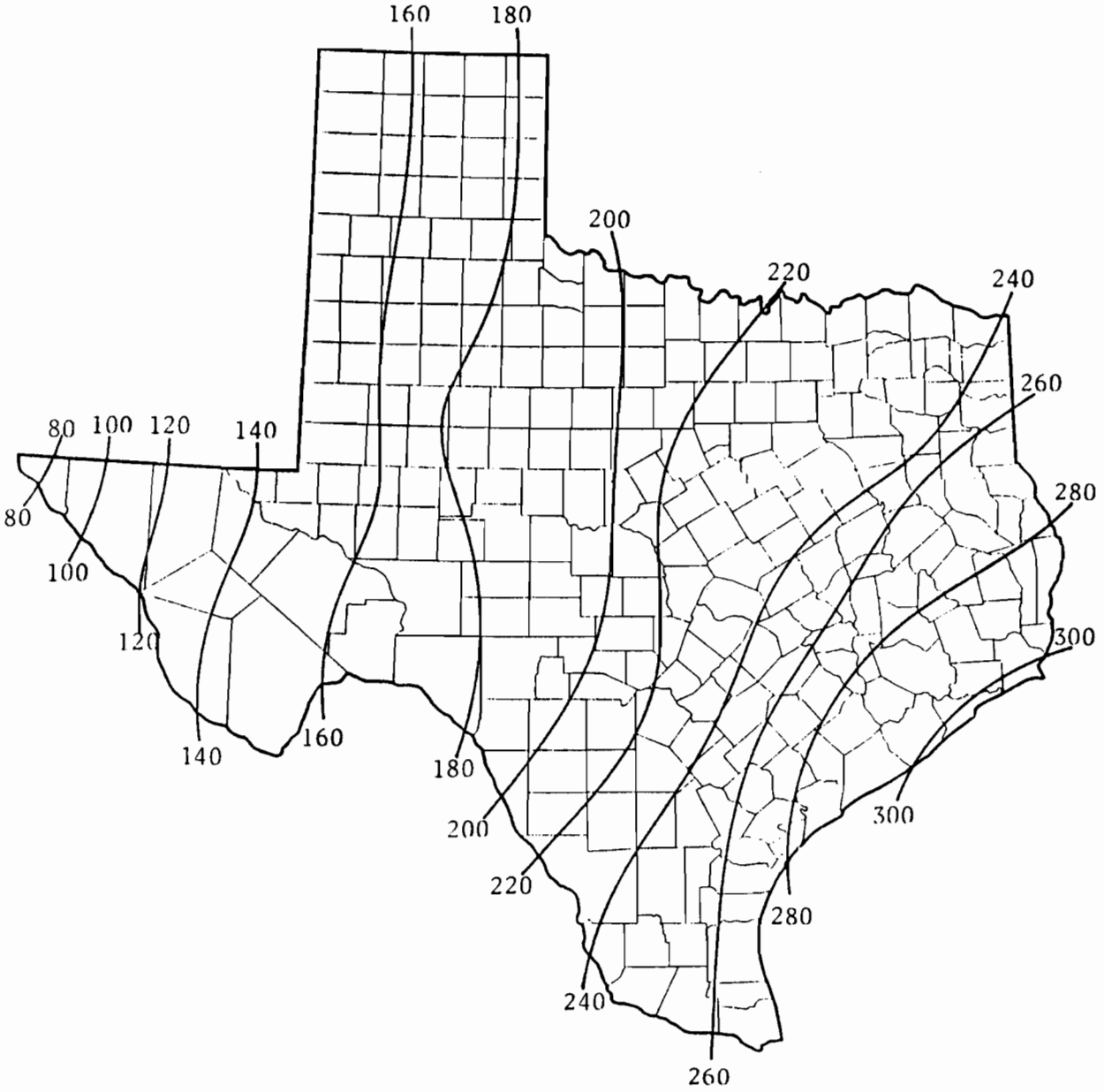

FIGURE 5 CONTOUR LINES THROUGHOUT TEXAS OF THE VALUES OF PARAMETER "a" IN THE INTENSITY - DEPTH - DURATION EQUATION FOR RAINSTORM EVENTS SHORTER THAN 120 MINUTES AND A RETURN PERIOD OF 5 YEAR

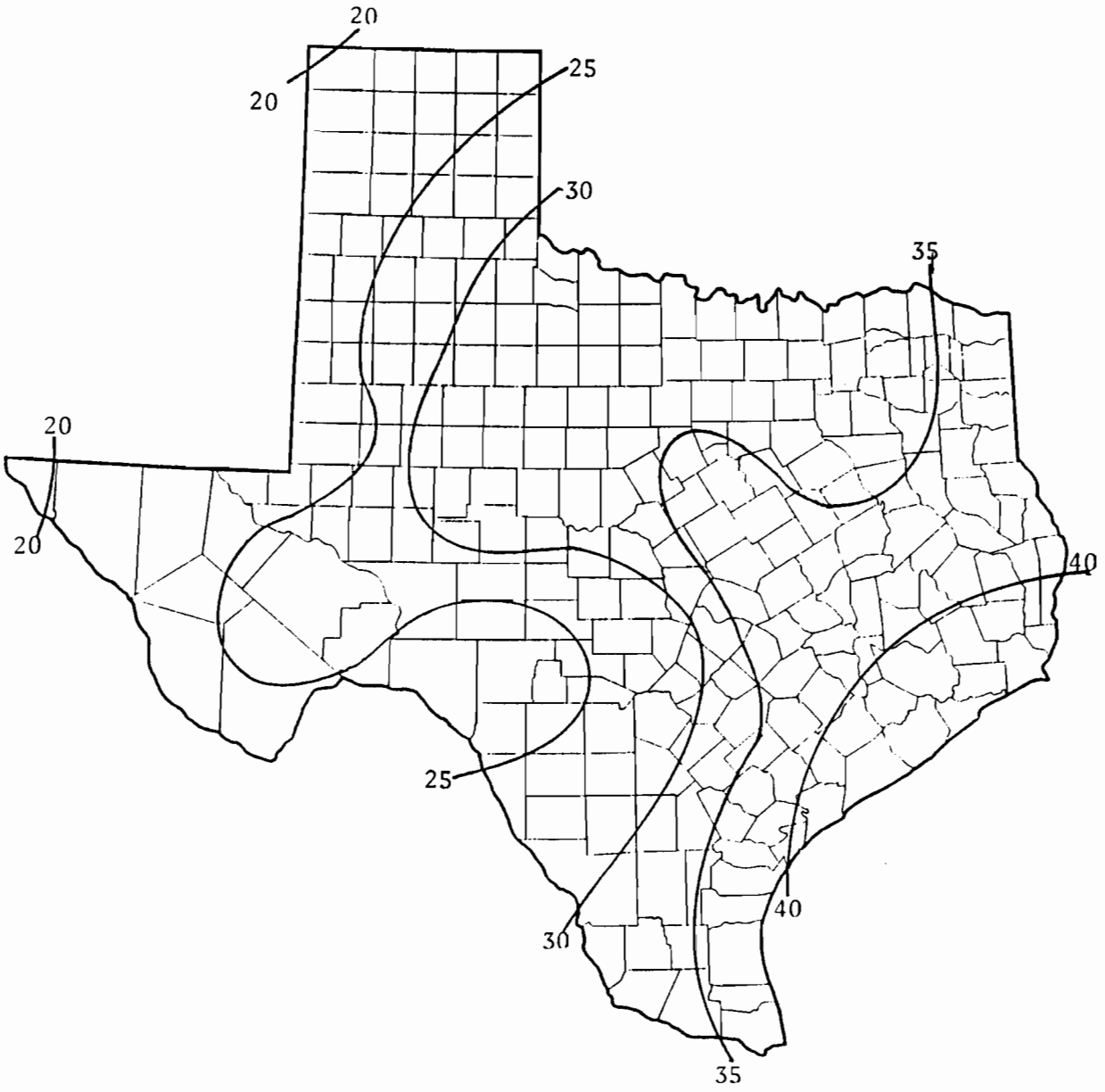

FIGURE 6 CONTOUR LINES THROUGHOUT TEXAS OF THE VALUES OF PARAMETER "b" IN THE INTENSITY - DEPTH - DURATION EQUATION FOR RAINSTORM EVENTS SHORTER THAN 120 MINUTES AND A RETURN PERIOD OF 5 YEAR

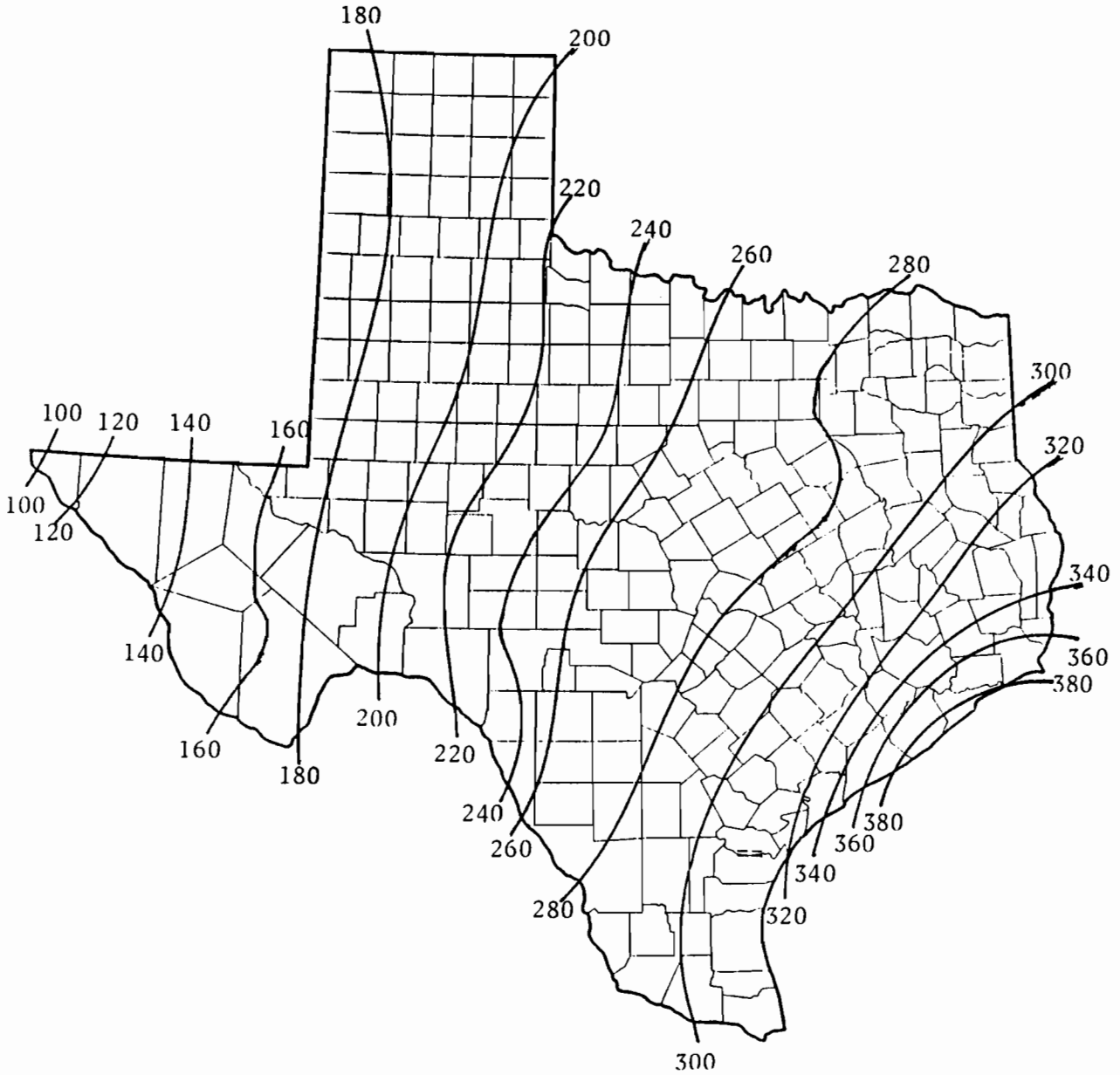

FIGURE 7 CONTOUR LINES THROUGHOUT TEXAS OF THE VALUES OF PARAMETER "a" IN THE INTENSITY - DEPTH - DURATION EQUATION FOR RAINSTORM EVENTS SHORTER THAN 120 MINUTES AND A RETURN PERIOD OF 10 YEAR

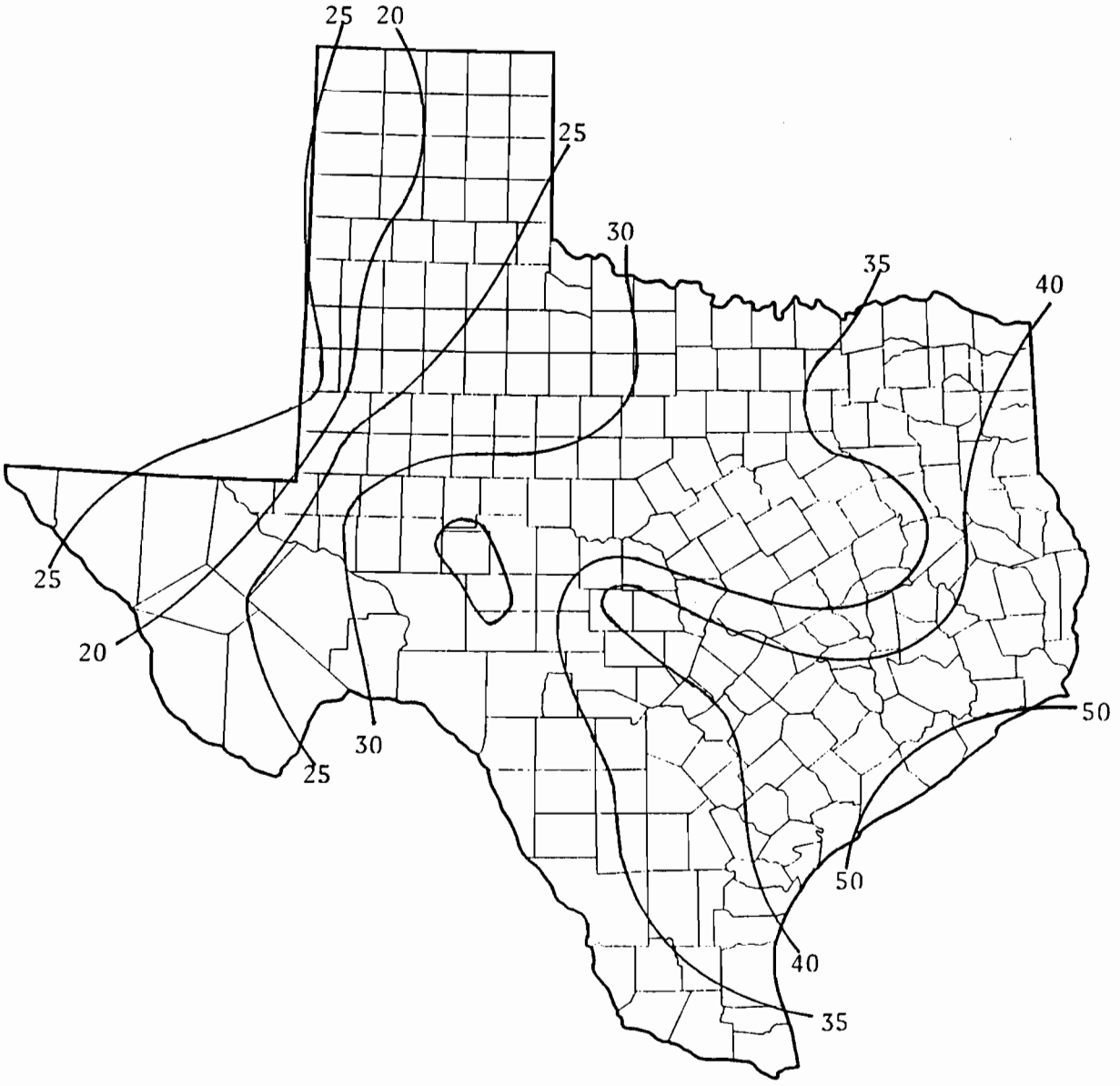

FIGURE 8 CONTOUR LINES THROUGHOUT TEXAS OF THE VALUES OF PARAMETER "b" IN THE INTENSITY - DEPTH - DURATION EQUATION FOR RAINSTORM EVENTS SHORTER THAN 120 MINUTES AND A RETURN PERIOD OF 10 YEAR

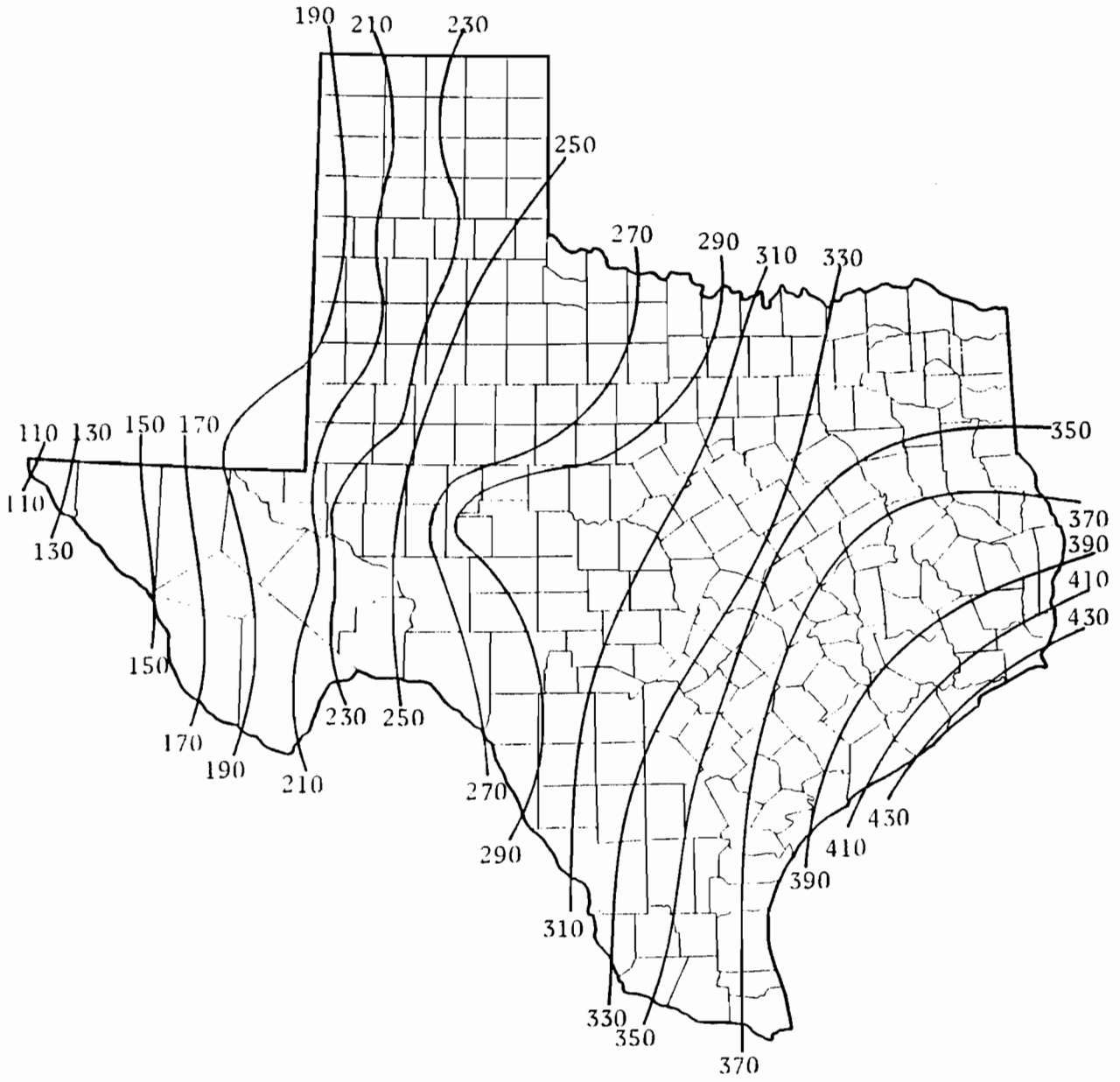

FIGURE 9 CONTOUR LINES THROUGHOUT TEXAS OF THE VALUES OF PARAMETER "a" IN THE INTENSITY - DEPTH - DURATION EQUATION FOR RAINSTORM EVENTS SHORTER THAN 120 MINUTES AND A RETURN PERIOD OF 25 YEAR

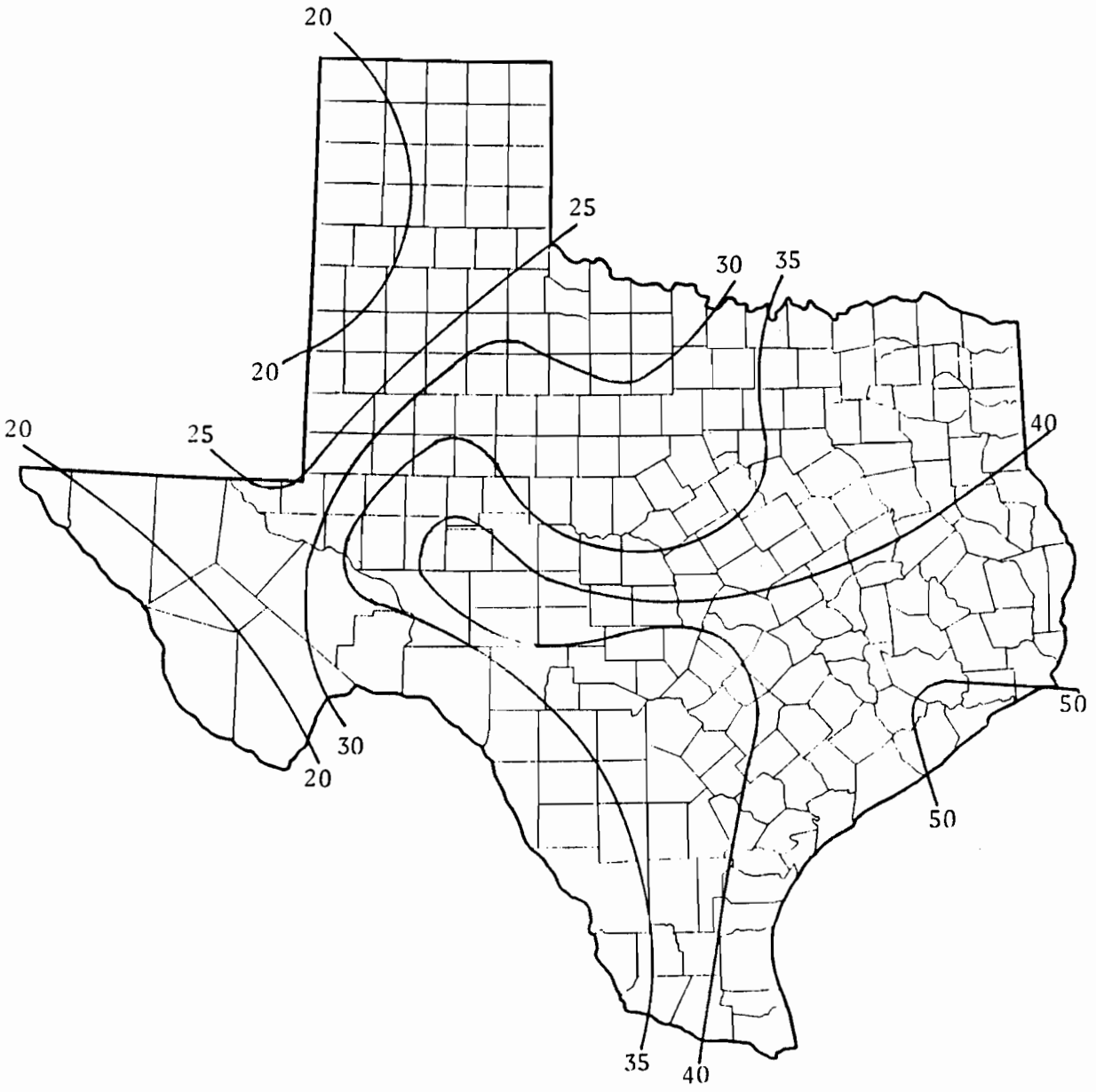

FIGURE 10 CONTOUR LINES THROUGHOUT TEXAS OF THE VALUES OF PARAMETER "b" IN THE INTENSITY - DEPTH - DURATION EQUATION FOR RAINSTORM EVENTS SHORTER THAN 120 MINUTES AND A RETURN PERIOD OF 25 YEAR

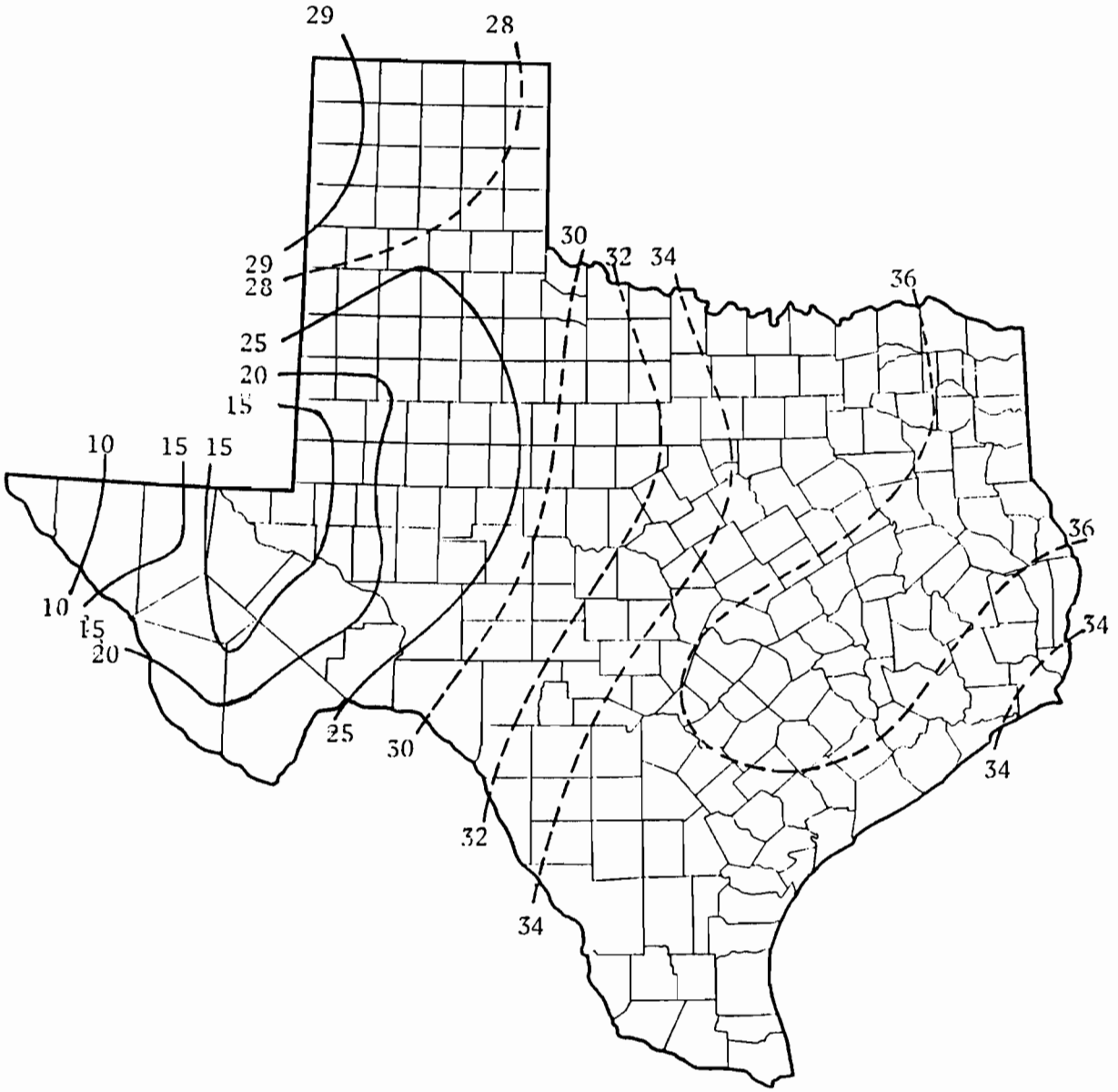

FIGURE 11 CONTOUR LINES THROUGHOUT TEXAS OF THE VALUES OF PARAMETER "K" IN THE INTENSITY - DEPTH - DURATION EQUATION FOR RAINSTORM EVENTS LONGER THAN 120 MINUTES

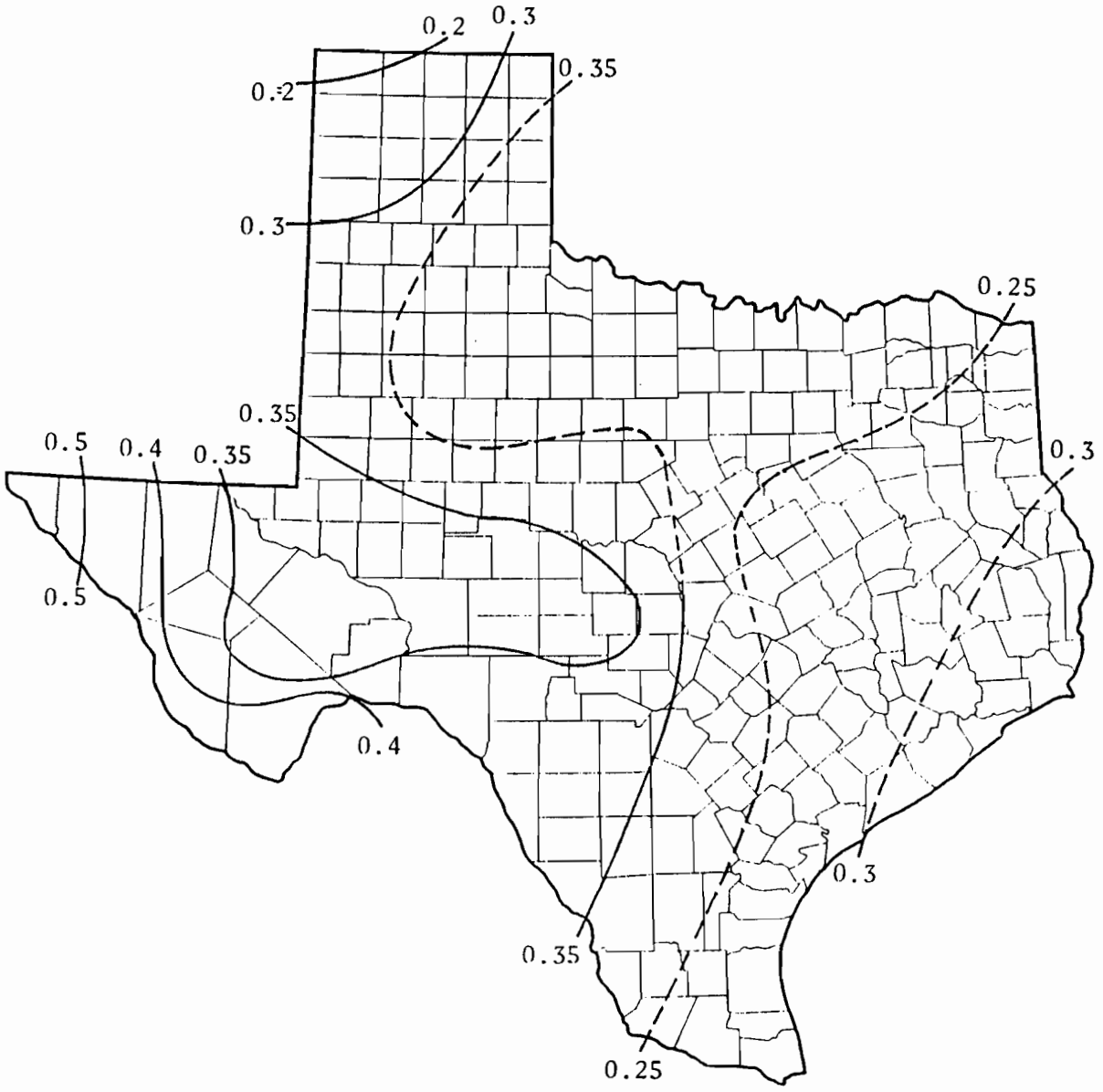

FIGURE 12 CONTOUR LINES THROUGHOUT TEXAS OF THE VALUES OF PARAMETER "x" IN THE INTENSITY - DEPTH - DURATION EQUATION FOR RAINSTORM EVENTS LONGER THAN 120 MINUTES

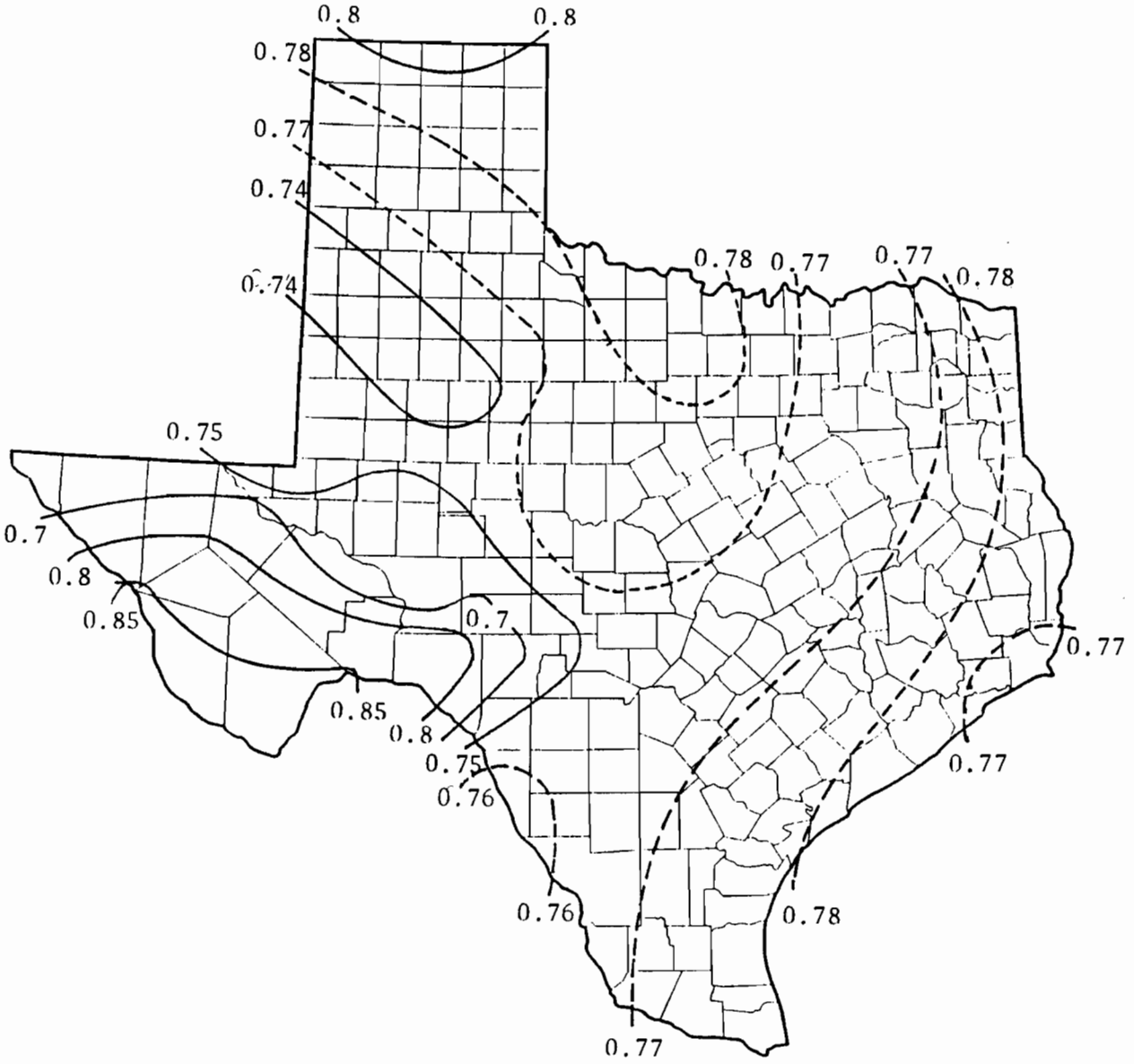

FIGURE 13 CONTOUR LINES THROUGHOUT TEXAS OF THE VALUES OF PARAMETER "n" IN THE INTENSITY - DEPTH - DURATION EQUATION FOR RAINSTORM EVENTS LONGER THAN 120 MINUTES

The computer program selects the return period by choosing a random number. For the short duration rainstorms (t<120 min), this random number is between 0.0 and 0.04. For the long durations rainstorm the random number is between 0 and 1. From the depth of rainfall and the return period selected, the program determines whether a short duration rainfall is possible; if not, the intensity is selected with the relationship for durations longer than 120 minutes.

After the duration of the storm has been found, the program selects the time of the day when the storm starts. This is selected based on another random number with the constraint that the rainstorm has to occur within the 24 hours of the day in question.

Potential Evapotranspiration

The program offers the user the possibility of estimating the Potential Evapotranspiration from two sets of data:

1) From Pan Evaporation Measurements. The user can specify a constant factor to transform the Pan evaporation data to potential evapotranspiration or can use a default factor (0.8) included in the program.
2) From Raw Meteorological Data. The meteorological data needed includes the following mean daily parameters: wind velocity, relative humidity, air temperature and net radiant energy.

The first step is to calculate the potential evapotranspiration "PET". Then the program forms two histograms with the relative frequency of occurrence; one histogram with the "PET" on dry days and the second histogram with the "PET" on for wet days.

As for the rainfall depth, the program fits a theoretical distribution to each histogram. Since the potential evapotranspiration is limited by the amount of energy available at the surface, and this energy is limited by the net incoming radiation, the theoretical distribution has to have a finite range of possible values. This consideration lead to choose a beta distribution. This distribution was fitted to the histogram using the mean, standard deviation, and the upper bound of potential evapotranspiration. The upper bound was obtained by trial and error as the value that minimized the test statistic that was assumed to follow a chi-square distribution.

Seasonal Variability

To account for the effect of the seasons on the rainfall depth and potential evapotranspiration, the program forms independent histograms for each month of the year. Thus the program forms thirty six histograms: twelve of rainfall depth on wet days with more than trace of rain, twelve of potential evapotranspiration on dry days, and twelve of potential evapotranspiration on wet days.

The histograms obtained with the program and the fitted distributions for rainfall depth and PET for a record of fourteen years of El Paso weather are presented in Appendix I. A summary of the theoretical distributions of PET for dry days are presented in Figures 14 and 15, and for PET on wet days in Figures 16 and 17. These distributions show the large effect that the month of the year has on PET and thus highlights the need to consider monthly distributions.

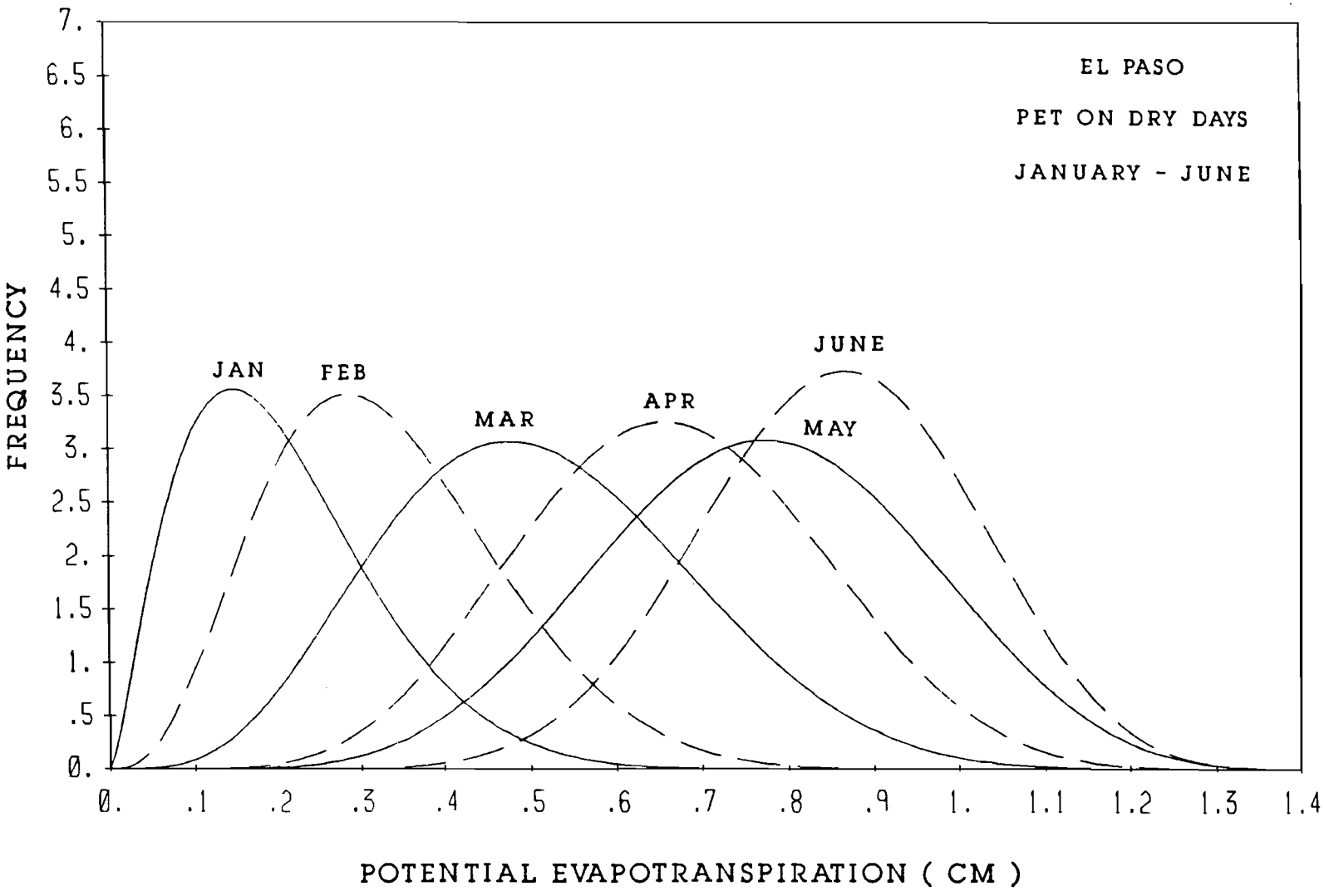

FIGURE 14 FITTED BETA DISTRIBUTION TO THE POTENTIAL EVAPOTRANSPIRATION ON DRY DAYS FROM JANUARY TO JUNE

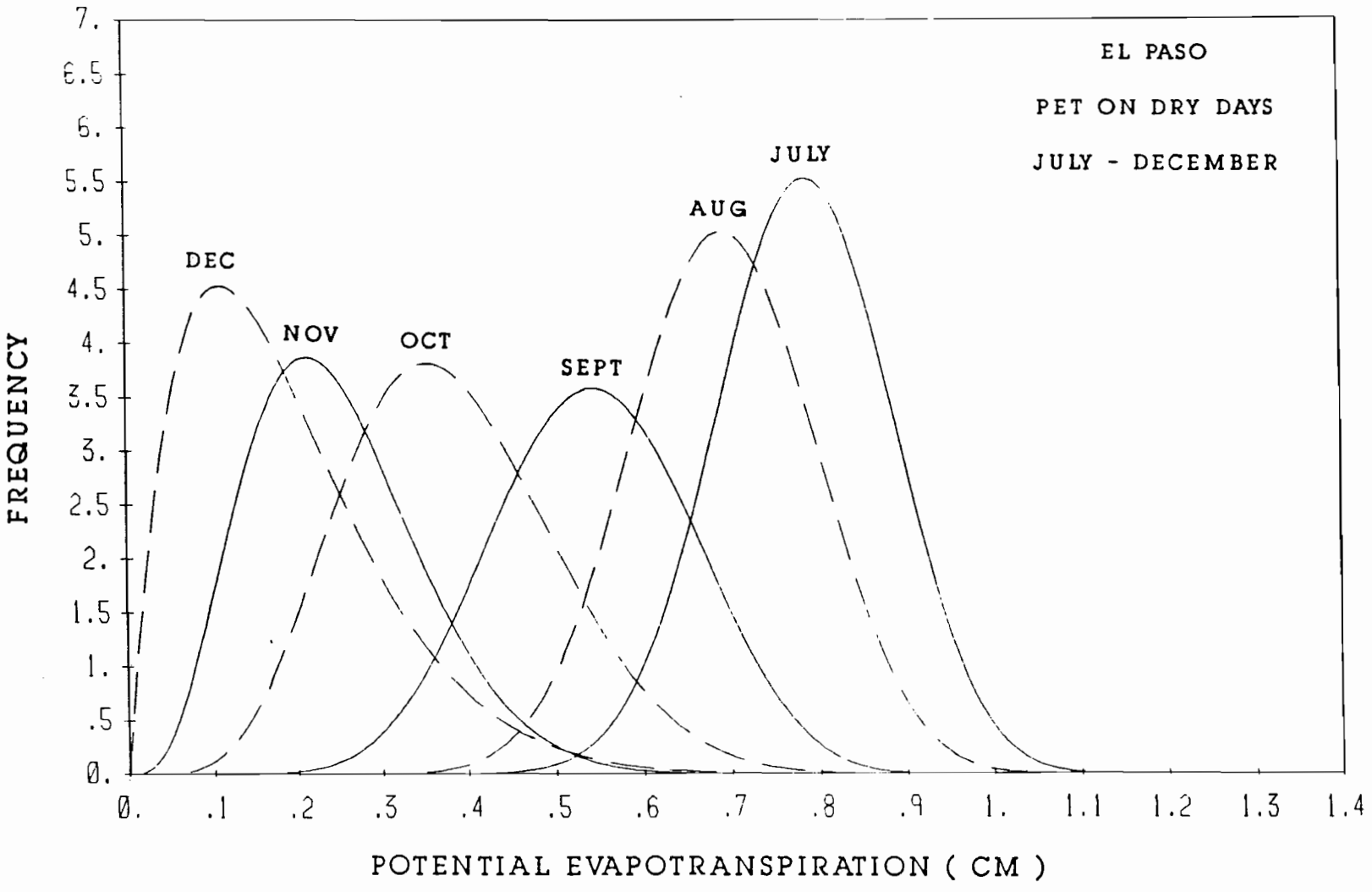

FIGURE 15 FITTED BETA DISTRIBUTION TO THE POTENTIAL EVAPOTRANSPIRATION ON DRY DAYS FROM JULY TO DECEMBER

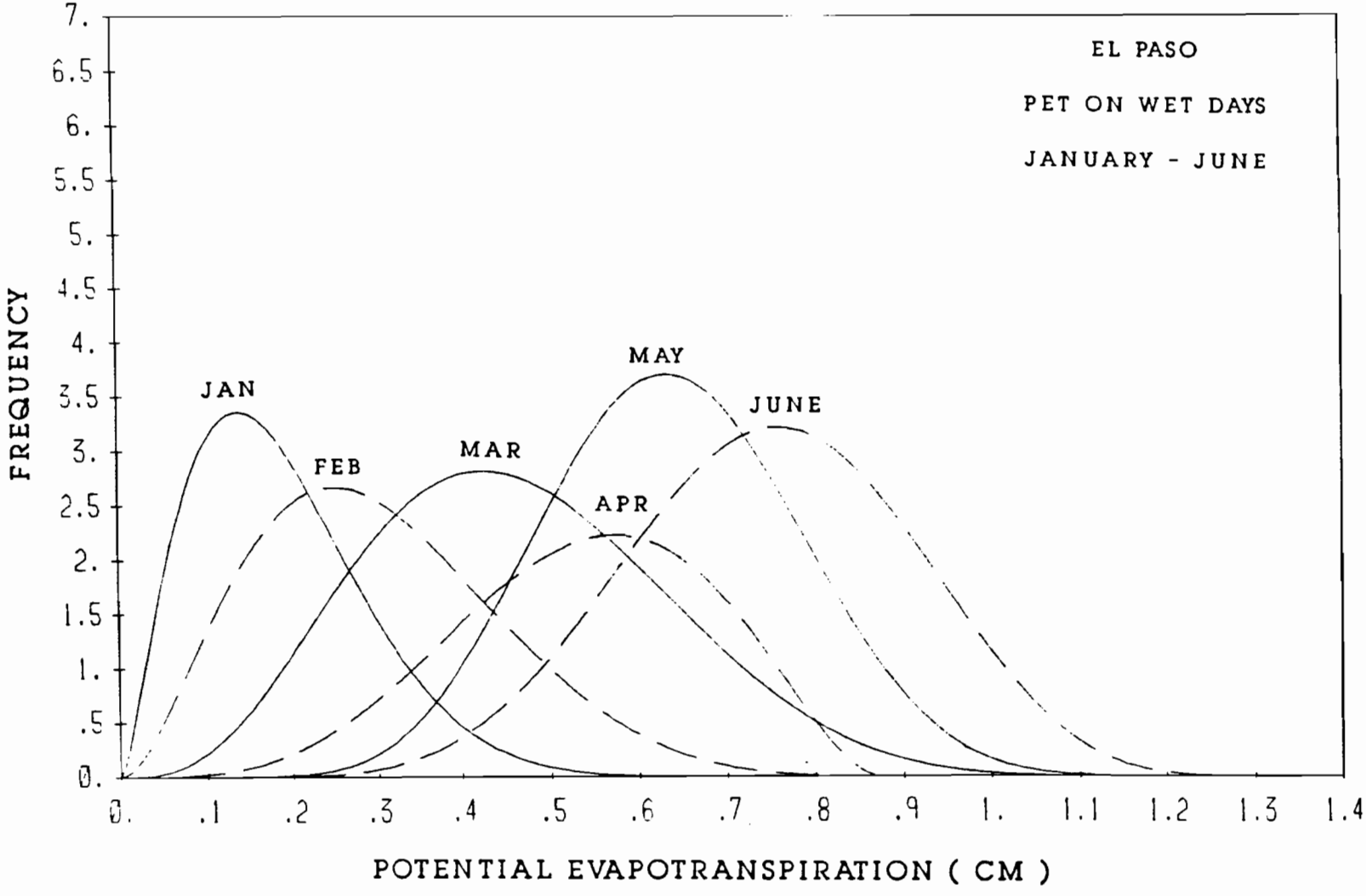

FIGURE 16 FITTED BETA DISTRIBUTION TO THE POTENTIAL EVAPOTRANSPIRATION ON WET DAYS FROM JANUARY TO JUNE

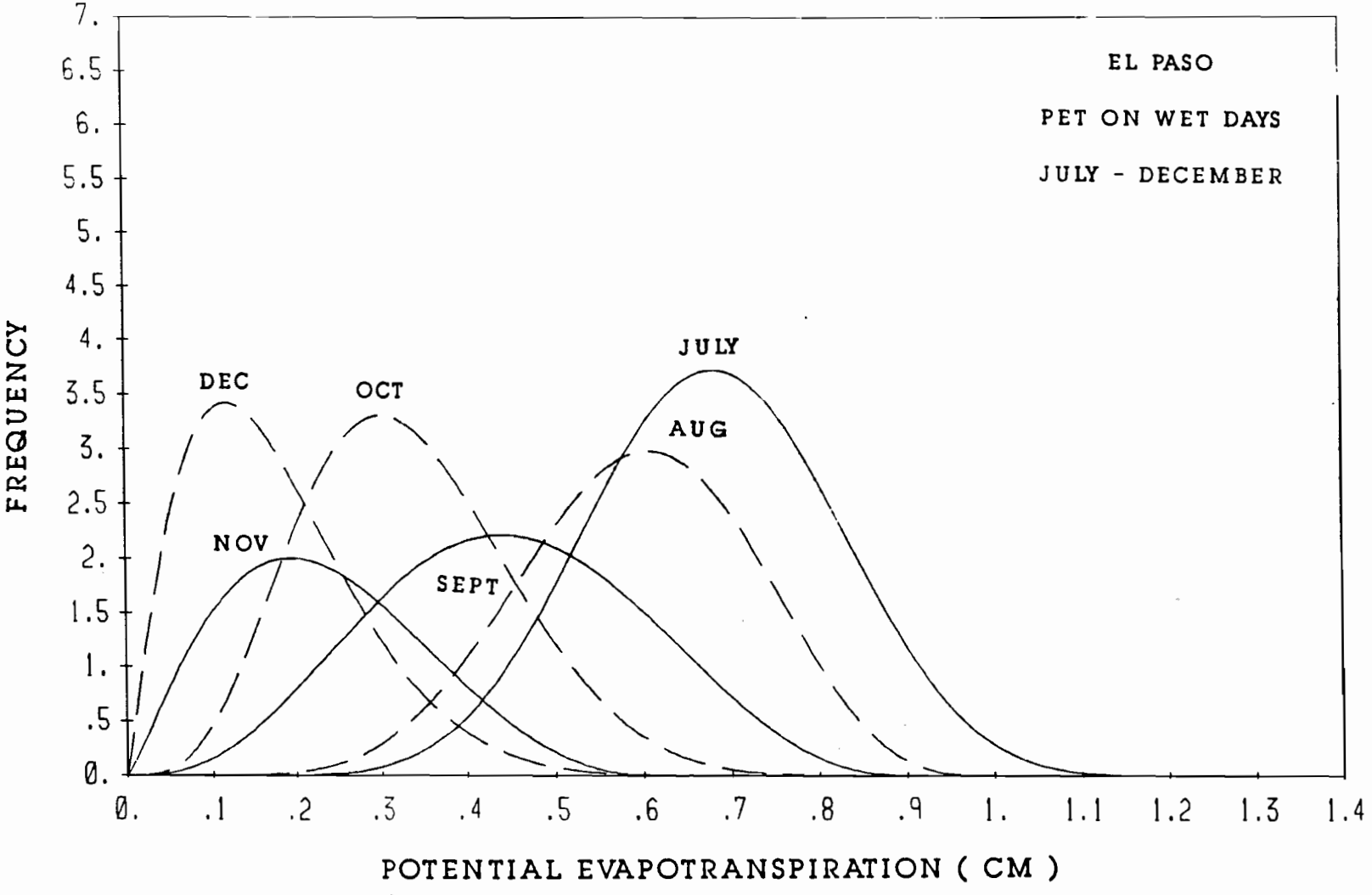

FIGURE 17 FITTED BETA DISTRIBUTION TO THE POTENTIAL EVAPOTRANSPIRATION ON WET DAYS FROM JULY TO DECEMBER

Stochastic Simulation

The stochastic simulation consists of a first order Markov chain to simulate the occurrence of rainfall following the recommendations of Larsen et al [23]. The first step consists of determining the state of the day:wet or dry. The program achieves this goal by selecting a random number between 0 and 1 and then comparing this number with the corresponding transition probability for the month in question. If the random number exceeds the transition probability the state of the following day changes relative to the preceding day.

If the following day is a dry day, the program selects another random number between 0 and 1 that is considered to be the probability of occurrence of an event smaller or equal to the selected event. This probability is used in conjunction with the distribution of PET on dry days to select the PET for the following day.

When the following day is a wet day, the program first determines whether will be trace or more than trace of rainfall. For this purpose, the program selects another random number that is compared with the probability of trace of rain on wet days for the month in question. If the day is to have more than trace of rain another random number is selected to choose the rainfall depth from the corresponding monthly distribution of rainfall depth. To select the rainstorm duration, another random number is chosen to be used as the probability of occurrence together with the frequency/intensity relations described earlier.

The PET on wet days (whether trace or more than trace rainfall) is selected based on another random number and the corresponding monthly distributions of PET on wet days.

The stochastic simulation part of the program was tried by generating a 100-year sequence of daily events. This sequence was then used as input to the program. The program reformed 36 histograms and new distributions were fitted to the new histograms. A sample of the comparison of these results and the original distributions are presented in Figures 18 through 23. These results illustrate that with the stochastic simulation over a period of many years it is possible to recover the original distributions. Figures 18,20 and 22 are examples of the best agreement observed between the original and simulated distributions for rainfall depth, and PET on dry and wet days. Figures 19, 21, and 23 are examples of the largest difference observed between the original and the simulated distributions.

SITE CONDITIONS

General

The computer program allows the user to choose the length of the section of highway, measured along the longitudinal axis, that is considered in the simulation. The crack fabric characteristics such as crack volume available for storage are those corresponding to the selected length of the highway section. Similarly, all the water balances formed also correspond to this same length of highway section.

Some of the soil mass characteristics required by the computer program, such as the crack fabric or linear shrinkage profile, are not readily available. The computer program allows the user to select several default characteristics described in the technical literature. These alternatives should only be used if evidence exists that would indicate that they are reasonable assumptions. Furthermore, some of

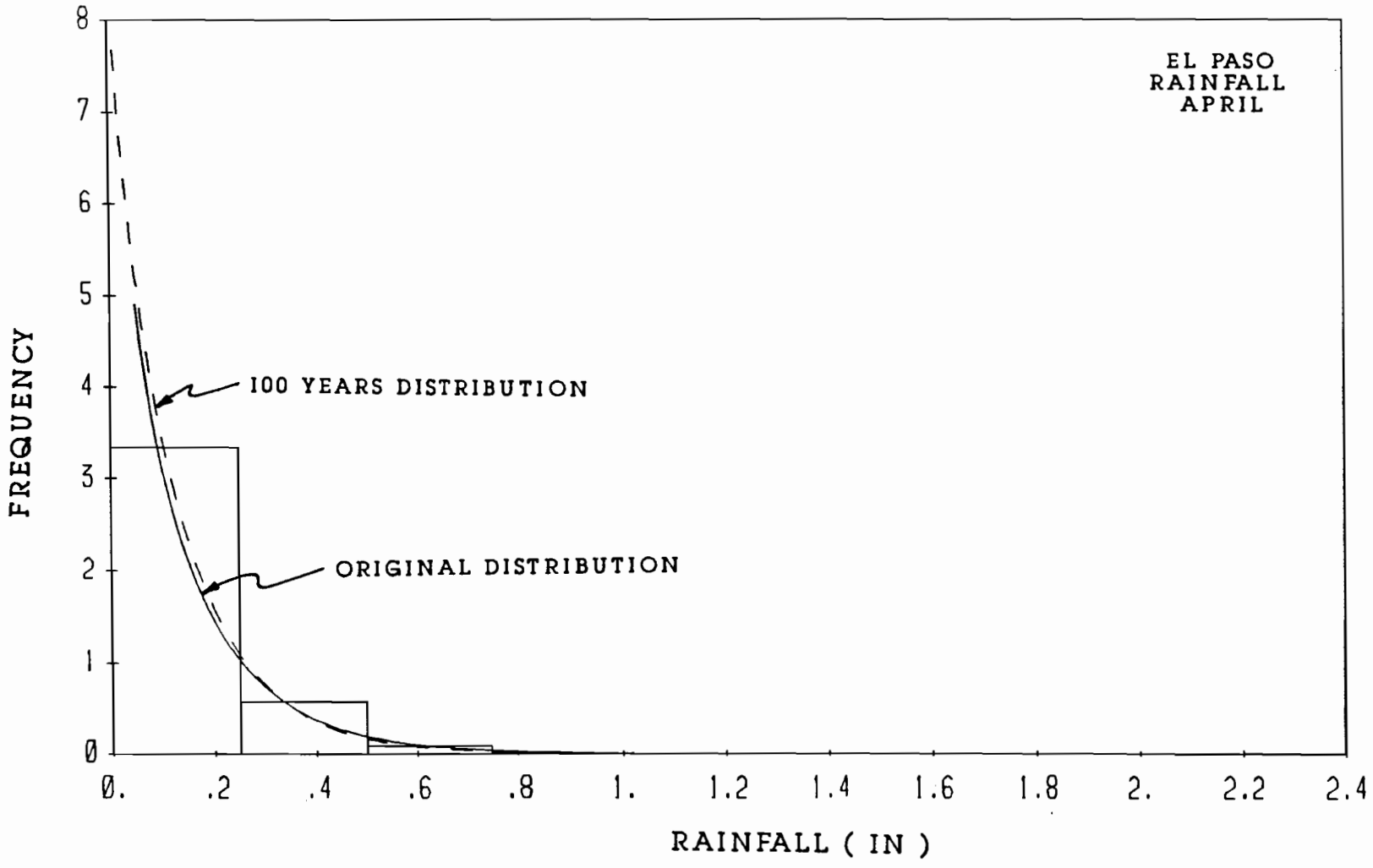

FIGURE 18 EXAMPLE OF CLOSE AGREEMENT BETWEEN ORIGINAL AND FITTED DISTRIBUTIONS TO A 100 YEAR STOCHASTIC SEQUENCE OF RAINFALL

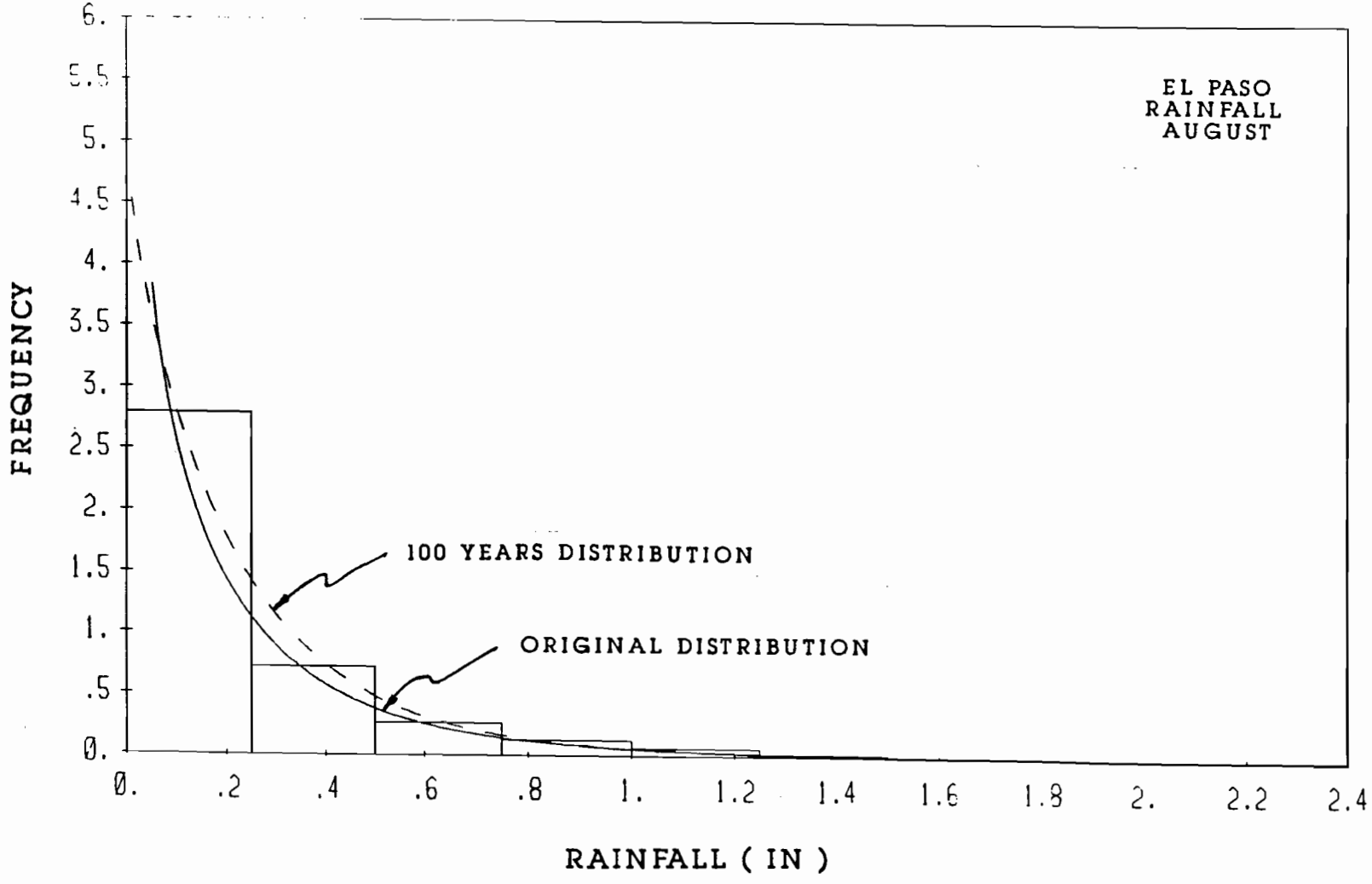

FIGURE 19 EXAMPLE OF POOR AGREEMENT BETWEEN ORIGINAL AND FITTED DISTRIBUTIONS TO A 100 YEAR STOCHASTIC SEQUENCE OF RAINFALL

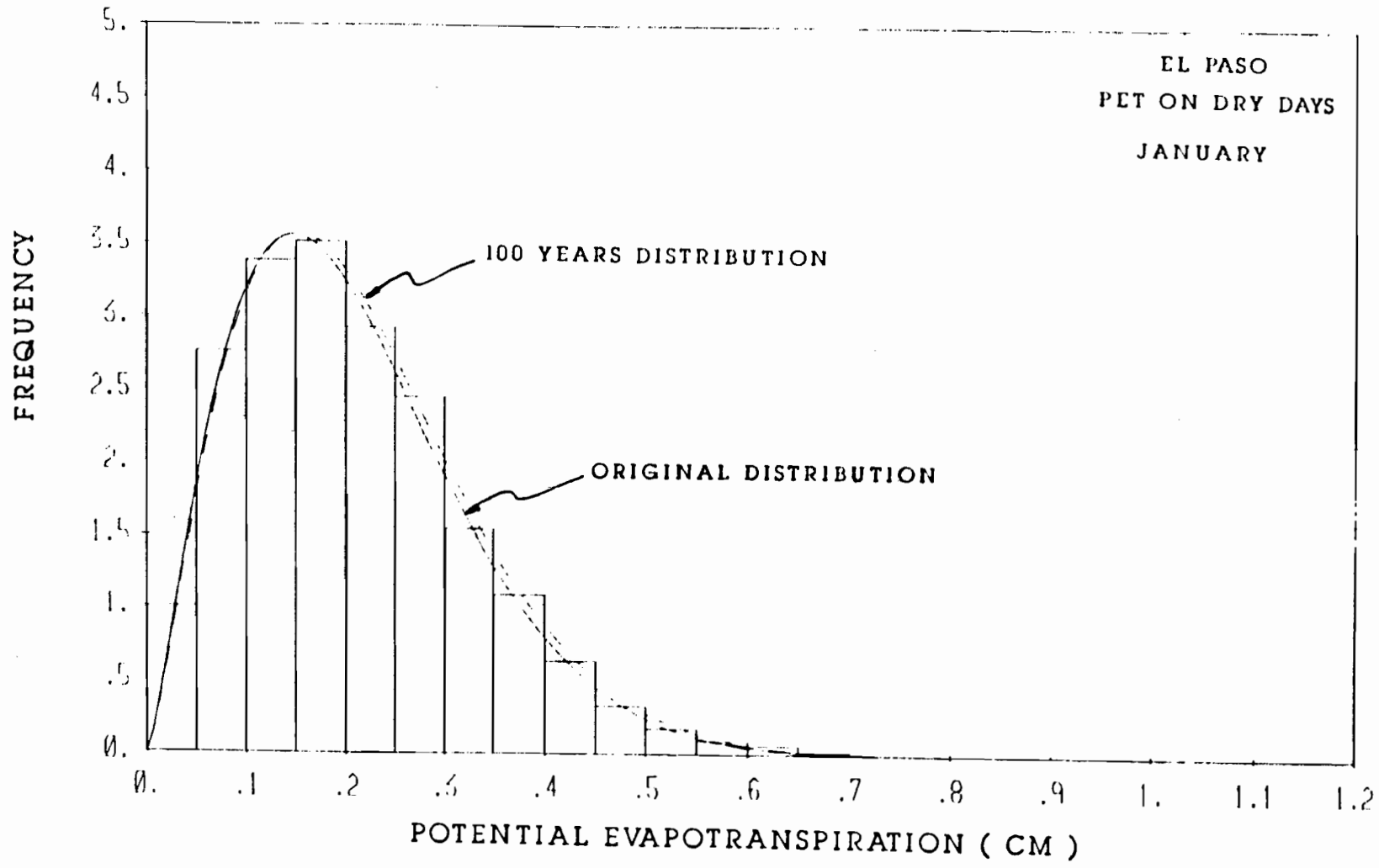

FIGURE 20 EXAMPLE OF CLOSE AGREEMENT BETWEEN ORIGINAL AND FITTED DISTRIBUTIONS TO A 100 YEAR STOCHASTIC SEQUENCE OF POTENTIAL EVAPOTRANSPIRATION ON DRY DAYS

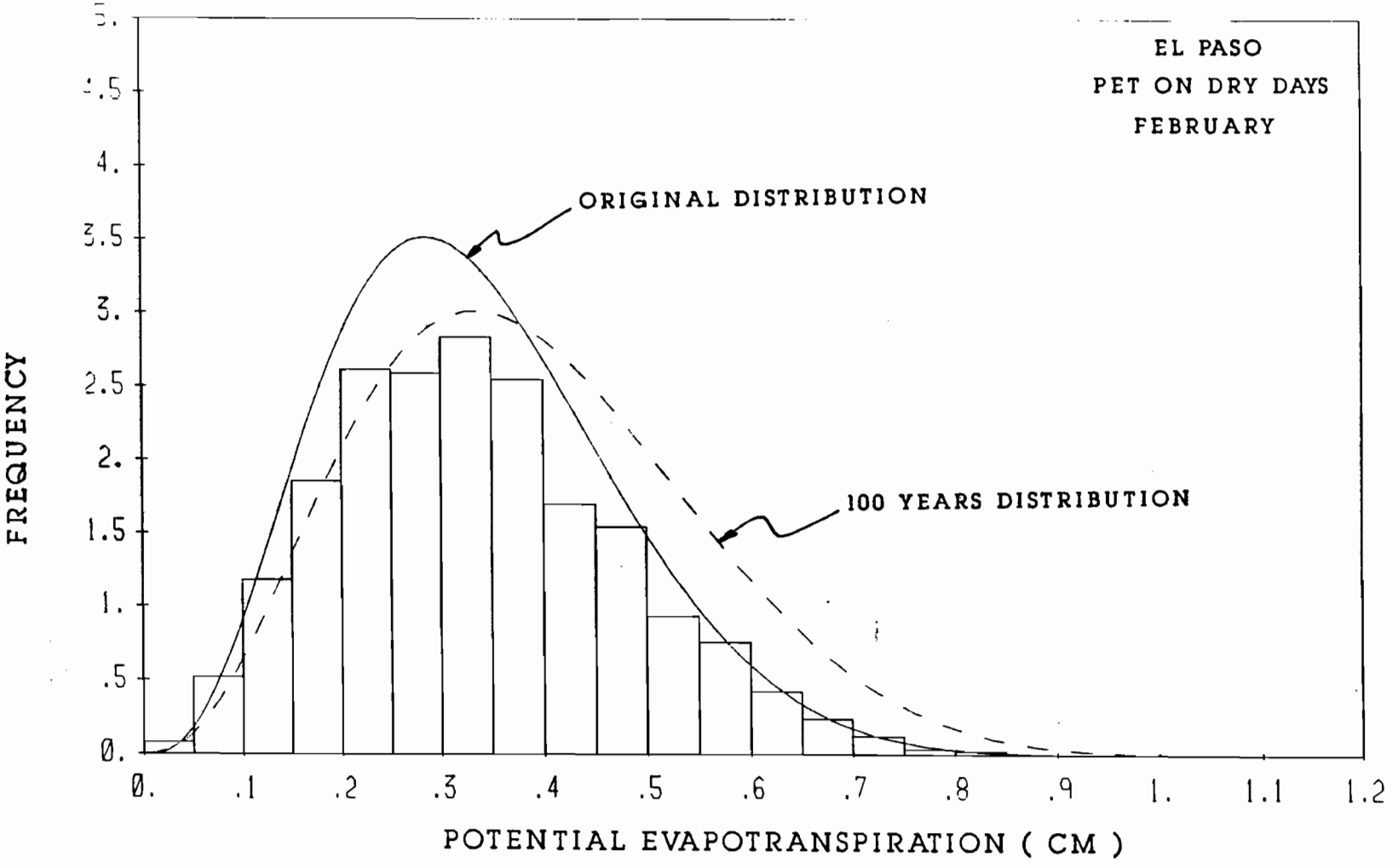

FIGURE 21 EXAMPLE OF POOR AGREEMENT BETWEEN ORIGINAL AND FITTED DISTRIBUTIONS TO A 100 YEAR STOCHASTIC SEQUENCE OF POTENTIAL EVAPOTRANSPIRATION ON DRY DAYS

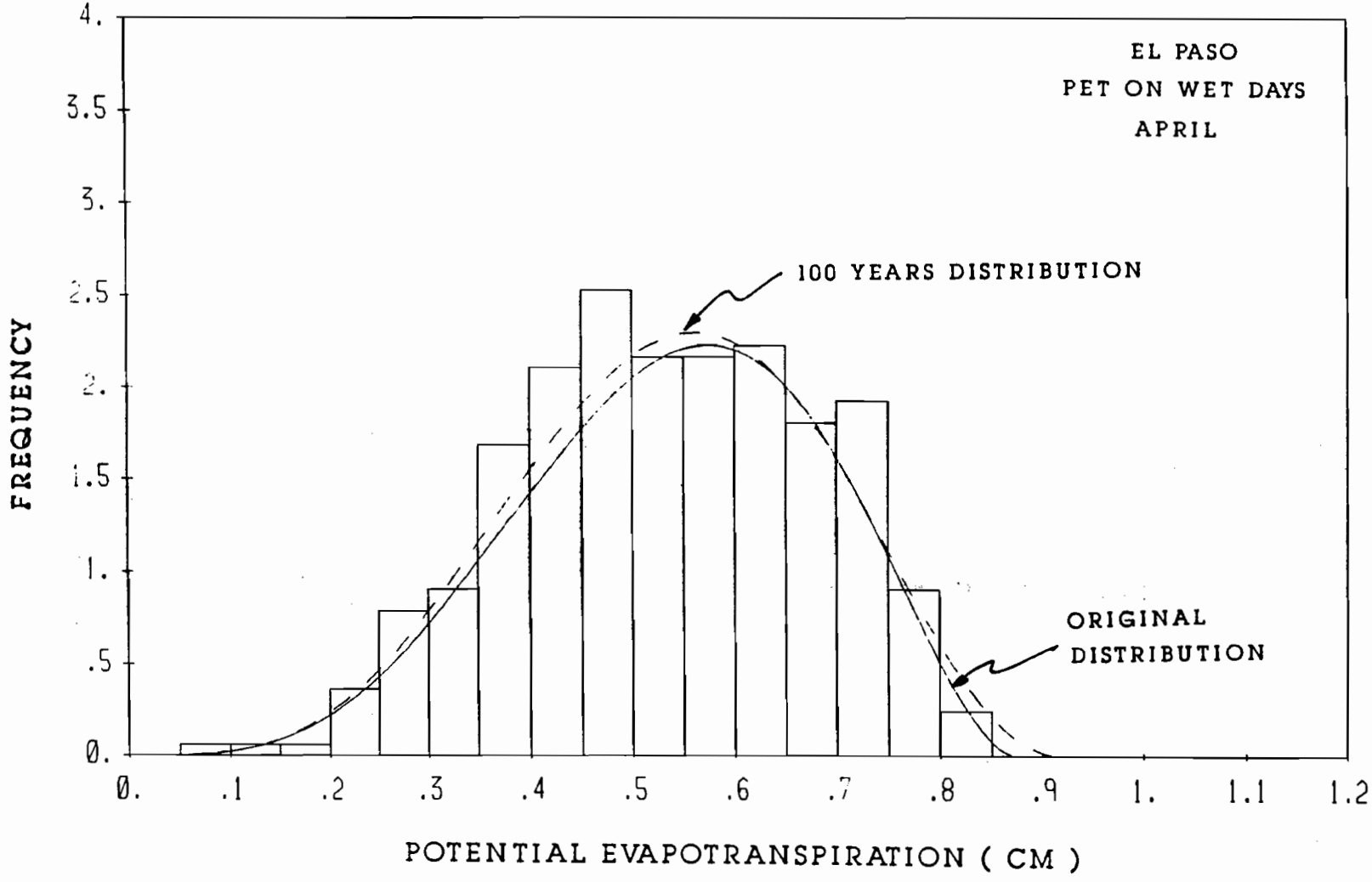

FIGURE 22 EXAMPLE OF CLOSE AGREEMENT BETWEEN ORIGINAL AND FITTED DISTRIBUTIONS TO A 100 YEAR STOCHASTIC SEQUENCE OF POTENTIAL EVAPOTRANSPIRATION ON WET DAYS

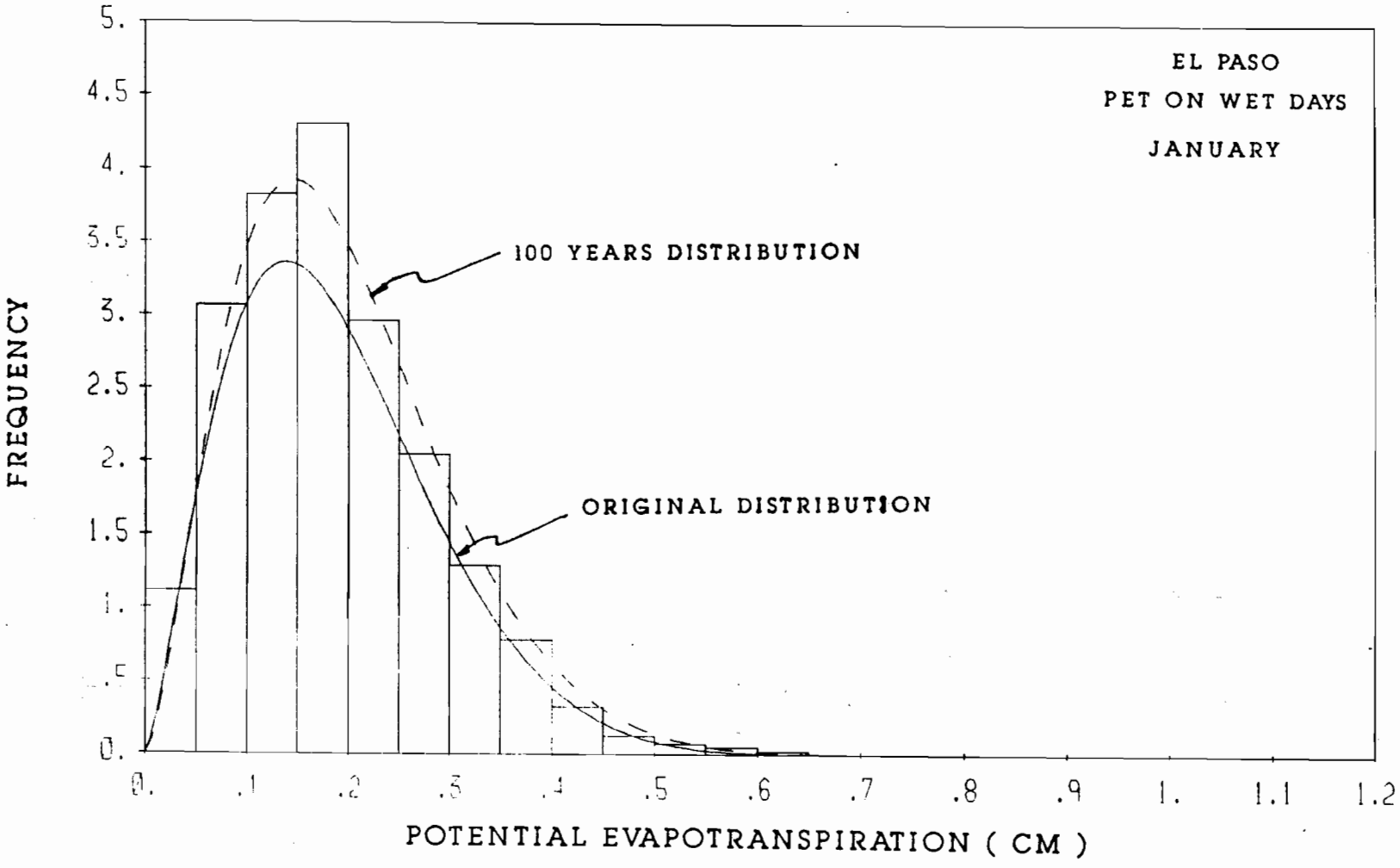

FIGURE 23 EXAMPLE OF POOR AGREEMENT BETWEEN ORIGINAL AND FITTED DISTRIBUTIONS TO A 100 YEAR STOCHASTIC SEQUENCE OF POTENTIAL EVAPOTRANSPIRATION ON WET DAYS

these characteristics are interrelated and their selection should be based on a consistent soil model.

Cross Section Definition

The first part of the simulation consists of developing a model for the cross section of the highway. This includes the characteristics of the pavement itself, of the moisture barrier, and the crack fabric within the subbase soils. The cross section model only contemplates one half of the pavement surface split alongside the centerline of the highway. A typical cross section is shown in Figure 24.

The surface of the subbase is considered to be horizontal. The program starts by fitting the series of soil blocks specified by the user from the subgrade surface down to the depth of the cracks in the soil region underneath the pavement. This is the region labelled "Pavement" and "Edge" in Figure 24. In the region labelled "Uncovered" in Figure 24, the program places the blocks starting at the same elevation. In this soil region and above the subgrade elevation, the program considers the soil divided in equal blocks identical in size and properties to those of the first block below the surface of the subgrade.

The program allows the user to define the width of the pavement surface, the distance from the edge of the pavement to the drainage ditch, and the distance from the ditch to the boundary of the region considered by the analysis. The user can also specify the slope of the pavement surface and the three slopes indicated in Figure 24 on the "Uncovered" ground surface adjacent to the pavement.

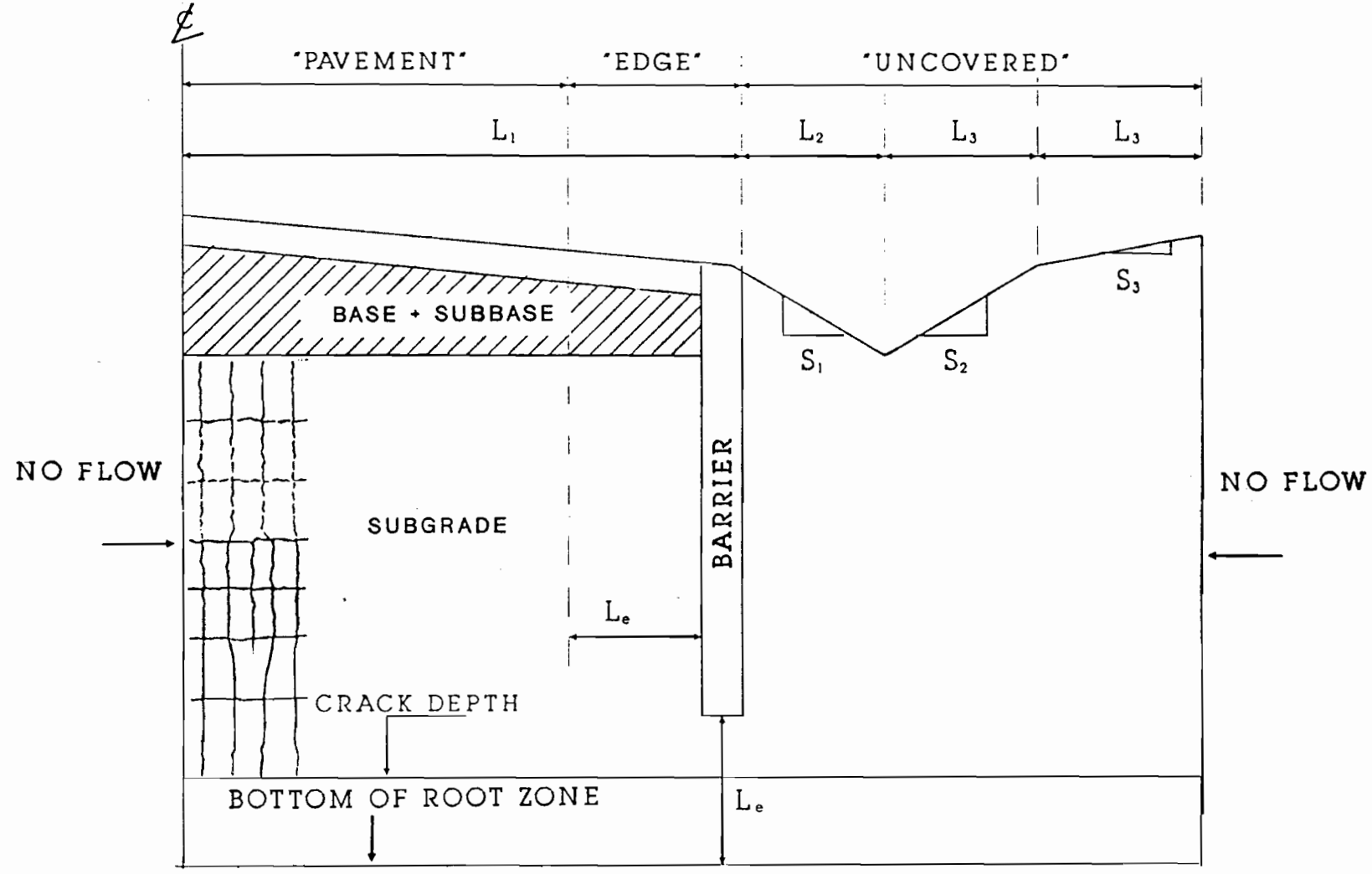

FIGURE 24 MAIN FEATURES OF HIGHWAY CROSS SECTION

The user can specify the thickness of the base and the depth and width of the vertical moisture barrier. The user can also specify the rooting depth of the roadside vegetation. This depth will be in general equal or larger than the initial depth of the shrinkage cracks. Based on the relative depth of the barrier and the roadside vegetation, the program divides the cross section into three zones; "Pavement", "Edge", and "Uncovered" soil as indicated in Figure 24. The width of the "Edge" zone is selected to be equal to the distance from the tip of the barrier to the bottom of the root zone of the roadside vegetation. The program considers that the roadside vegetation can develop roots within this zone and thus evapotranspiration can remove soil water from the cracks and the soil blocks within this region.

Shrinkage Crack Fabric

The program defines the crack fabric at the beginning of the simulation based on a list of block sizes input by the user. Morphological observations [10] in dry clayey soils indicates that the soil mass is divided into parallelepipeds of increasing sizes with depth. Figure 25 shows some of the block sizes identified for several soil conditions. To the authors knowledge, this type of information is not available for typical Texas soils. Hence this four block size sets have been included in the program as default values.

From the block size list, the program starts to fit blocks in the subgrade soils, under the barrier, if applicable, and within the soil mass in the region "Uncovered". The next step is to shrink the soil blocks according to the initial conditions (i.e. initial suction). An example of a cross section fitted with a sequence of blocks is presented in Figure 26. The computer program, during the simulation

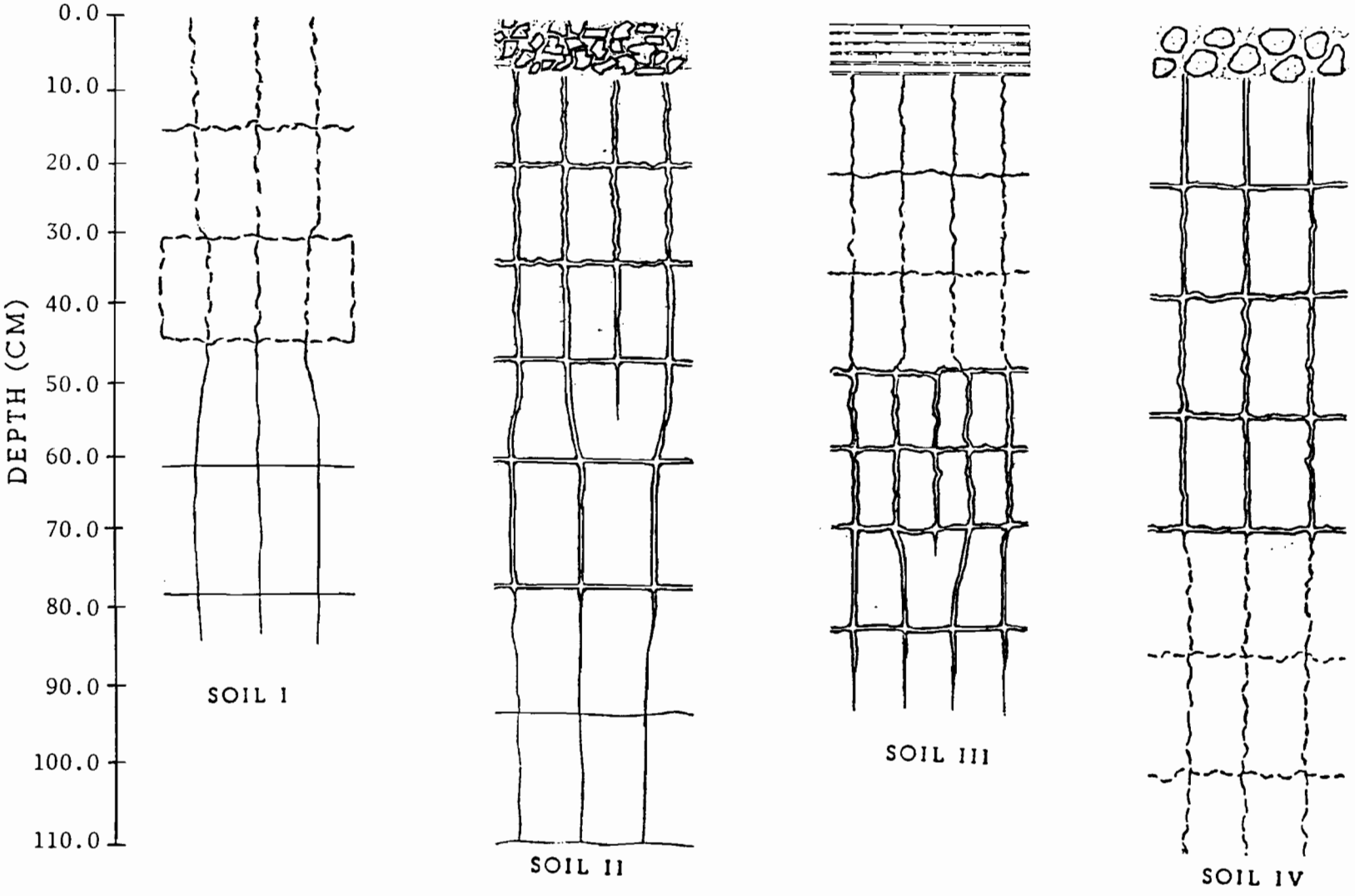

FIGURE 25 SOIL BLOCK SIZES FOR SEVERAL DIFFERENT SOILS (REDRAWN FROM REFERENCE [10])

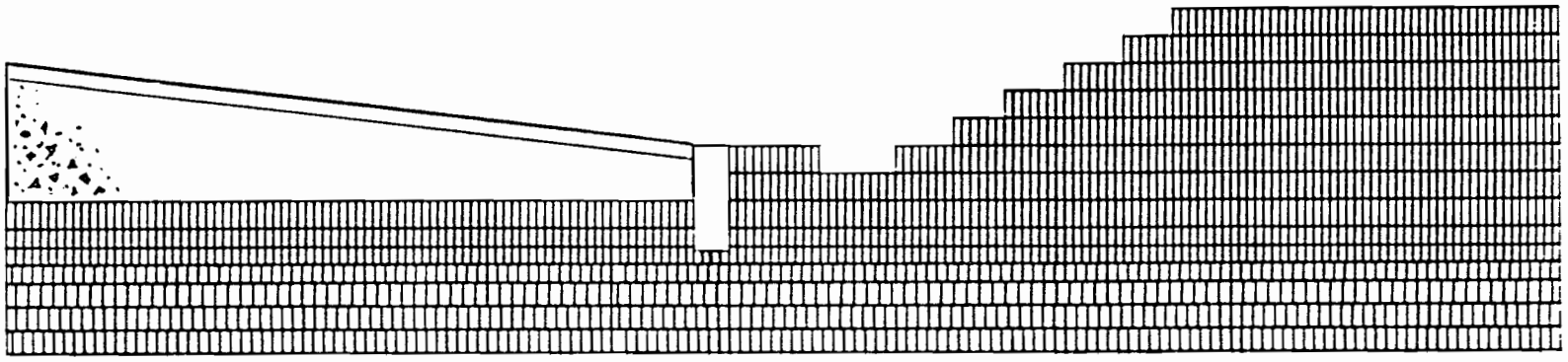

FIGURE 26 EXAMPLE OF THE CROSS SECTION WITH SOIL BLOCKS

keeps track of the position of the center of each block, and the sizes of the block. Based on the relative positions of all blocks and their sizes the program calculates the volume of cracks available for storage of rainfall.

Initial Subsurface Conditions

The program allows the user to define the soil properties making up each block. Thus, it is possible to define as many soil layers as block sizes are included in the set of soil blocks. Then, several alternatives are available to input the required soil properties. The program does not check for consistency of the input properties; therefore, the user needs to make sure that all soil properties are consistent.

In outline, it is necessary to describe the initial state of the subsurface soils and the flow properties of each soil block. The initial state of the subgrade can be described by a shrinkage profile with depth. Typical shrinkage profiles in swelling soils of the Sudan [9] have been included as default values in the computer program. Another alternative offered to the user is to calculate the linear shrinkage profile from the initial suction profile. In this last case, it is necessary to provide the swelling (γ_h) and compressibility (γ_σ) coefficients of the soil for each block. Then the linear shrinkage for each block is taken to be one third of the volumetric strain calculated from the following relationship [27]:

$$\frac{\Delta V}{V} = - \gamma_h \log_{10} (h_f/h_s) - \gamma_\sigma \cdot \log_{10} (\sigma_f/\sigma_t)$$

where: h_f is the initial soil suction,

h_s is the wettest field condition possible normally taken to be 1000 cm of water,

γ_h is the swelling coefficient,

γ_σ is the compressibility coefficient,

σ_f is the applied octahedral normal stress, and

σ_t is a threshold octahedral normal stress below which the stress does not restrict volume changes.

The two coefficients γ_h and γ_σ have to be selected in agreement with the specific moisture capacity discussed later.

This is necessary because two alternative methods of calculating volume changes are used. It has been shown [25] that clayey soils remained essentially saturated to very high suctions, such as 100 bar. In this study, the range of suctions of interest expands from field capacity to the wilting point of the vegetation around 15 bar. Thus, it is reasonable to assume that the volume changes that would take place in the soil are identical to the volume of water gained/lost from the soil. This volume of water is controlled by the specific moisture capacity; that is, the slope of the moisture characteristic curve of the soil.

The flow properties of the soil are specified independently for each block. Again two alternatives are offered to the user. The first one is to specify in table form the moisture capacity and permeability for a range of suctions from zero to above 15 bars. The second alternative is to use proposed analytical relationships [26] between the two properties and the soil suctions, such as:

$$K = \frac{A}{1+B \cdot h} + C \qquad \text{and}$$

$$\frac{dh}{d\theta} = D + E \cdot h$$

where: K is the permeability coefficient,

h is the suction (in cm of water),

θ is the volumetric moisture content, and

A,B,C,D & E are constants characteristic of the soil.

Other properties required for each block are the unit weight and the initial suction at the beginning of the simulation.

Pavement Surface Conditions

The program estimates the fraction of rainfall depth infiltrating through the pavement with the same procedure outlined in reference [27]. This procedure allows two alternative ways to estimate the infiltration rate through the pavement surface depending on the information available. When there is no information about the type of pavement or the length of cracks and joints on the pavement surface, the infiltration is estimated based on the worst possible case of several published cases [28]. If the pavement surface conditions are known, then the infiltration through the pavement surface is determined based on the pavement type and the length of cracks and joints as proposed in reference [29].

Roadside Vegetation

The native vegetation growing along the roadside provides the most effective mechanism to remove soil-water from the soil mass within the

rooting depth of the vegetation. The amount of water removed by the plants is determined by the stress imposed on the plants by the environmental conditions and to some degree it depends on the exposure of the plants to the environment. This exposure is measured [19] by the leaf area index "LAI". This index measures the leaf surface area exposed per unit of ground surface area.

The taller the vegetation, the larger is the leaf area index. The mowing of roadside grasses is a common practice. The results of mowing is a large decrease of the "LAI", which implies a a reduced exposure of the vegetation to the environment and, thus, reduces the water removal from the soil mass. The computer program allows the user to specify a sequence of Leaf Area Indeces throughout the year and also includes a default sequence with "LAI" ranging from 1.0 to 2.5. The LAI's are assumed to increase linearly between consecutive mowings. This sequence includes three general mowings on days 150, 260, and 330. The computer program uses this sequence to estimate the actual evapotranspiration from the potential evapotranspiration as discussed later in this report.

SIMULATION SEQUENCE

General

The main tasks and decisions performed by the computer program are summarized in Figure 27. The first task performed is reading the pavement and subsurface site conditions. The second task is to read or develop the distribution of rainfall depth and potential evapotranspiration. The last step before the simulation starts is the development of master block curves for each soil block relating the

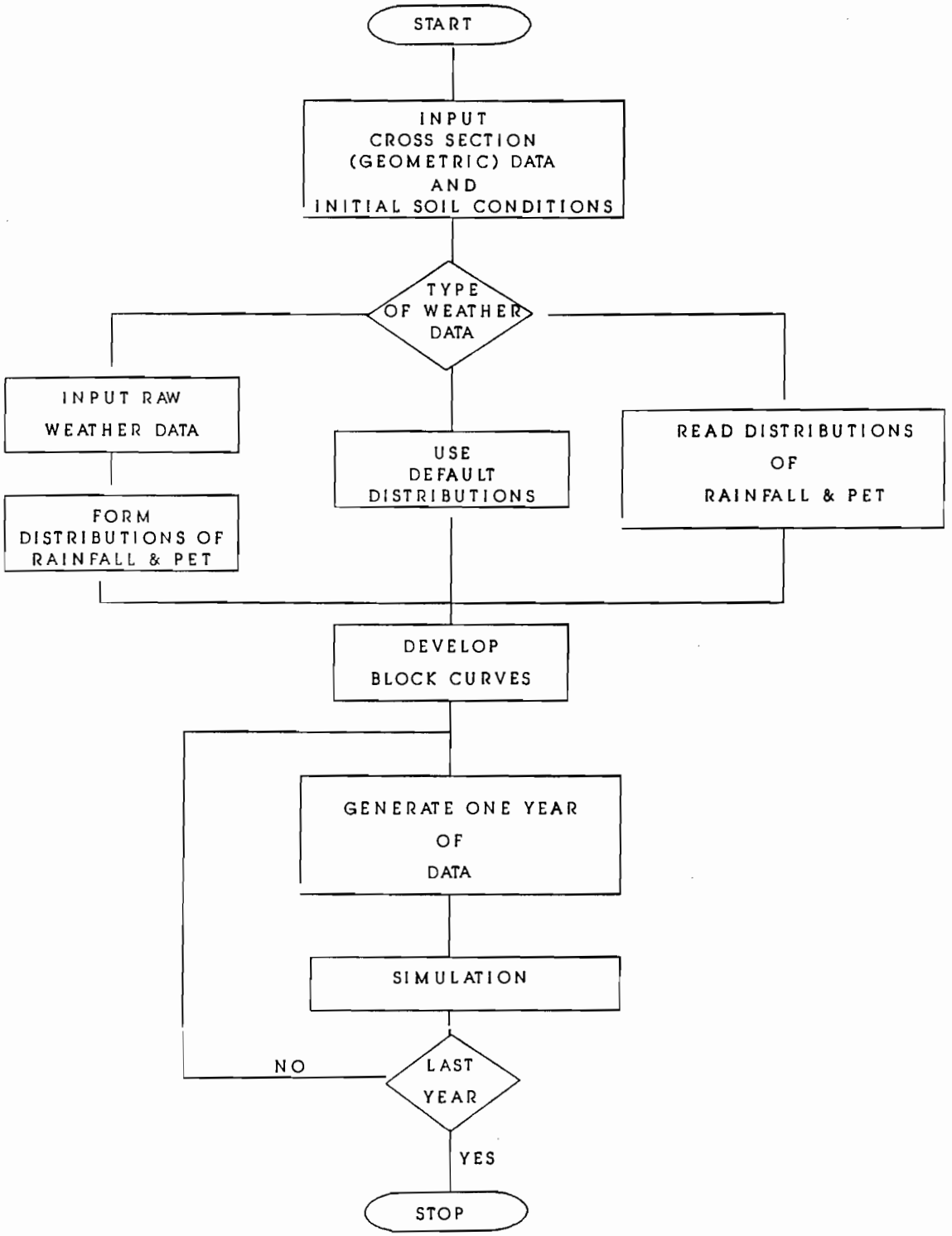

FIGURE 27 FLOWCHART OF COMPUTER PROGRAM

volume of water absorbed per day that the block is submerged under water.

The simulation itself is performed one year at a time. The first step is to generate stochastically a 365 days sequence of daily rainfall and daily potential evapotranspiration. At this point, the program initiates the simulation itself. A summary of the main tasks and decisions performed by the computer program during the simulation are presented as a flowchart in Figure 28. The rest of this section describes in more detail how the computer implements these tasks.

Development of Block Curves

One of the main assumptions behind this study is that rain water is quite mobile within the crack fabric; but when the water is absorbed by the soil blocks, the water is effectively immobilized in the blocks, unless it can be removed by the roots of the roadside vegetation. The program attempts to approximate the rate of absorption of water by the soil blocks with a master curve developed for each block size and soil type.

The master curve for each block is derived by modeling a one-dimensional unsaturated water flow within the soil block. The soil within a block is assumed to be at a constant suction initially. The water flow is assumed to take place along the shortest length of the soil block. The full master curve is developed in two steps: a wetting and a drying phase.

In the wetting phase the soil block is subjected to a zero suction at the two exposed faces. For every time step, the volume of water flowing into the block is calculated for both exposed faces. The volume of water absorbed by the block is assumed to be equal to the

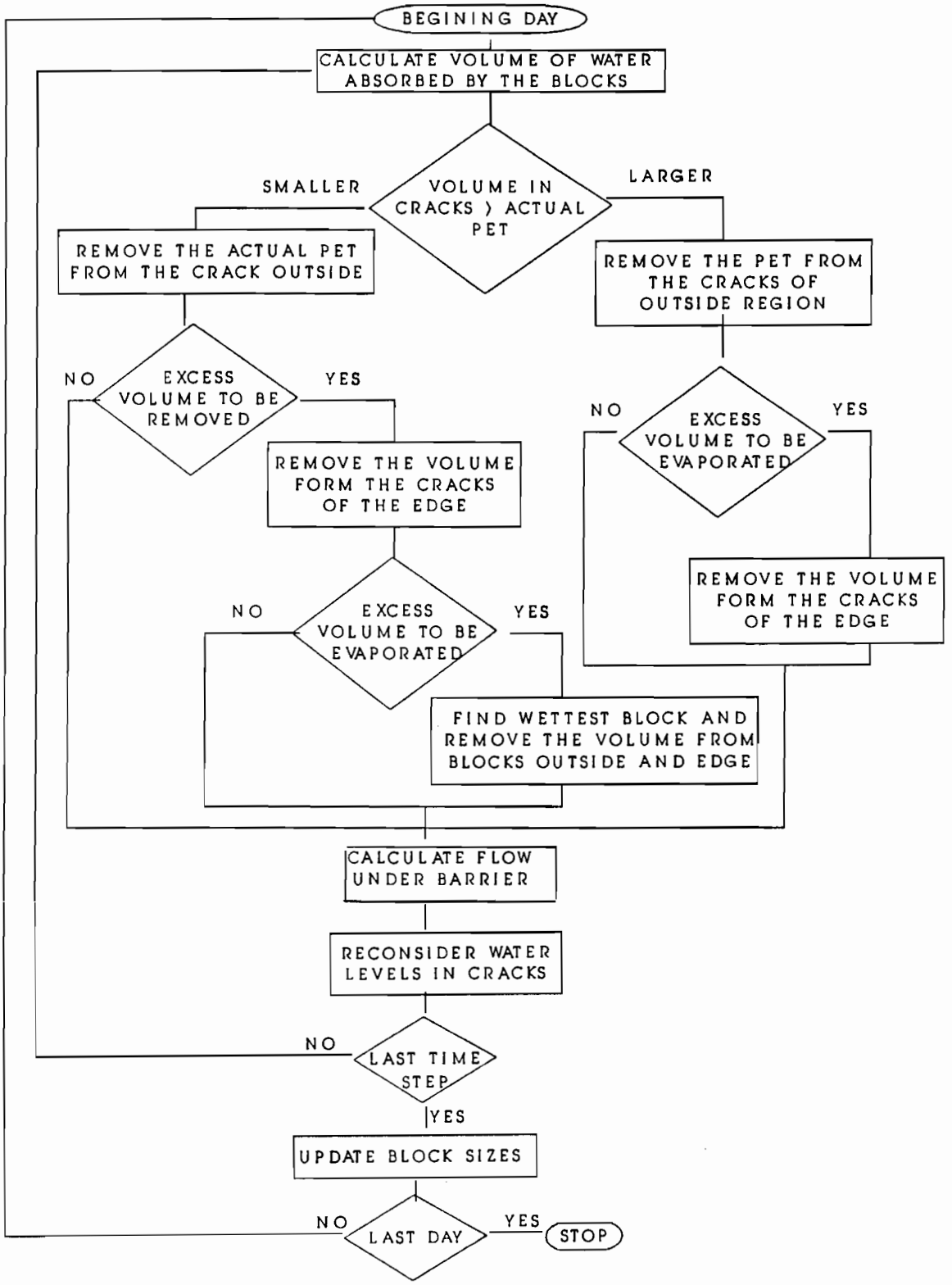

FIGURE 28 FLOWCHART OF THE SIMULATION SEQUENCE

volume heaved by the block; thus allowing to calculate the variation of the block's volume with time.

In the drying phase, the block at the same initial suction is exposed to a soil suction of 15 bars and the program calculates the volume of water extracted from the block at each time step. Again, the volume change of the block is assumed to be equal to the volume of water lost through both exposed faces. The simulation proceeds until the flow rate (intake on release) at the two exposed surfaces is smaller than 0.01 cm^3/day.

The results of the two phases are incorporated into a single master curve for each block. Examples of master curves for several block sizes are shown in Figure 29. These curves are used during the simulation to determine the rate of transfer of water from the crack fabric into the blocks and/or the change in sizes of the soil blocks upon absorbing or releasing soil water.

Rainfall Depth Assignment

The rainfall depth on the pavement surface of the highway section is split into two fractions. The first fraction corresponds to the infiltration through cracks and fissures of the pavement. The remaining rainfall is assigned to run off to the side drainage ditch.

The infiltration through the pavement is added to the water stored in crack fabric beneath the pavement. If the crack fabric within the subsoil and the base material fills with water, the remaining rainfall is assigned to run off to the side drainage ditch.

The infiltration into the soil adjacent to the pavement is the result of direct rainfall in the area plus the run off coming from the pavement surface. The run off from the pavement surface is multiplied

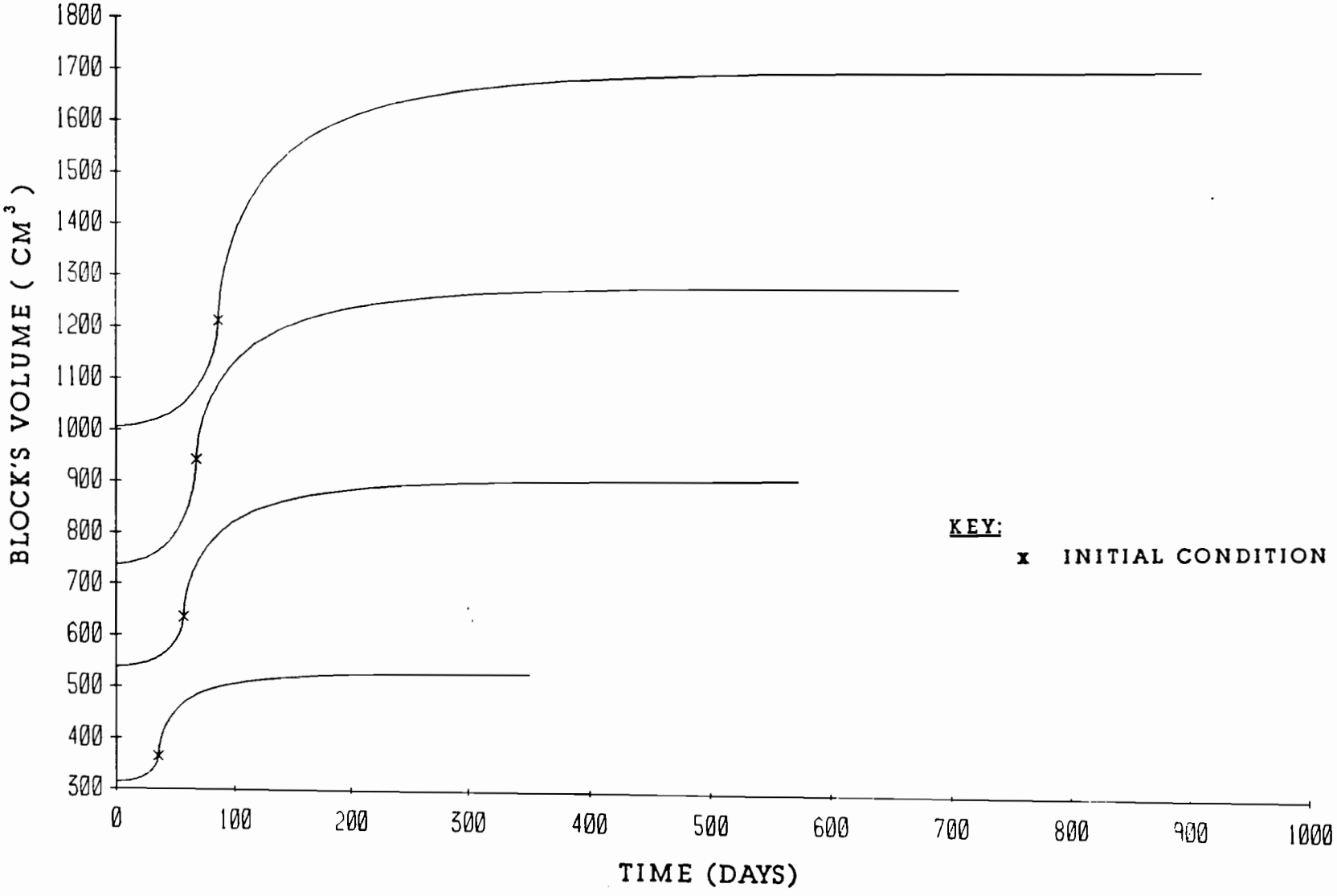

FIGURE 29 EXAMPLES OF MASTER BLOCK CURVES FOR SEVERAL BLOCK SIZES

times a factor, input by the user, to account for run off coming from higher areas of the pavement and drainage ditch.

The infiltration into these soils is also assumed to go straight to replenish the water within the crack fabric. The user can input a maximum depth of water that the program allows to accumulate within the drainage ditch. If the water level within the crack fabric accumulates to this limit, the rest of infiltration is lost.

The combined possibilities offered to the user by the depth of water ponding within the drainage ditch and the factor that multiplies the run off from the pavement cover all possible cases of drainage conditions for the section under study.

Moisture Removal Assignment

The actual removal of water from the soil mass is the result of the potential evapotranspiration and the amount of soil-water stored in the soil profile. To assign the removal of soil-water, the program first has to determine the "actual" evapotranspiration. After the "actual" evapotranspiration is known, it is necessary to assign the location from where the soil moisture will be removed: from the cracks, or the soil blocks.

Actual Evapotranspiration. The program estimates the actual evapotranspiration using a simplified procedure [30] verified for the climatic conditions of Central Texas. This procedure keeps track of the amount of water stored in the soil mass and the actual evapotranspiration is calculated based on the storage of soil-water available and the demand imposed by the potential evapotranspiration.

The total storage possible in the soil is calculated by the program from the set of blocks specified by the user and the difference

in soil-water stored within each block from field capacity to the wilting point of the vegetation (15 bar suction). The program calculates the volume of soil water stored on a daily basis. The gains are the rainfall depth plus the run off from the pavement and the loss is the actual evapotranspiration.

The program splits the potential evapotranspiration into potential soil evaporation and plant transpiration based on the Leaf Area Index "LAI". The effect of the stage of drying is then evaluated independently for the two components.

Soil evaporation is evaluated based on the matrix properties of the soil summarized in a parameter "α". The program allows the user to input this value or to select a value from a set of four default values that cover the range of most cases to be encountered.

Plant transpiration passes through several stages, but in all cases the actual plant transpiration is estimated based on the "LAI" and the monthly average of actual evapotranspiration.

After the two components have been evaluated, are added together to determine the actual evapotranspiration. The computer program considers that evapotranspiration occurs at a constant rate during 12 hours every day. The rate at which the water is pulled out of the soil is the actual evapotranspiration water depth divided into the 12 hours.

Subsurface Soil Regions. After the actual evapotranspiration is known the program has to assign from where the water has to be removed. The first choice is whether the water has to be removed from the cracks or from inside the soil blocks.

A second choice has to be performed; this refers to whether the water should come from the soil mass adjacent to the pavement or from the soil mass under the pavement. The evaporation from the soil

surface can only take place at the "Uncovered" soil surface outside the pavement area. However, plant transpiration removes water from the soil inside the root depth of the vegetation. Thus, if the vegetation can spread roots under the pavement the plant transpiration can be supplied by soil-water stored in the soils under the pavement.

For this purpose, the soil mass has been divided into the three regions shown in Figure 24. The soil region "Pavement" is not accessible to the roots of the roadside vegetation and, thus, the computer program assumes that the water absorbed by the soil blocks cannot be removed. This assumption implies that the soil blocks in this region can absorb water and, thus, swell in size; however, there is no mechanism to permit removal of water from these blocks.

The soil under the "Edge" as labelled in Figure 24, is assumed to be accessible to the root system of the roadside side vegetation and, thus, soil-water can also be removed from soil blocks in this region. The computer program allows the user to specify the rooting depth of the vegetation. The program estimates the width of the "Edge" by considering it to be equal to the vertical distance from the tip of the impermeable moisture barrier to the bottom of the rooting depth of the vegetation. Although this region is not accessible for the soil evaporation, the computer program considers that the actual evapotranspiration can remove water from this region with the preferential choices indicated in the remaining of this section.

The third region is the "Uncovered" soil mass adjacent to the pavement. This soil is the most exposed and thus the program assumes that the soil-water can be removed from this region by the two mechanisms: soil evapotranspiration and the plant transpiration.

In summary, the actual evapotranspiration is removed from the soil mass under the "Edge" and the "Uncovered" soil mass adjacent to the pavement. Therefore, the soil blocks in these two regions can experience swelling and shrinking, which implies that the cracks will close during wet periods but will open again during consistently dry periods. This is in contrast to what will happen to the cracks in the "Pavement" region that are only allowed to close.

The rooting depth of the roadside vegetation has a large influence because the shrinking under the "Edge" will open cracks allowing rainfall water to bypass the barrier, if the barrier did not extend to the rooting depth of the roadside vegetation.

Most commonly, the roadside vegetation are grasses. There is a wealth of information [16] indicating that grasses have maximum rooting depths of 8 ft to 9 ft. However, when shrubs or trees grow in the vicinity of the pavement, much larger rooting depths should be expected.

Removal of Soil-Water from Cracks. The soil-water stored in the cracks is free water and is, thus, the water that requires the least amount of energy to be absorbed by the rooting system of the vegetation. Therefore, the computer program first tries to take all the actual evapotranspiration from water stored in the cracks. When the cracks do not hold enough water to satisfy all the actual evapotranspiration, the remaining is taken from the soil blocks in the "Edge" and "Uncovered" regions.

The water stored in the crack fabric of the soils within the "Uncovered" region is the first source of water. The water in the crack fabric in the "Edge" region is the next source, after the "Uncovered" soil region has been depleted of water in the cracks.

Removal of Soil-Water from Soil Blocks. When the water in the crack fabric has been depleted, the actual evapotranspiration is taken from the soil blocks. At this time, it is necessary to select the soil block or blocks from which the water has to be removed. The vegetation will remove the water from the blocks that require the minimum amount of energy to be spent to remove the water and transport it to the leaves. In this sense, the plants will go to the wettest block closest to the soil surface.

This has been approximated by neglecting the transport component, since it will only have a minimal influence. Thus, the program removes the water from the soil block that is under the wettest conditions. The decision of which block is the wettest block is based on the position of the actual block state along the master block curve. The blocks included in this search are the soil blocks located in the "Edge" and "Uncovered" regions.

The selection of the wettest block is performed with a set of dimensionless master block curves. An example of this set of dimensionless master block curves is presented in Figure 30. The set is formed by plotting percentages instead of actual volumes. Zero percent corresponds to the driest condition at 15 bar and one-hundred percent to the wettest condition. The program considers that the soil block with the highest percentage is the wettest block and it is selected as the source of soil water to satisfy the actual evapotranspiration.

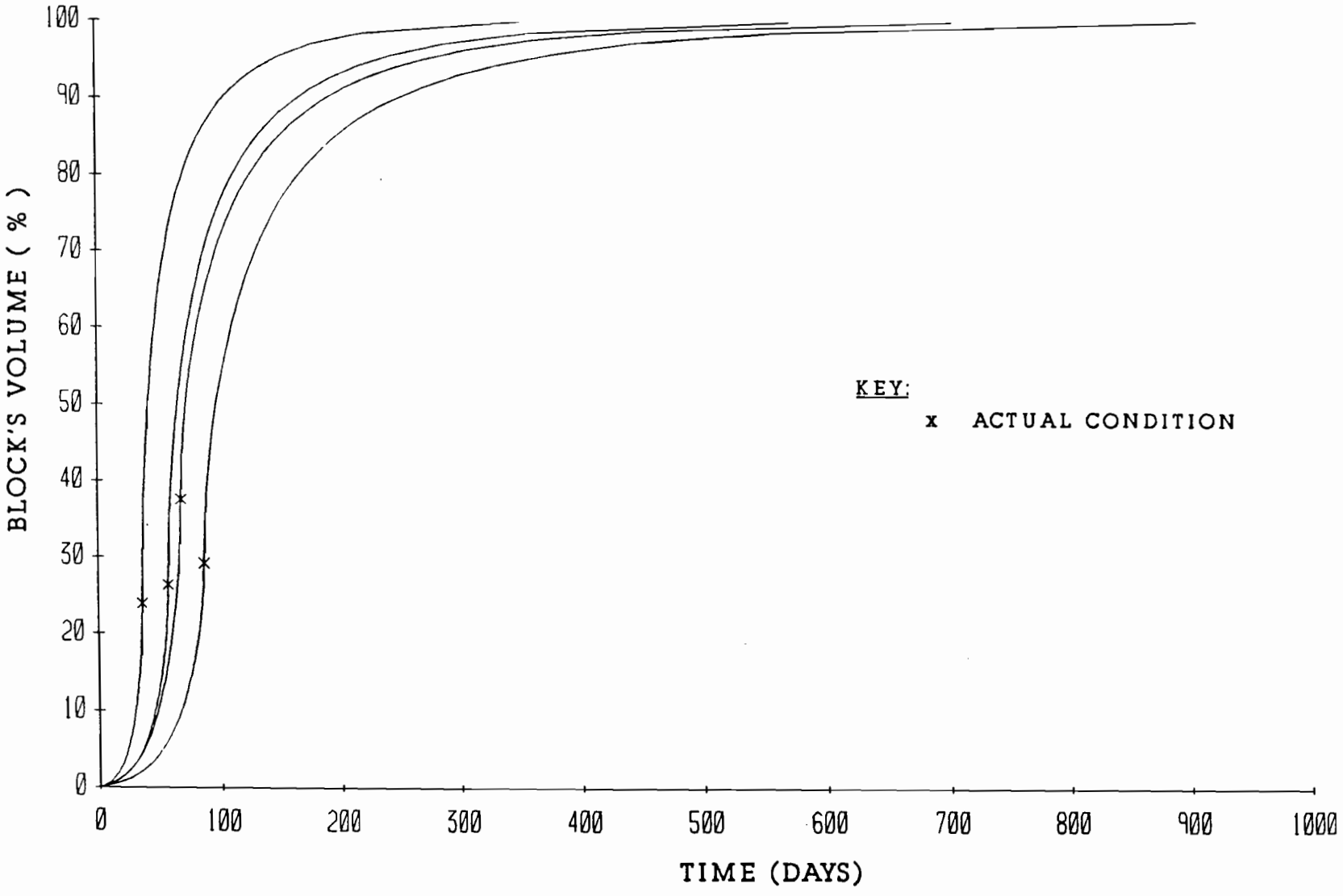

FIGURE 30 EXAMPLES OF MASTER BLOCK CURVES REDUCED TO A COMMON VOLUME SCALE

Block Absorption/Desorption

The program keeps track of three sets of blocks; one on each of the three soil regions: "Pavement", "Edge", and "Uncovered". For each block, the program records at every time step the coordinates of the center of the block, the width, length, and height of the block, the total volume of the block and the relative volume of each block.

The total volume of the soil block at any time indicates the position of the soil block along the master block curve. This position also determines the volume increase of the soil block for any period of time that the soil block is submerged beneath the water level within the crack fabric. This increase is obtained from the master block curve by increasing the time by the step desired and finding the corresponding new volume of the block. When the exposed faces of the soil block are not completely covered by the water within the cracks, the program considers that the fraction of face covered represents the fraction of volume increased by the soil block.

The master block curves were developed imposing zero suction on the exposed faces. However, when the blocks are submerged the water inside the cracks will impose positive pressures on the exposed surfaces; although this positive pressures will be small compared to suction levels dealt with. Thus, the assumption of developing the master block curves imposing zero suction will have a negligible effect on the rate of water uptake by the blocks.

An additional assumption is that the change in volume of the soil block will be equal to the volume of water absorbed or released by the block. This assumption is quite appropriate in light of Holmes [25] measurements and the suction levels of interest.

The rate of desorption of the soil blocks subject to water removal by the root system of the vegetation is determined based on the approximate method described earlier to calculate the actual evapotranspiration. The water removal will cause the blocks to slide down along the master block curve. Upon rewetting the block will start from a lower position along the master block curve.

Crack Fabric

The crack fabric depth is evaluated and tracked by the program within the three soil regions: "Pavement", "Edge", and "Uncovered"; and within the soils just beneath the vertical moisture barrier.

The soils in the first region "Pavement" are only allowed to absorb water and thus cracks will progressively close as rainfall reaches this soil zone and is available for absorption by the blocks. The program keeps track of one set of soil blocks. The changes occurring in this set of blocks times the number of soil blocks fitted within the region are used to calculate crack opening changes within the region.

The soils within the second and third soil regions are subject to drying by the root system of the vegetation. Thus the crack depth in these zones is subjected to closing during wet spells and crack opening upon dry spells. The program keeps track of one set of blocks for each region and assumes that the rest of the blocks within each region behave identically to the set of blocks tracked. Thus the changes recorded for the set of block times the number of blocks fitted initially inside the region is used to calculate crack openings within the regions.

The soil region underneath the vertical moisture barrier plays a critical role. Since when the cracks in this soil zone close the moisture transfer from "Uncovered" to the "Edge" or vice-versa is halted.

Water Transfer Underneath the Barrier

The program considers two water levels on either side of the barrier. The transfer of water from one side to the other is assumed to take place through the shrinkage cracks in the soil underneath the vertical moisture barrier. If these cracks close, the program stops all transfer of water between the two sides.

The water transfer when the cracks are opened is impelled by the difference in elevation between the two water levels. The flow of water through the cracks is estimated using Maning's formula and adopting a hydraulic gradient equal to the difference in water levels divided into the horizontal distance between the midpoints of the two regions on either side of the barrier. The hydraulic radius is calculated at every step taking into account the wetted perimeter of all shrinkage crack included in the highway section being analyzed.

Time Step of the Simulation

The computer program selects the time step of the simulation based on the difference in water levels on both sides of the barrier. The shortest time step is one minute and the longest time step is one day. When the cracks are empty the simulation proceeds on a daily basis and the program calculates the water balances once a day.

During rainstorms and when water levels on both sides of the barrier are different by more than 1 cm, the program calculates the

water balances every minute. If after some time the water levels reach the same elevation the program takes the rest of the day as the next time step.

Water Balances

The program enforces two nearly independent water balances: one for the soil region "Uncovered", and the second is for the two soil regions "Edge", and "Pavement". The result is that only two water levels are tracked: one under the pavement and the second within the cracks of the soil adjacent to the pavement.

At every selected time step the computer program considers the initial volume of water stored inside cracks, then adds to it 1) any rainfall assigned for this period, and 2) any volume of water transferred underneath the barrier. Then substracts: 1) the volume water absorbed by all the soil blocks, 2) the volume of water taken by the actual evapotranspiration. Based on the volume absorbed by the soil blocks, the geometry of the crack fabric is reconsidered.

COMPUTER PROGRAM

The computer code has been written in Fortran. The listing of the program, the user's guide and copies of data files for trial runs have been collected in Volume II of this report.

The user's guide is included as Appendix G. An example of the input data required for the weather analysis at a site is included in Appendix H. The output of this weather analysis is presented in Appendix I. An example of the input data for a simulation is included as Appendix J. An example of the output produced for a one year

simulation is included as Appendix K. The complete FORTRAN listing of the computer code is included as Appendix L.

RESULTS OF TRIAL RUNS AND DISCUSSION

General

The computer code has been used in several trial runs to insure that is working properly and to illustrate the effect of some of the parameters on the absorption of rainfall by the subbase soils. The first part consisted of illustrating the analysis of the climatic conditions at a site. This part was performed for the climatic conditions of El Paso.

The simulation was performed for several representative climatic conditions in Texas. Houston's climatic conditions were adopted as an example of the wettest conditions in Texas. El Paso's climatic conditions were taken as an example of the driest condition in Texas. Then the climatic conditions of San Antonio, and Dallas - Fort Worth were used as examples of the predominant weather conditions in Central Texas.

Several extra simulations were performed for the climatic conditions of San Antonio for several different depths of moisture barrier to illustrate the effect that the barrier has on the wetting process of the subgrade soils.

Climatic Conditions Analysis

The first part of the computer program that handles the raw meteorological data to form distributions of rainfall depth and PET has been tried for the climatic conditions of El Paso, Texas. For this

purpose, fourteen years of data (1969-1983) were collected to be used as input data for the program. A list of these data is presented in Appendix H.

The output of the program consists of the parameters of the monthly distributions of rainfall depth, PET on dry days, and PET on wet days. The summary of parameters selected in this run have been assembled by month of the year and are included in Appendix I. Also included in this appendix are plots of the histograms formed and plots of the distributions fitted to those histograms. These plots are not the normal output of the computer program written and they are only included in this report to provide the reader with a graphical representation of the goodness of fit achieved.

Simulation Results for Different Climatic Areas

The first set of simulations was to test the sensitivity of the wetting process of the subbase soils to the climatic conditions. All these runs were performed for the same subsurface soil and pavement conditions. Specifically, an impermeable moisture barrier was installed to an elevation of fifty centimeters for all these runs. The subgrade was placed at elevations 120 cm and the base was 50 cm thick. The period of simulation was five years for the climatic conditions of Houston, Dallas - Fort Worth, and San Antonio; for El Paso the simulation extended over ten years.

The results of the simulation at each site are summarized in a set of four plots per year of the simulation. The first plot shows the daily rainfall for everyday of the year; also included is the rainfall depths infiltrating through the pavement surface, and the infiltration depth into the soils in the "Uncovered" region. The second plot shows

the daily PET and actual ET for every day of the year. The third plot shows the water level elevations within the crack fabric under the "Pavement" and within the crack fabric of the "Uncovered" region for every day of the year. When the cracks are empty of water the water level shown in these figures corresponds to the elevation of the crack tip. The fourth plot shows the elevation of the shrinkage crack tips in the three regions: "Pavement", "Edge", and "Uncovered".

San Antonio. The plots prepared from the results of the simulation for San Antonio, Texas, are included as Appendix A.

The water levels in the crack fabric show a general increasing trend with occasional fluctuations during the first two years. In general, the water level in the "Uncovered" region lags behind the water level within the "Pavement" region. The crack tip elevations show that about 2 months after the beginning of the simulation the cracks under the barrier close, and about 18 months from the beginning, the cracks in the "Pavement" region have closed to the subgrade. During the first two years, all crack tips show a general increasing elevation trend with the cracks in the "Uncovered" region lagging somewhat. After the first two years the cracks in the "Edge" and "Uncovered" regions have closed and show only occasional drops during the summer months.

Houston. The plots obtained from the simulation for Houston, Texas are presented in Appendix B.

The water levels in the crack fabric fill the cracks in about four months and remain full thereafter with the exception of a few short periods when they drop below the subgrade.

In about one month time the cracks under the moisture barrier close and never open again. All the cracks in the three soil zones close to the subgrade in about four month. Thereafter the cracks open annually for periods of one or two months, and then close again for the rest of the year.

Dallas - Fort Worth. The plots obtained from the simulation results for Dallas - Fort Worth are presented in Appendix C.

The water level within the soil underneath the "Pavement" are filled to the top of the subbase in less than one year. The water level within the cracks of the soil in the region "Uncovered" lag slightly behind those under the "Pavement", nevertheless, within the first year also reaches the subgrade elevation. The remaining 4 years of the simulation, the water levels remain very high with small summer drops, below the subgrade elevation, for periods ranging from the 2 to 3 months.

The cracks within the soils under the barrier close within six weeks of the beginning of the simulation. Within about 10 months of the beginning, the cracks of the soil under the "Pavement" have completely closed. The cracks in the regions "Edge" and "Uncovered" also progressively close but lag behind the cracks under the "Pavement". At the beginning of the second year, the cracks in all three regions have closed to the subgrade elevation. Thereafter, the cracks within the "Edge" and "Uncovered" regions remain closed except for summer periods ranging from 4 to 6 months per year.

El Paso. The plots of the simulation results for El Paso's climatic conditions are presented in Appendix D. Due to the extremely dry conditions in El Paso, the simulation was performed for a 10 year series.

The actual evapotranspirations in El Paso are much smaller than the PET and this is strickingly different than for the other regional areas studied. The large strings of asterisks indicating durations of dry periods are clearly evident in the evapotranspirations plots included in Appendix D.

The plots showing the water levels indicate a slow gradual increase for the water in the cracks underneath the "Pavement". Nevertheless, it is necessary to keep in mind that in these plots, the elevation of the water level when the cracks are empty is indicated as the elevation of the crack tip. Thus, some of the rise seen in water level elevation is in fact the result of closing the cracks underneath the pavement. In stark contrast to what happen in the simulations for the other areas, the water levels in the cracks within the "Uncovered" region never accumulate water for more than a few days.

The cracks in the "Uncovered" region never close by any amount; that is, the crack tip never changes during the 10 year simulation. This prediction of the program is in agreement with visual observations by the authors that shrinkage cracks are always open in the El Paso area. Furthermore, it took about three years of simulation to close the cracks within the soil under the moisture barrier.

The cracks, in the soil mass within the "Pavement" region of the pavement, closed gradually, although at a very slow pace. It took about seven years of simulation for these cracks to close to the subgrade elevation. The cracks within the "Edge" region of the pavement also exhibit a slow trend of gradually closing; however, these cracks closed to the subgrade elevation only sporadically.

Effect of Barrier's Depth

Several trial runs were performed to illustrate the effect that a deeper barrier might have on the rate of moisture uptake by the sub-base soils. These runs were performed for identical soil conditions and for the climate conditions of San Antonio, Texas. Two runs for barrier tips at 25 cm and at 0.0 cm elevations were performed. The second of these runs corresponds to the case that the barrier tip reaches the bottom of the initial crack depth. The plots of the results of the simulation for the barrier with the tip at elevations 25 cm are included in Appendix E. The results of the simulation for a barrier with the tip at elevation 0.0 cm are presented in Appendix F.

The results for the barrier with tip at elevation 25 cm indicate that a deeper barrier had the effect of accelerating the changes under the pavement while it retarded the changes outside the pavement. In this sense, the cracks under the pavement closed in one year while for the earlier run it had taken fifty percent more time. By way of contrast, the outside cracks were slower to close by more than half a year.

The same trend is observed for the barrier with the tip at elevation 0.0 cm. The sub-base soils wetted up even faster; in this sense, all the cracks were closed under the pavement in about 8 months. While the cracks outside the pavement did not close during the period of the simulation. The results of these simulations indicate that when the pavement is cracked or fissured, a large fraction of the rainfall is directed towards the sub-base. In this case, the subrade soil gains moisture at a faster rate than the unpaved soils. These results would explain the observed behavior [3] in IH-30 that seemed to be in

conflict with previous observations at other vertical moisture barrier sites [5].

Computer Resources Needed

The trial runs have been performed on a VAX 11/780 computer with 12 megabytes RAM. The CPU time spent on each simulation ranged from 1 hour 30 minutes to more than 5 hours for the five-year simulations. The ten years simulation for el El Paso used more that 3 hr. 15 min. of CPU time. Thus, on the average, 20 minutes of CPU time are required for each year of simulation.

The development of the master block curves for a block sequence of seven different blocks used 20 minutes of CPU time.

SUMMARY AND CONCLUSIONS

A computer program has been assembled to simulate the movement of water under a pavement on a cracked, swelling soil subbase. Specifically, it was desired that the program could account for the infiltration of rainfall through cracks and joints on the pavement surface and the horizontal water flow through the shrinkage crack fabric.

The assumptions have been that the crack fabric displays a simple geometric configuration of superimposed parallelepipeds. The water is assumed to flow through the cracks under positive pressure and then is slowly absorbed by the soil blocks. As the water is absorbed, the blocks swell and the geometry of the crack fabric changes. The water absorbed by the blocks is assumed to be immobilized unless the road side vegetation has stablished roots within the blocks.

Trial runs for some climatic conditions of Texas show a wide range of possible behavior. From the wettest conditions of Houston where the cracks close in a matter of a few months to the driest case studied of El Paso where the cracks remain open during the ten years of simulation.

These results have shown that the shrinkage crack fabric under the pavement steadily close even under the dry conditions of El Paso climate. The wetter the climate, the faster that the cracks close; from a minimum of four months in Houston to a maximum of seven years in El Paso.

Trial runs performed with several moisture barrier depths have shown that if the pavement surface has cracks and joints that allow water infiltration, the moisture barrier can cause faster swelling under the pavement than that for the surrounding soils.

The program requires some information about the sizes of the soil blocks in order to form the shrinkage crack fabric. This data is not readily available in the literature for the typical sub-surface soil conditions in Texas. The usefulness of the program could be increased dramatically if such information would become available.

REFERENCES

1. Velasco, M.O., and R.L. Lytton, 1981, "Pavement Roughness on Expansive Clays," Research Report No. 284-2, Texas Transportation Institute, Texas A&M University, College Station, Texas.

2. Steinberg, M.L., 1980, "Deep Vertical Fabric Moisture Seals," Proceedings, 4th International Conference on Expansive Soils, D. Snethen, Editor, American Society of Civil Engineers.

3. Gay, D.A., and R.L. Lytton, 1988, "Moisture Barrier Effects on Pavement Roughness," in Measured Performance of Shallow Foundations, Geotechnical Special Publication No. 15, American Society of Civil Engineers.

4. Picornell, M., 1985, "The Development of Design Criteria to Select the Depth of a Vertical Moisture Barrier," Dissertation, Submitted to Texas A&M University, College Station.

5. Picornell, M., R.L. Lytton, and M.L. Steinberg, 1983, "Matrix Suction Instrumentation of a Vertical Moisture Barrier," Transportation Research Record 945, Transportation Research Board, National Academy of Sciences, Washington D.D.

6. Kissel, D.E., J.T. Ritchie, and E. Burnett, 1973, "Chloride Movement in Undisturbed Swelling Clay Soil," Proceedings, Soil Science Society of America, Vol. 37, pp. 21-24.

7. Blake, G., E. Schlichting, and U. Zimmermann, 1973, "Water Recharge in a Soil with Shrinkage Cracks," Proceedings, Soil Science Society of America, Vol. 37, pp. 669-672.

8. Johnston, J.R., and H.O. Hill, 1944, "A Study of the Shrinking and Swelling Properties of Rendzina Soils," Proceedings, Soil Science Society of America, Vol. 9, pp. 24-29.

9. El Abedine, A.Z., and G.H. Robinson, 1971, "A Study on Cracking in Some Vertisols of the Sudan," Geoderma, Vol. 5, pp. 229-241.

10. Bouma, J., and L.W. Dekker, 1978, "A Case Study on Infiltration Into Dry Clay Soil. I. Morphological Observations," Geoderma, Vol. 20, pp. 27-40.

11. Barenblatt, G.I., Y.P. Zheltov, and I.N. Kochina, 1960, "Basic Concepts in the Theory of Seepage of Homogeneous Liquids in Fissured Rocks," Prike. Mat. Mekh., Vol. 24, pp. 1286-1303.

12. Richards, B.G., 1968, "A Mathematical Model for Moisture Flow in Horsham Clay," Civil Engineering Transactions, Institution of Engineers, Australia, Vol. CE10, No. 2, pp. 220-224.

13. Ritchie, J.T., and J.E. Adams, 1974, "Field Measurements of Evaporation from Soil Shrinkage Cracks," Soil Science Society of America, Proceedings, Vol. 38, pp. 131-134

14. Williams, A.A.B., and J.T. Pidgeon, 1983, "Evapo-Transpiration and Heaving Clays in South Africa," Geotechnique, Vol. 23, No. 2, pp. 141-150.

15. Richards, B.J., 1967, "Moisture Flow and Equilibria in Unsaturated Soils for Shallow Foundations," Permeability and Capillarity of Soils, ASTM STP 417, pp. 4-34.

16. Picornell, M., and R.L. Lytton, "Behavior and Design of Vertical Moisture Barriers," Transportation Research Record 1137, Transportation Research Board, National Research Council, Washington, D.C., pp. 71-82.

17. Thornthwaite, C.W., 1948, "An Approach Towards a Rational Classification of Climate," Geographical Review 38, pp. 55-94.

18. Penman, H.L, 1948, "Natural Evaporation from Open Water, Bare Soil, and Grass," Proceedings, Royal Society of London, A193, pp. 120-146.

19. Ritchie, J.T., 1972, "A Model for Predicting Evaporation from a Row Crop with Incomplete cover," Water Resources Research, Vol. 8, No. 5, pp. 1204-1213.

20. Greenwood, J.A., and D. Durand, 1960, "Aid for Fitting the Gamma Distribution by Maximum Likelihood," Technometrics 2, pp. 55-65.

21. Bernard, M.M., 1932, "Formulas for Rainfall Intensities of Long Durations," Transactions, ASCE, Vol. 96, pp. 592-624.

22. Hershfield, D.M., 1961, "Rainfall Frequency Atlas of the United States," Technical Paper 40, U.S. Weather Bureau, Washington.

23. Larsen, G.A., and R.B. Pense, 1982, "Stochastic Simulation of Daily Climatic Data for Agronomic Models," Agronomy Journal, vol. 74, pp. 510-514.

24. Picornell, M., and R.L. Lytton, 1984, "Modelling the Heave of Heavily Loaded Foundation," Proceedings, Fifth Inter. Conference on Expansive Soils, Adelaide South Australia, pp. 104-108.

25. Holmes, J.W., 1955, "Water Sorption and Swelling of Clay Blocks," Journal of Soil Science 6, No. 2, pp. 200-208.

26. Richards, B.G., 1974, "Behaviour of Unsaturated Soils," in Soil Mechanics - New Horizons, Ed. i.k. Lee, Newnes - Butterworths Australia, pp. 112-157.

27. Liu, S.J. and R.L. Lytton, 1985, "Environmental Effects on Pavements - Drainage Manual," Report FHWA/RD-84/116, Texas Transportation Institute, Texas A&M University.

28. Dempsey, B.J., and Q.L. Robnett, 1979, "Influence of Precipitation, Joints, and Sealing on Pavements Drainage," Transportation Research Record, 705, National Research Council, Washington, D.C., pp. 13-23.

29. Ridgeway, H.H., 1976, "Infiltration of Water Through the Pavement Surface," Transporation Research Record, 616, National Research Council, Washington, D.C., pp. 98-100.

30. Richardson, C.W., and Ritchie J.T., 1973, "Soil Water Balance for Small Watersheds," Transactions of the American Society of Agricultural Engineers, pp. 72-77.

APPENDIX A

SIMULATION RESULTS FOR SAN ANTONIO

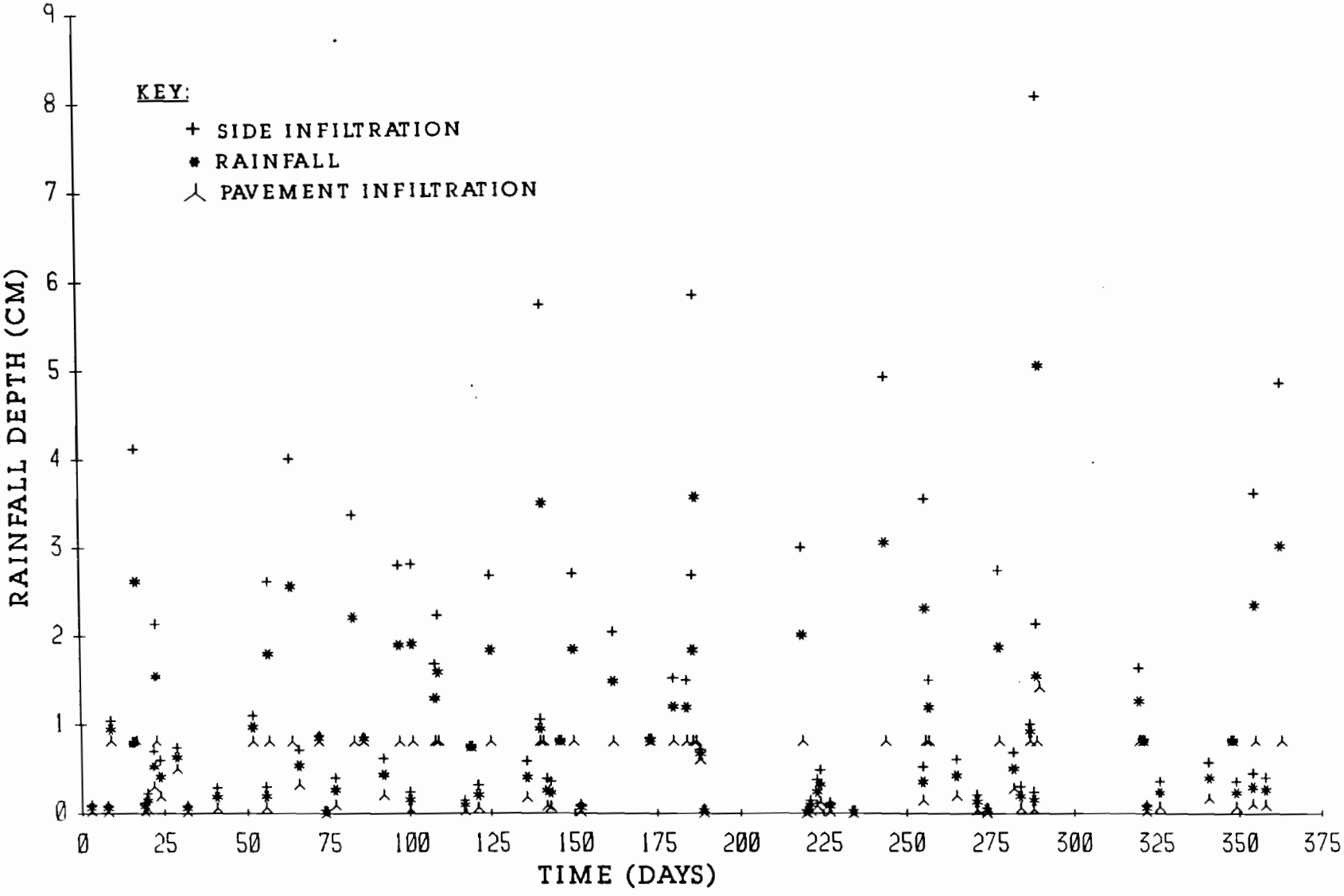

FIGURE A1.1 RAINFALL AND INFILTRATION DEPTHS FOR FIRST YEAR IN SAN ANTONIO

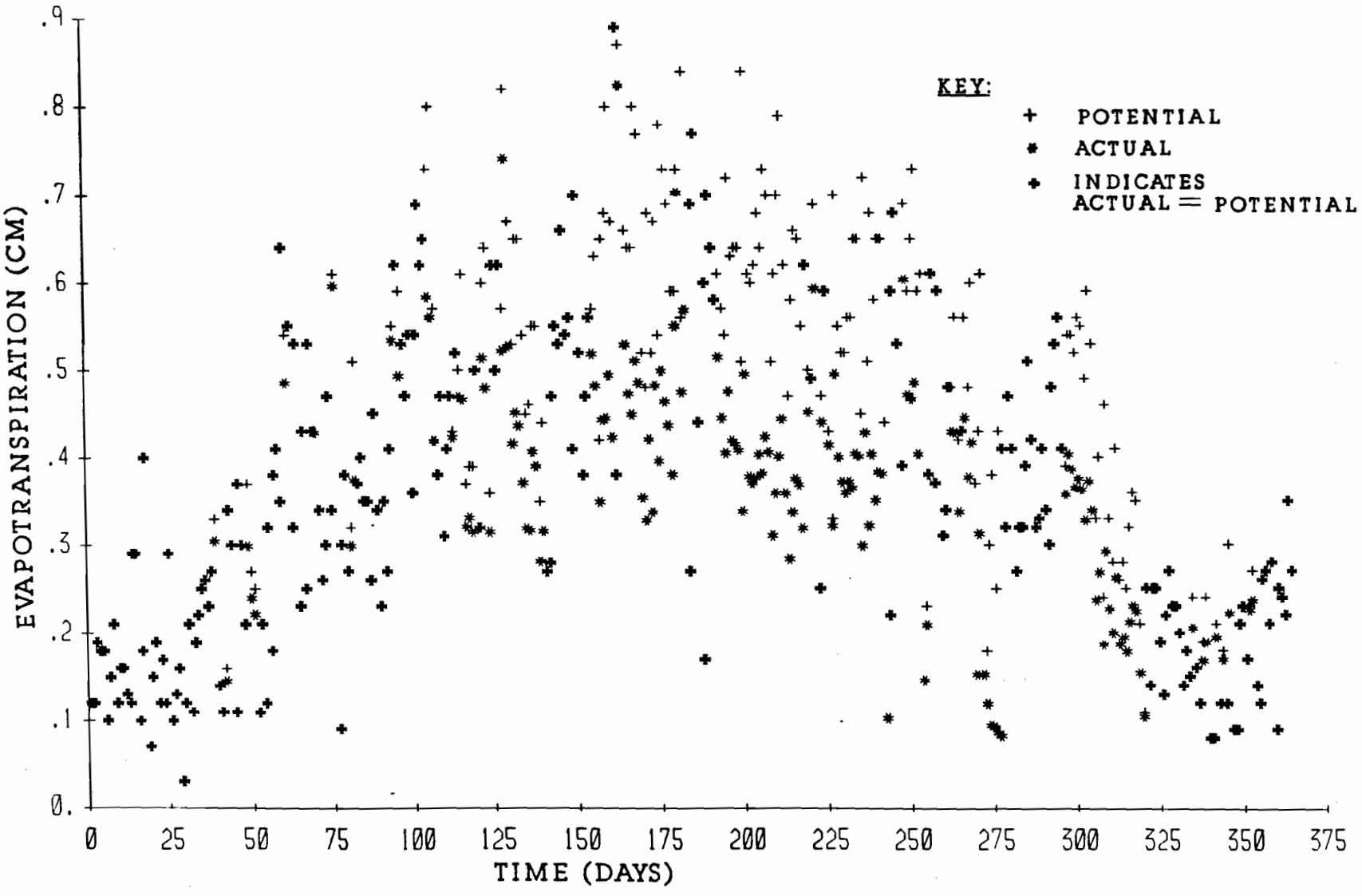

FIGURE A2.1 EVAPOTRANSPIRATION FOR FIRST YEAR IN SAN ANTONIO

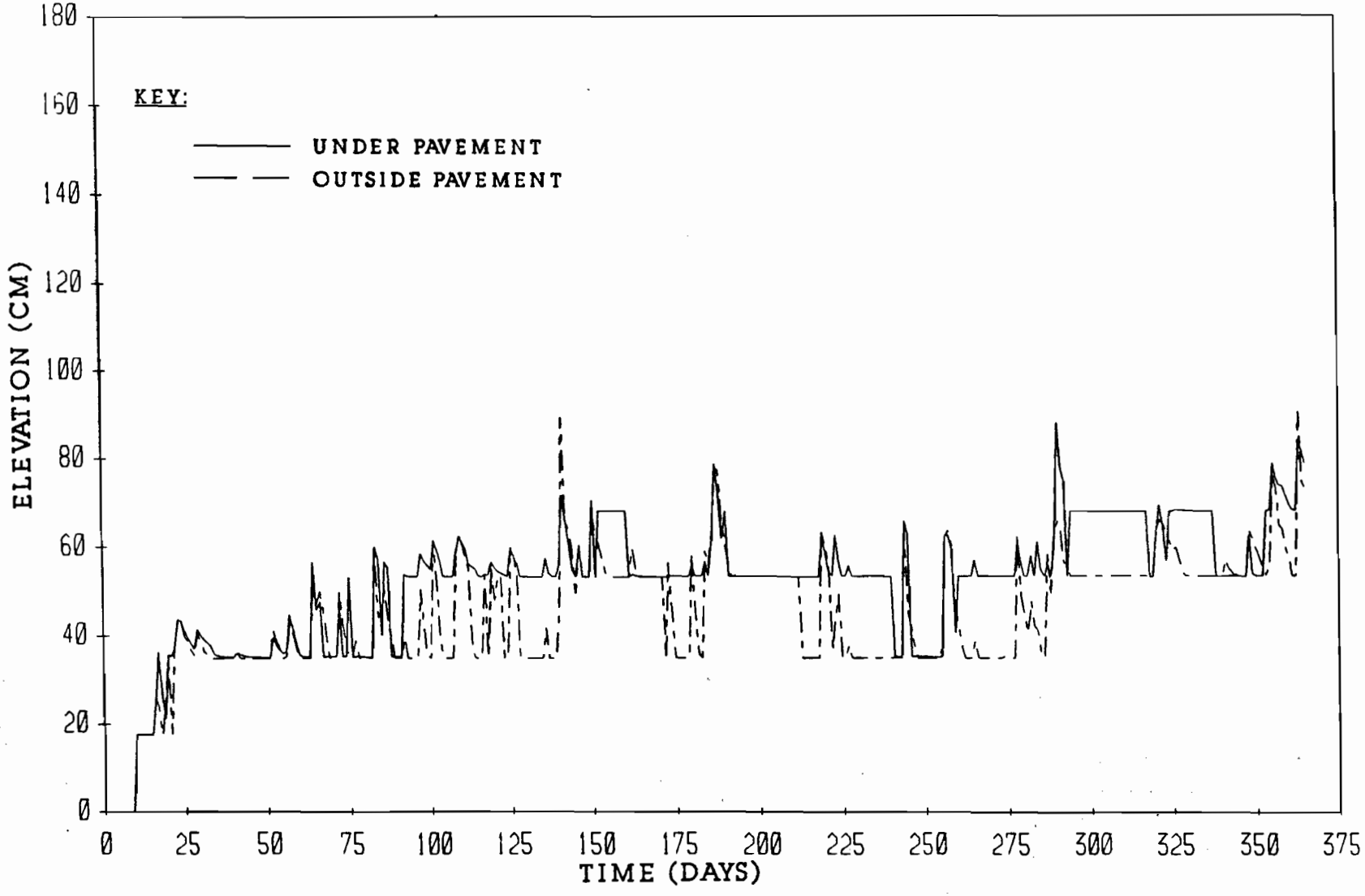

FIGURE A3.1 WATER LEVELS WITHIN THE CRACK FABRIC FOR FIRST YEAR IN SAN ANTONIO

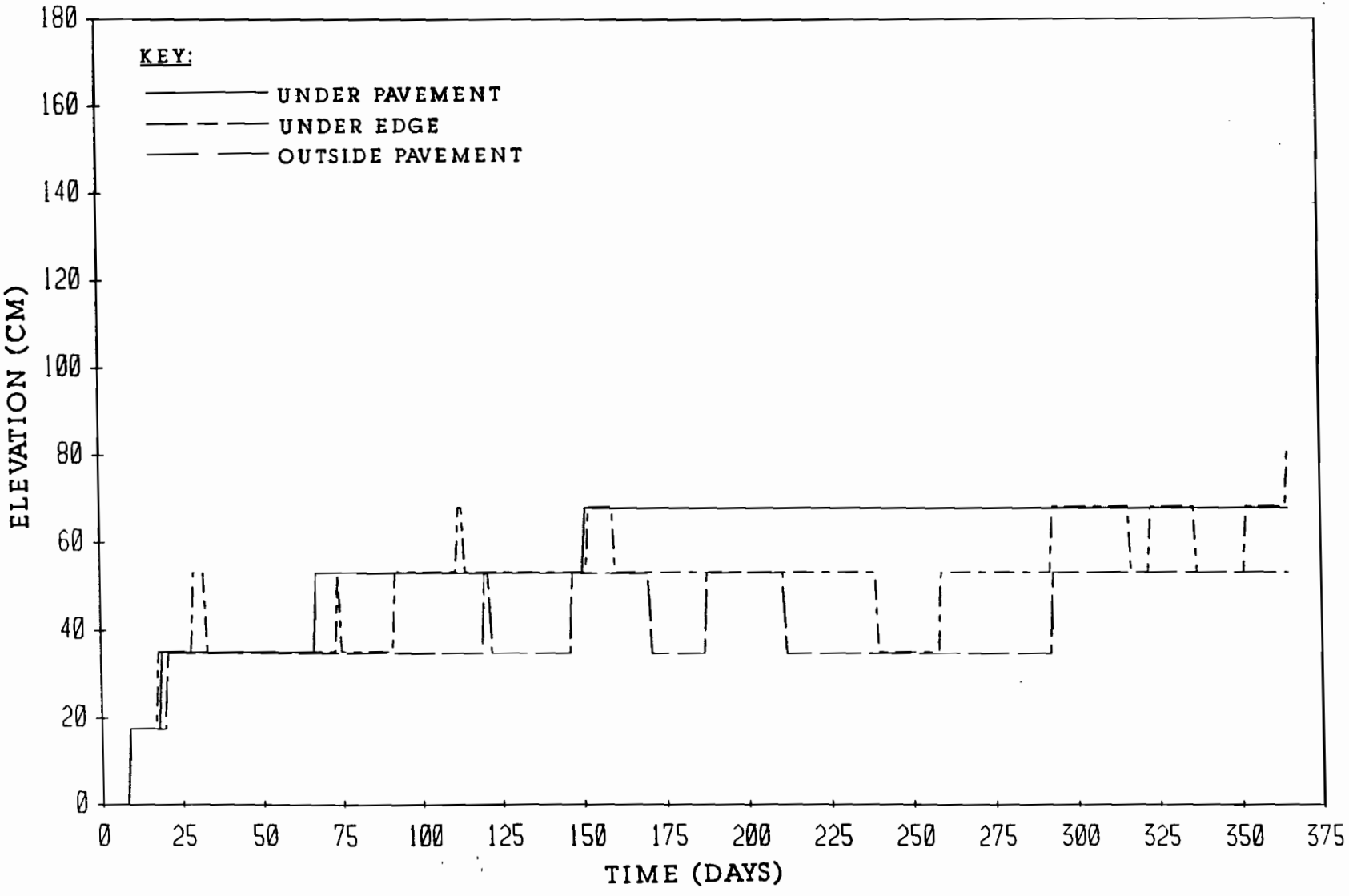

FIGURE A4.1 CRACK TIP ELEVATIONS FOR FIRST YEAR IN SAN ANTONIO

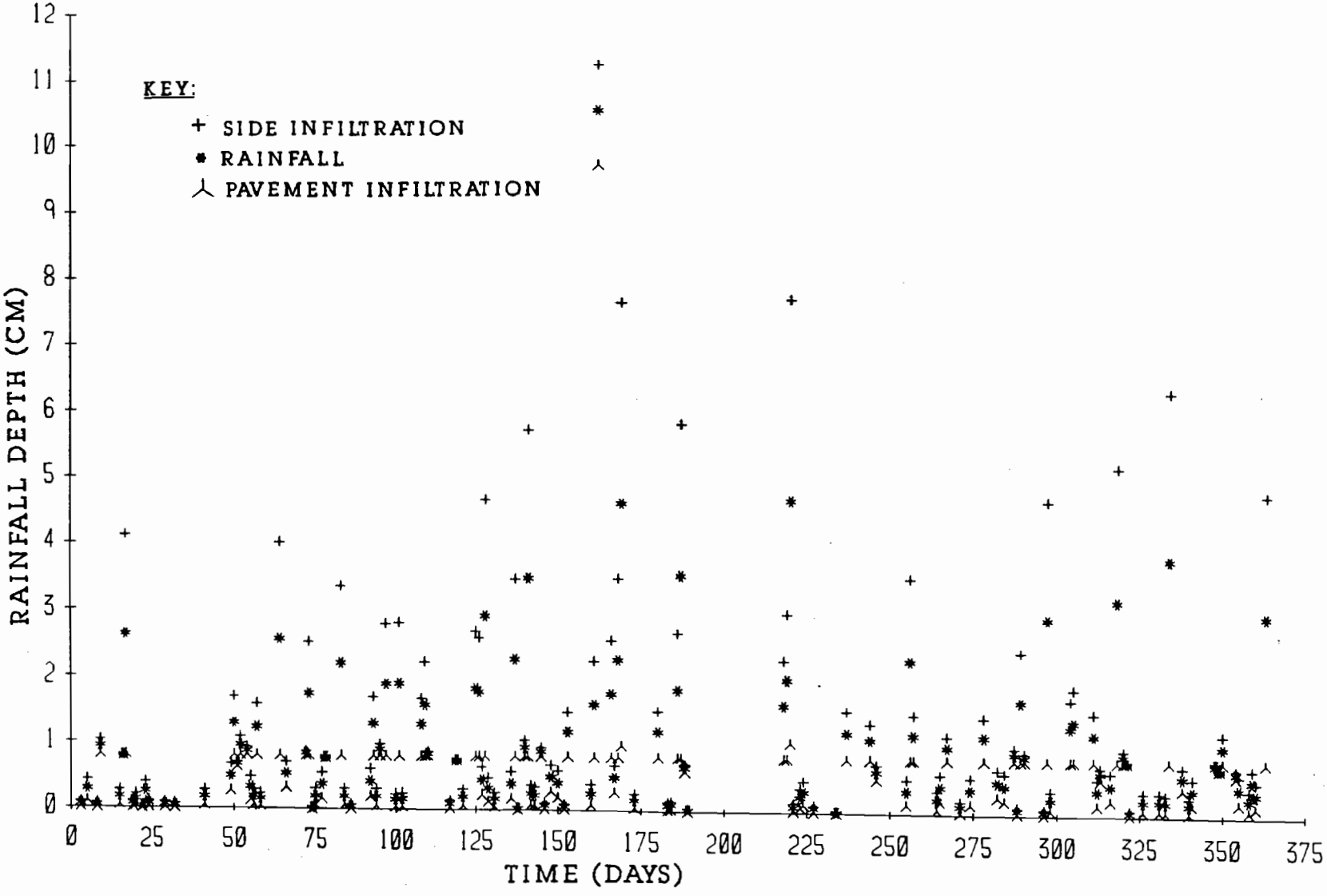

FIGURE A1.2 RAINFALL AND INFILTRATION DEPTHS FOR SECOND YEAR IN SAN ANTONIO

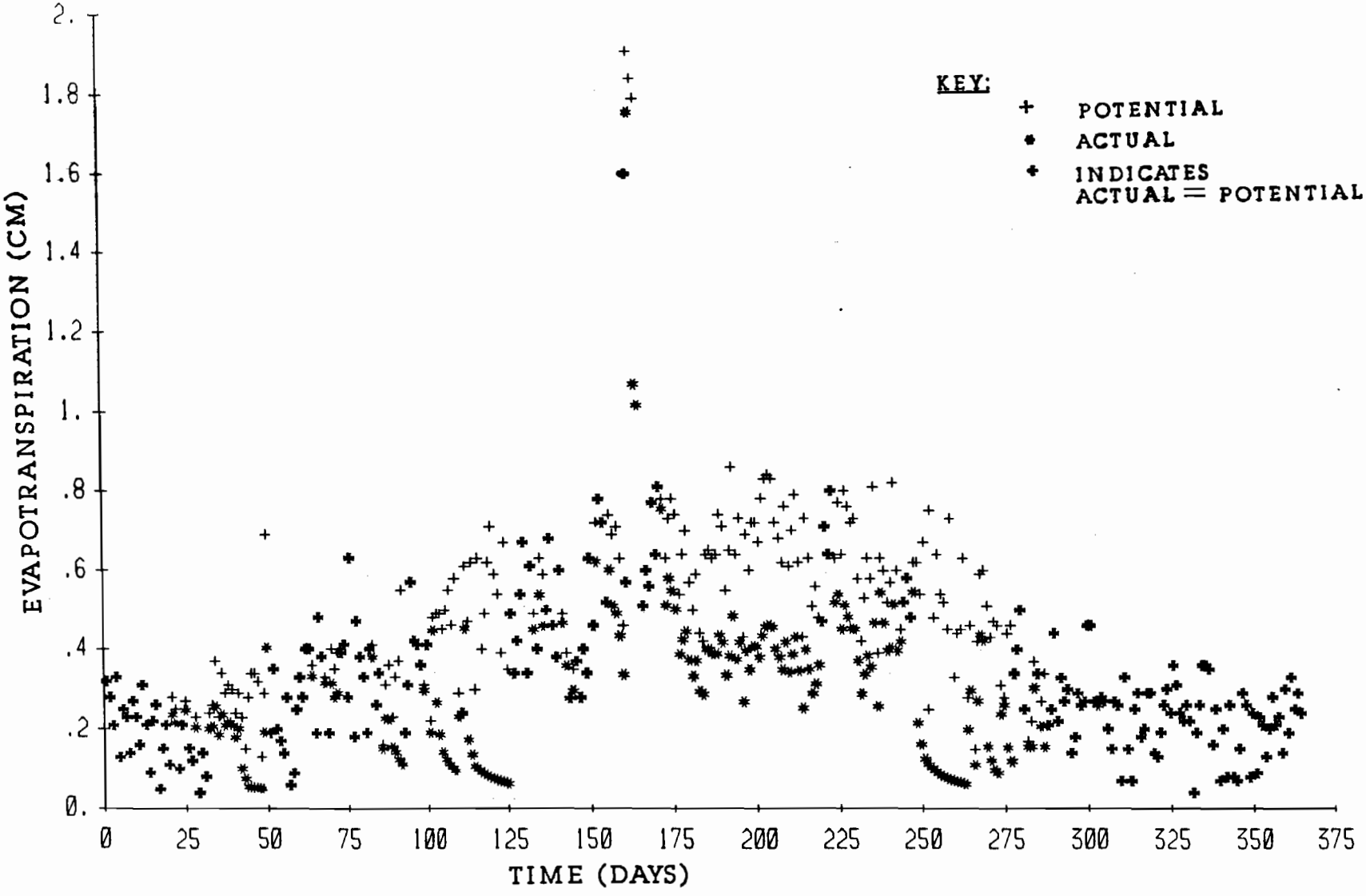

FIGURE A2.2 EVAPOTRANSPIRATION FOR SECOND YEAR IN SAN ANTONIO

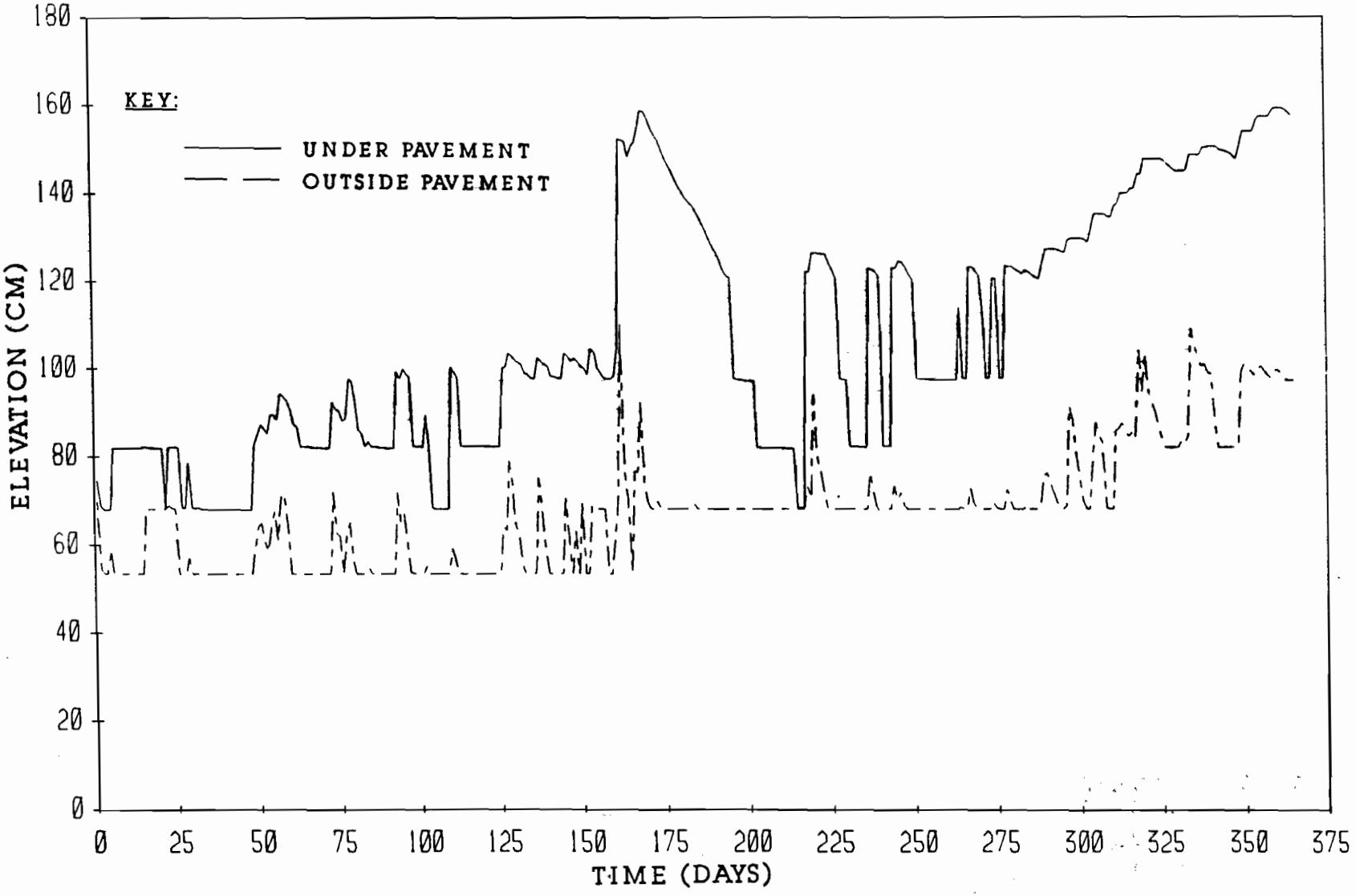

FIGURE A3.2 WATER LEVELS WITHIN THE CRACK FABRIC FOR SECOND YEAR IN SAN ANTONIO

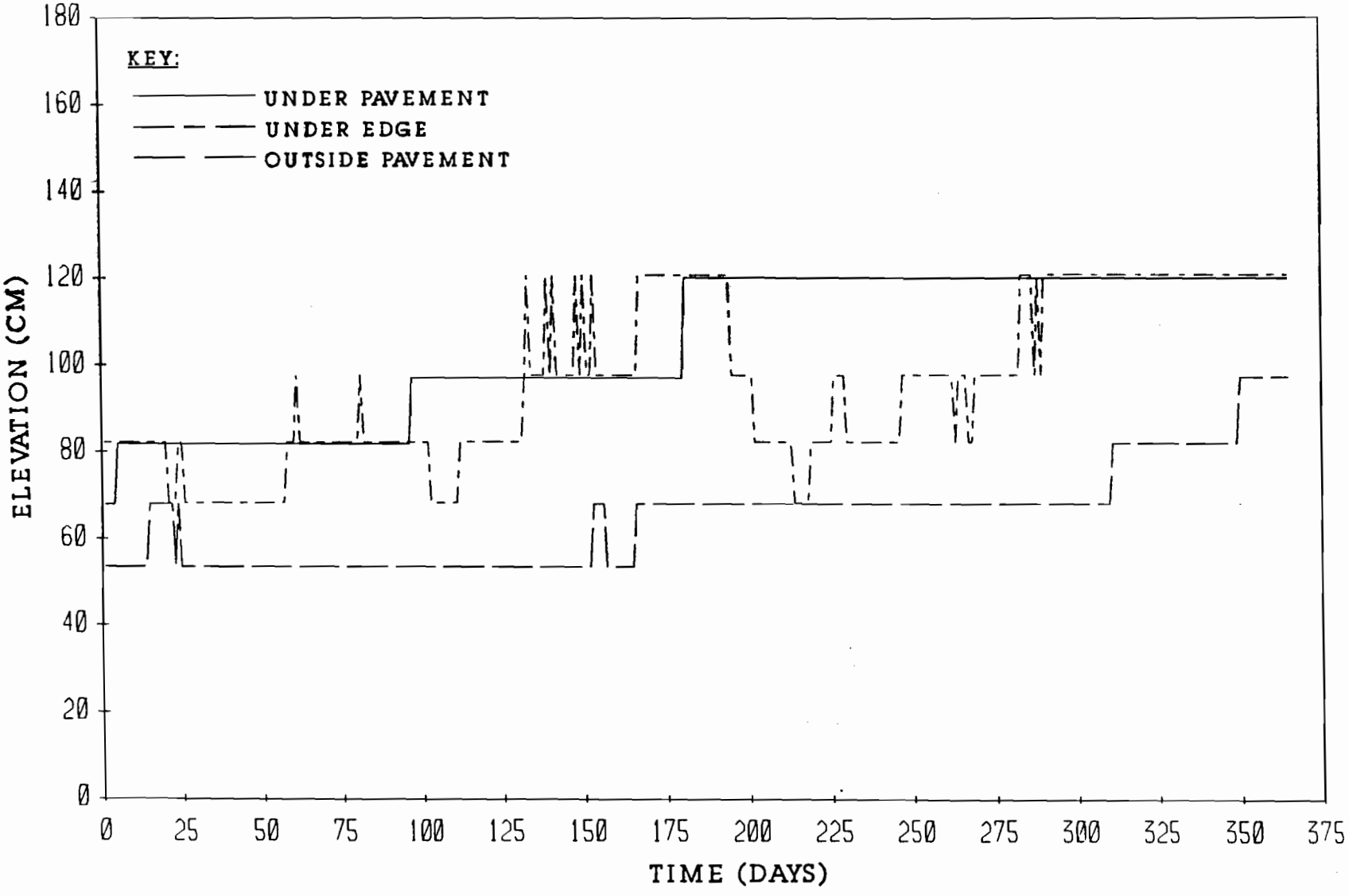

FIGURE A4.2 CRACK TIP ELEVATIONS FOR SECOND YEAR IN SAN ANTONIO

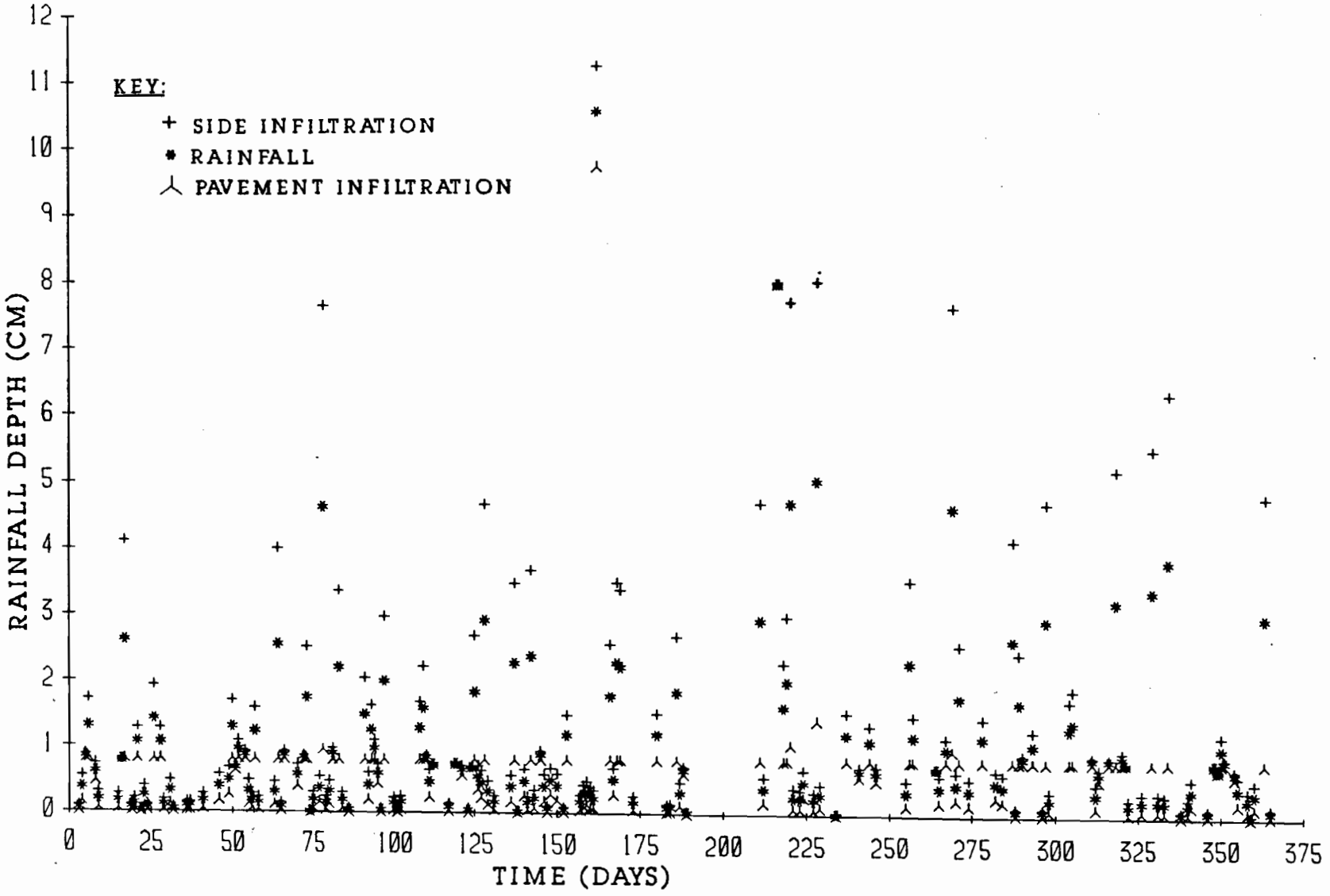

FIGURE A1.3 RAINFALL AND INFILTRATION DEPTHS FOR THIRD YEAR IN SAN ANTONIO

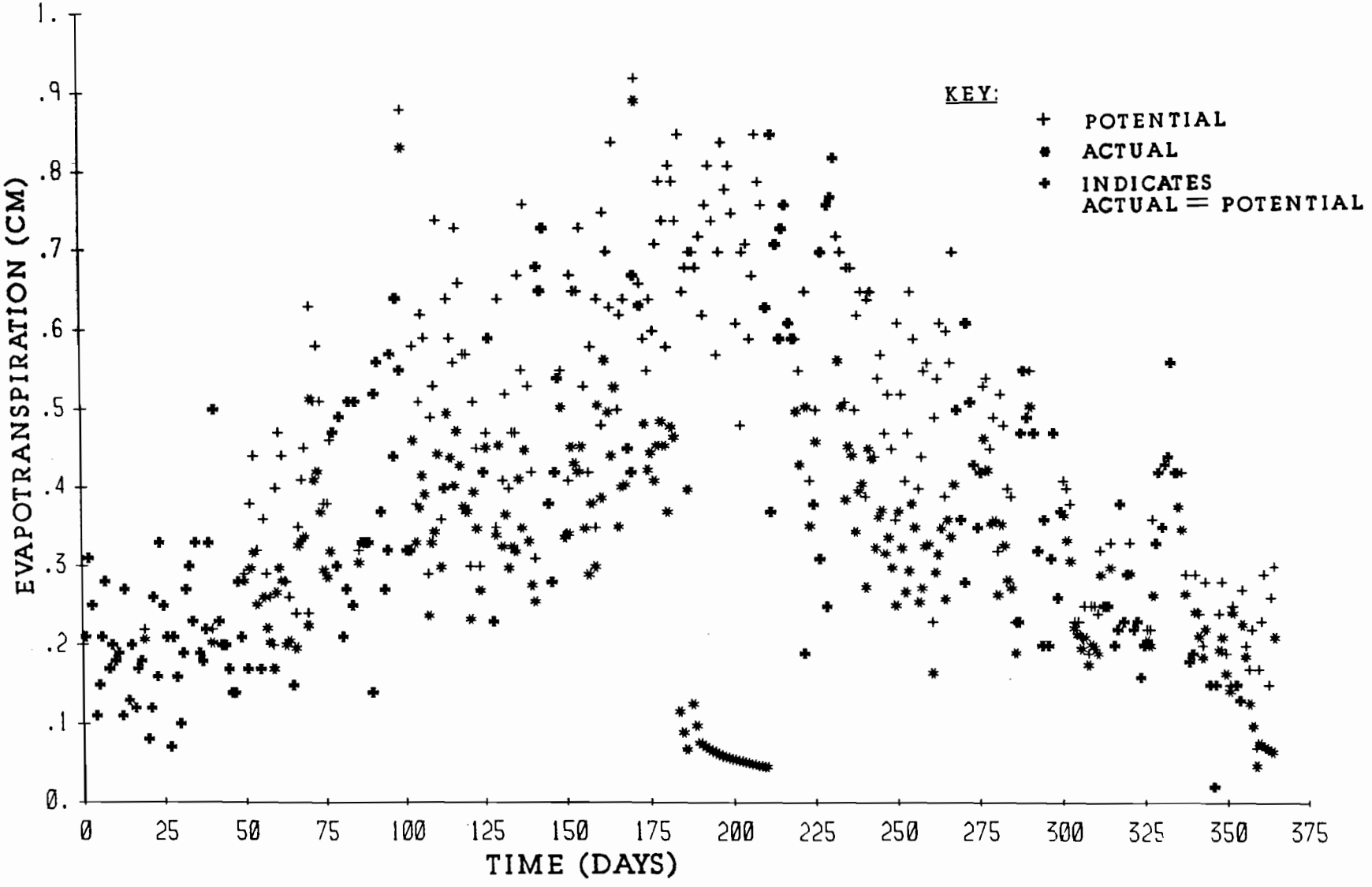

FIGURE A2.3 EVAPOTRANSPIRATION FOR THIRD YEAR IN SAN ANTONIO

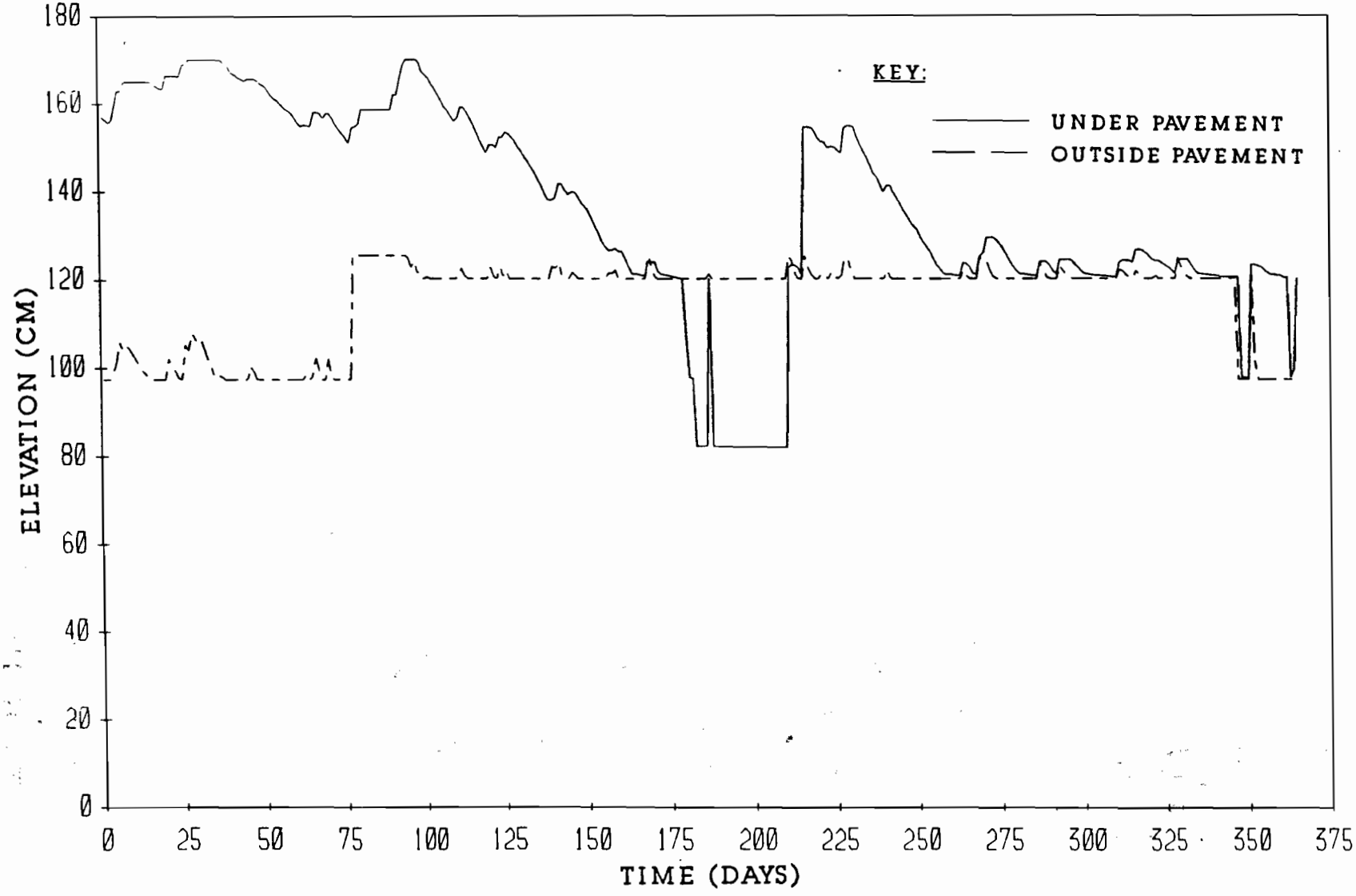

FIGURE A3.3 WATER LEVELS WITHIN THE CRACK FABRIC FOR THIRD YEAR IN SAN ANTONIO

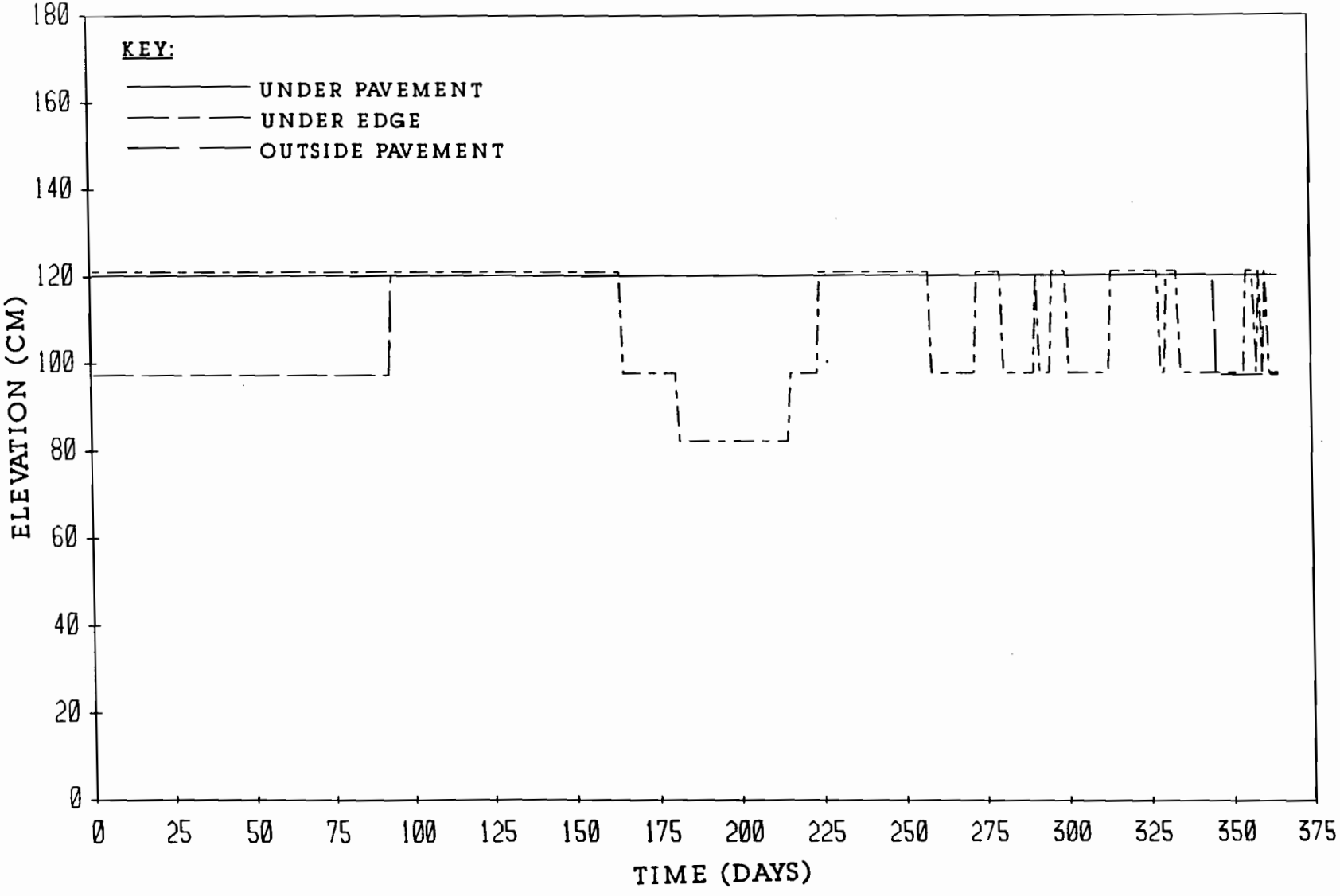

FIGURE A4.3 CRACK TIP ELEVATIONS FOR THIRD YEAR IN SAN ANTONIO

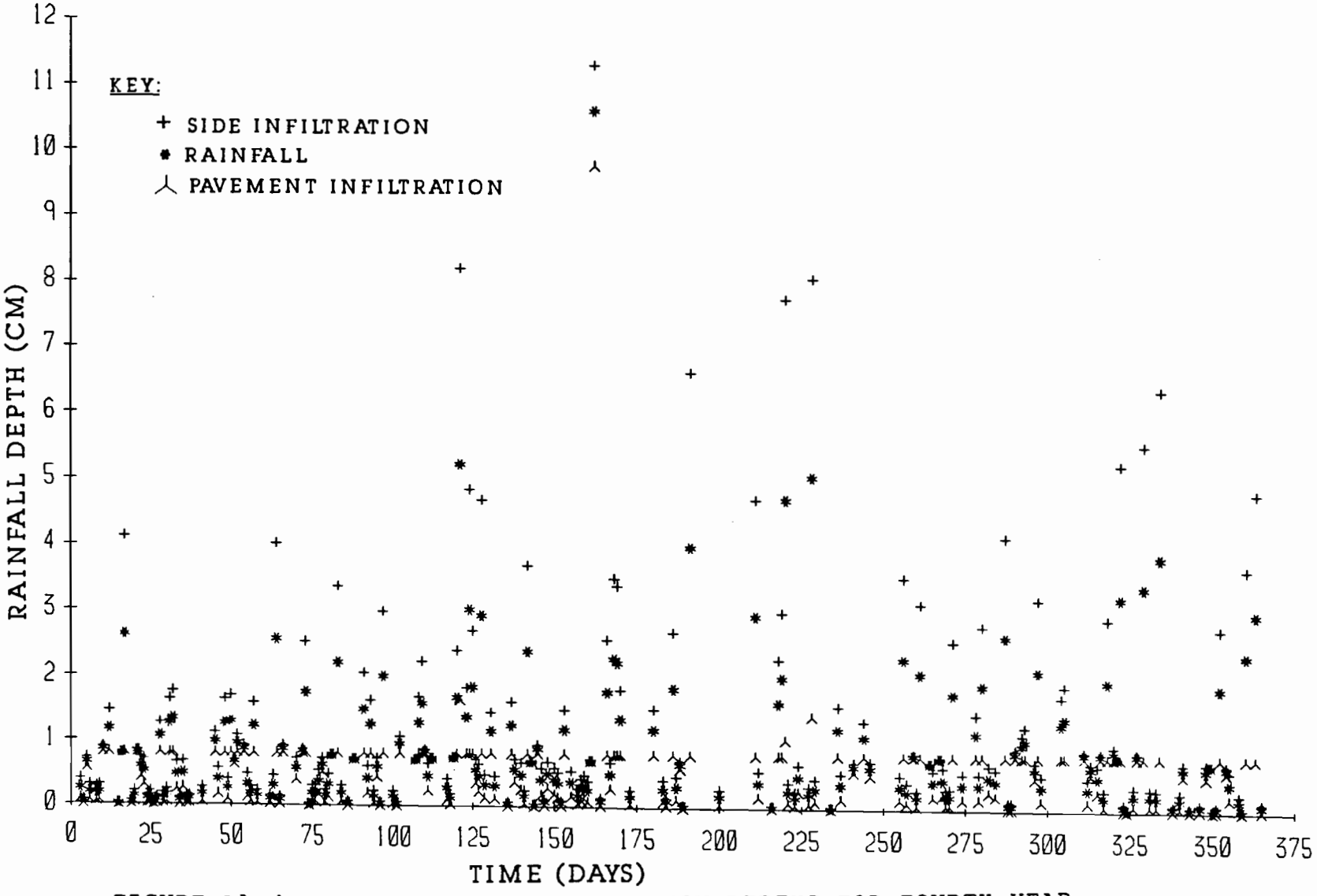

FIGURE A1.4 RAINFALL AND INFILTRATION DEPTHS FOR FOURTH YEAR IN SAN ANTONIO

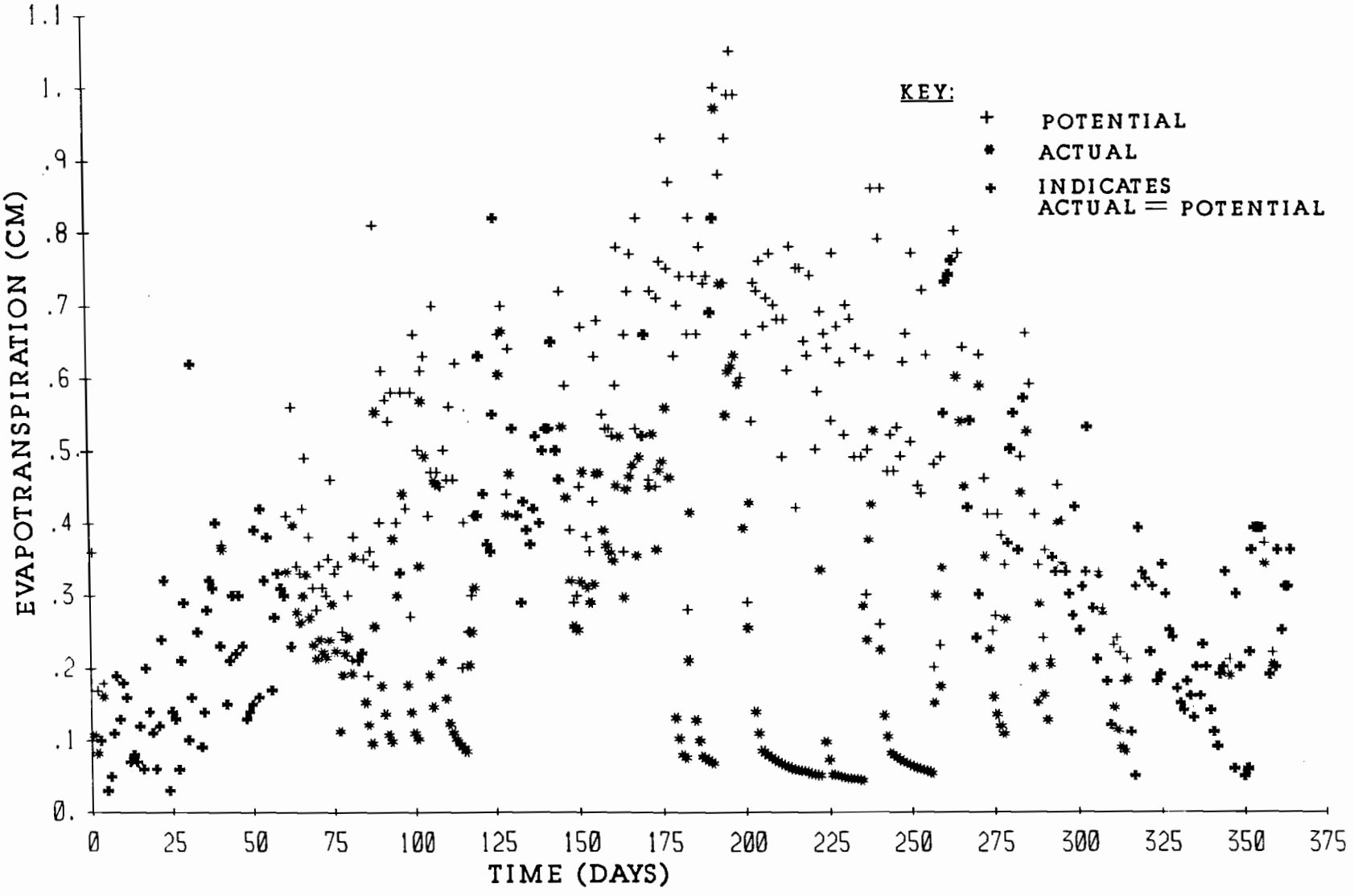

FIGURE A2.4 EVAPOTRANSPIRATION FOR FOURTH YEAR IN SAN ANTONIO

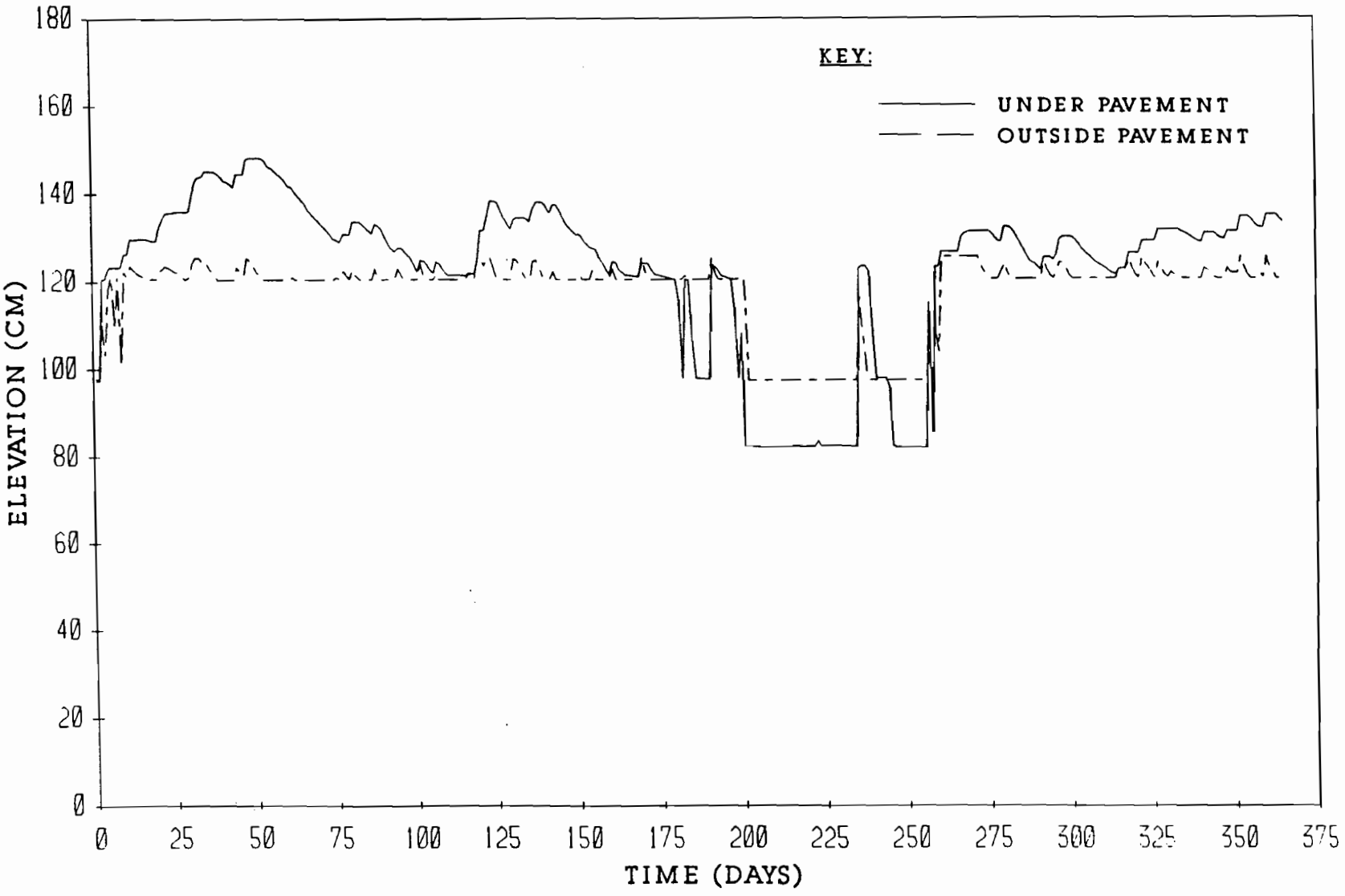

FIGURE A3.4 WATER LEVELS WITHIN THE CRACK FABRIC FOR FOURTH YEAR IN SAN ANTONIO

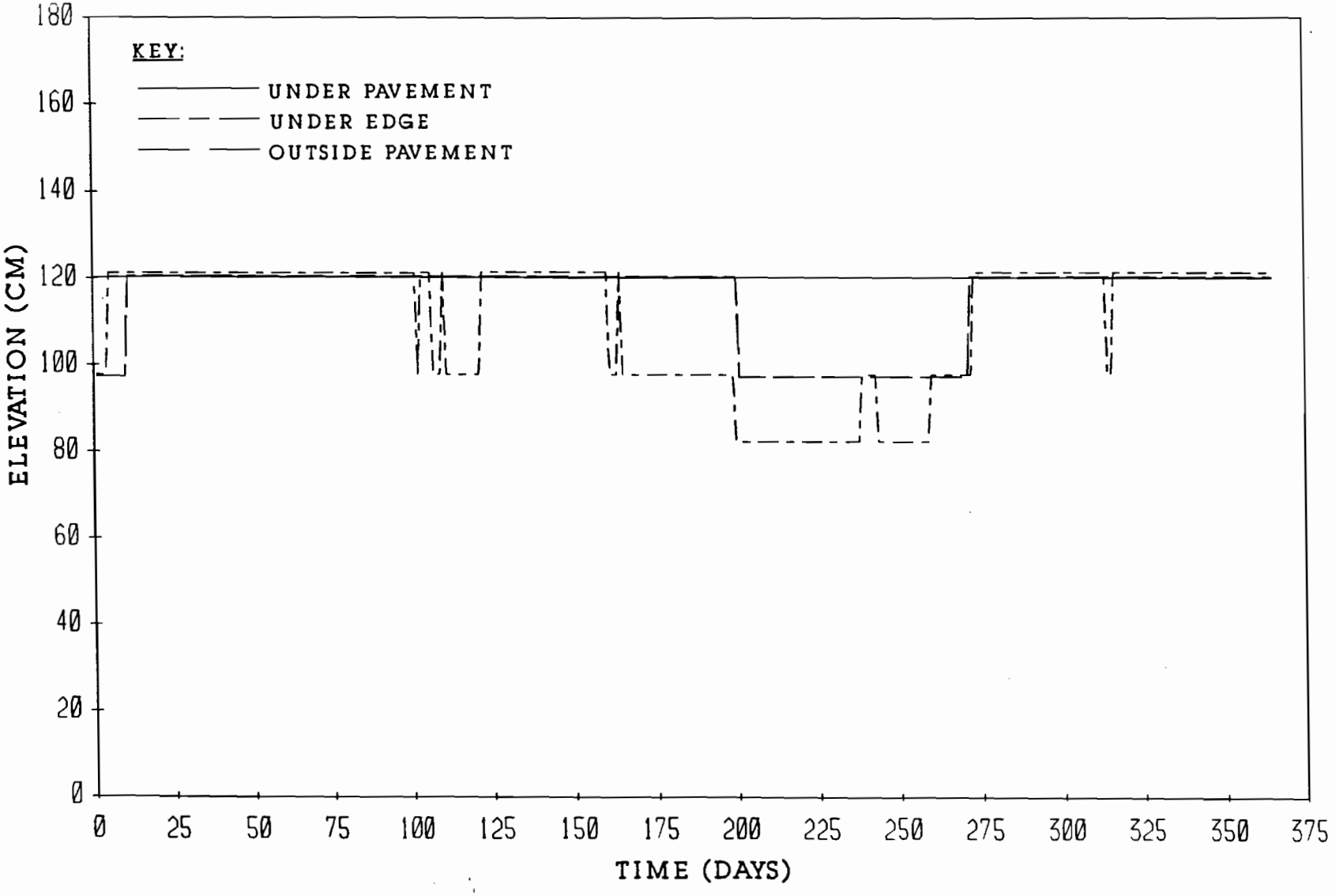

FIGURE A4.4 CRACK TIP ELEVATIONS FOR FOURTH YEAR IN SAN ANTONIO

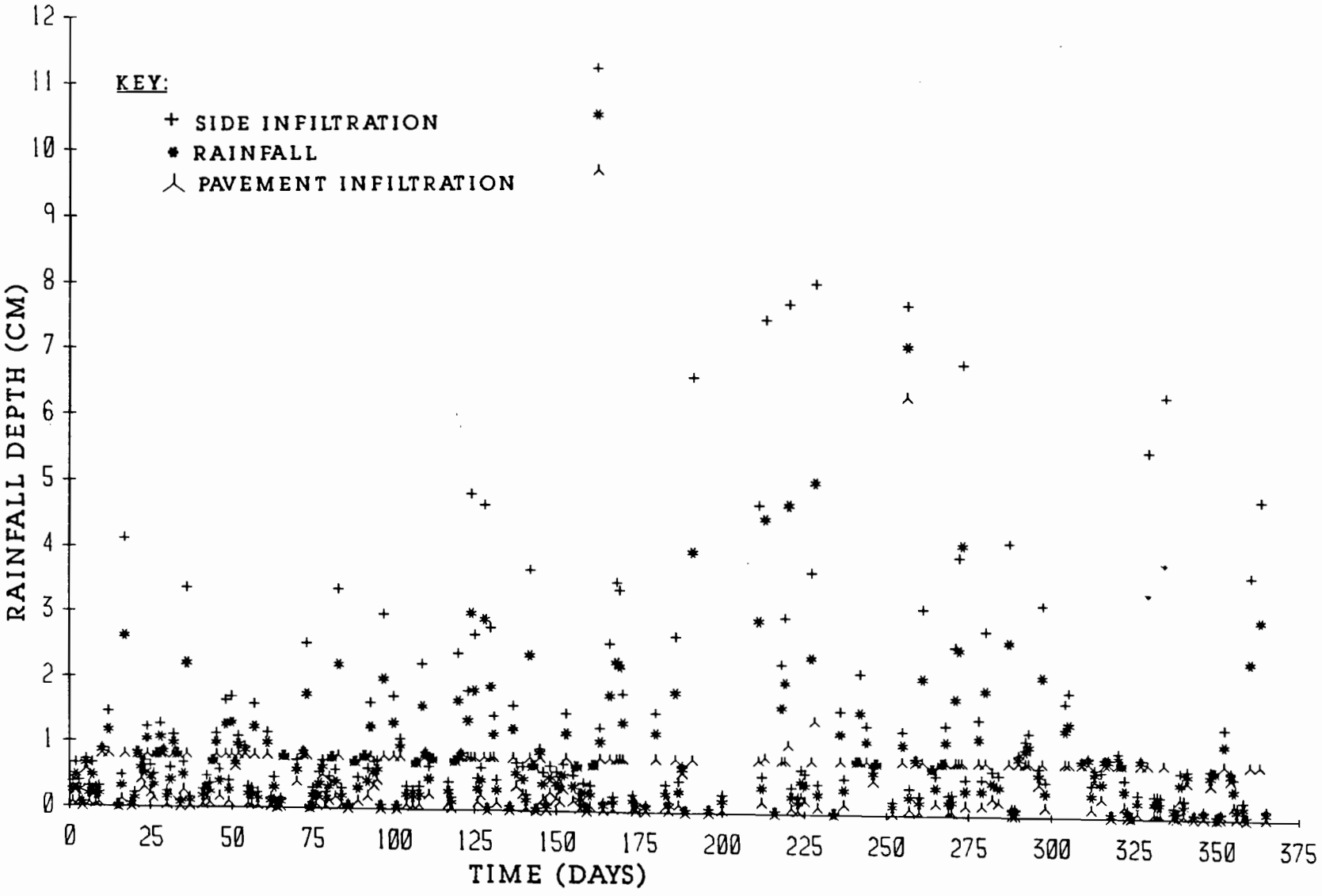

FIGURE A1.5 RAINFALL AND INFILTRATION DEPTHS FOR FIFTH YEAR IN SAN ANTONIO

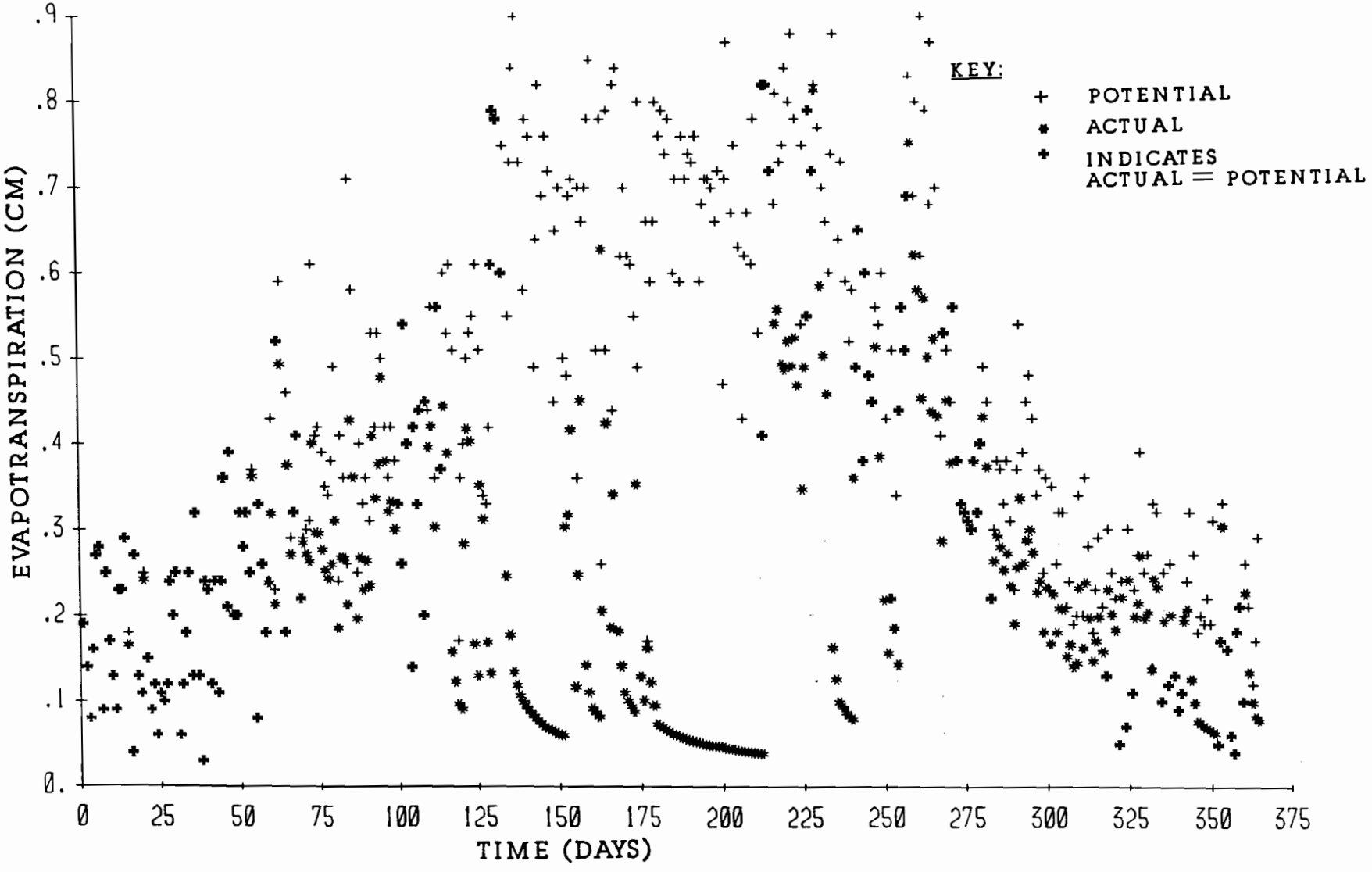

FIGURE A2.5 EVAPOTRANSPIRATION FOR FIFTH YEAR IN SAN ANTONIO

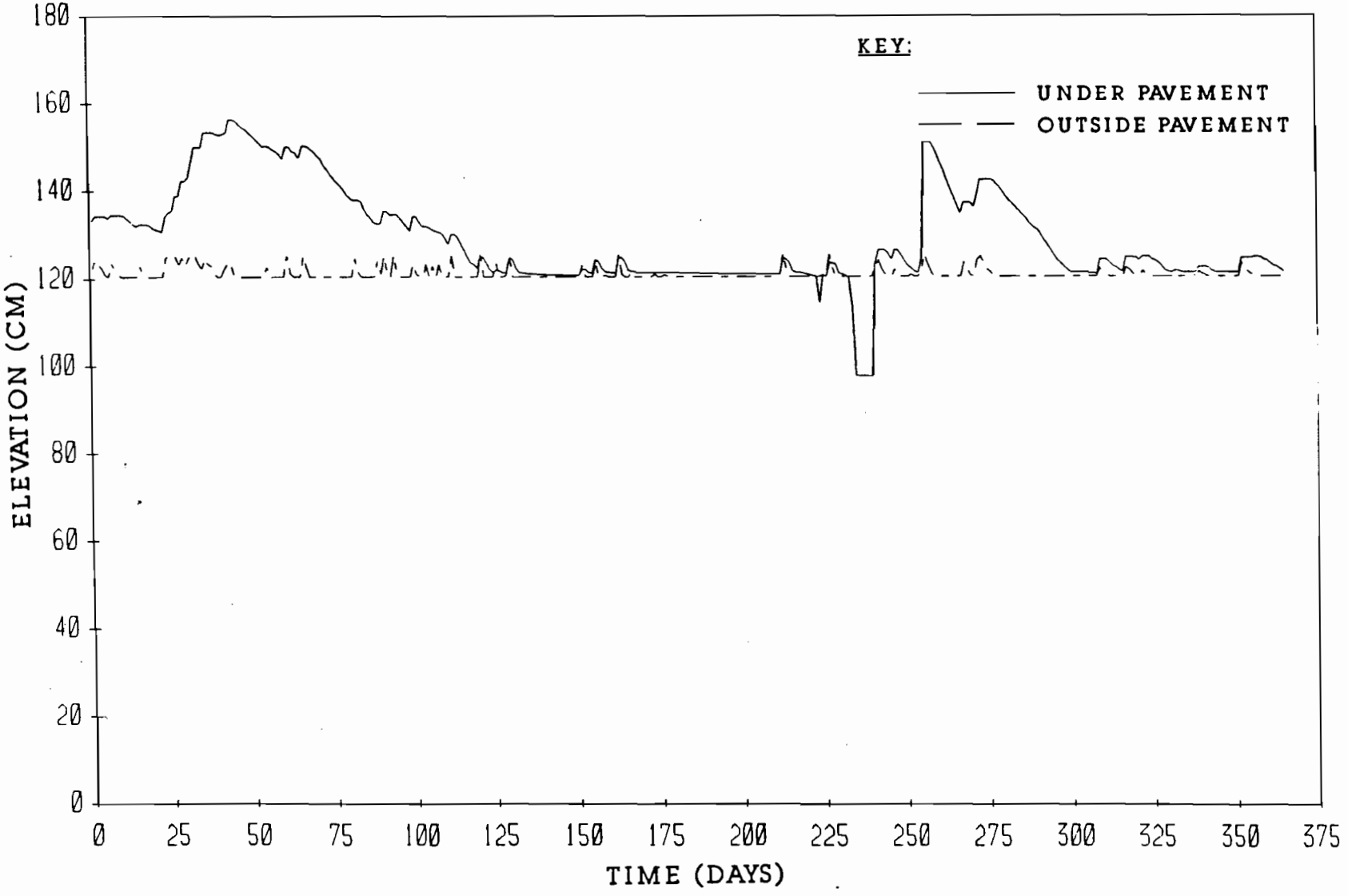

FIGURE A3.5 WATER LEVELS WITHIN THE CRACK FABRIC FOR FIFTH YEAR IN SAN ANTONIO

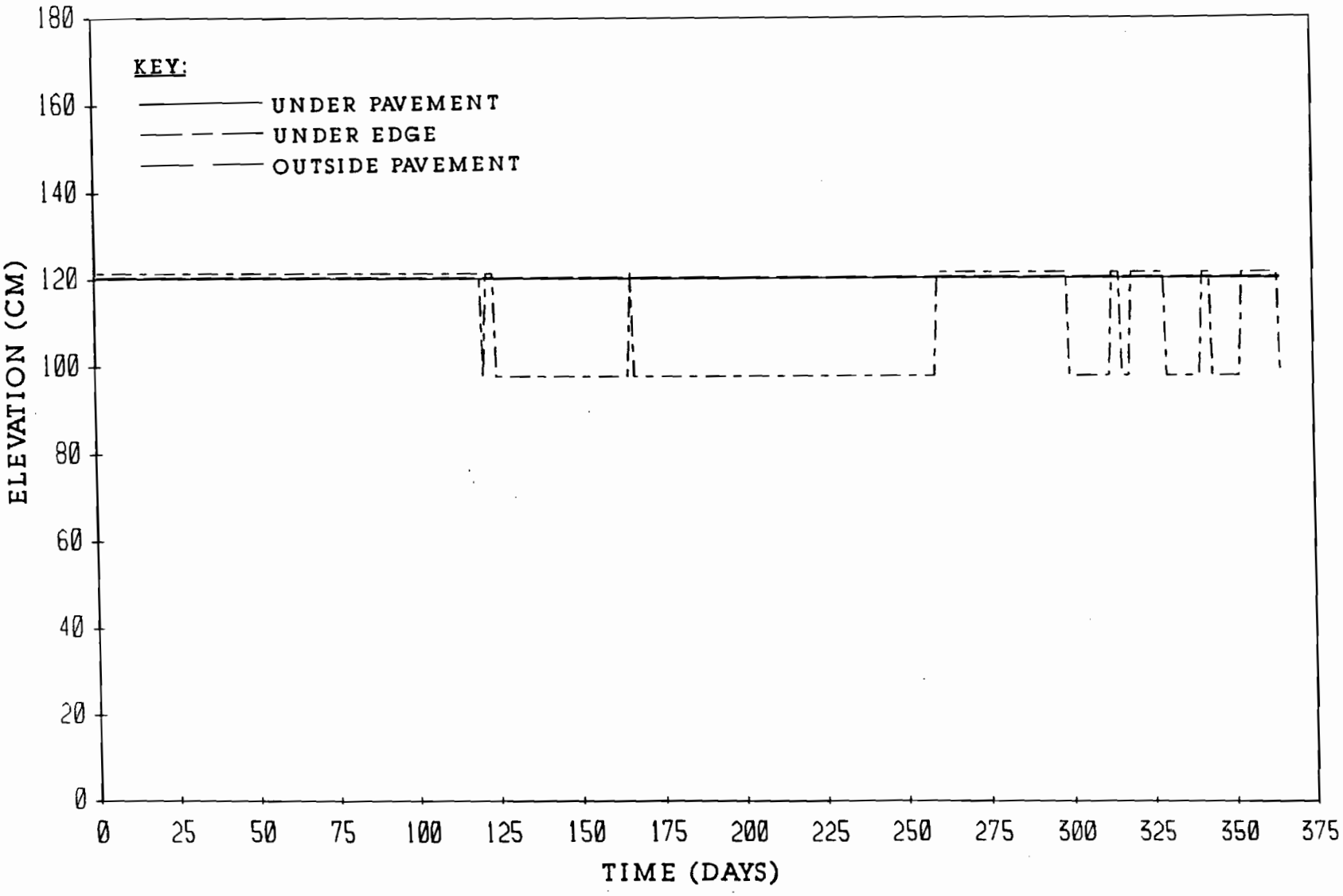

FIGURE A4.5 CRACK TIP ELEVATIONS FOR FIFTH YEAR IN SAN ANTONIO

APPENDIX B

SIMULATION RESULTS FOR HOUSTON

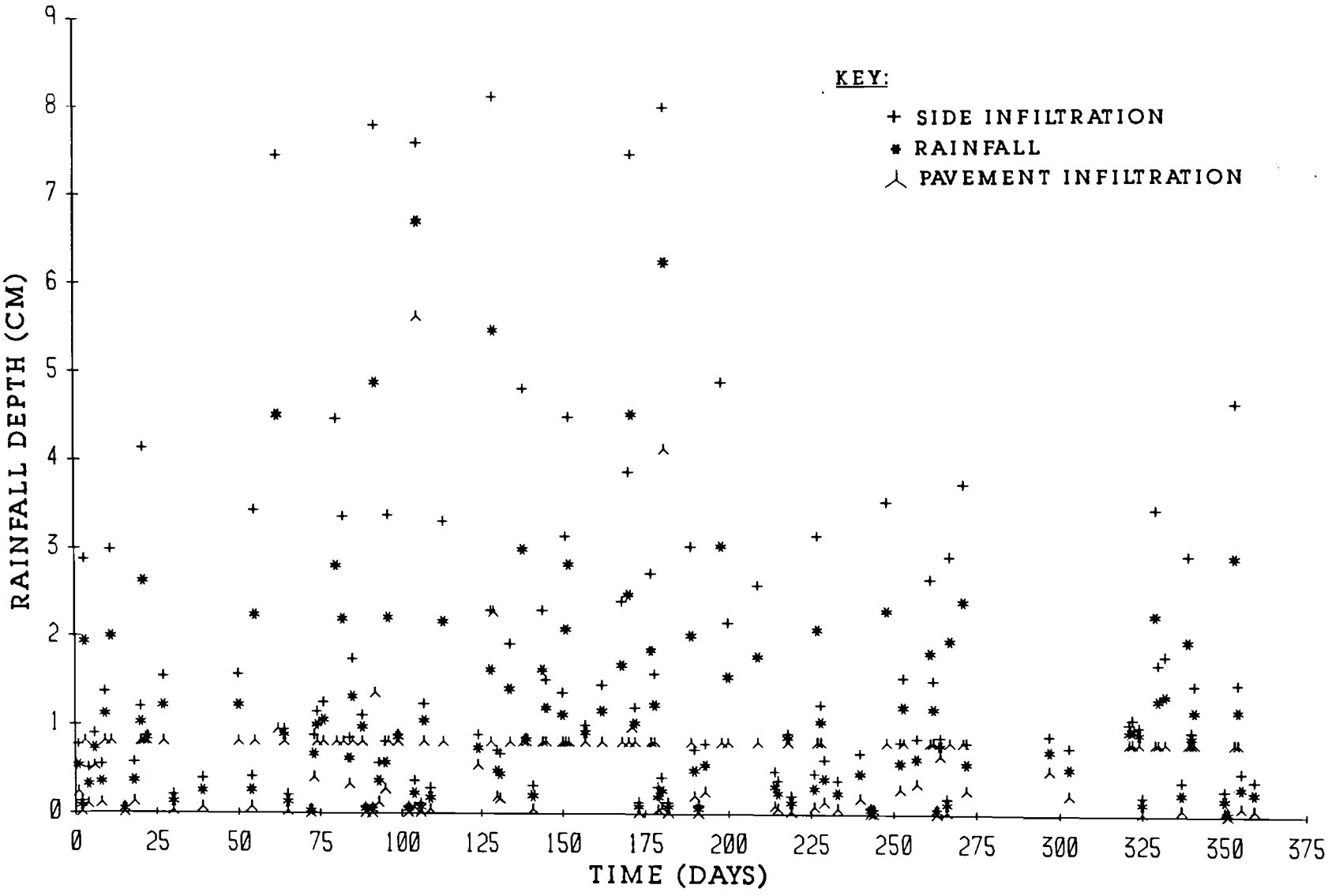

FIGURE B1.1 RAINFALL AND INFILTRATION DEPTHS FOR FIRST YEAR IN HOUSTON

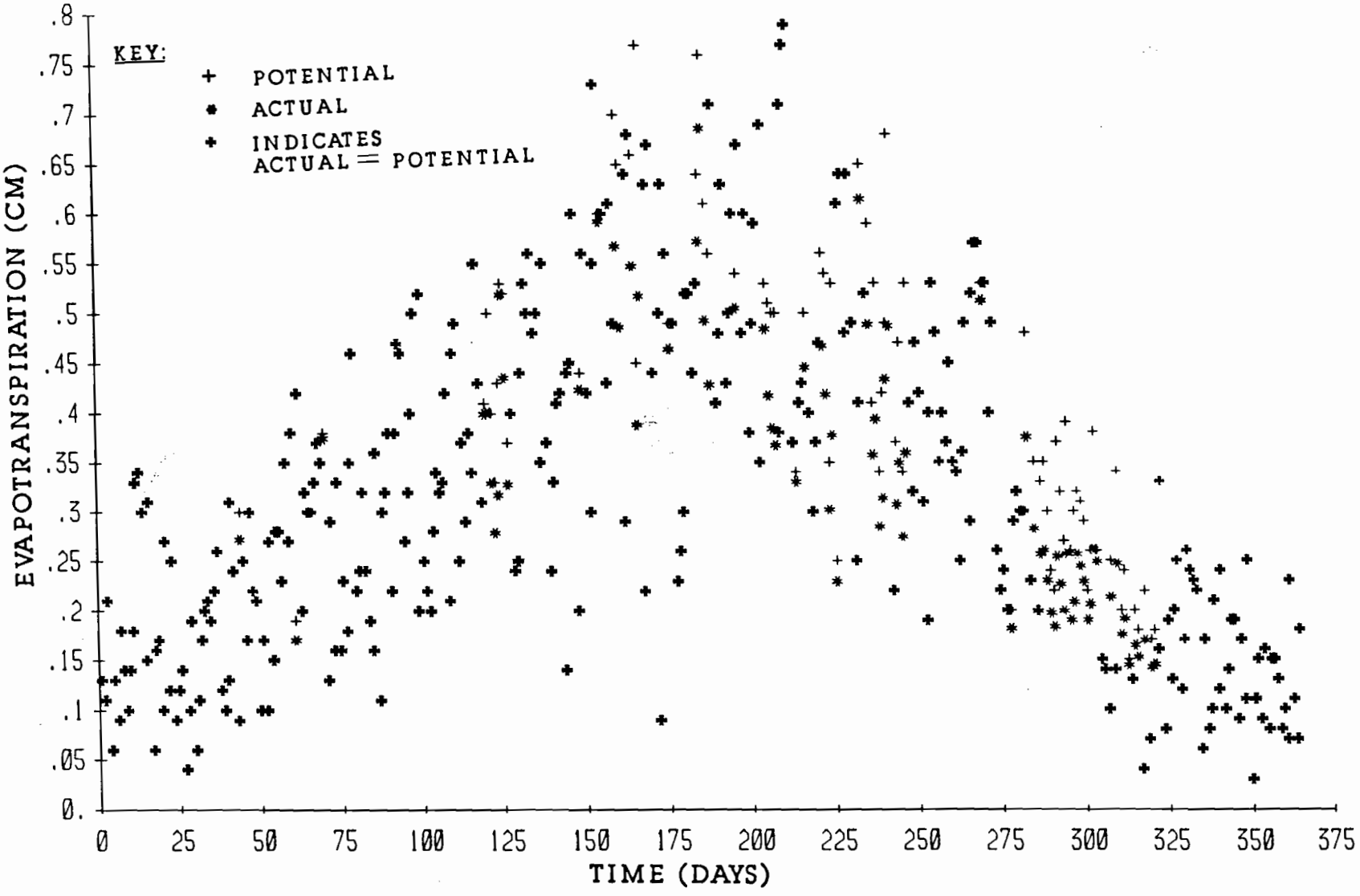

FIGURE B2.1 EVAPOTRANSPIRATION FOR FIRST YEAR IN HOUSTON

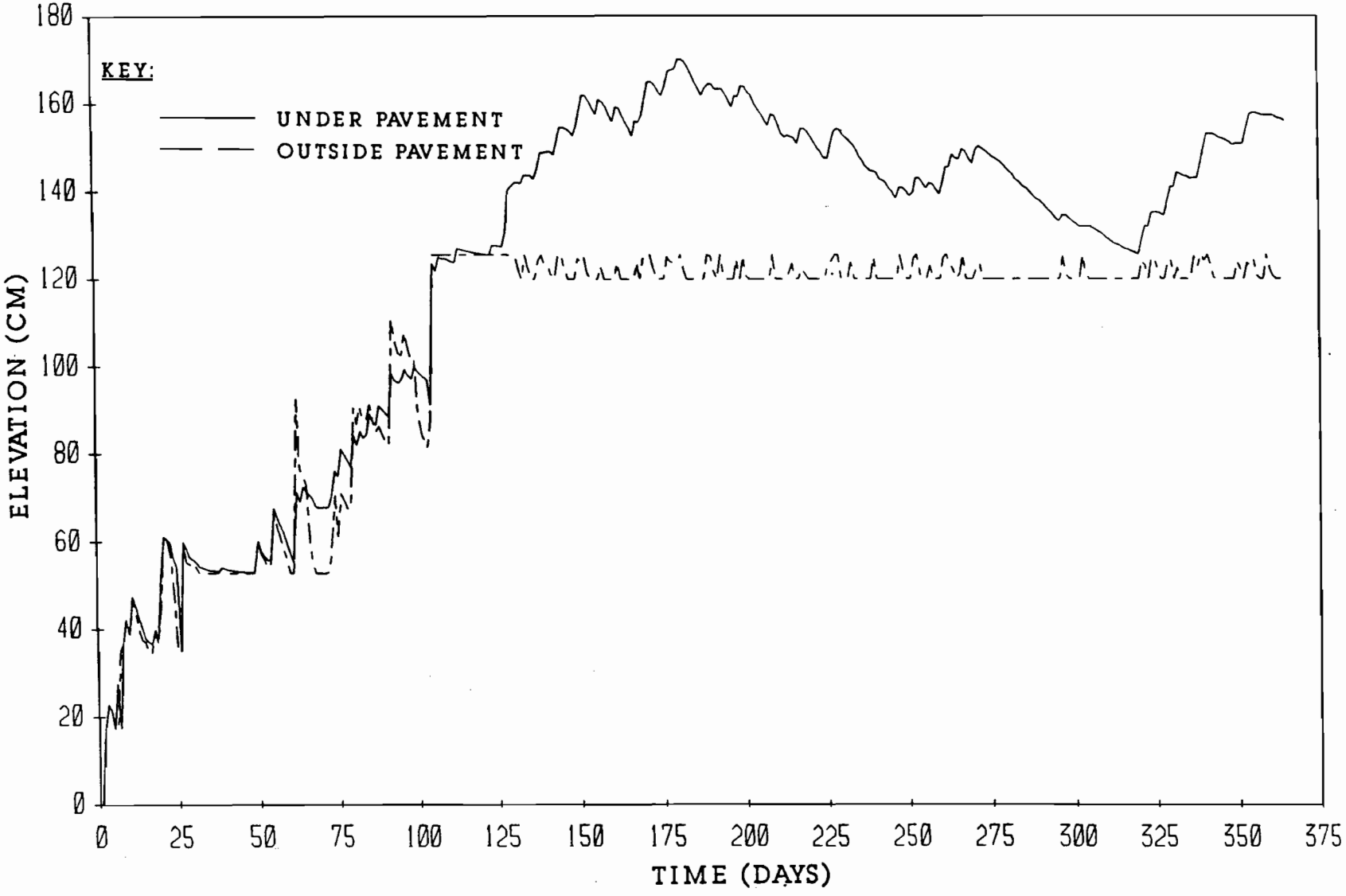

FIGURE B3.1 WATER LEVELS WITHIN THE CRACK FABRIC FOR FIRST YEAR IN HOUSTON

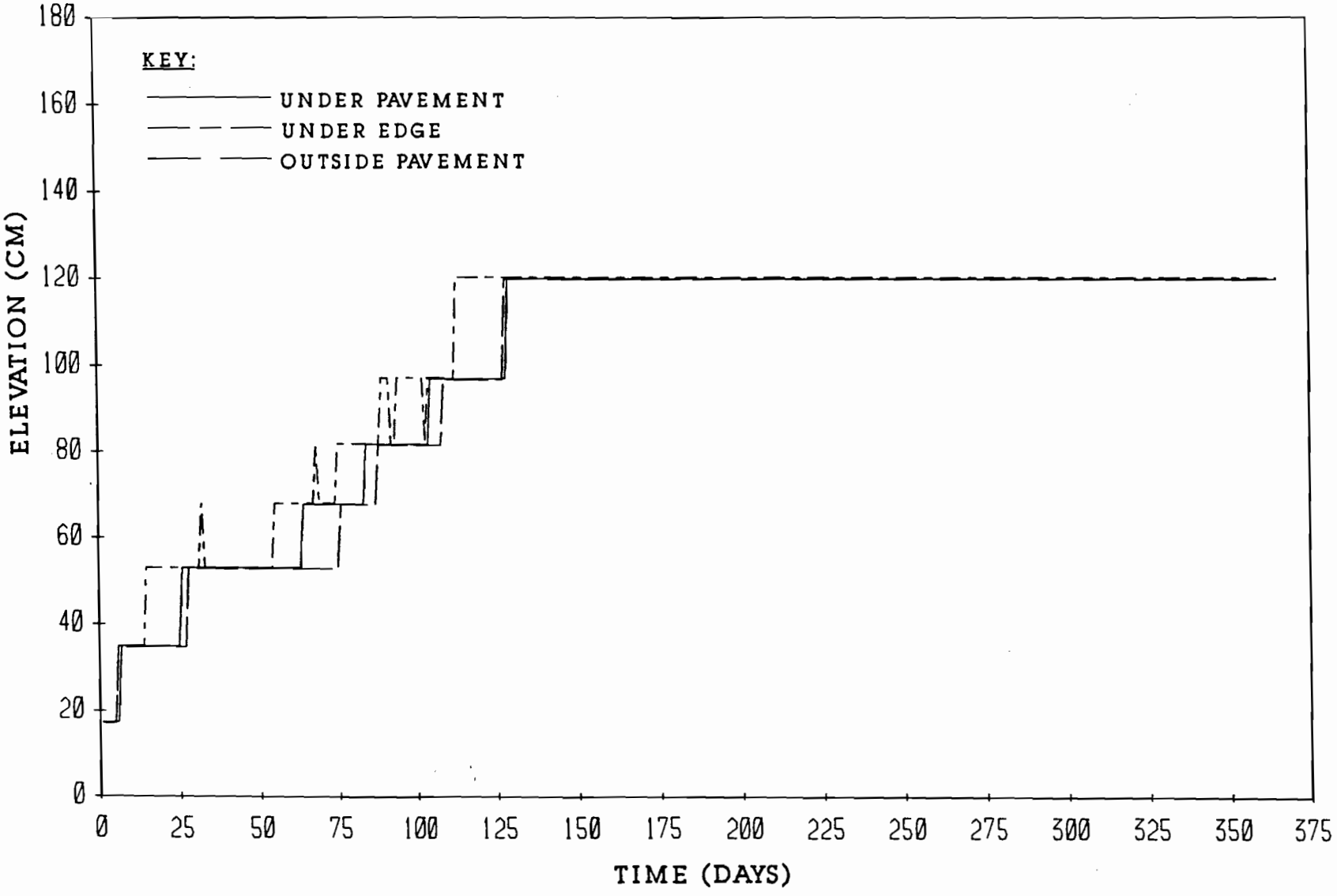

FIGURE B4.1 CRACK TIP ELEVATIONS FOR FIRST YEAR IN HOUSTON

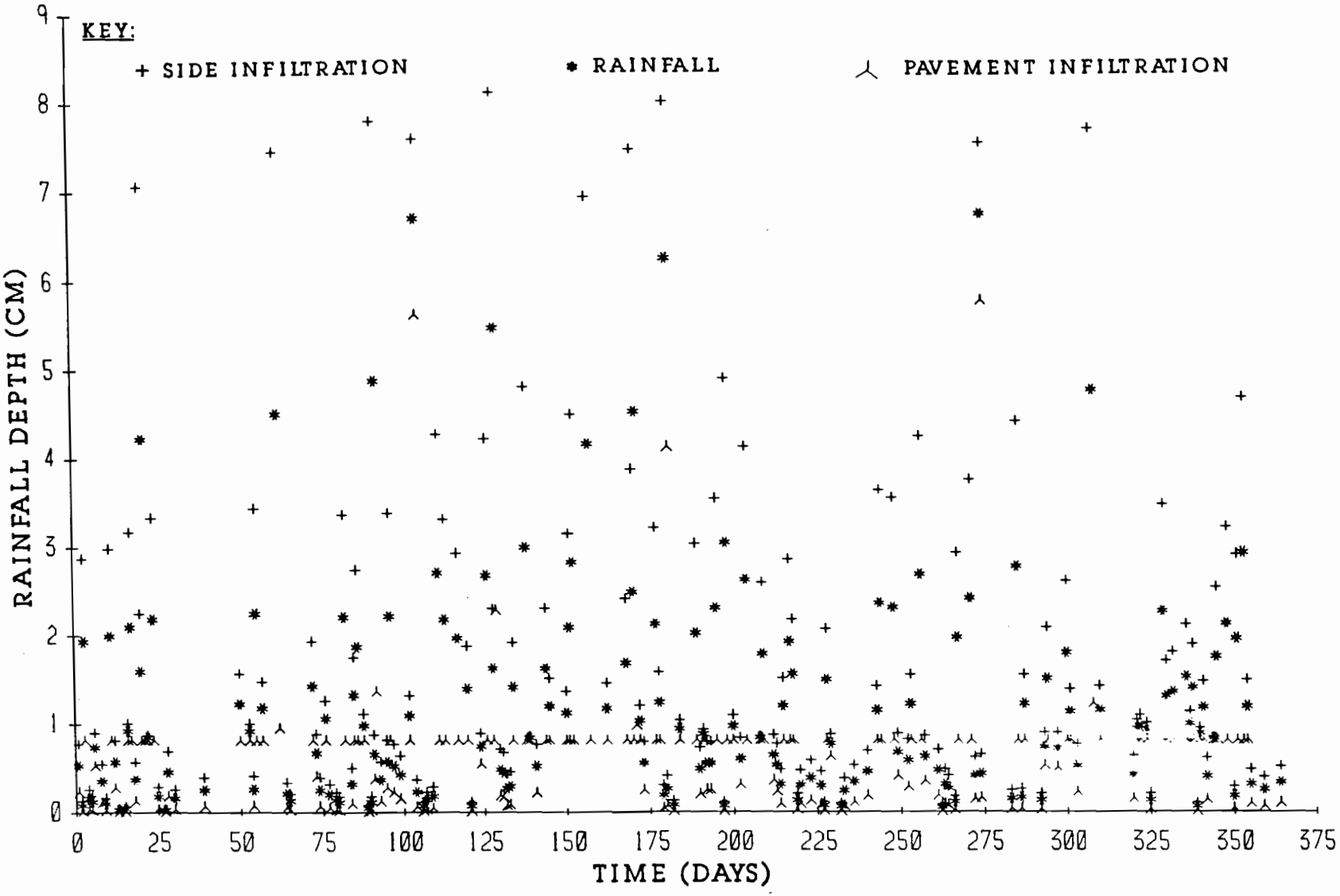

FIGURE B1.2 RAINFALL AND INFILTRATION DEPTHS FOR SECOND YEAR IN HOUSTON

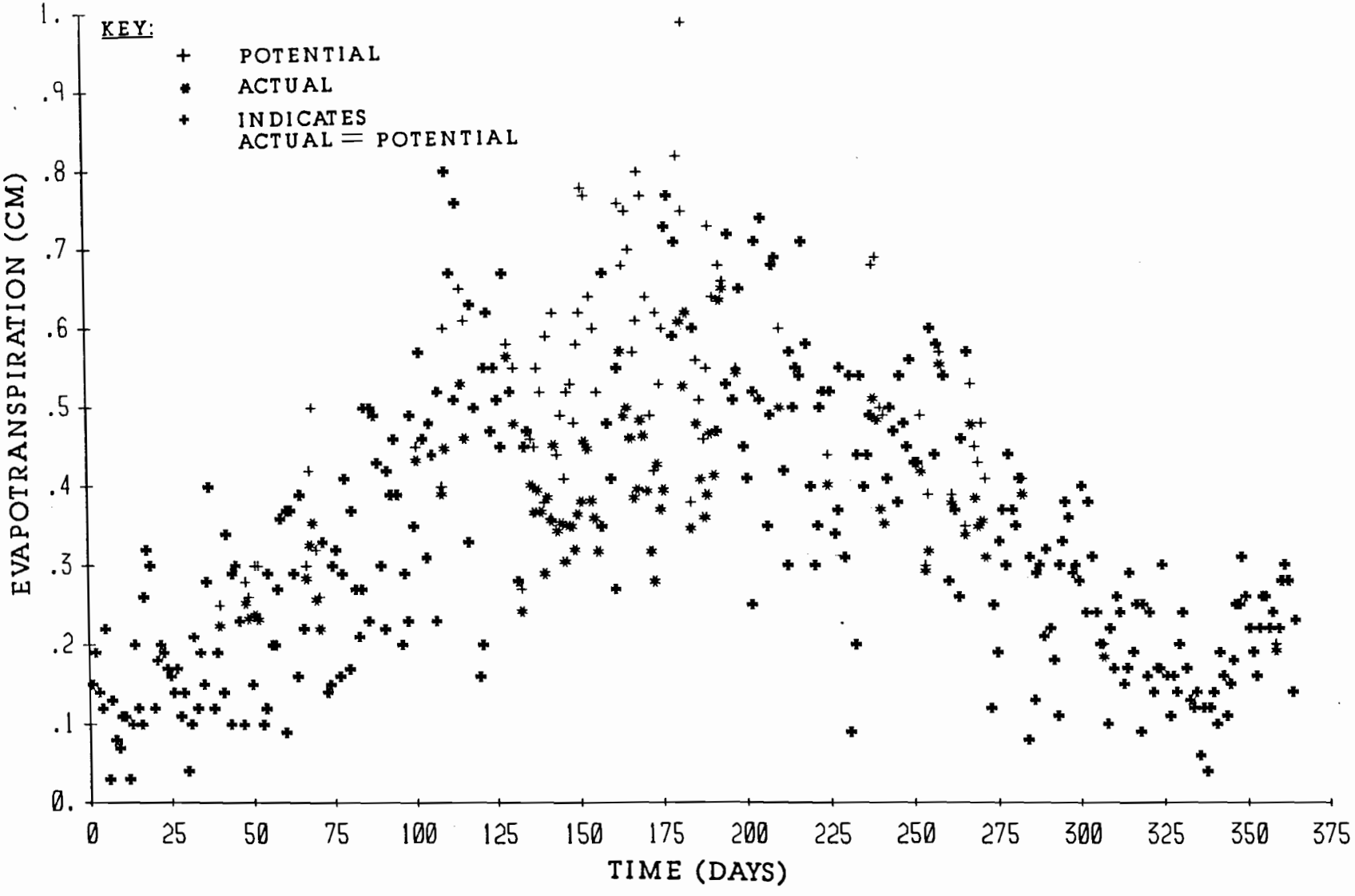

FIGURE B2.2 EVAPOTRANSPIRATION FOR SECOND YEAR IN HOUSTON

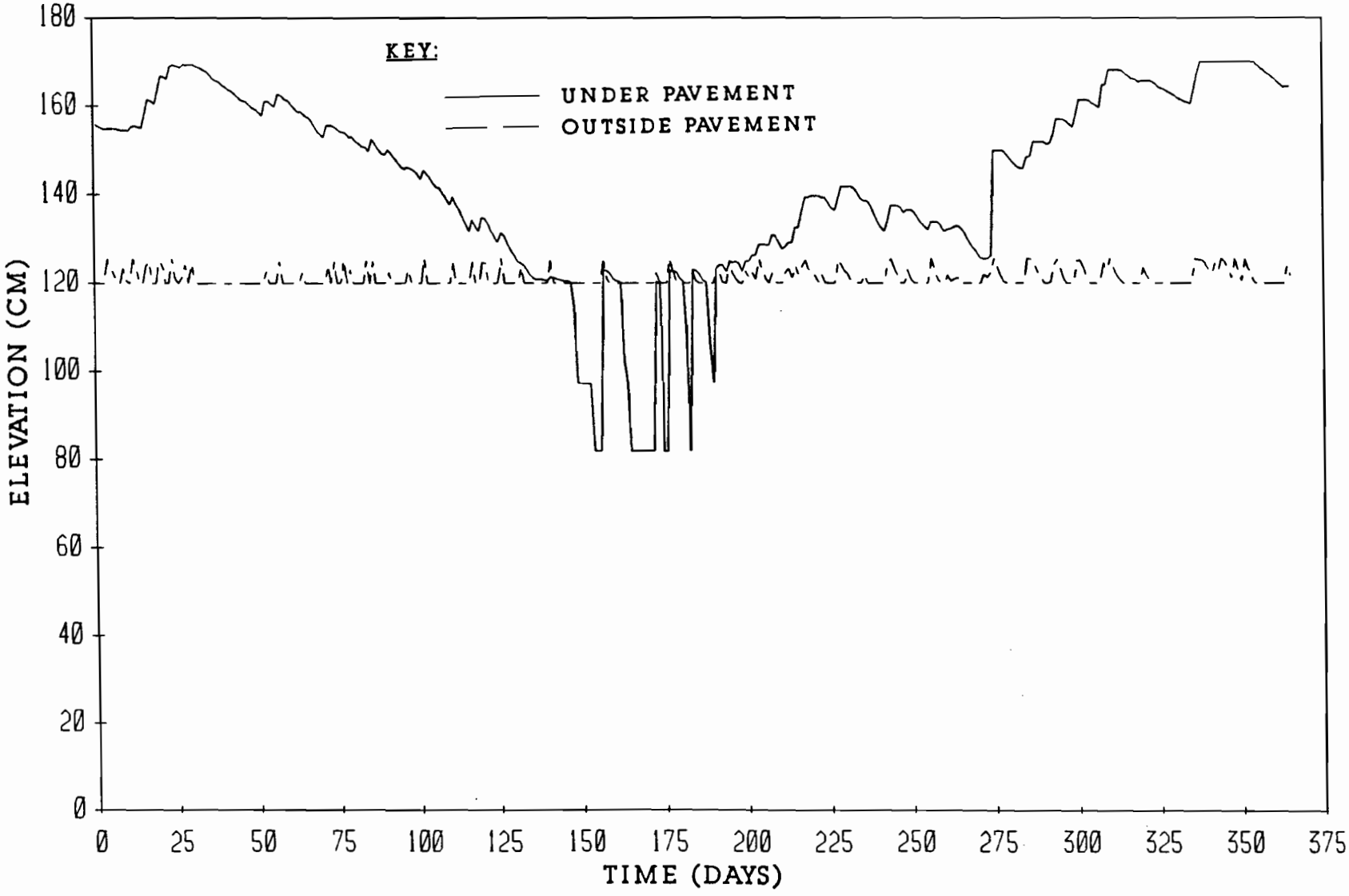

FIGURE B3.2 WATER LEVELS WITHIN THE CRACK FABRIC FOR SECOND YEAR IN HOUSTON

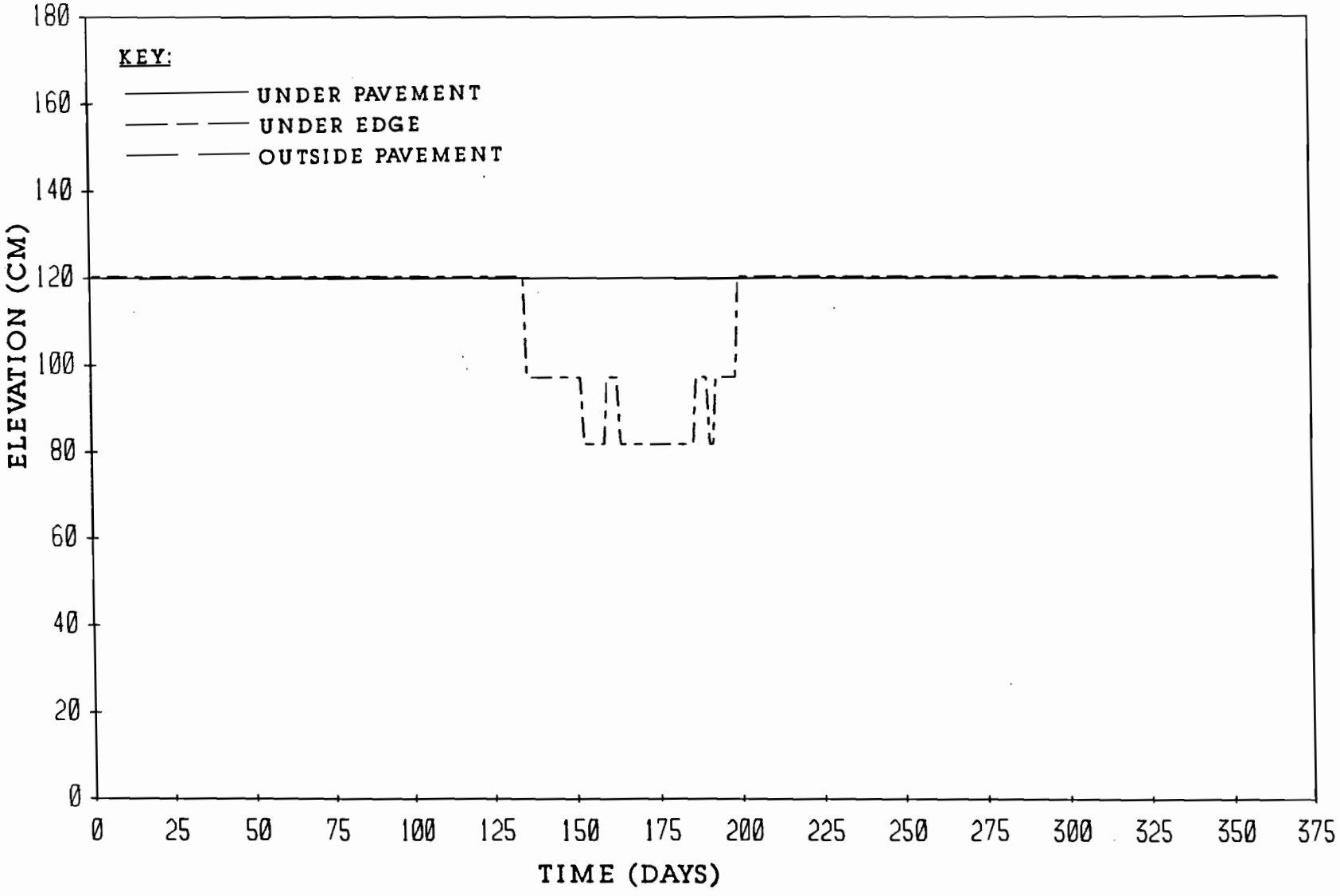

FIGURE B4.2 CRACK TIP ELEVATIONS FOR SECOND YEAR IN HOUSTON

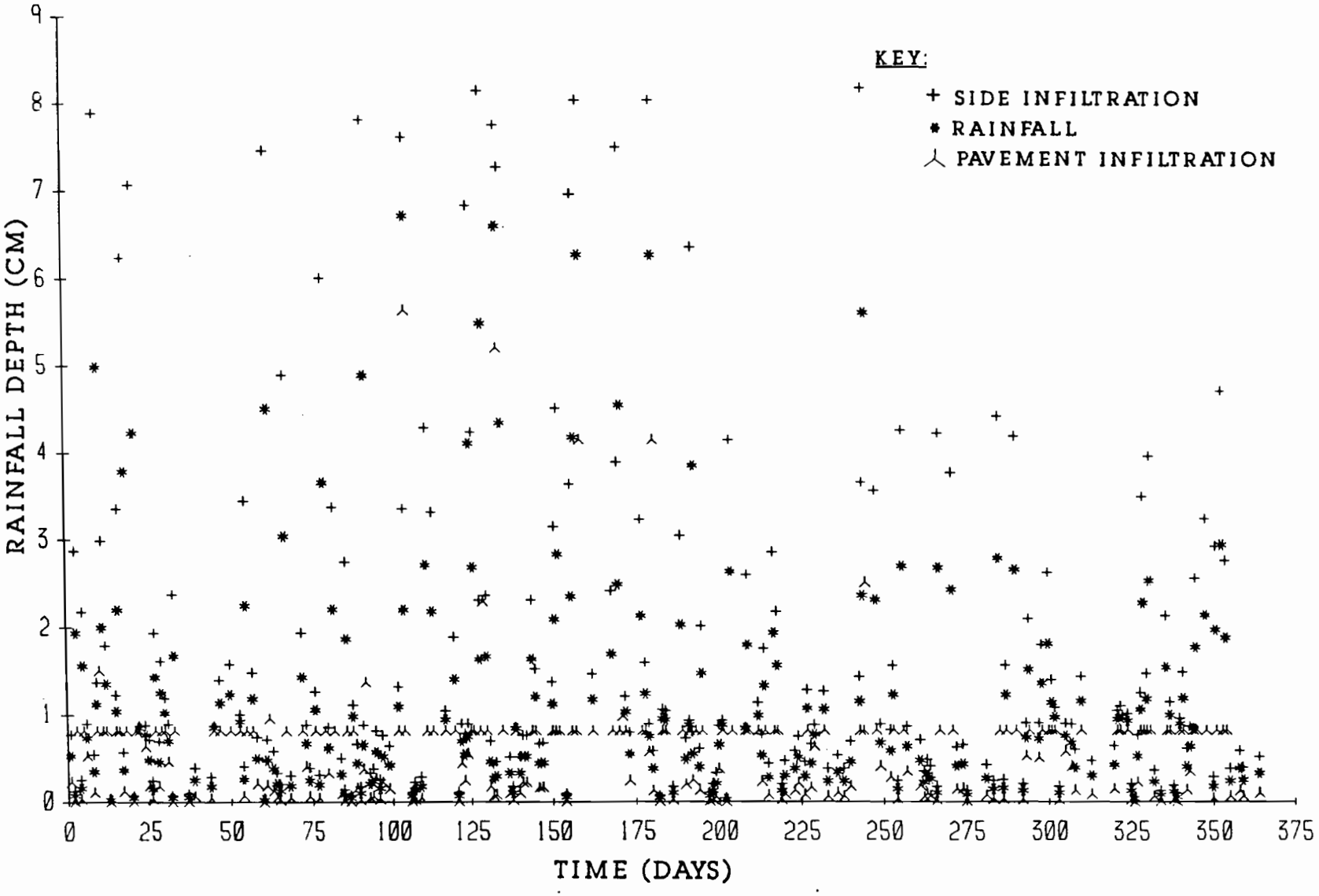

FIGURE B1.3 RAINFALL AND INFILTRATION DEPTHS FOR THIRD YEAR IN HOUSTON

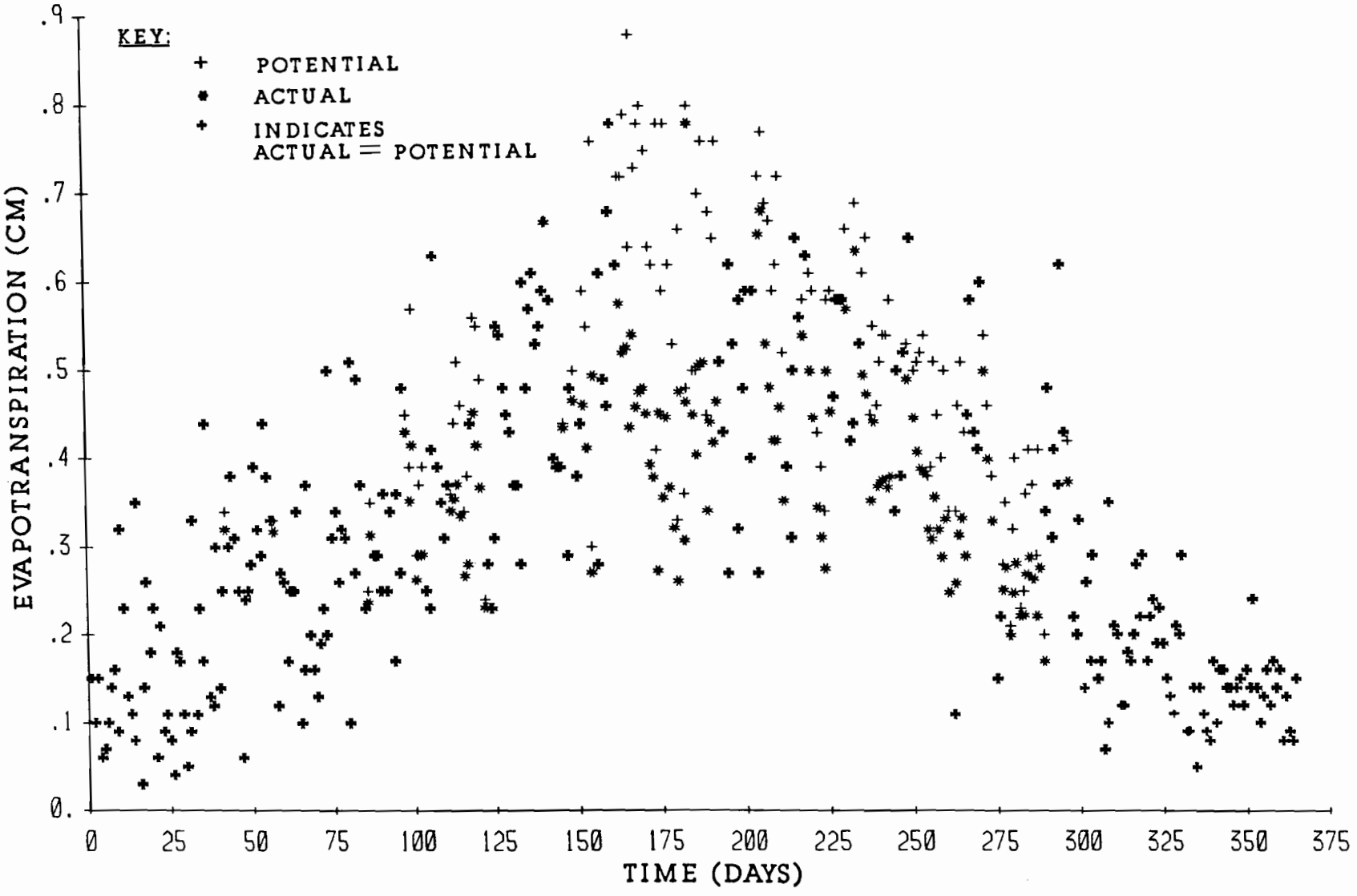

FIGURE B2.3 EVAPOTRANSPIRATION FOR THIRD YEAR IN HOUSTON

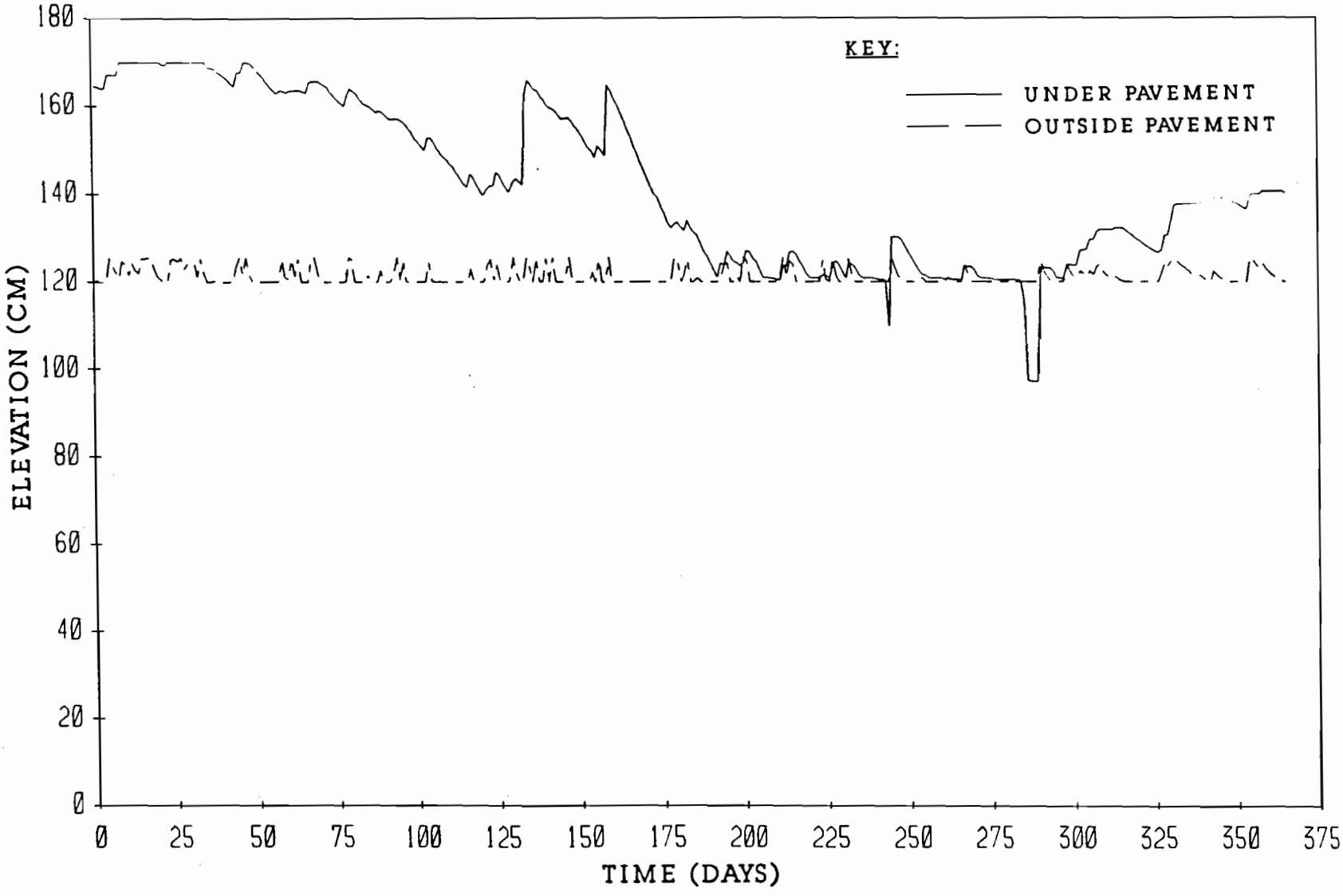

FIGURE B3.3 WATER LEVELS WITHIN THE CRACK FABRIC FOR THIRD YEAR IN HOUSTON

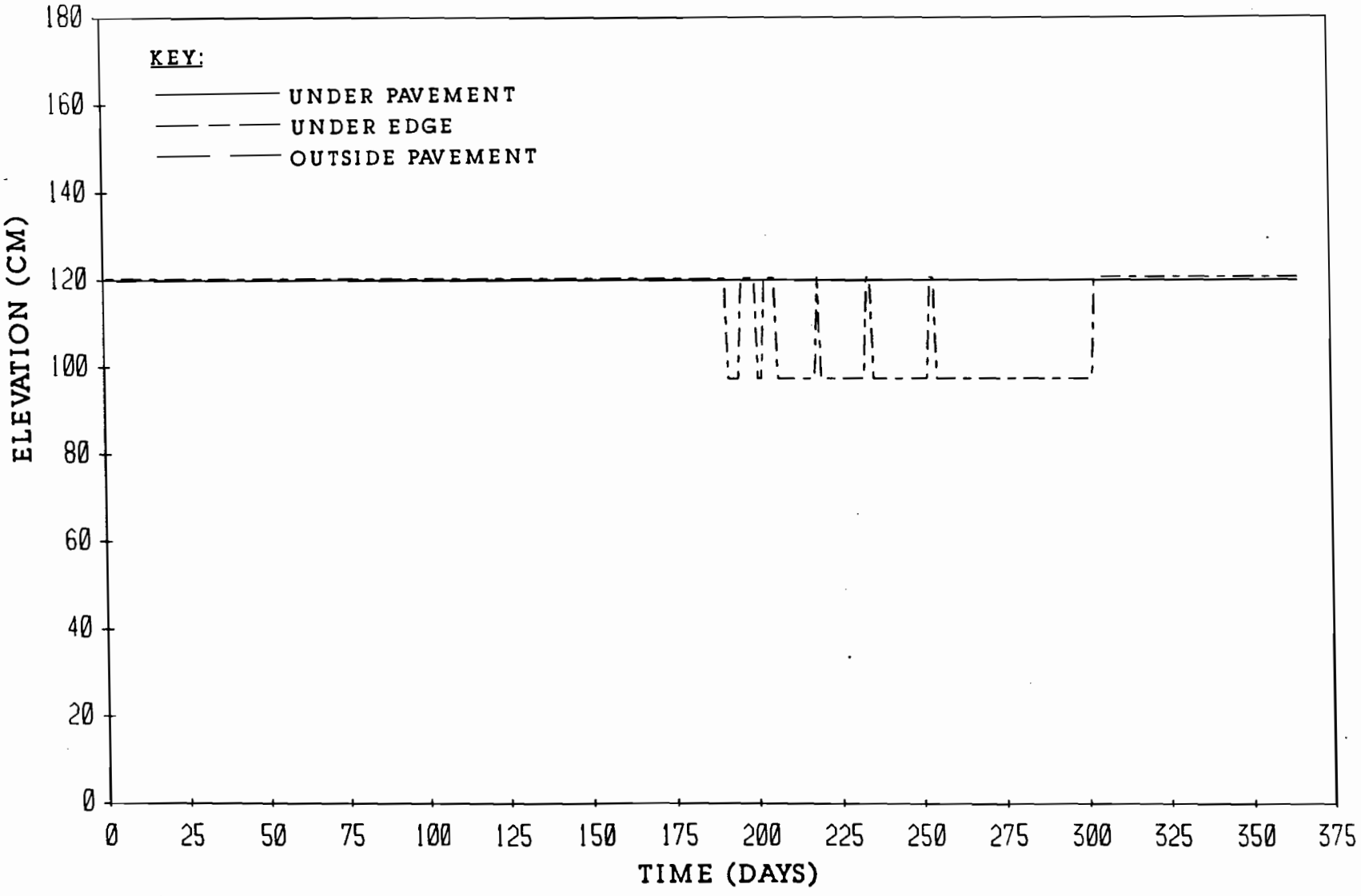

FIGURE B4.5 CRACK TIP ELEVATIONS FOR THIRD YEAR IN HOUSTON

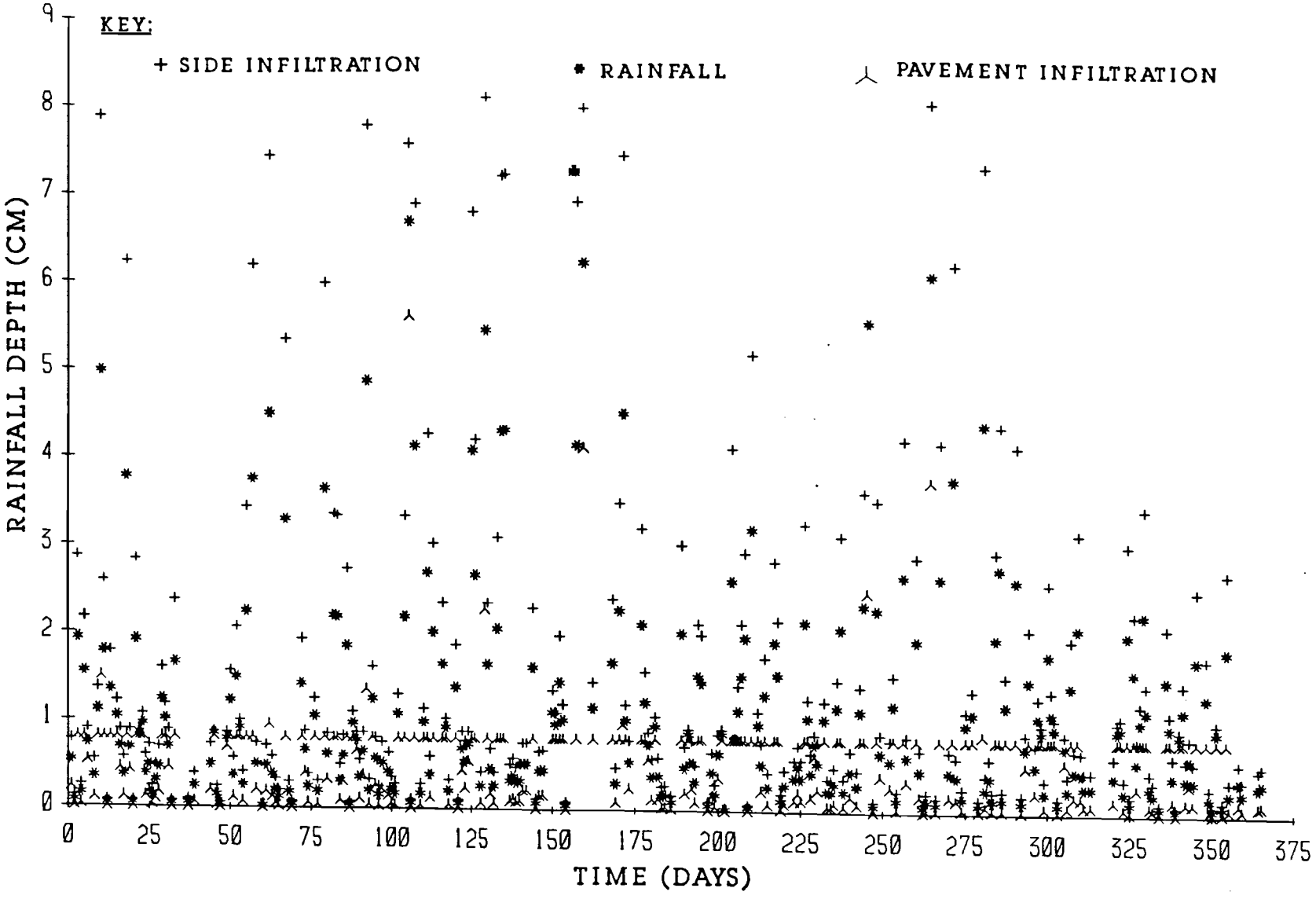

FIGURE B1.4 RAINFALL AND INFILTRATION DEPTHS FOR FOURTH YEAR IN HOUSTON

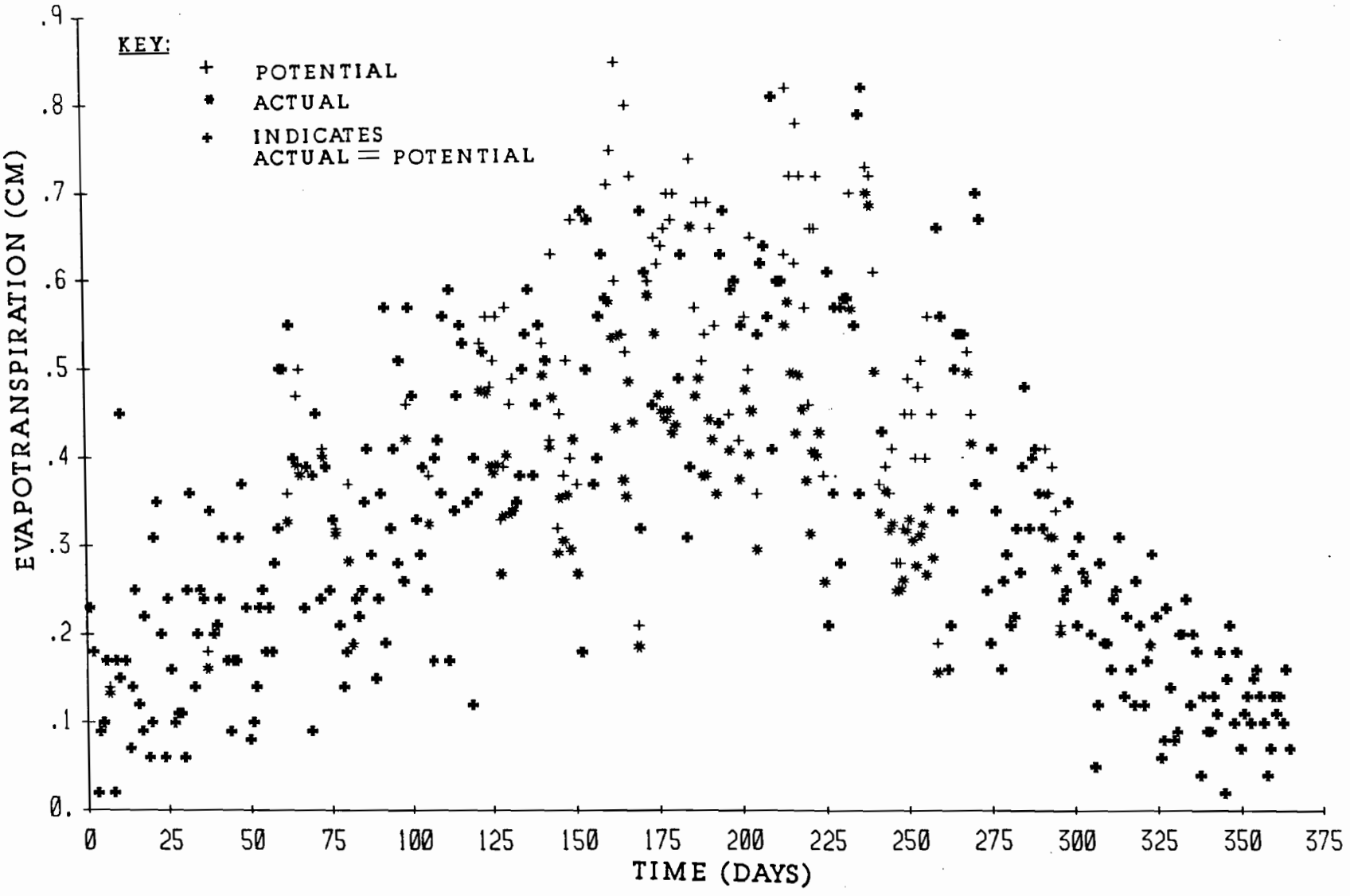

FIGURE B2.4 EVAPOTRANSPIRATION FOR FOURTH YEAR IN HOUSTON

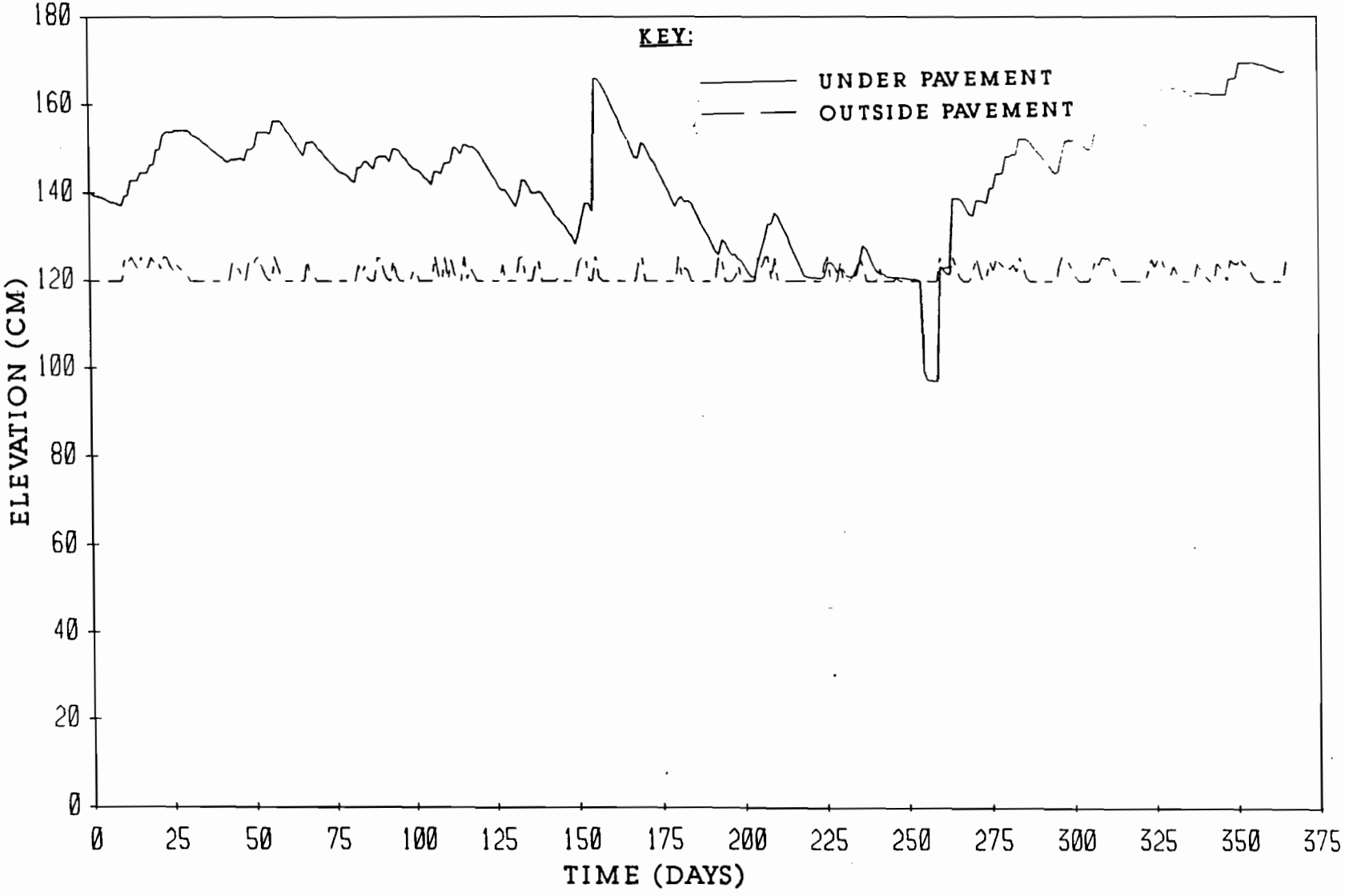

FIGURE B3.4 WATER LEVELS WITHIN THE CRACK FABRIC FOR FOURTH YEAR IN HOUSTON

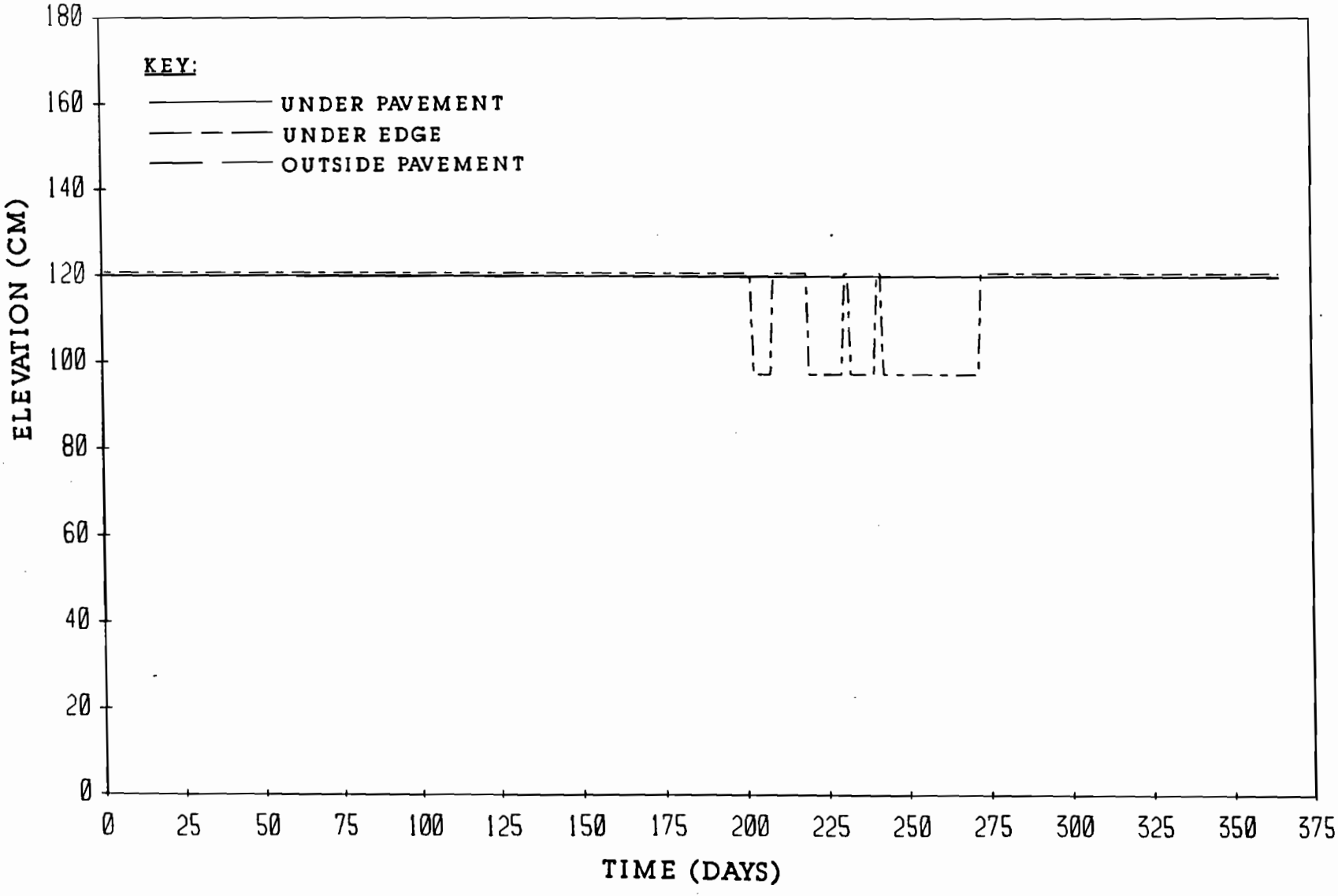

FIGURE B4.4 CRACK TIP ELEVATIONS FOR FOURTH YEAR IN HOUSTON

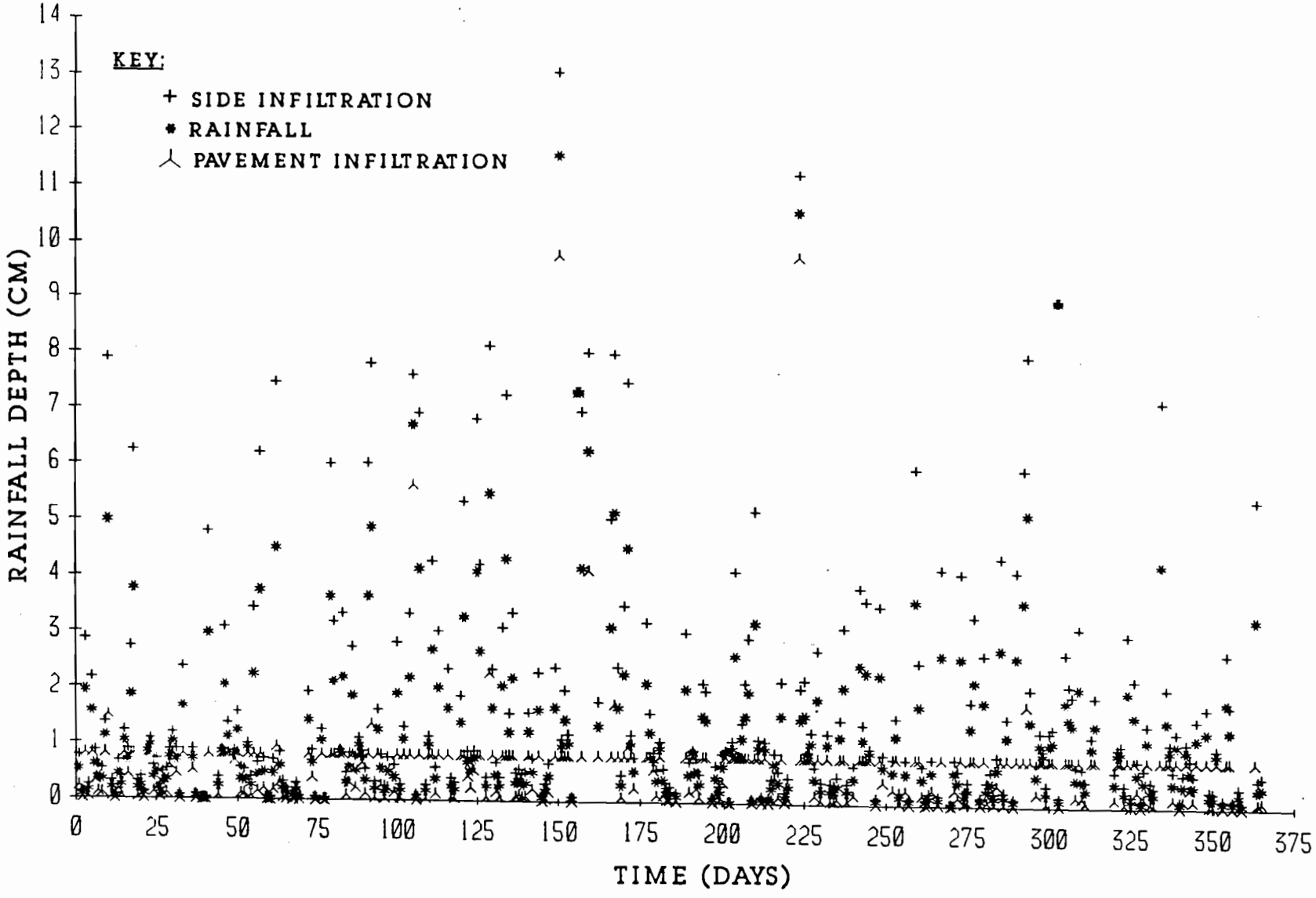

FIGURE B1.5 RAINFALL AND INFILTRATION DEPTHS FOR FIFTH YEAR IN HOUSTON

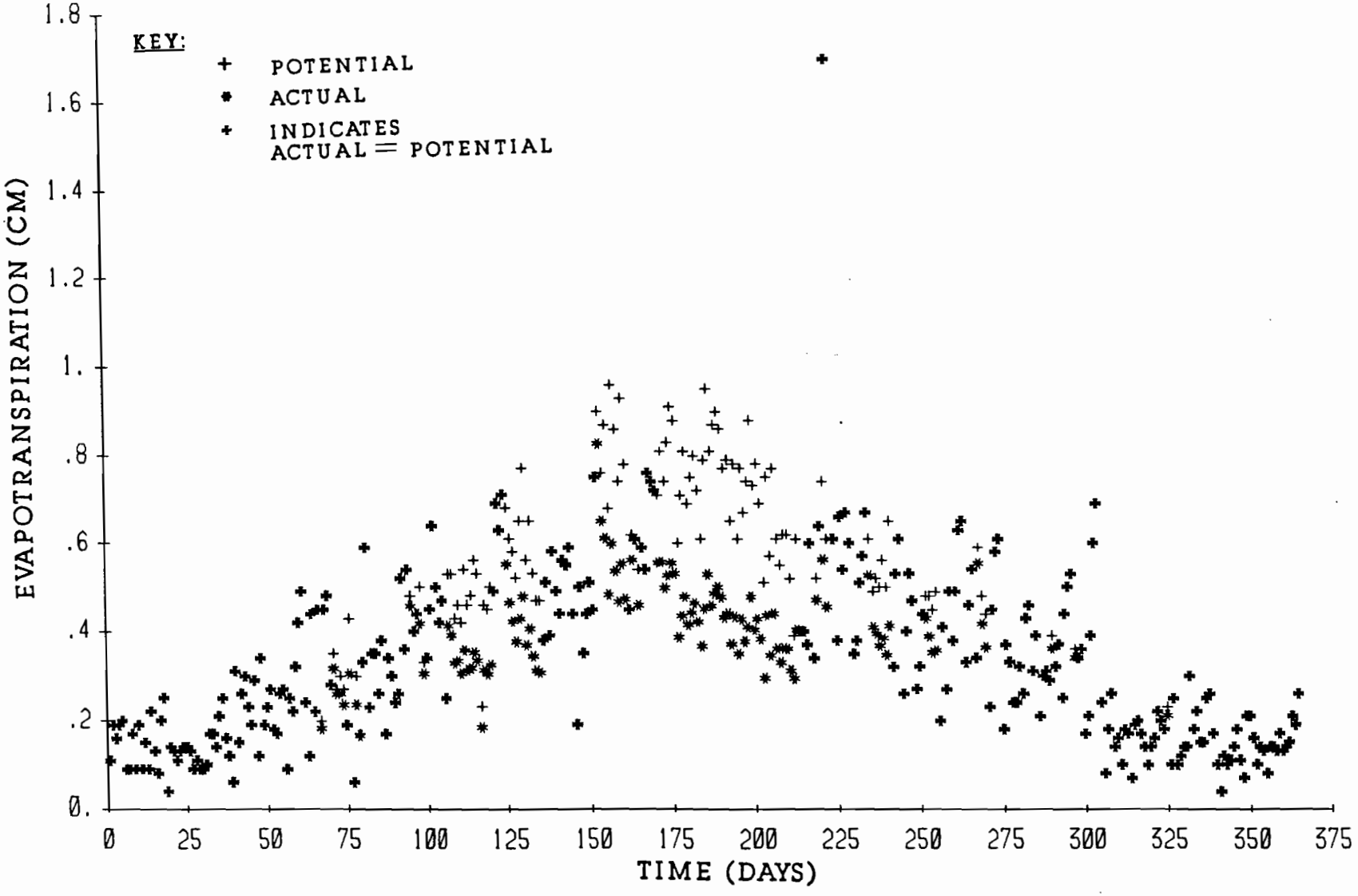

FIGURE B2.5 EVAPOTRANSPIRATION FOR FIFTH YEAR IN HOUSTON

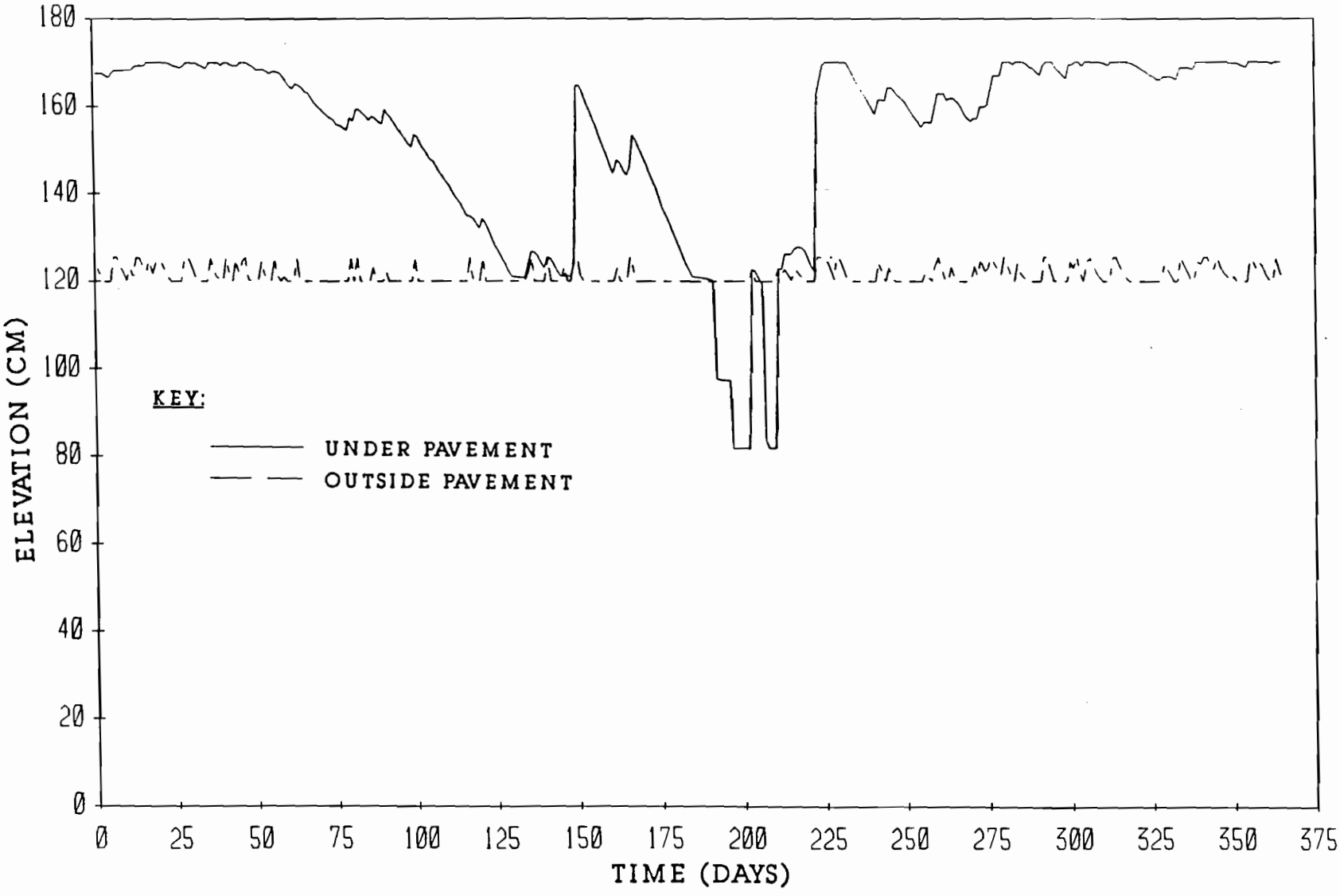

FIGURE B3.5 WATER LEVELS WITHIN THE CRACK FABRIC FOR FIFTH YEAR IN HOUSTON

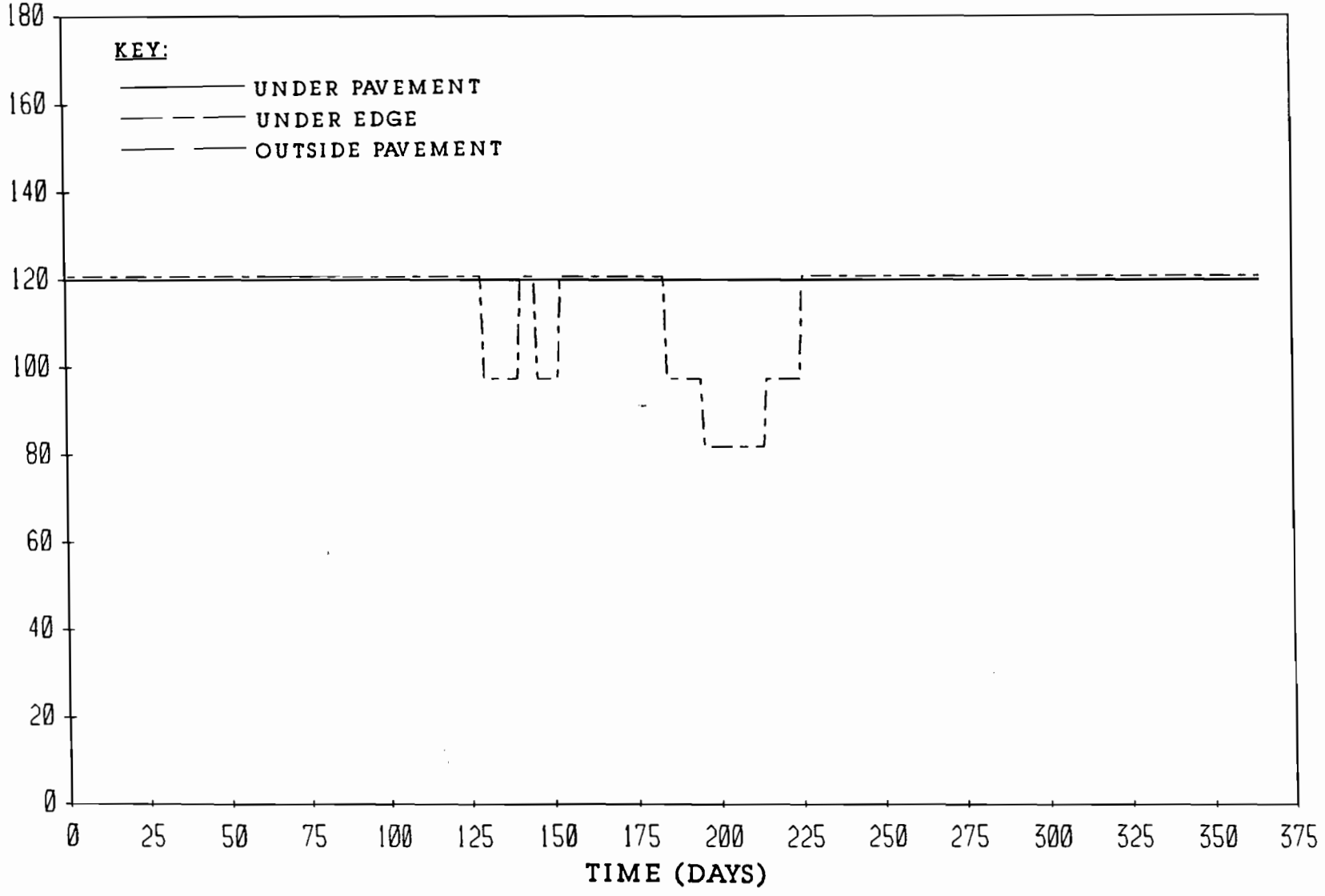

FIGURE B4.5 CRACK TIP ELEVATIONS FOR FIFTH YEAR IN HOUSTON

APPENDIX C

SIMULATION RESULTS FOR DALLAS - FORT WORTH

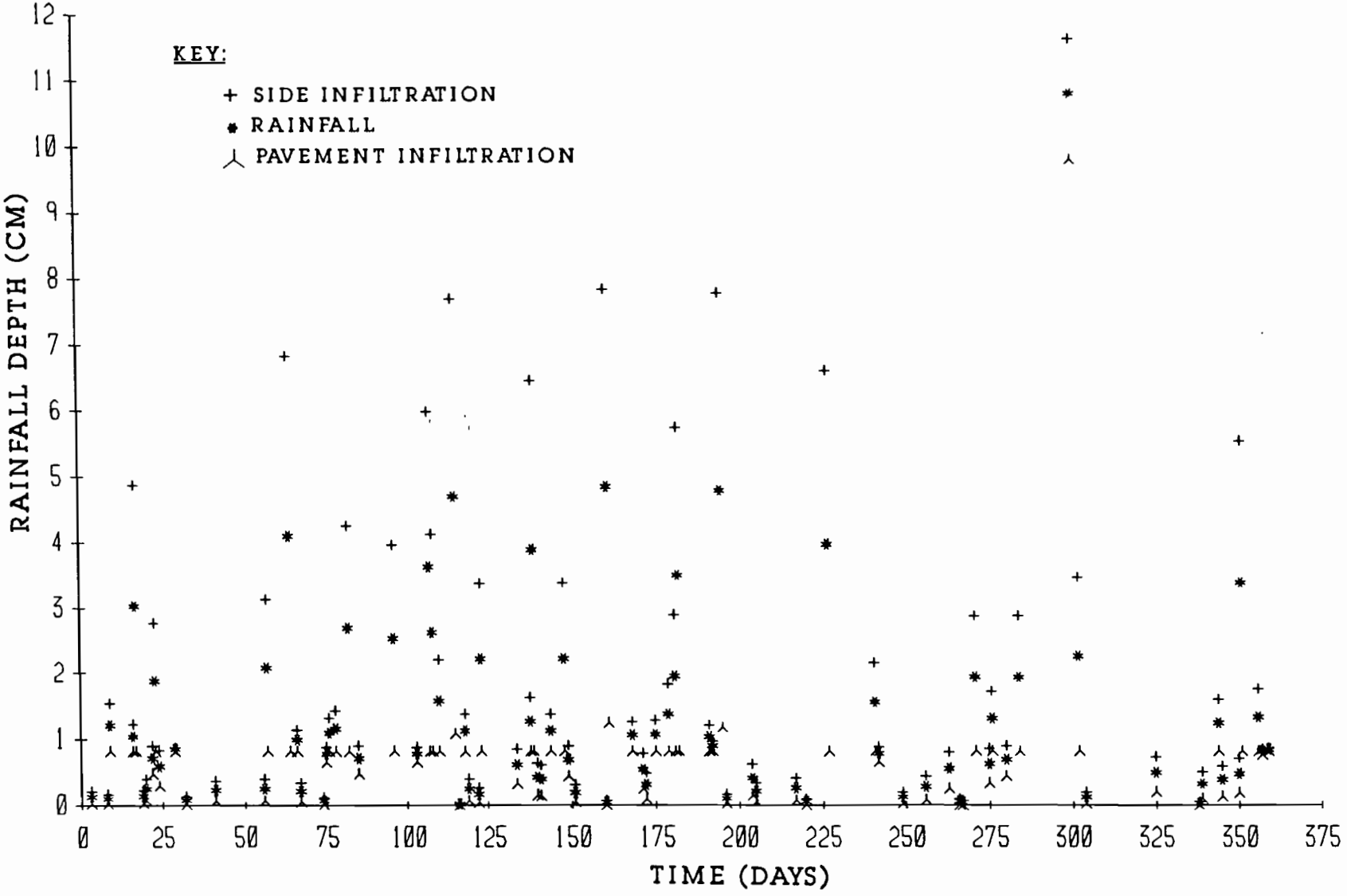

FIGURE C1.1 RAINFALL AND INFILTRATION DEPTHS FOR FIRST YEAR IN DALLAS - FORT WORTH

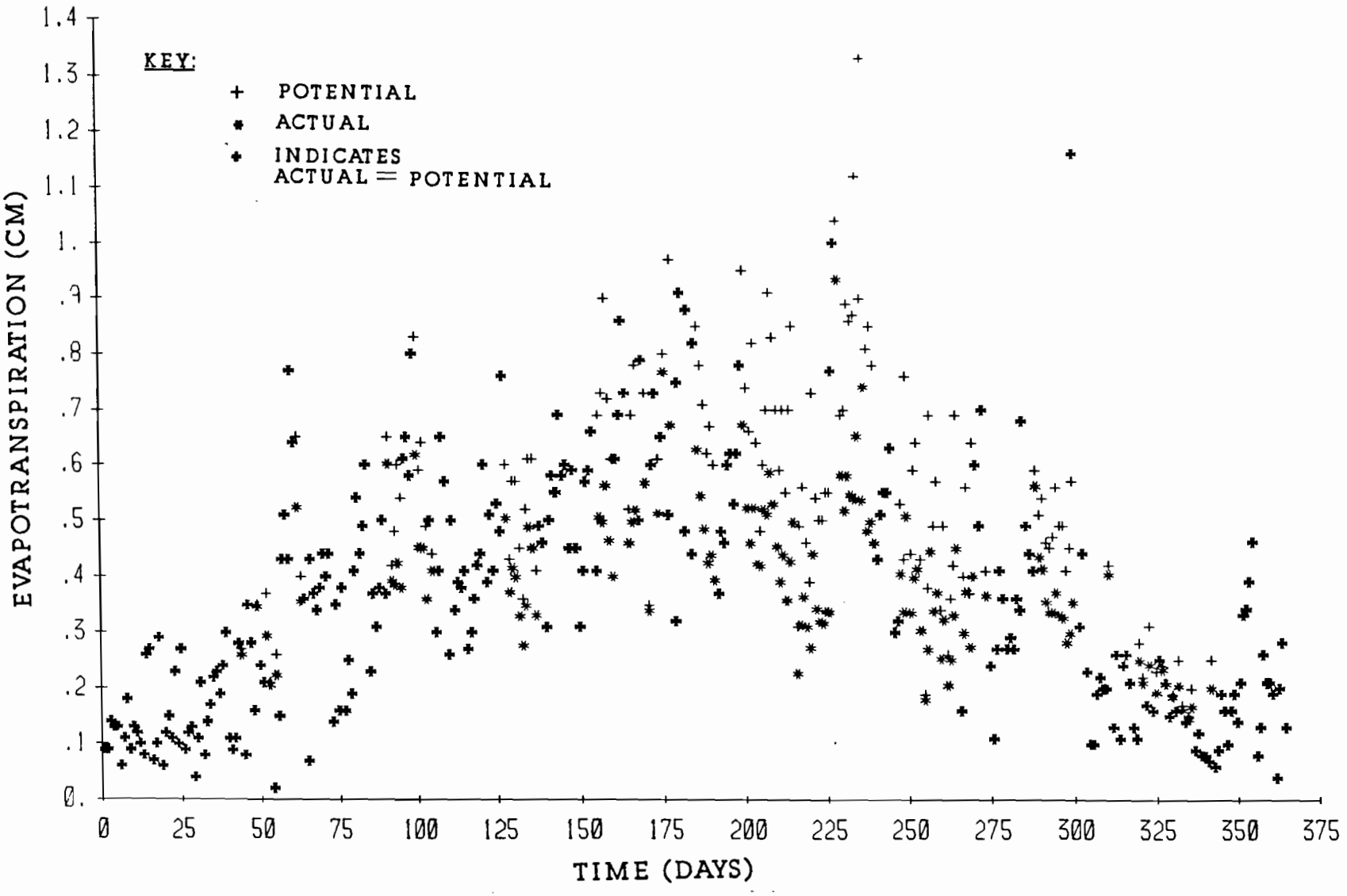

FIGURE C2.1 EVAPOTRANSPIRATION FOR FIRST YEAR IN DALLAS - FORT WORTH

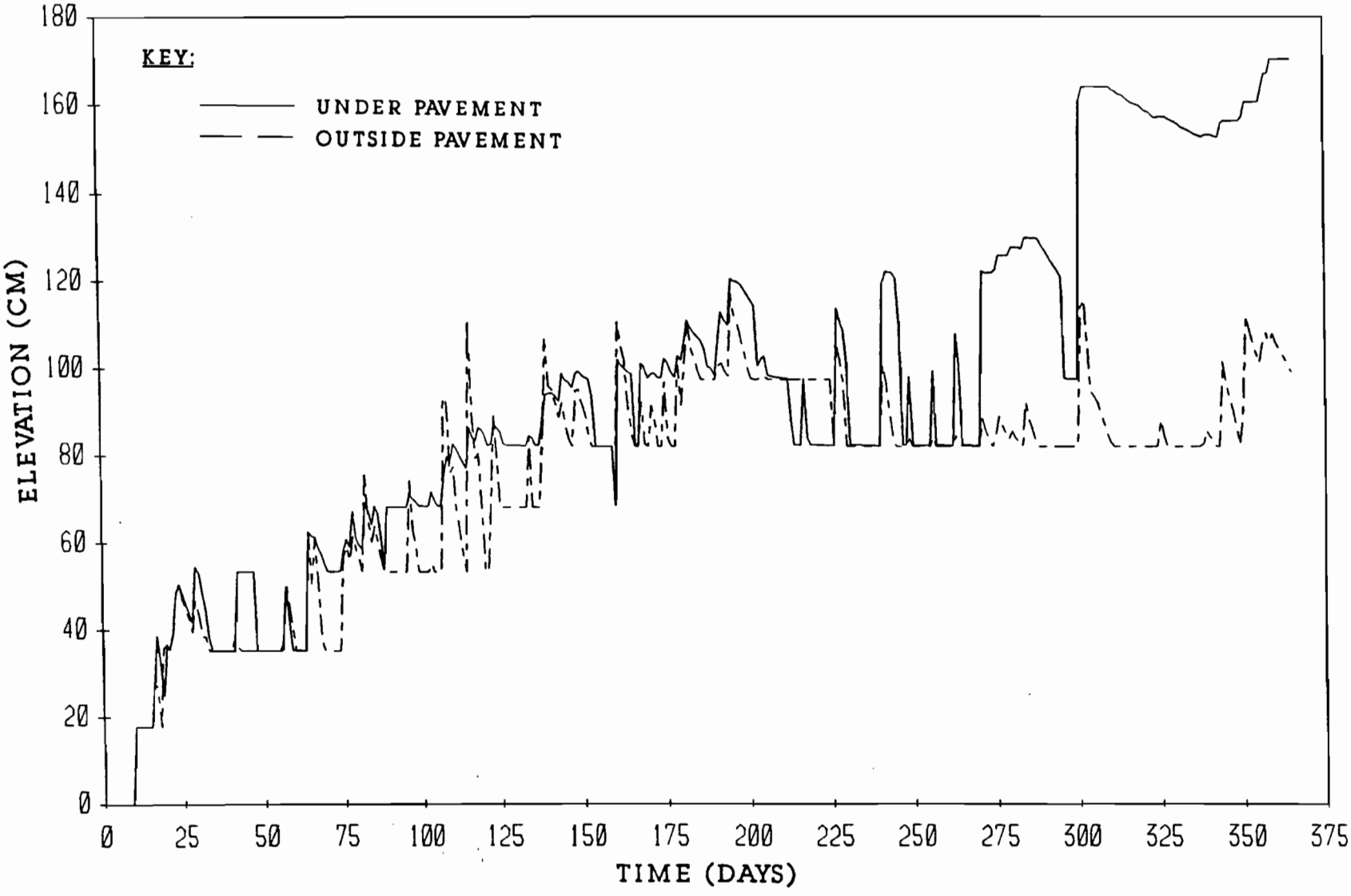

FIGURE C3.1 WATER LEVELS WITHIN THE CRACK FABRIC FOR FIRST YEAR IN DALLAS - FORT WORTH

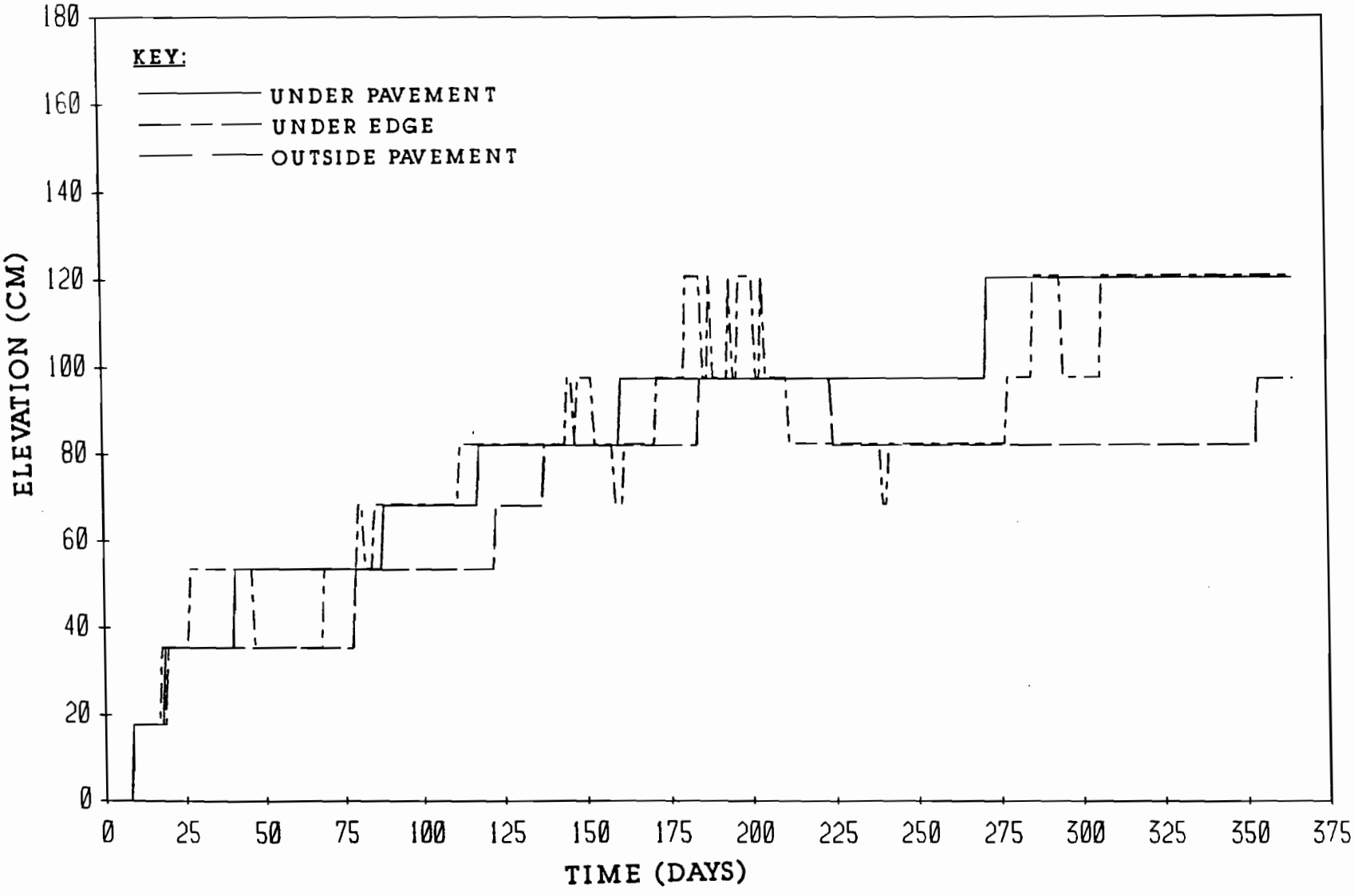

FIGURE C4.1 CRACK TIP ELEVATIONS FOR FIRST YEAR IN DALLAS - FORT WORTH

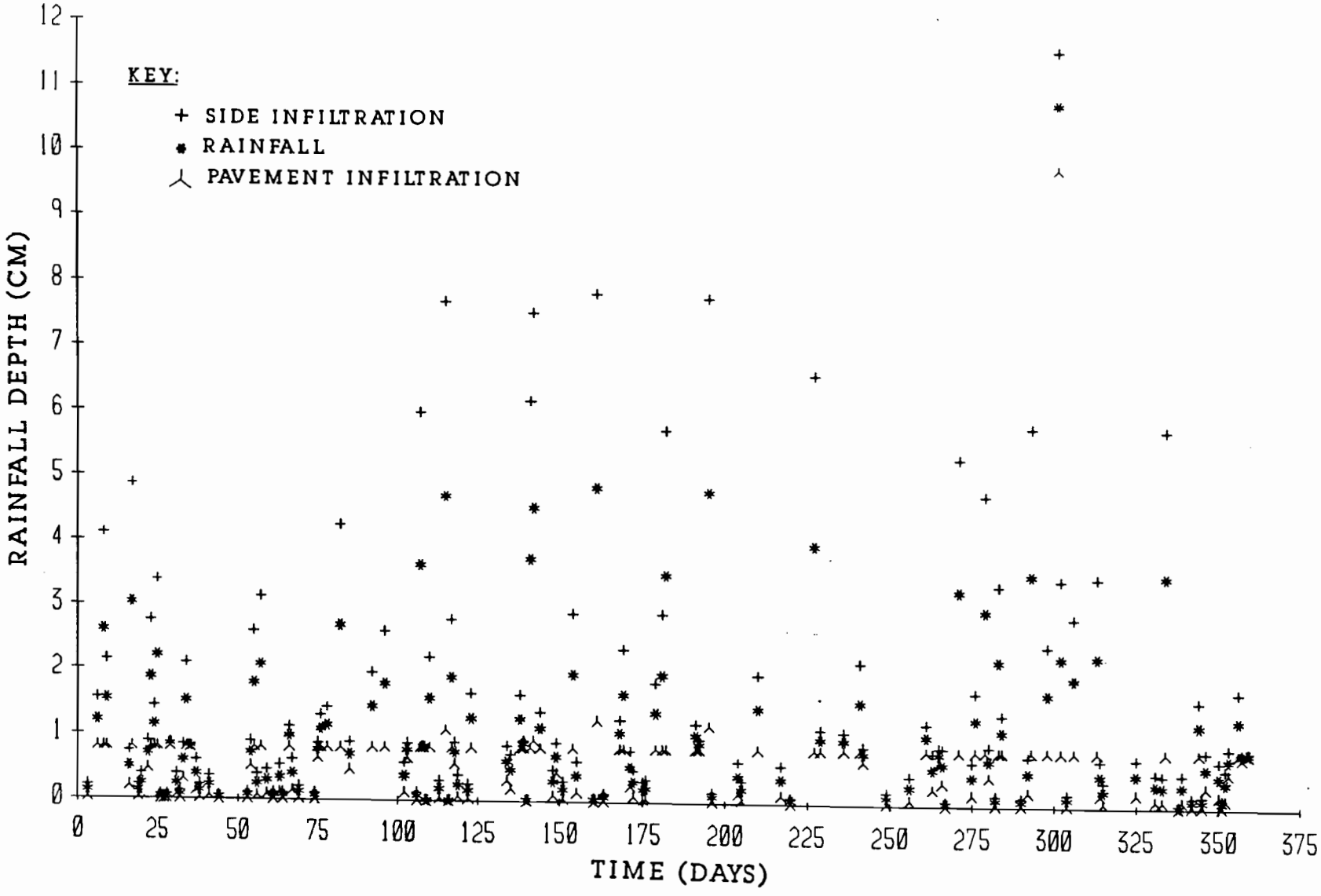

FIGURE C1.2 RAINFALL AND INFILTRATION DEPTHS FOR SECOND YEAR IN DALLAS - FORT WORTH

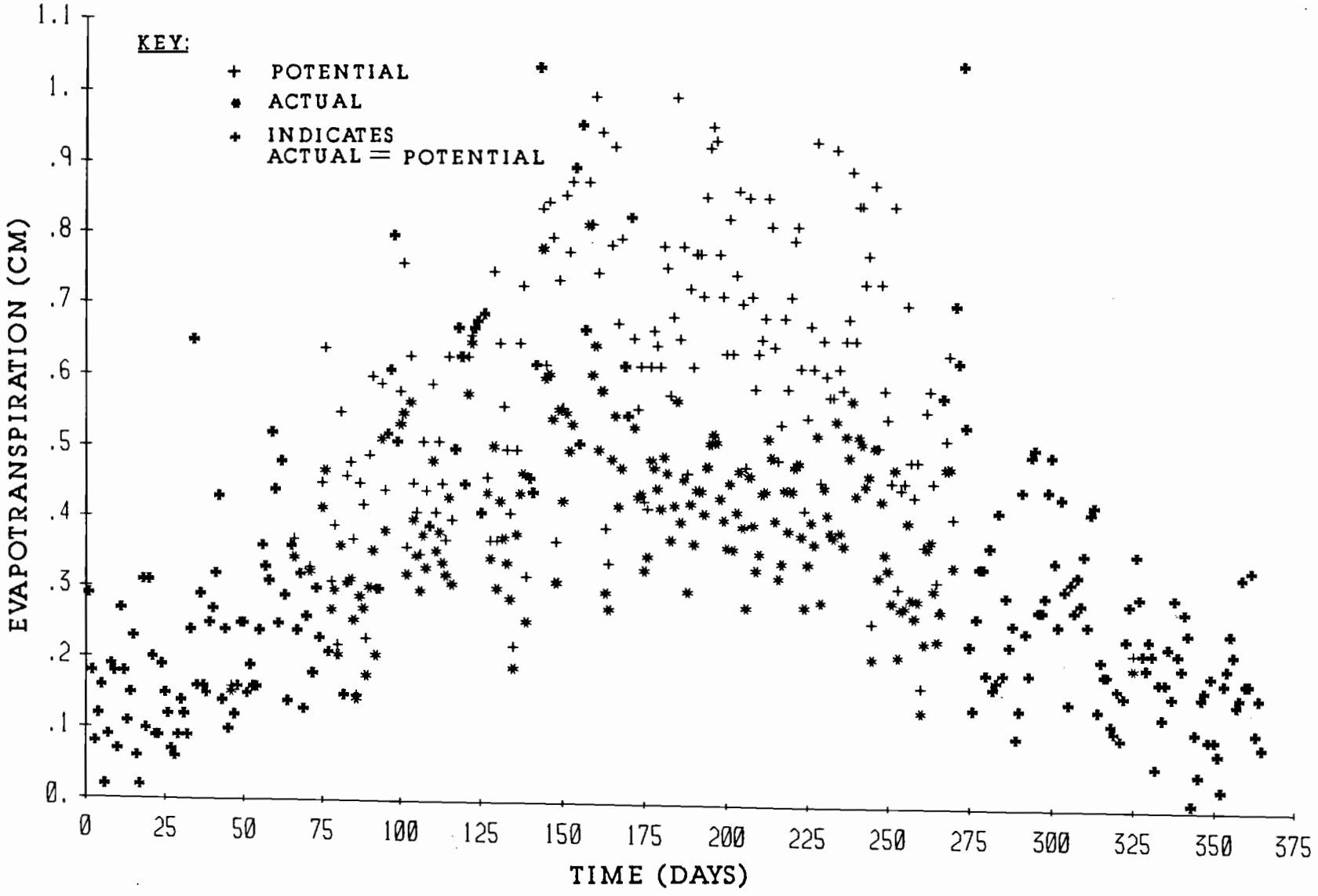

FIGURE C2.2 EVAPOTRANSPIRATION FOR SECOND YEAR IN DALLAS - FORT WORTH

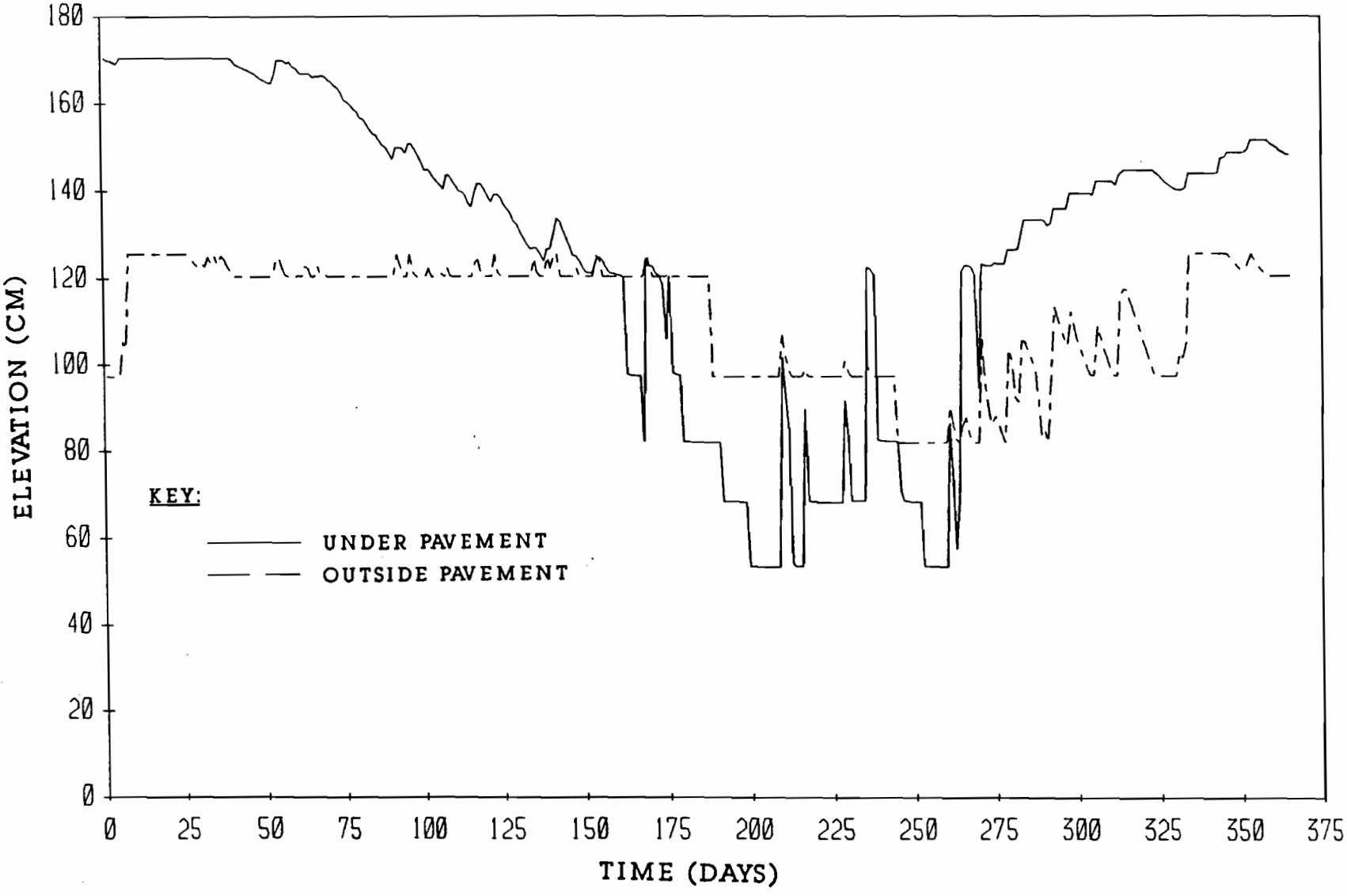

FIGURE C3.2 WATER LEVELS WITHIN THE CRACK FABRIC FOR SECOND YEAR IN DALLAS - FORT WORTH

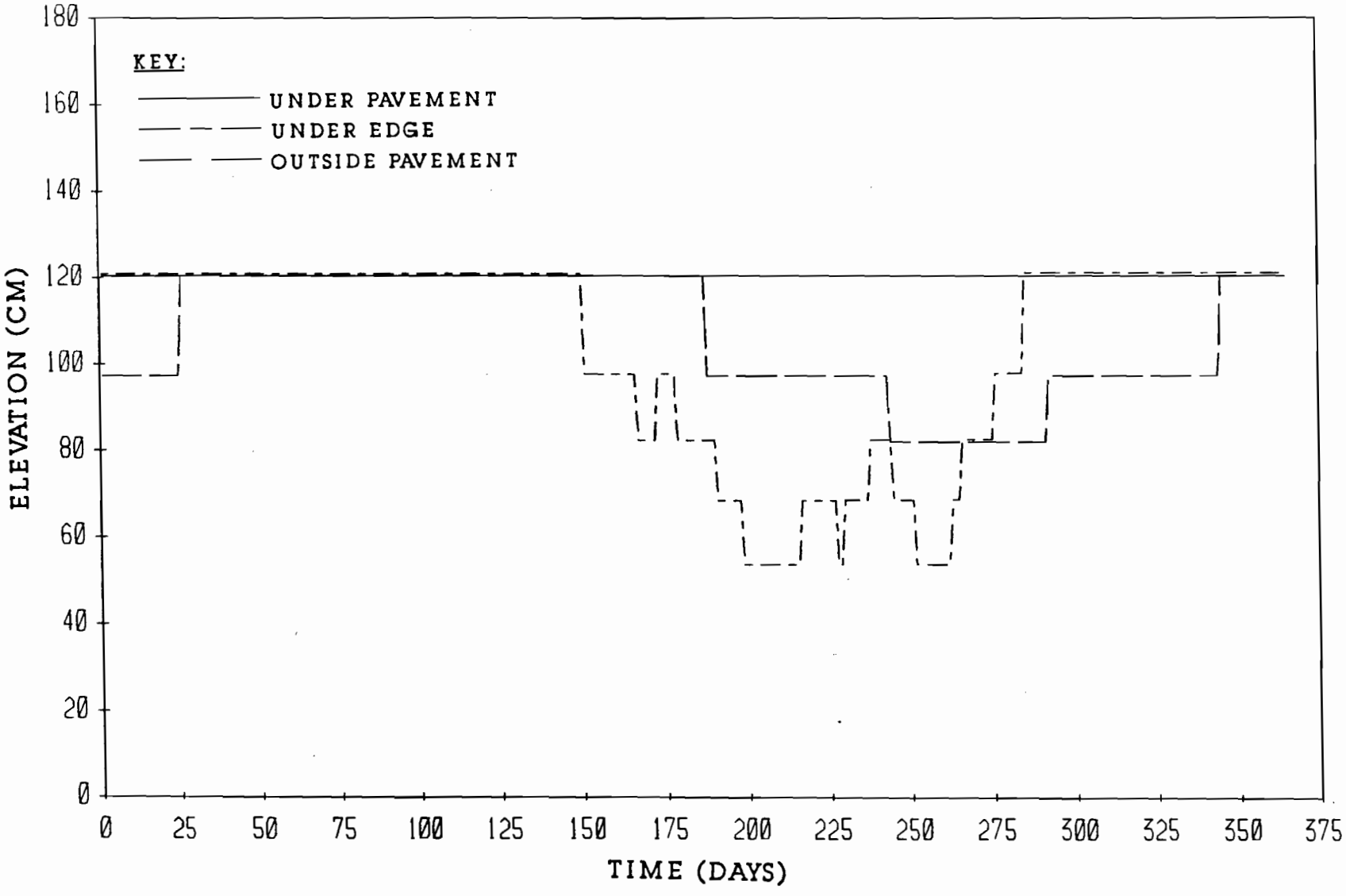

FIGURE C4.2 CRACK TIP ELEVATIONS FOR SECOND YEAR IN DALLAS - FORT WORTH

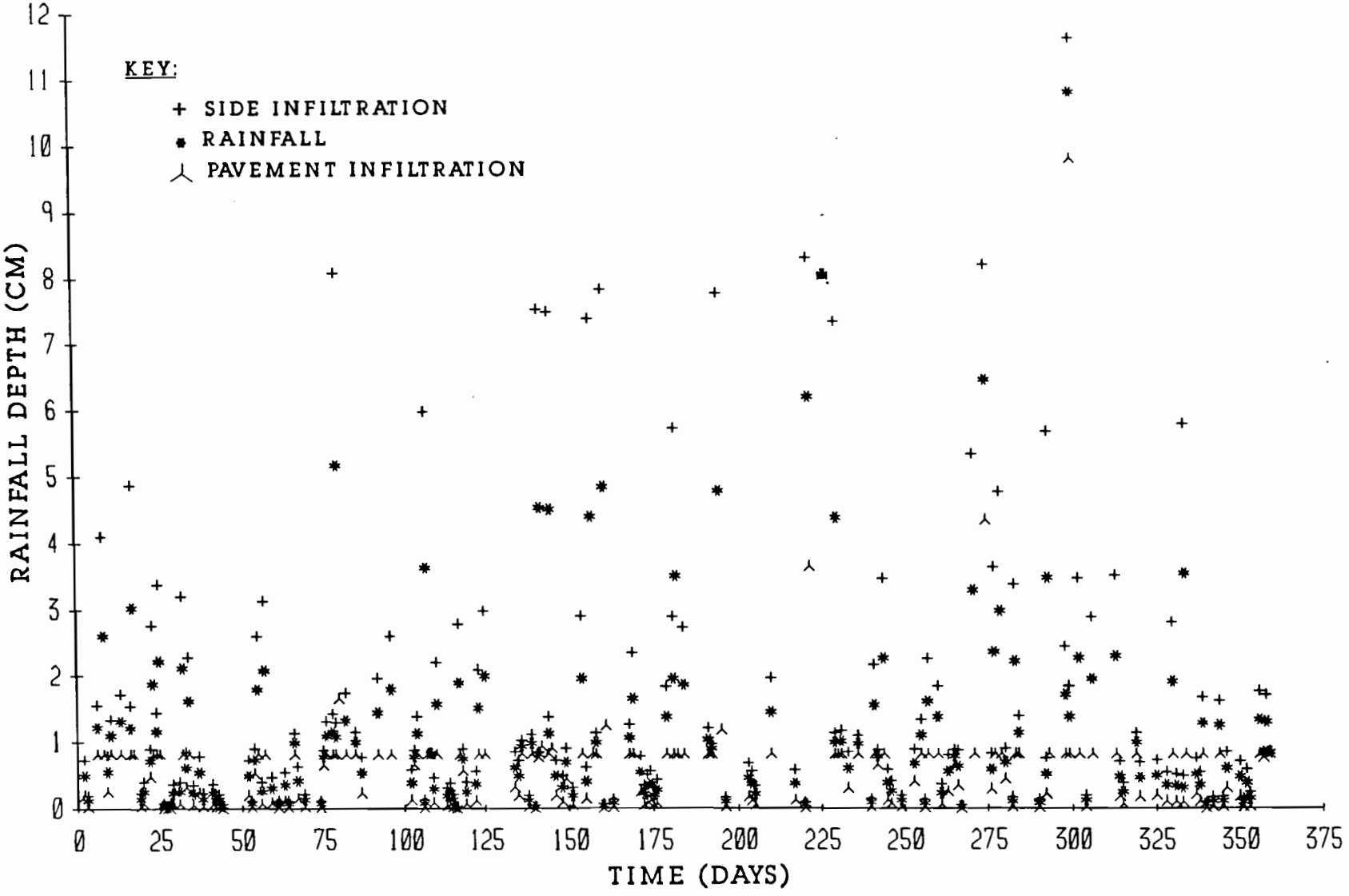

FIGURE C1.3 RAINFALL AND INFILTRATION DEPTHS FOR THIRD YEAR IN DALLAS - FORT WORTH

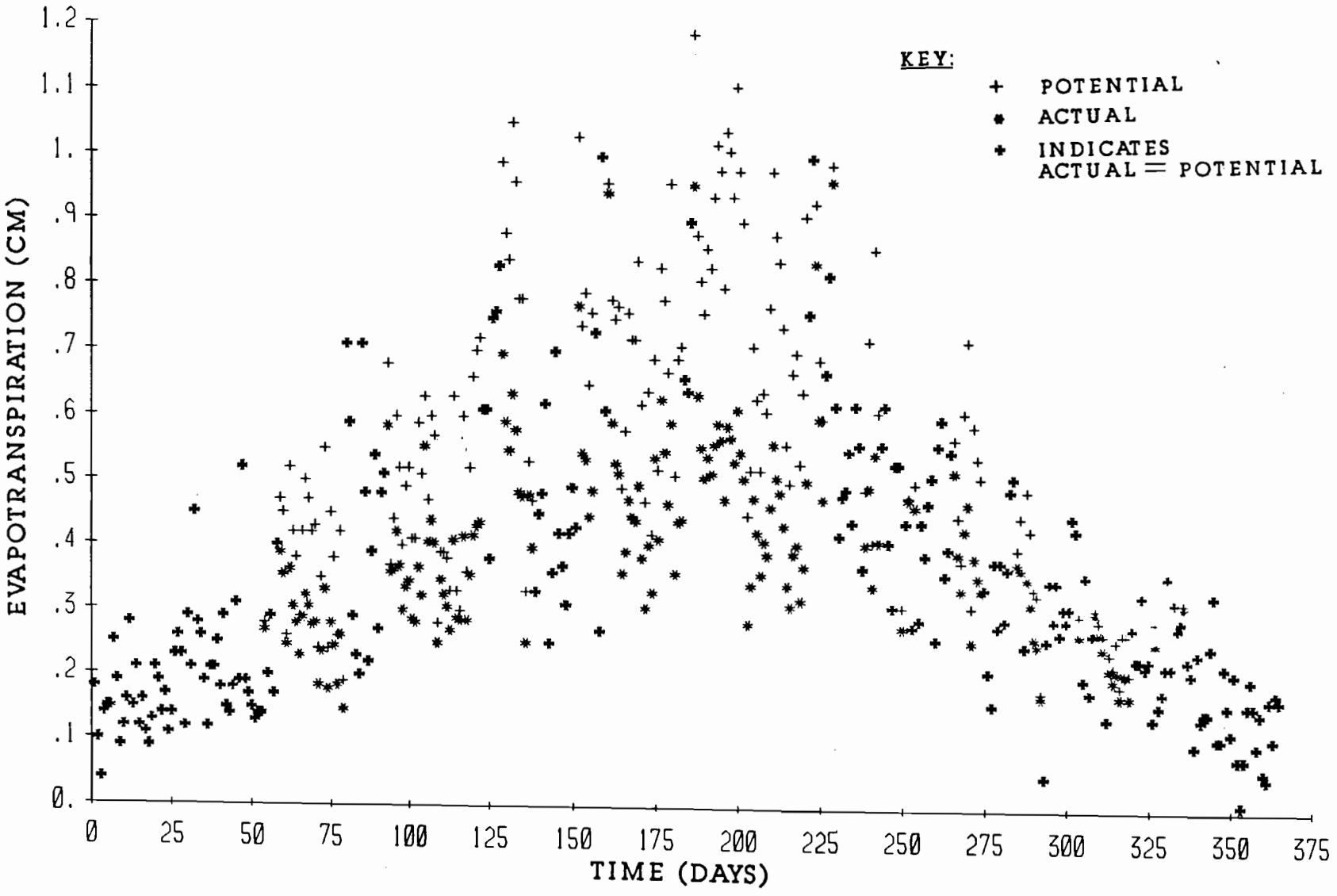

FIGURE C2.3 EVAPOTRANSPIRATION FOR THIRD YEAR IN FORT WORTH

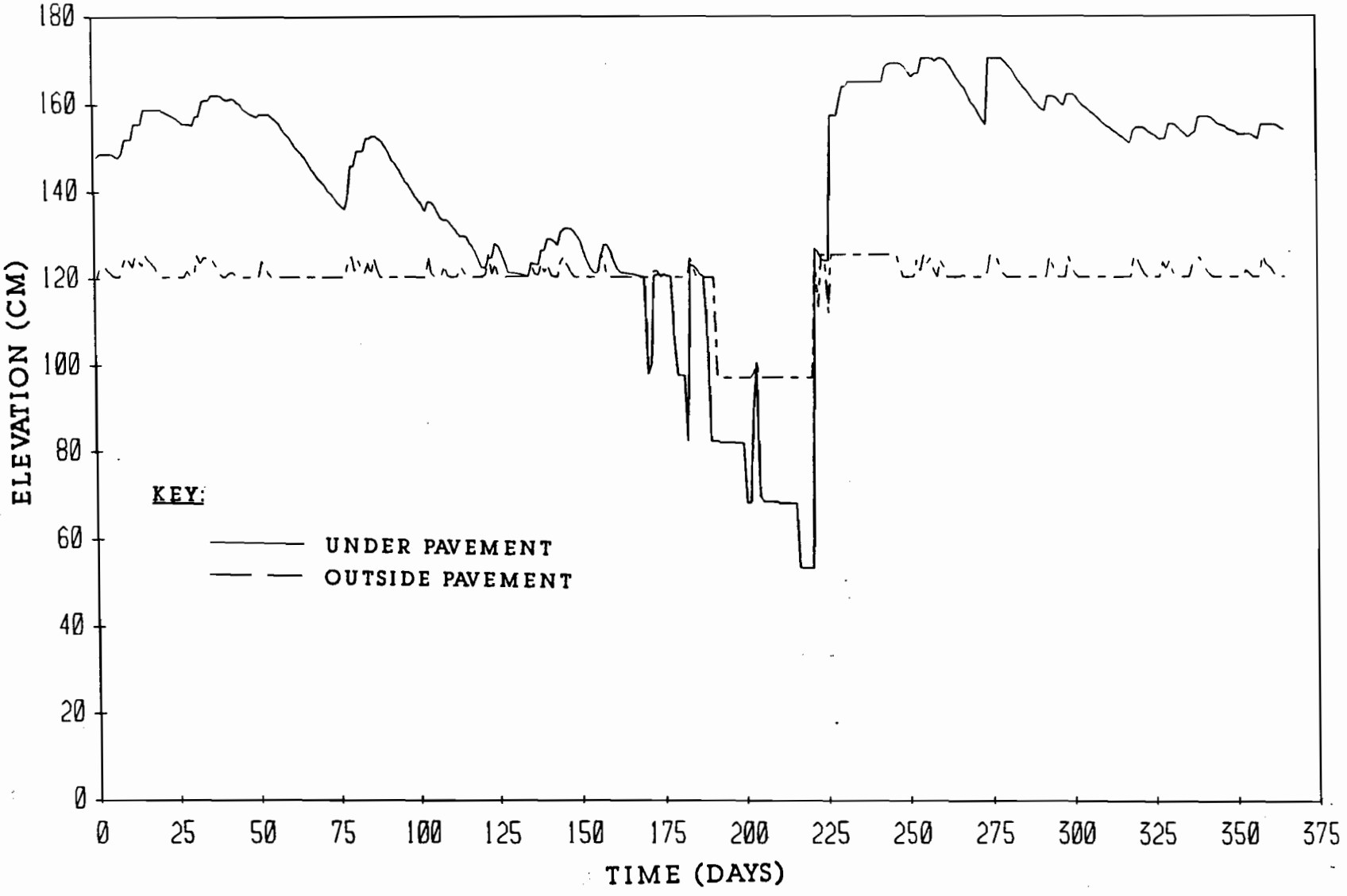

FIGURE C3.3 WATER LEVELS WITHIN THE CRACK FABRIC FOR THIRD YEAR IN DALLAS - FORT WORTH

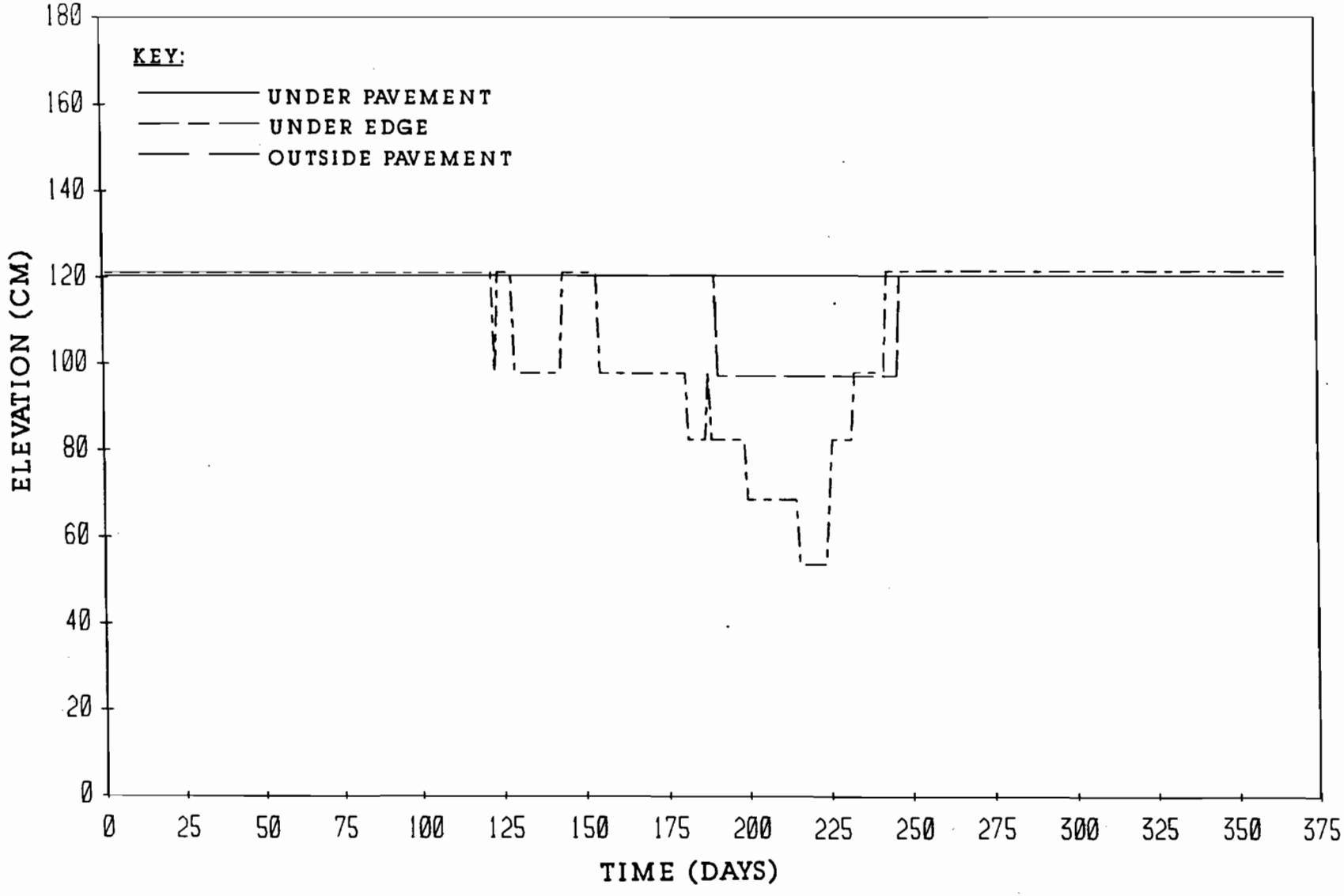

FIGURE C4.3 CRACK TIP ELEVATIONS FOR THIRD YEAR IN DALLAS - FORT WORTH

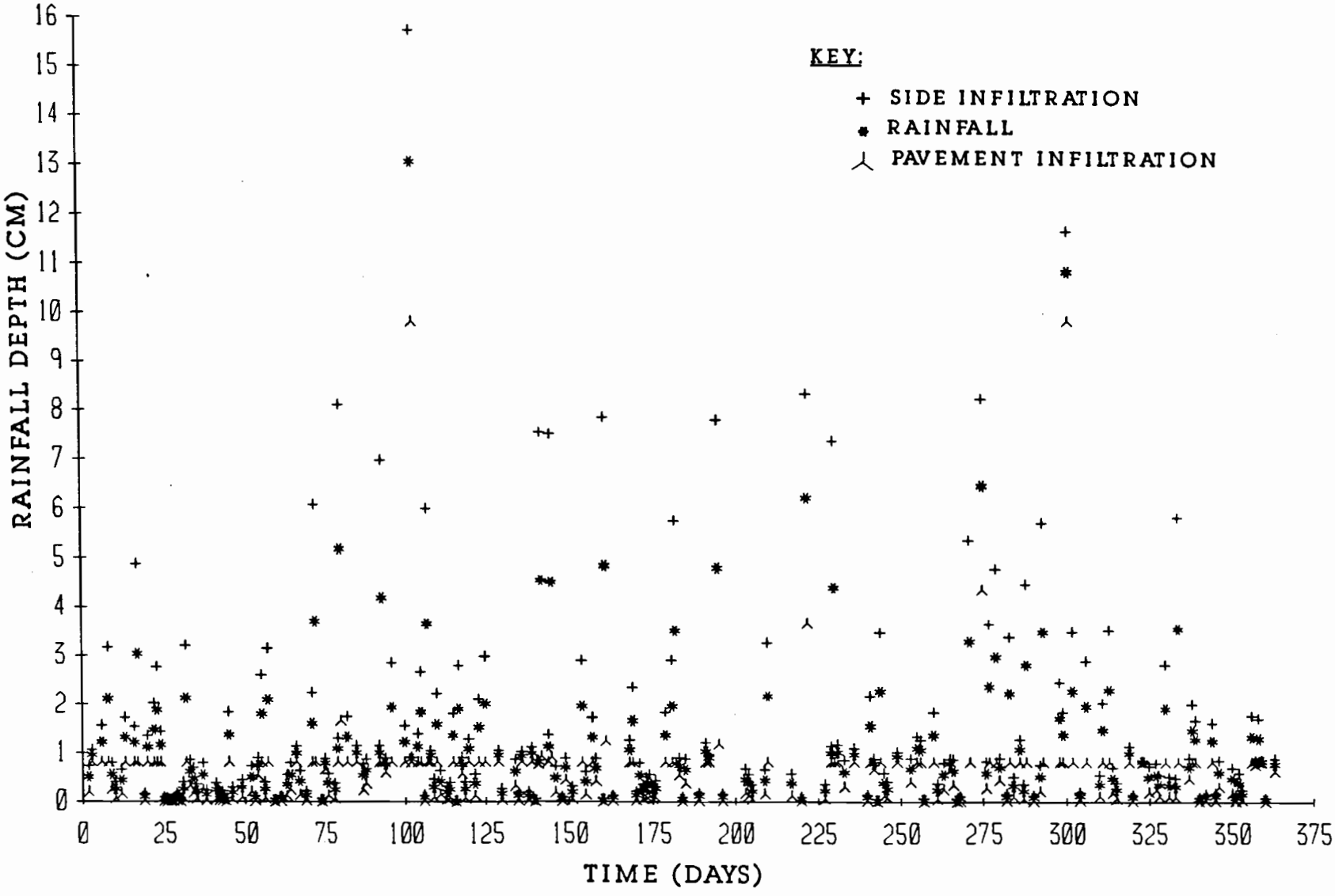

FIGURE C1.4 RAINFALL AND INFILTRATION DEPTHS FOR FOURTH YEAR IN DALLAS - FORT WORTH

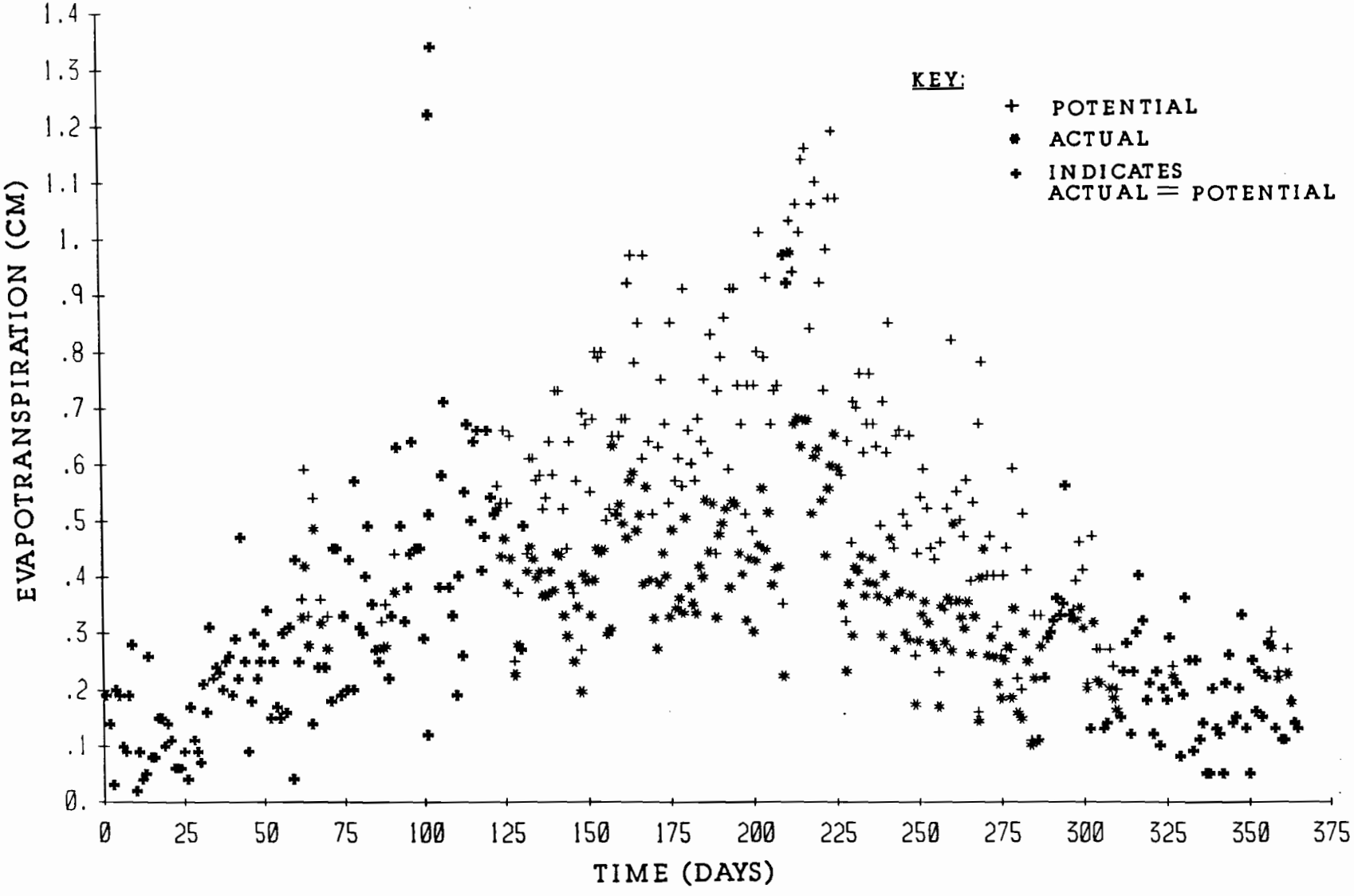

FIGURE C2.4 EVAPOTRANSPIRATION FOR FOURTH YEAR IN DALLAS - FORT WORTH

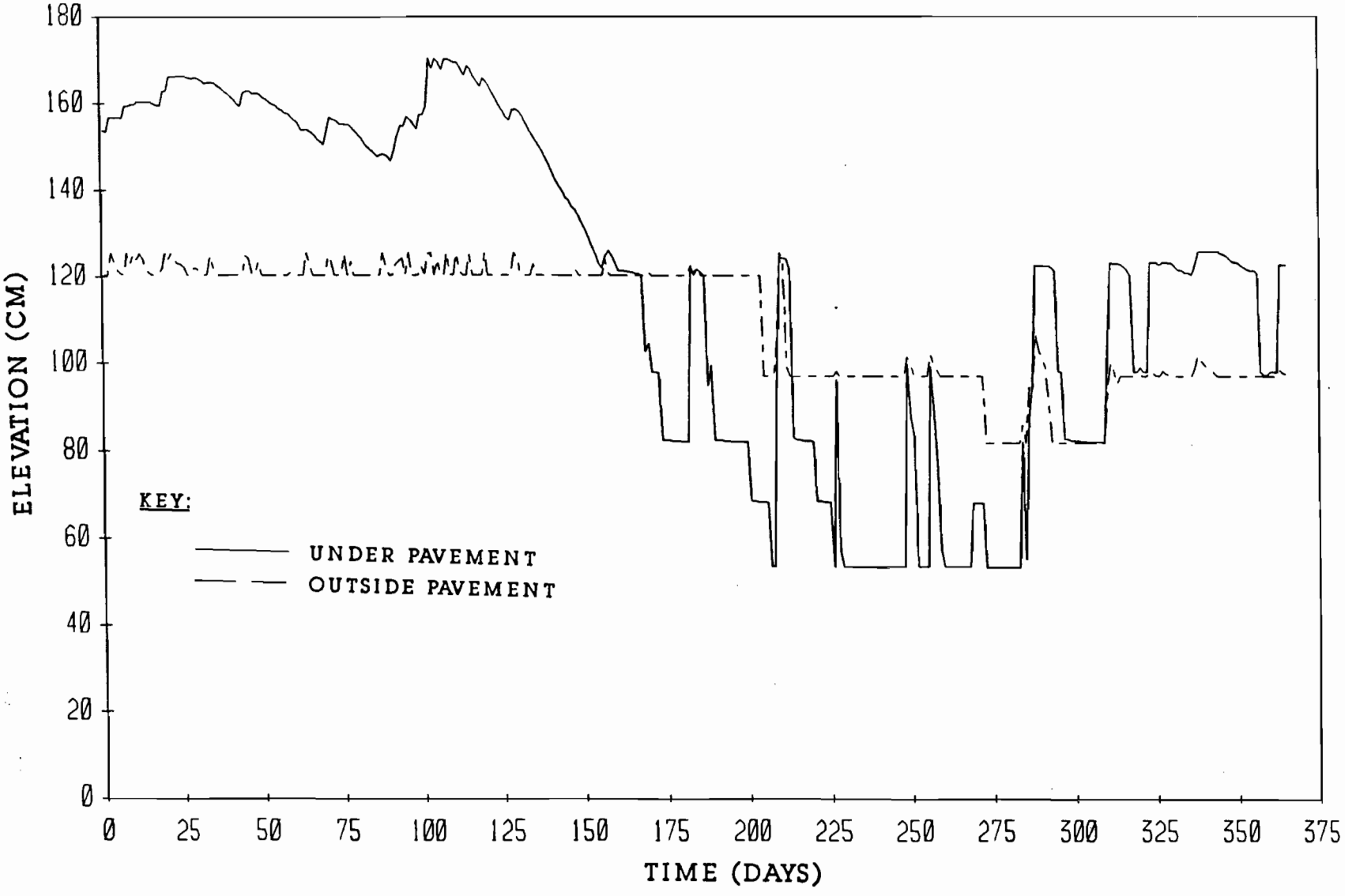

FIGURE C3.4 WATER LEVELS WITHIN THE CRACK FABRIC FOR FOURTH YEAR IN DALLAS - FORT WORTH

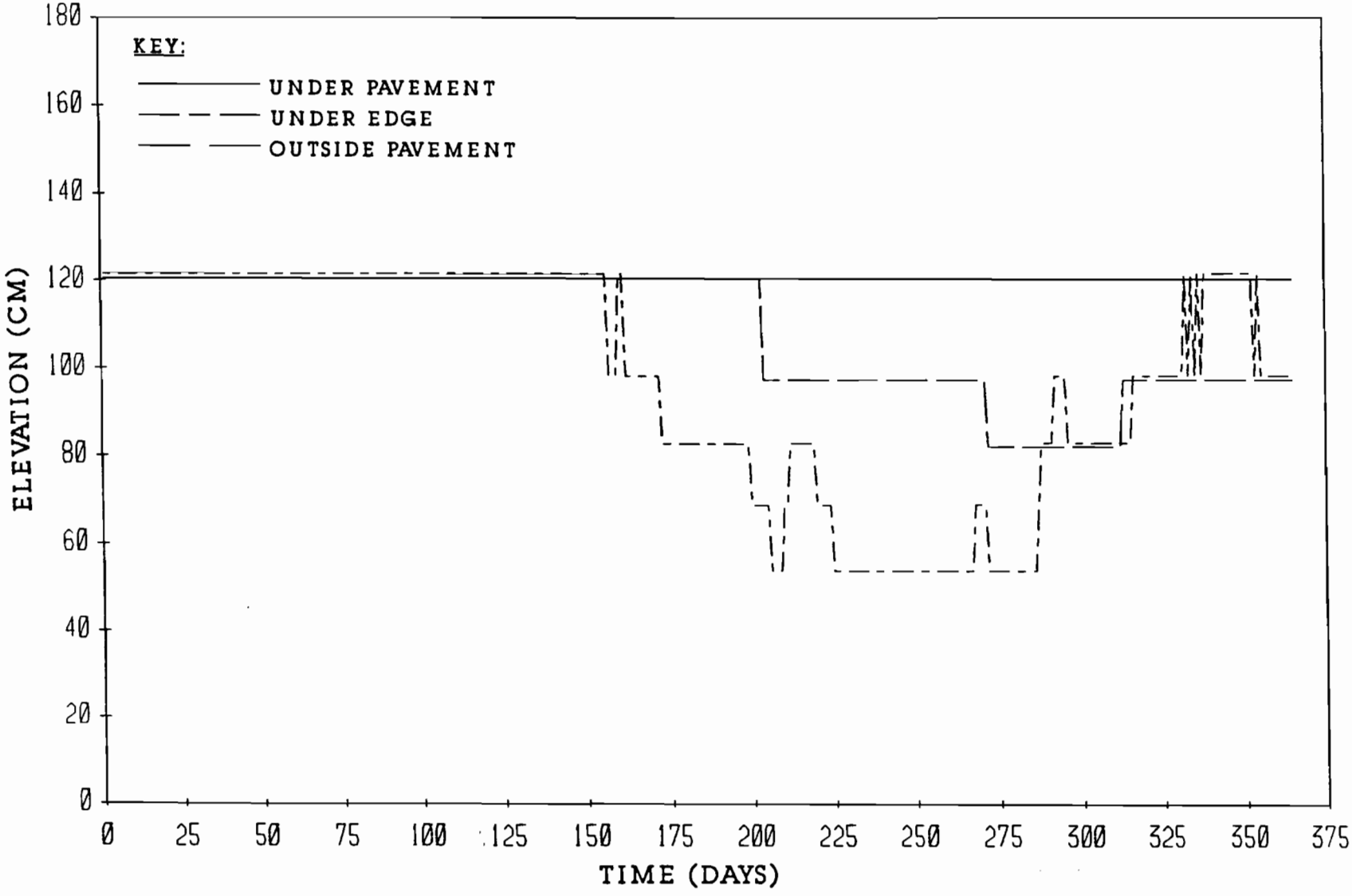

FIGURE C4.4 CRACK TIP ELEVATIONS FOR FOURTH YEAR IN DALLAS - FORT WORTH

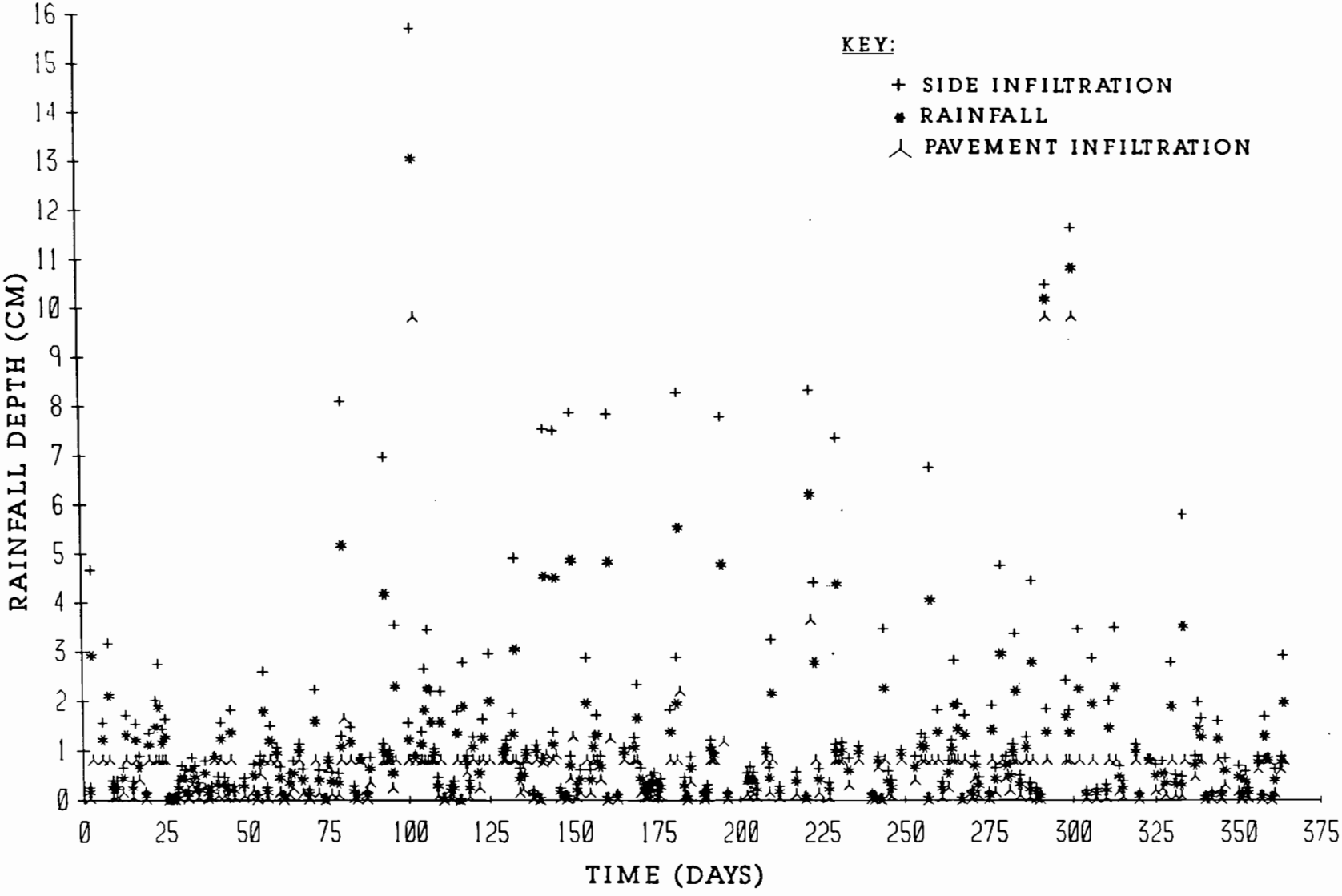

FIGURE C1.5 RAINFALL AND INFILTRATION DEPTHS FOR FIFTH YEAR IN DALLAS - FORT WORTH

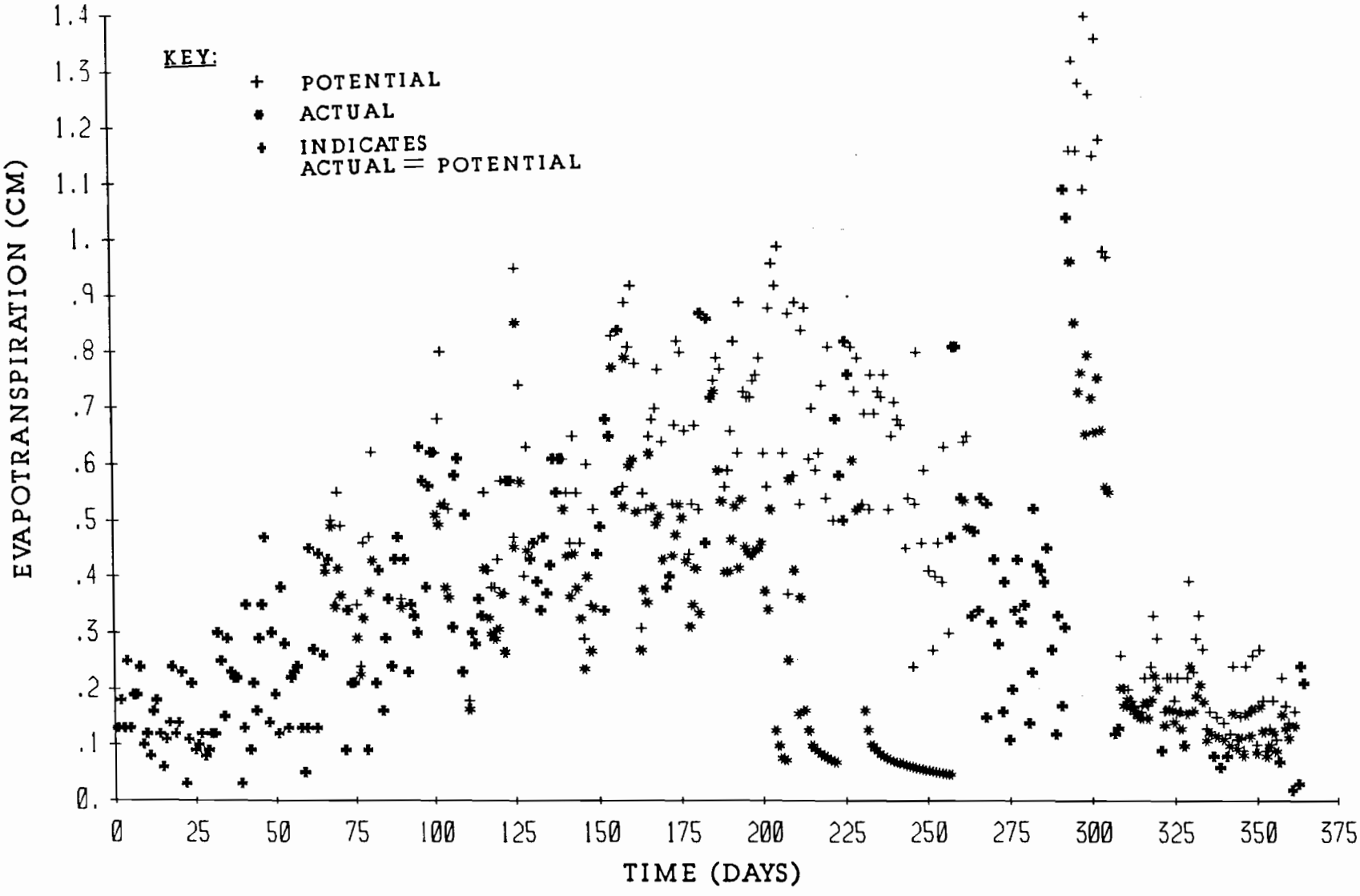

FIGURE C2.5 EVAPOTRANSPIRATION FOR FIFTH YEAR IN DALLAS - FORT WORTH

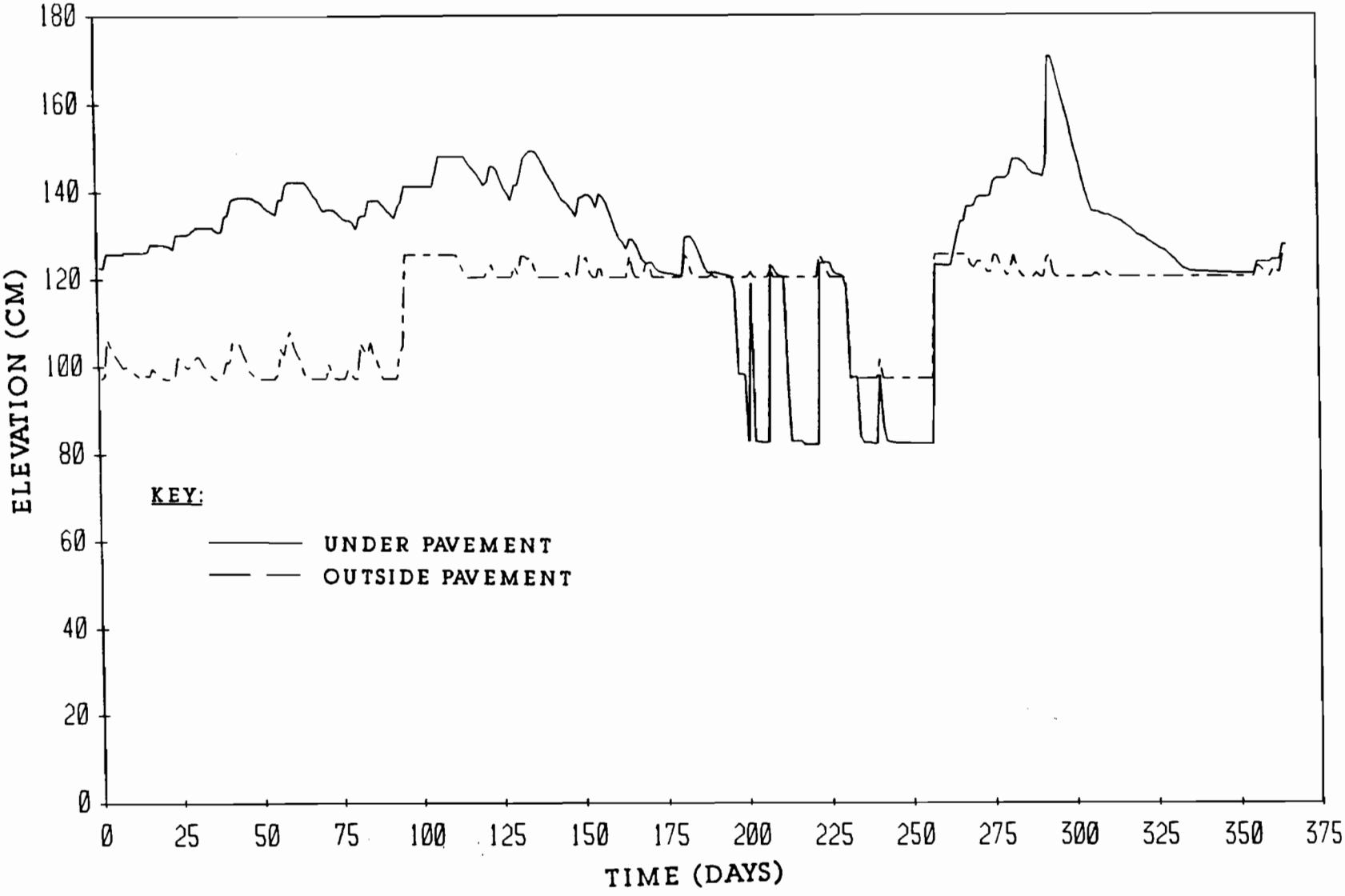

FIGURE C3.5 WATER LEVELS WITHIN THE CRACK FABRIC FOR FIFTH YEAR IN DALLAS - FORT WORTH

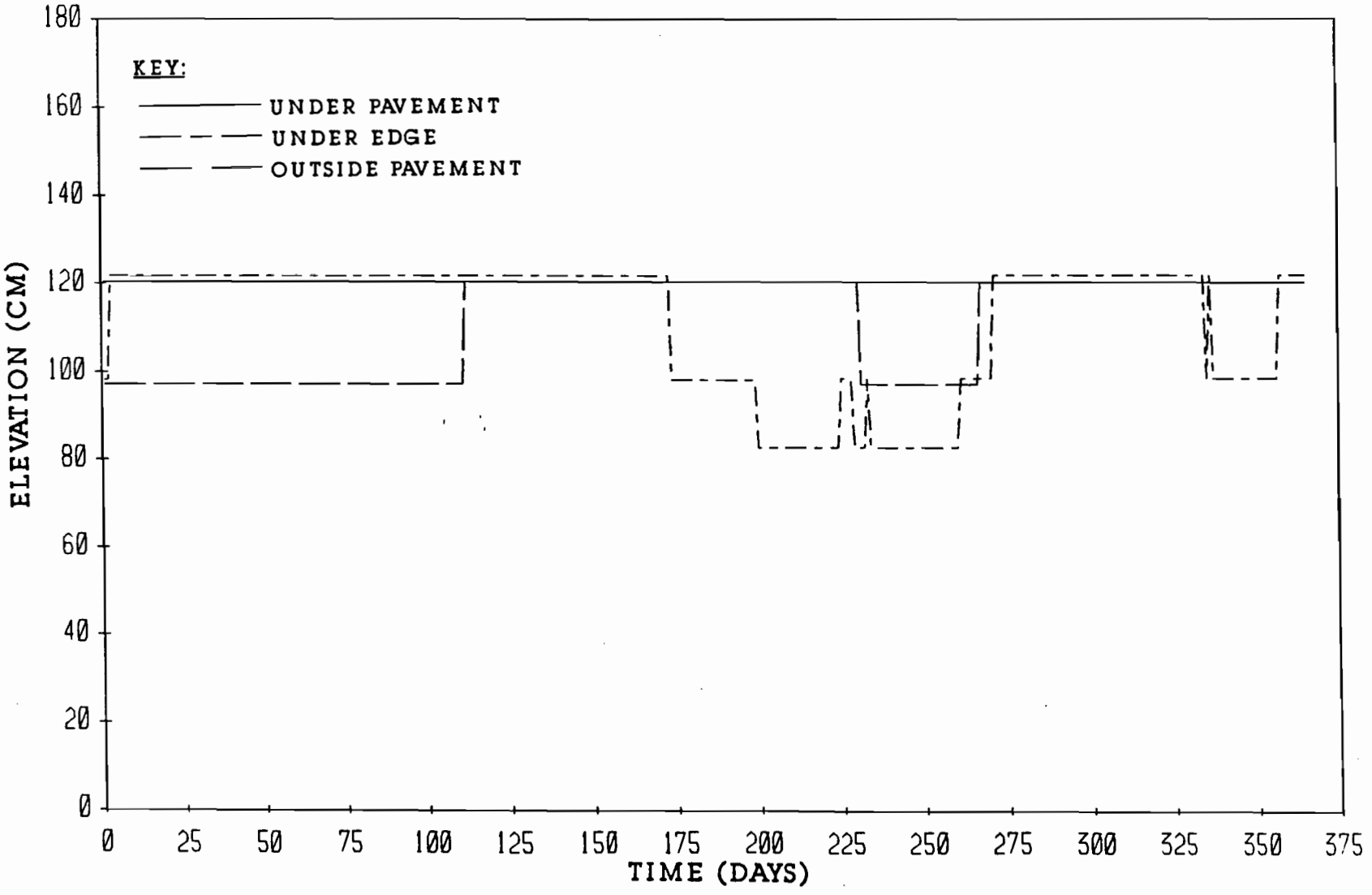

FIGURE C4.5 CRACK TIP ELEVATIONS FOR FIFTH YEAR IN DALLAS - FORT WORTH

APPENDIX D

SIMULATION RESULTS FOR EL PASO

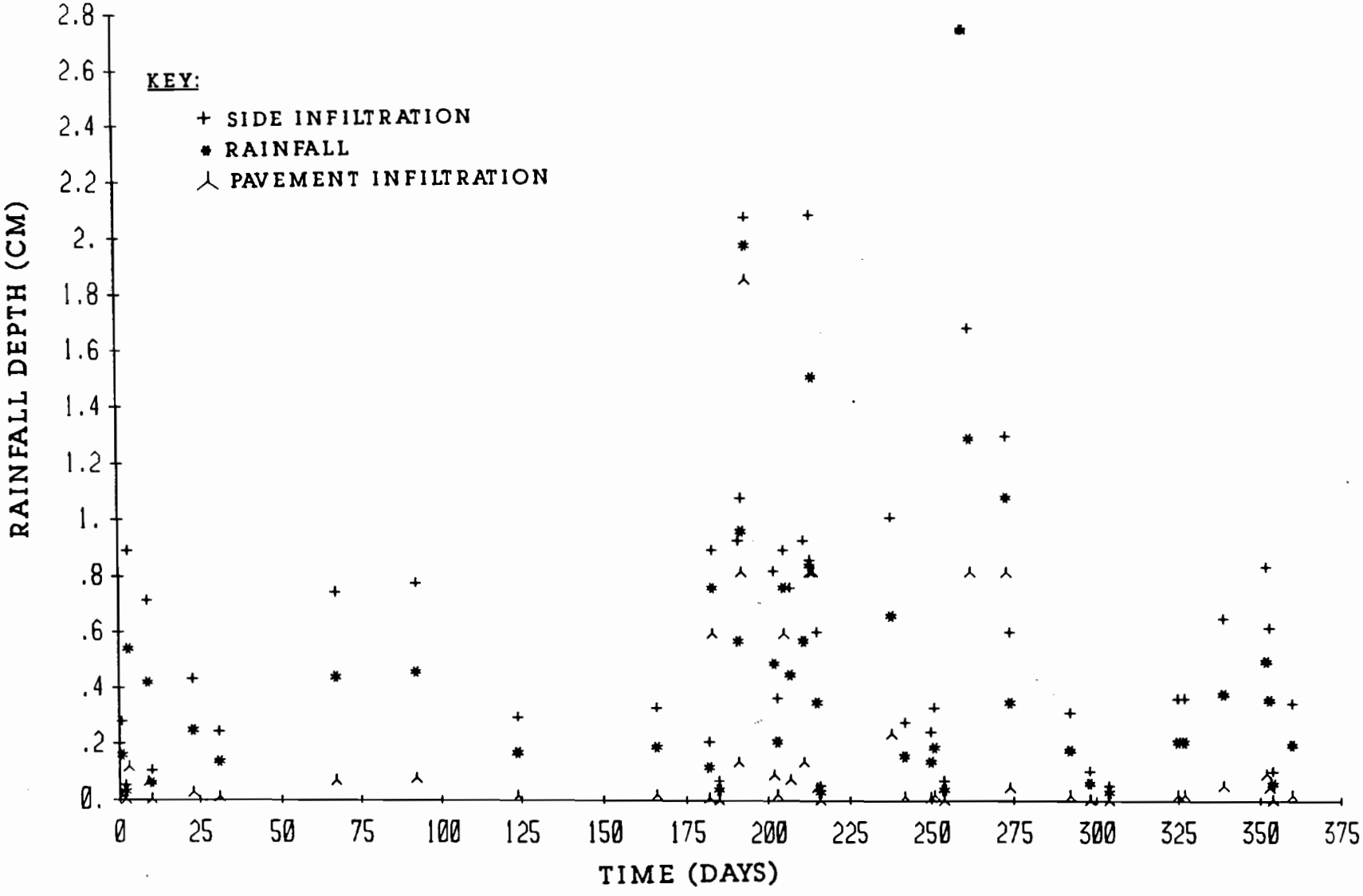

FIGURE D1.1 RAINFALL AND INFILTRATION DEPTHS FOR FIRST YEAR IN EL PASO

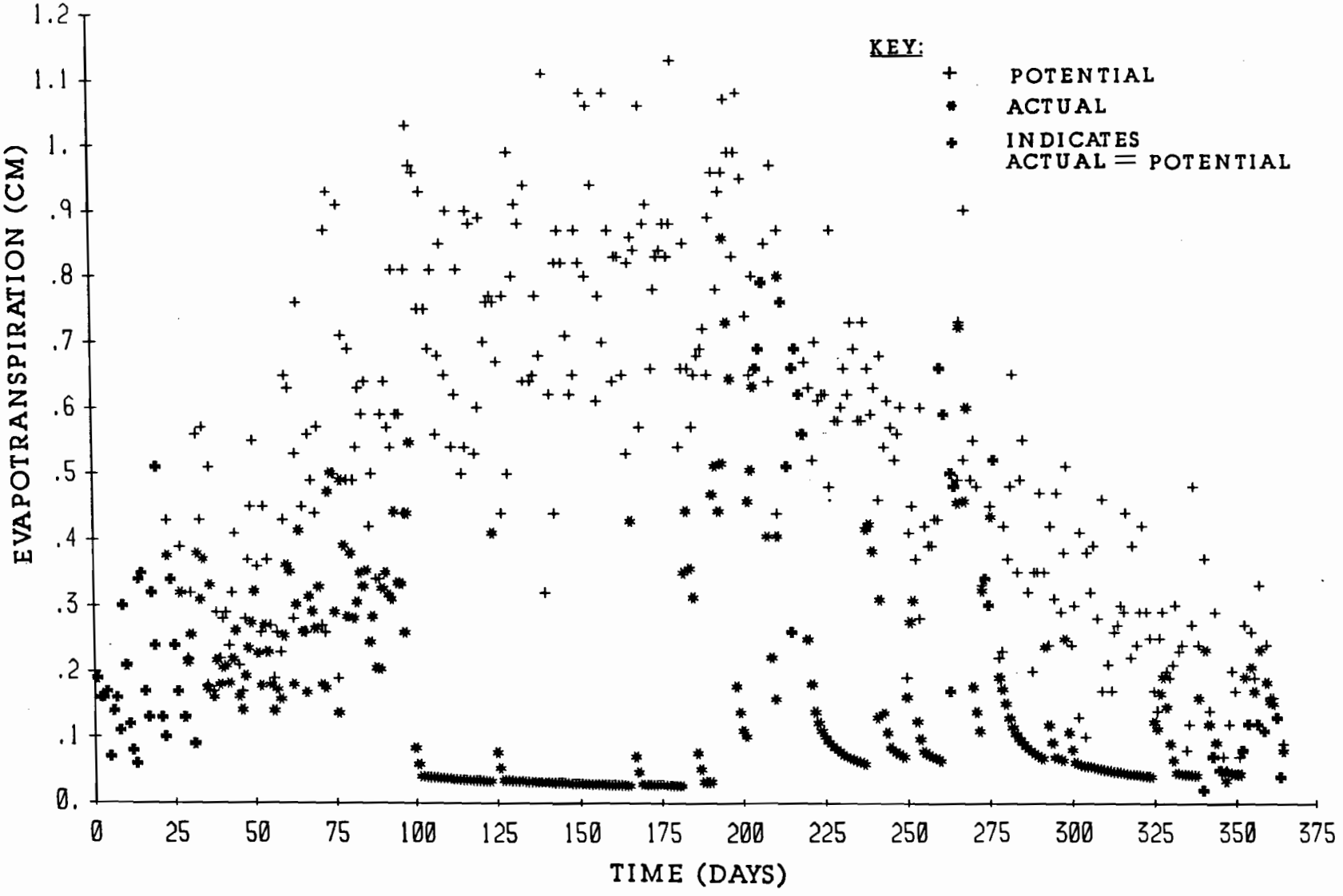

FIGURE D2.1 EVAPOTRANSPIRATION FOR FIRST YEAR IN EL PASO

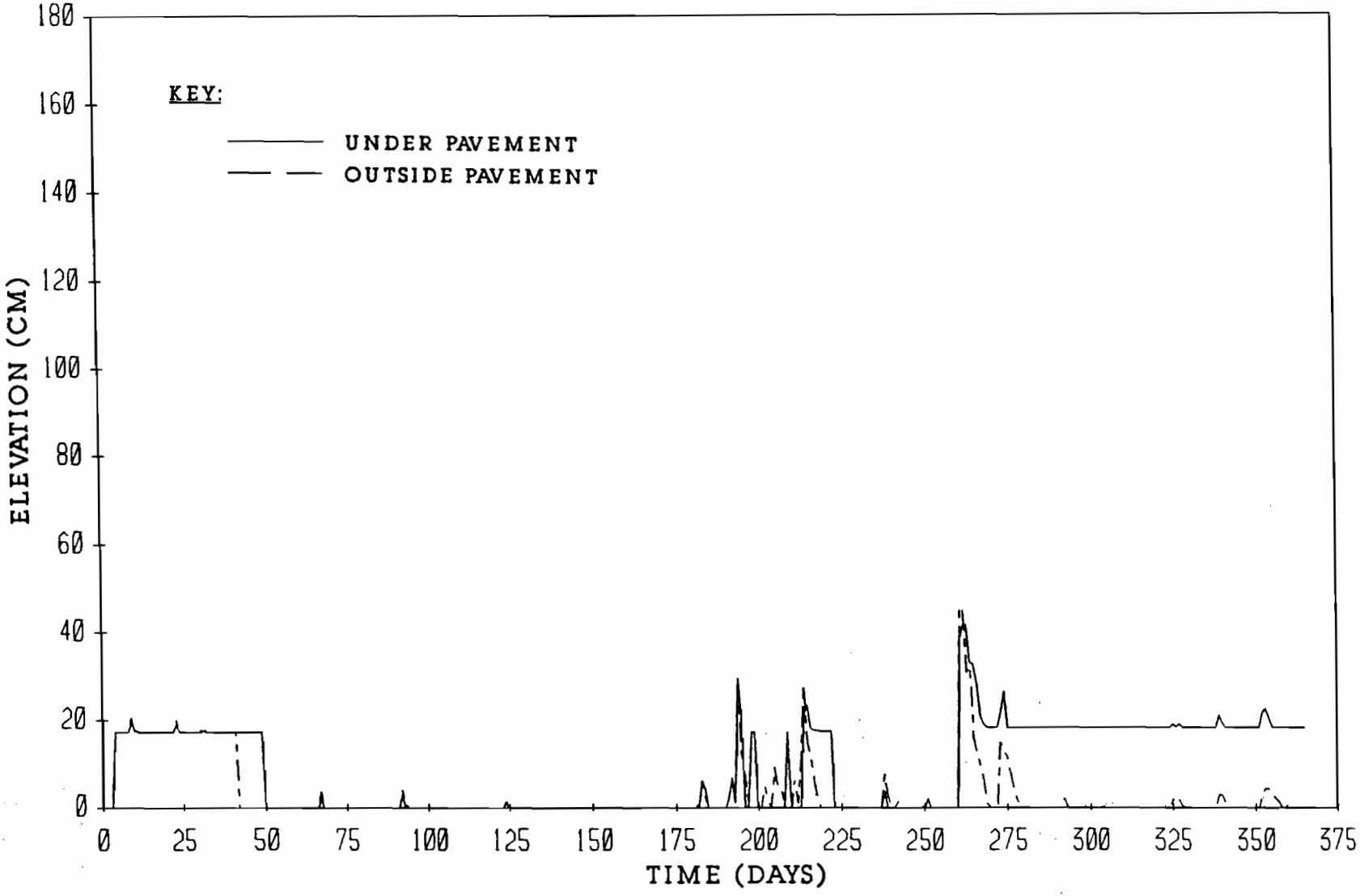

FIGURE D3.1 WATER LEVELS WITHIN THE CRACK FABRIC FOR FIRST YEAR IN EL PASO

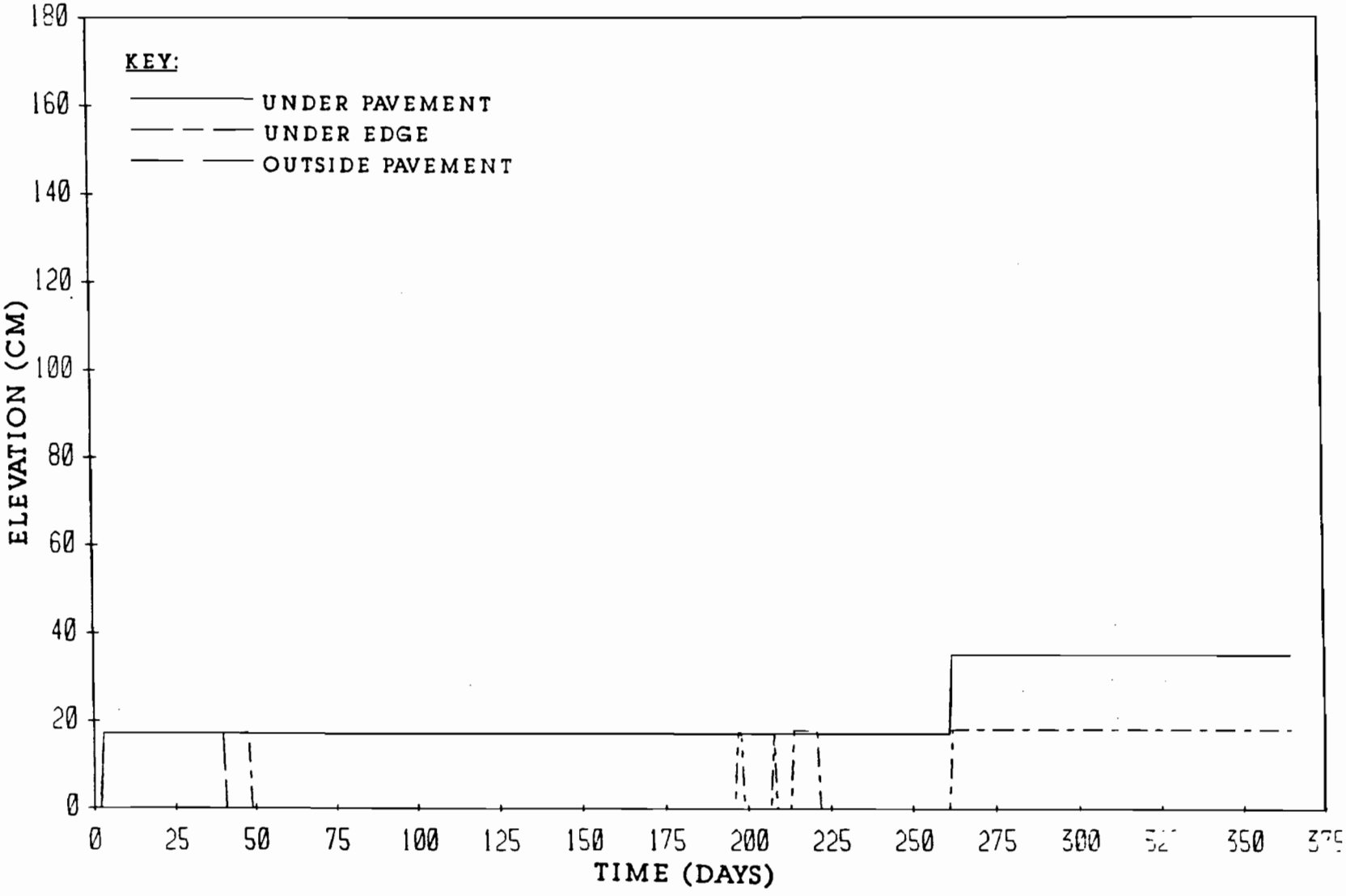

FIGURE D4.1 CRACK TIP ELEVATIONS FOR FIRST YEAR IN EL PASO

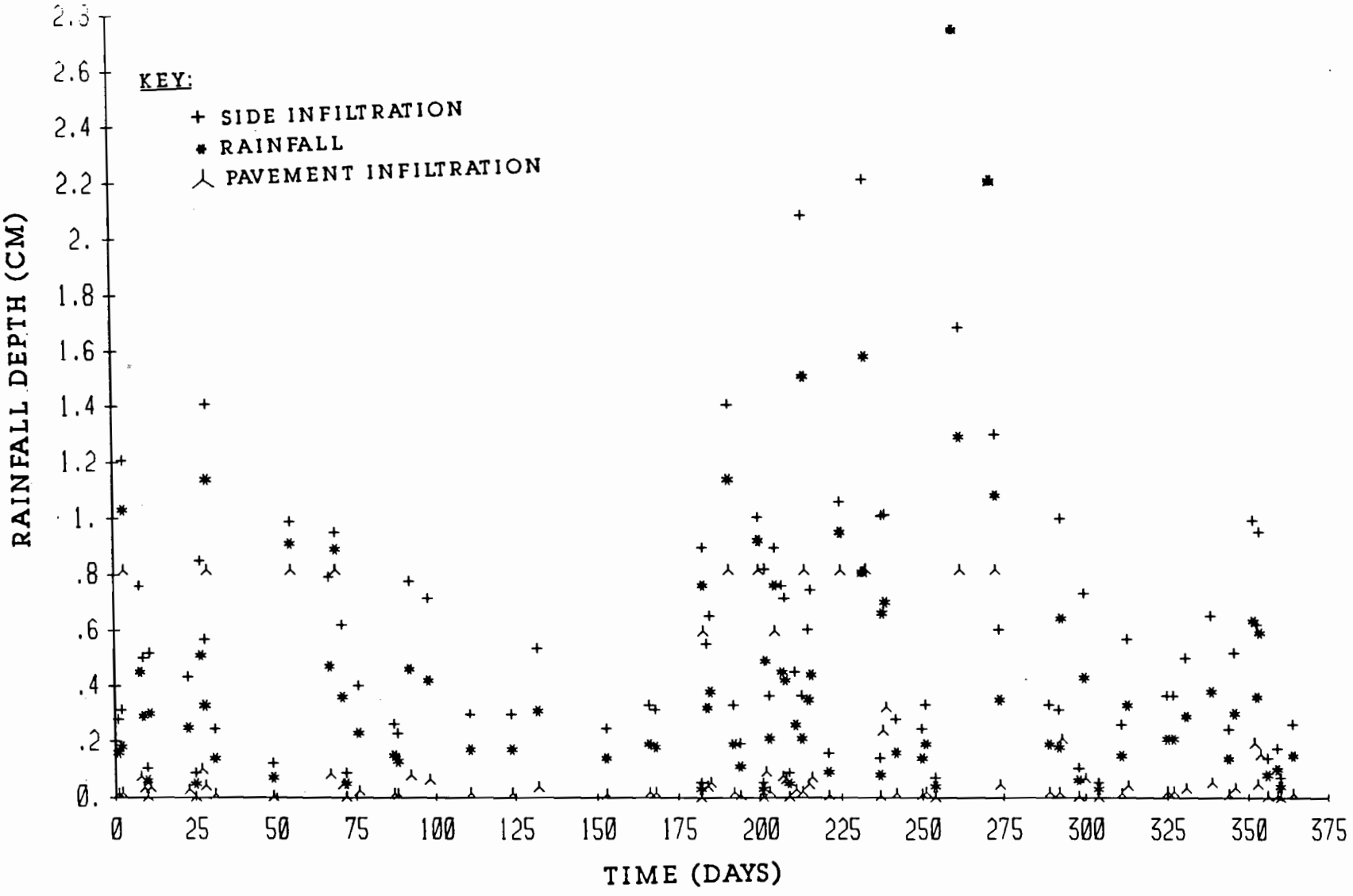

FIGURE D1.2 RAINFALL AND INFILTRATION DEPTHS FOR SECOND YEAR IN EL PASO

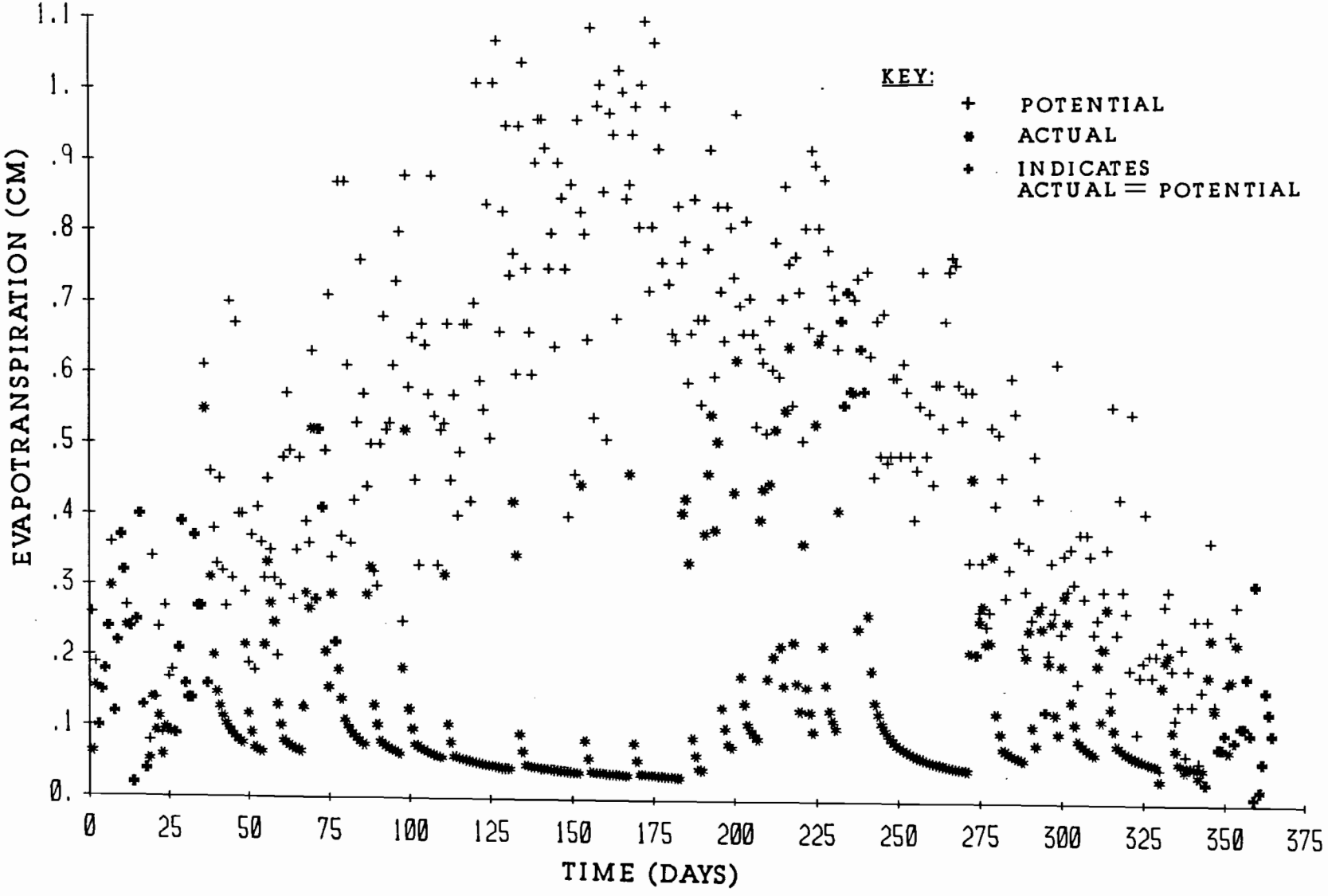

FIGURE D2.2 EVAPOTRANSPIRATION FOR SECOND YEAR IN EL PASO

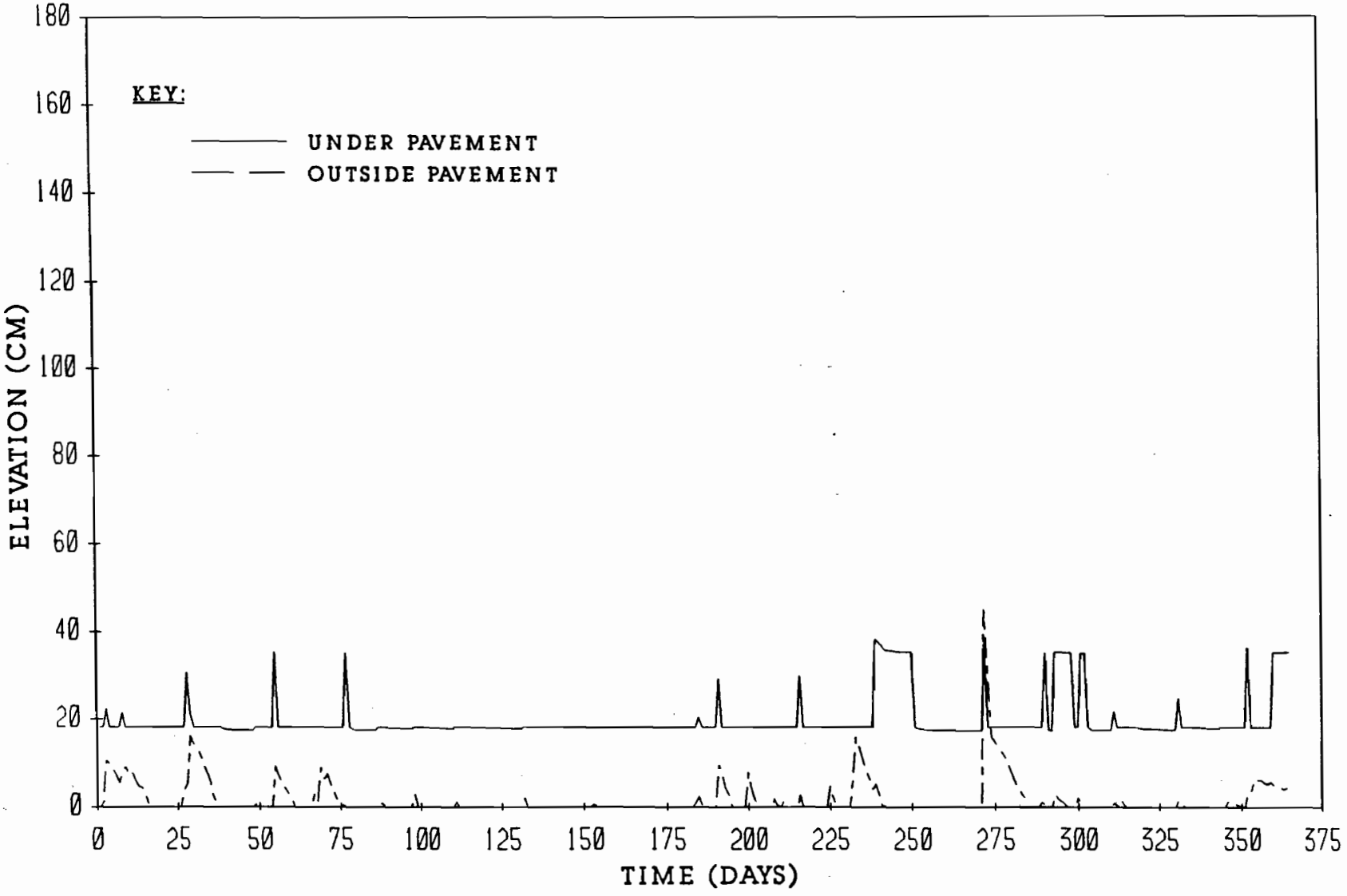

FIGURE D3.2 WATER LEVELS WITHIN THE CRACK FABRIC FOR SECOND YEAR IN EL PASO

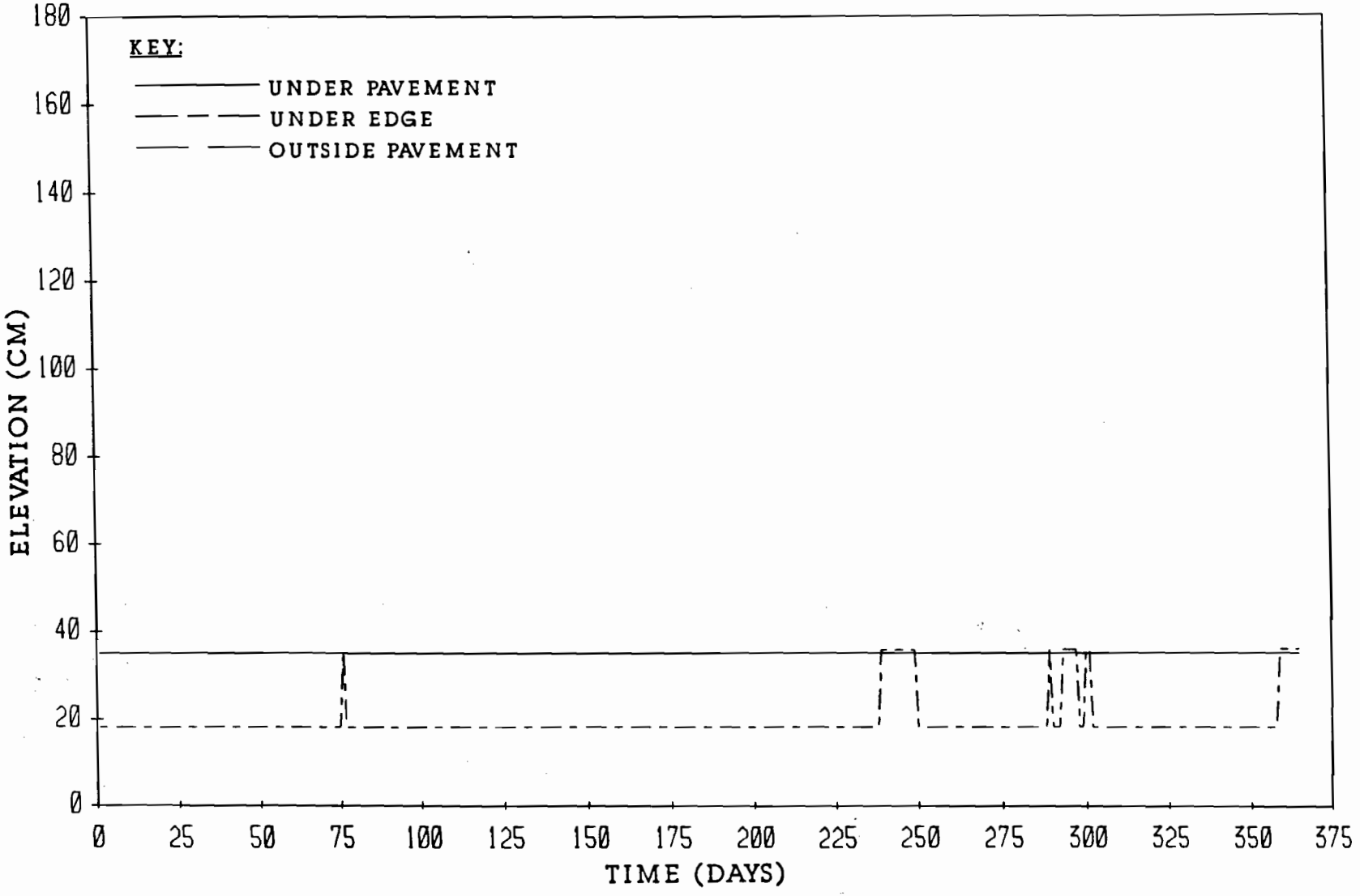

FIGURE D4.2 CRACK TIP ELEVATIONS FOR SECOND YEAR IN EL PASO

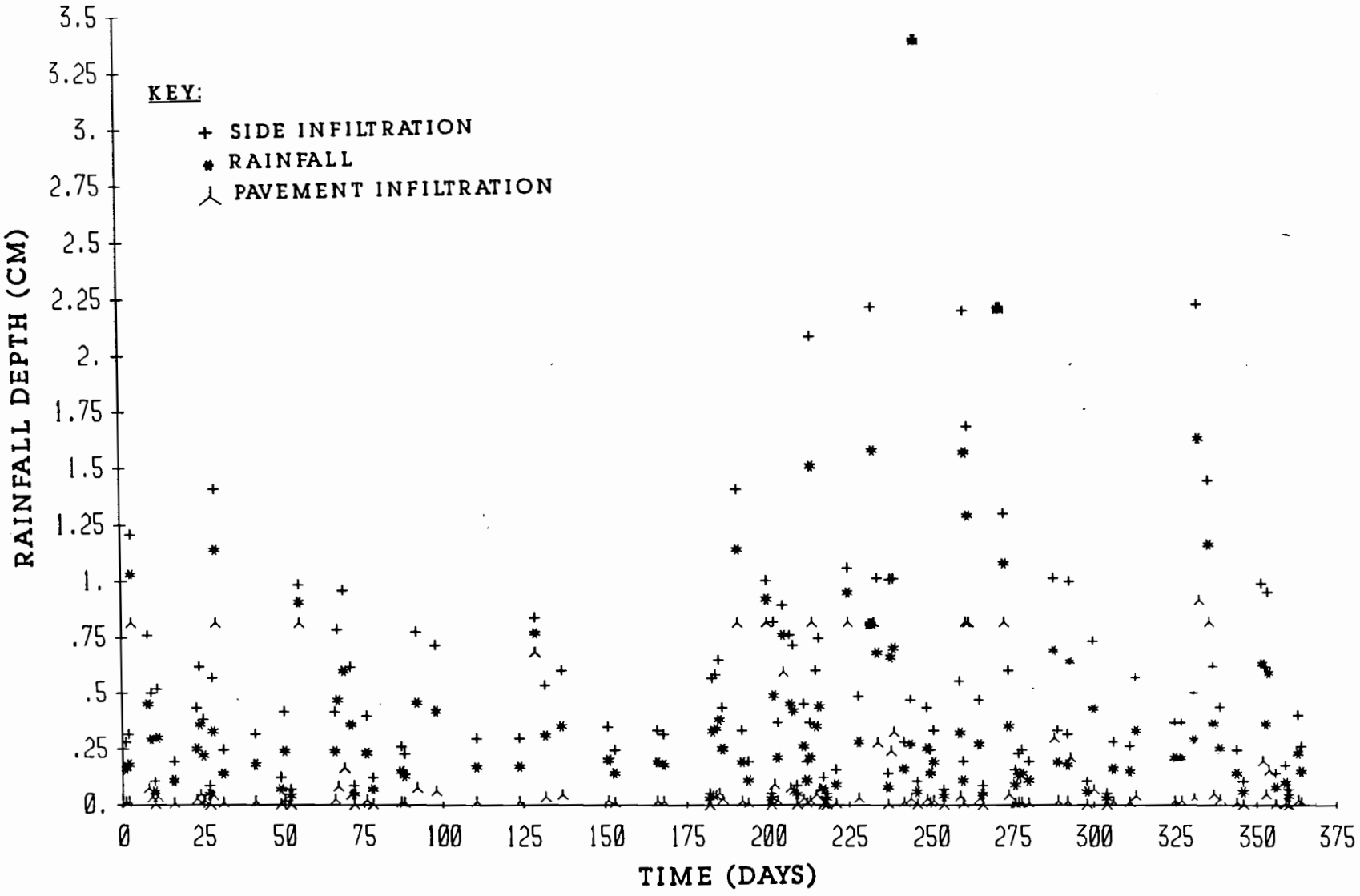

FIGURE D1.3 RAINFALL AND INFILTRATION DEPTHS FOR THIRD YEAR IN EL PASO

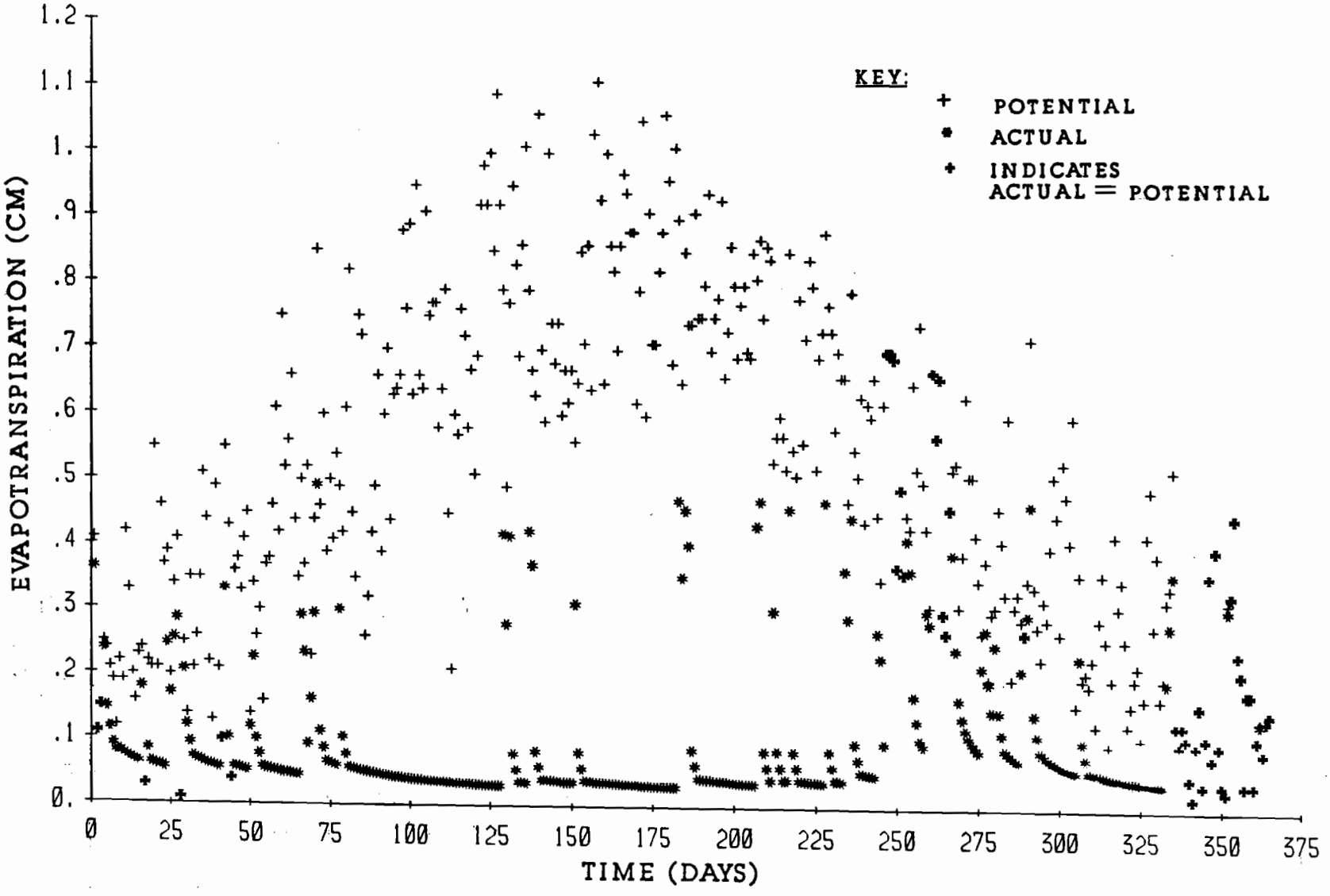

FIGURE D2.3 EVAPOTRANSPIRATION FOR THIRD YEAR IN EL PASO

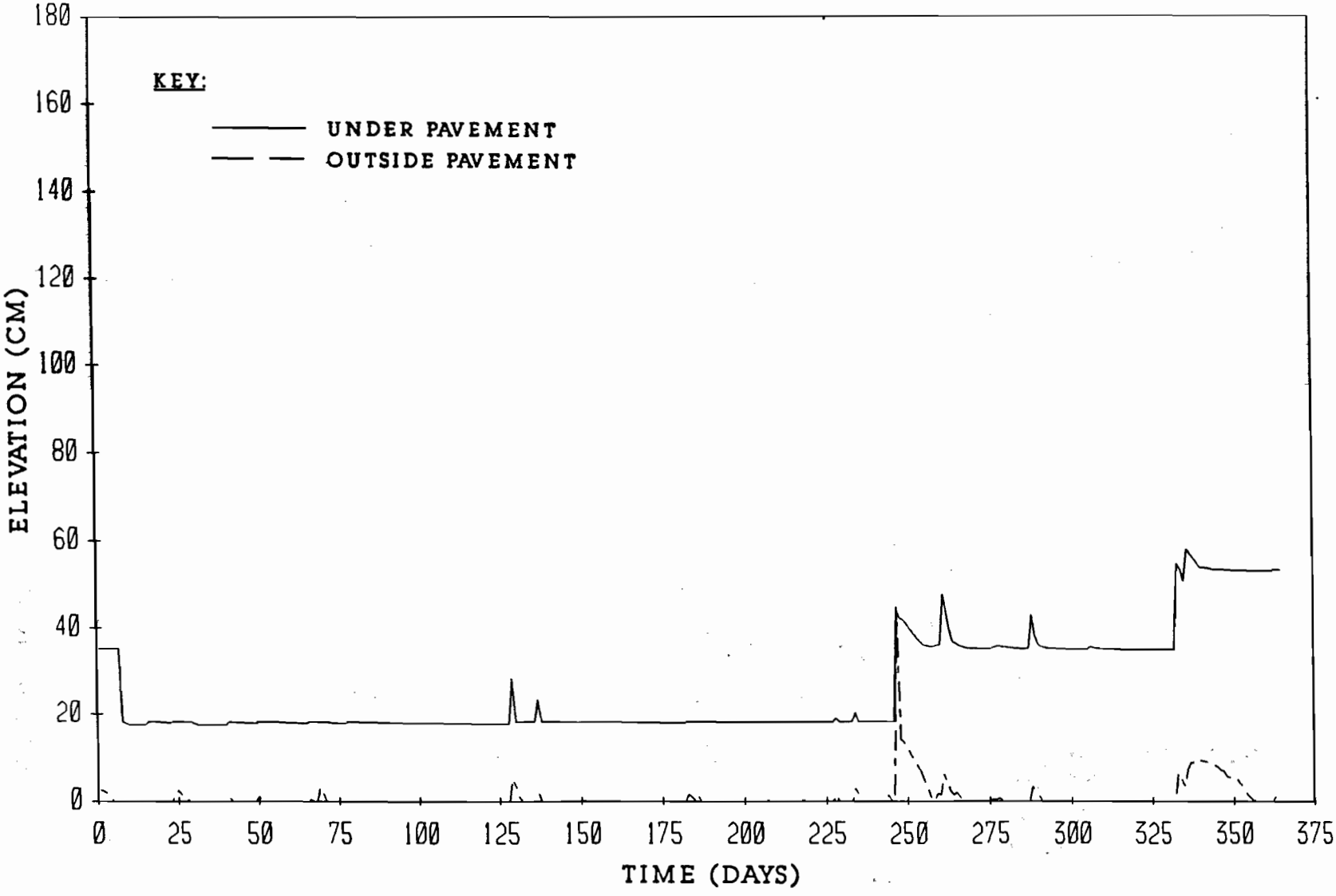

FIGURE D3.3 WATER LEVELS WITHIN THE CRACK FABRIC FOR THIRD YEAR IN EL PASO

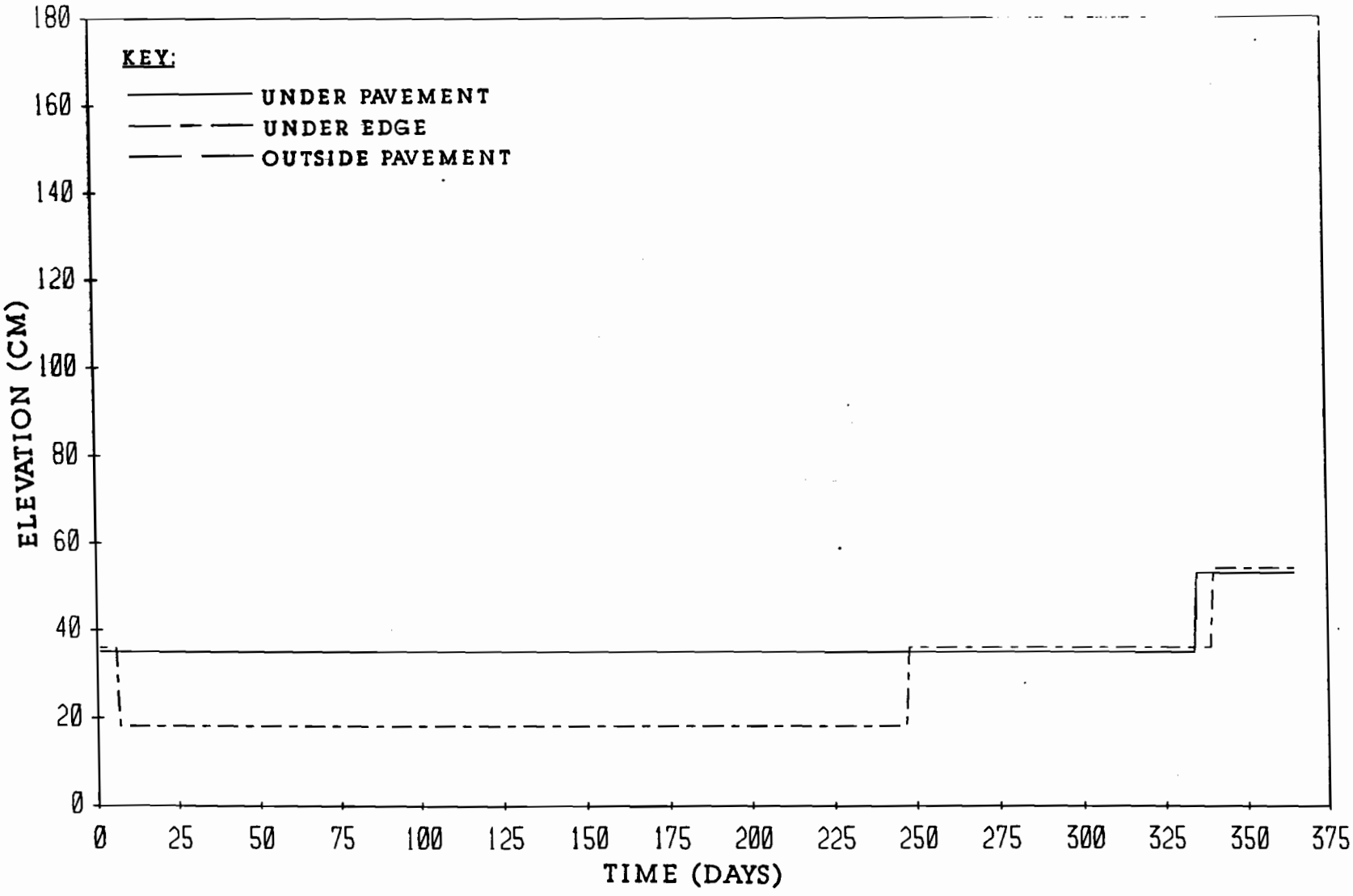

FIGURE D4.3 CRACK TIP ELEVATIONS FOR THIRD YEAR IN EL PASO

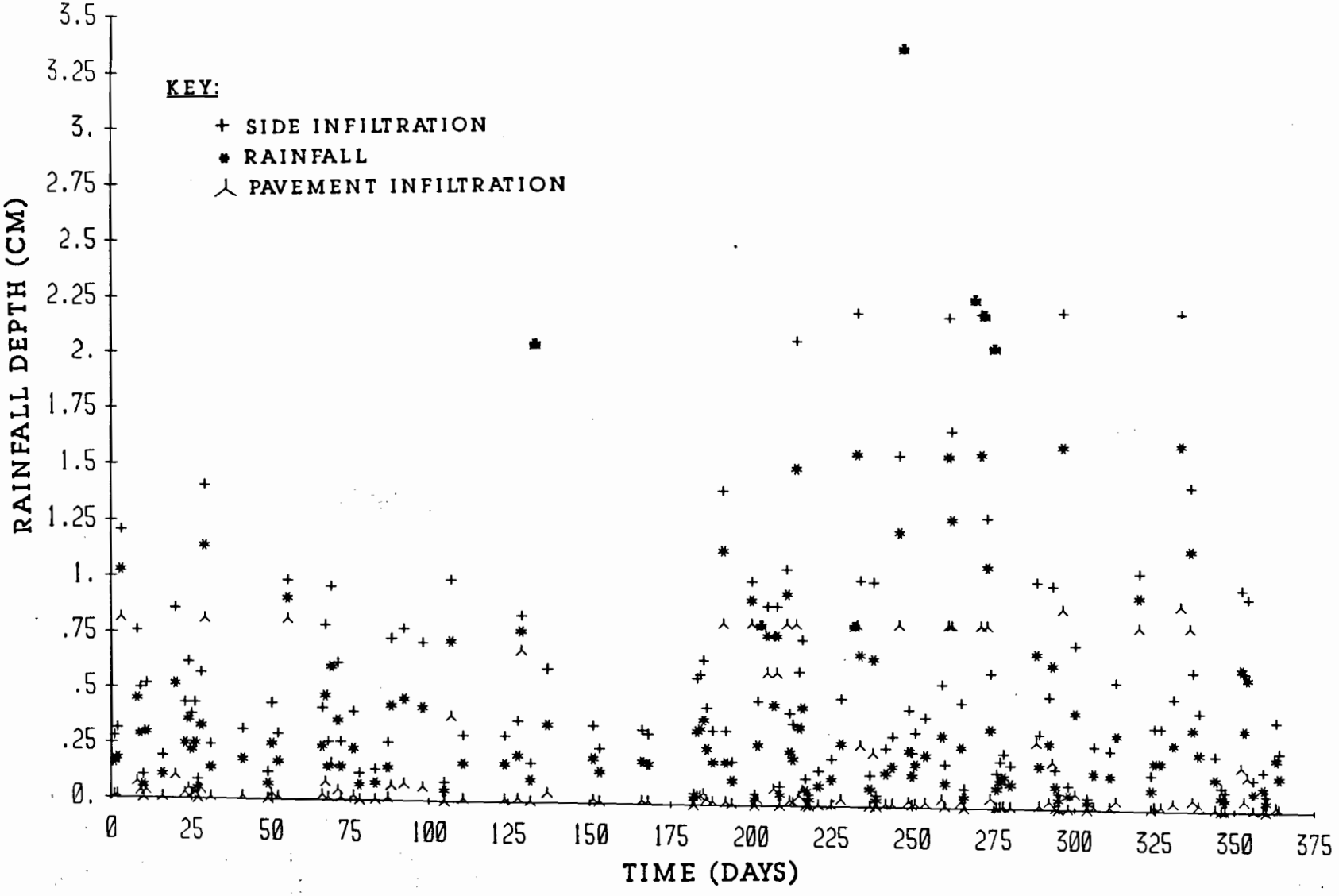

FIGURE D1.4 RAINFALL AND INFILTRATION DEPTHS FOR FOURTH YEAR IN EL PASO

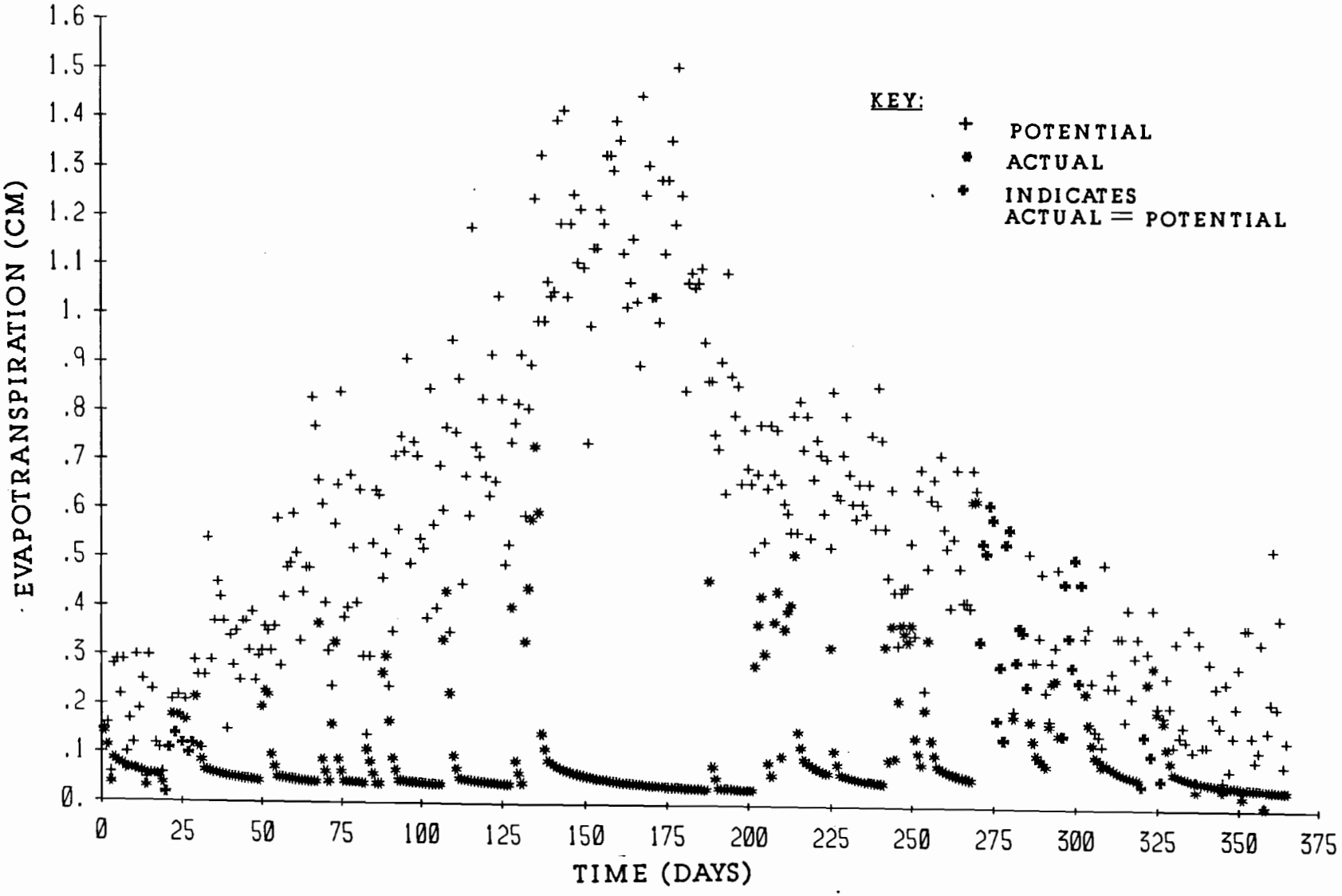

FIGURE D2.4 EVAPOTRANSPIRATION FOR FOURTH YEAR IN EL PASO

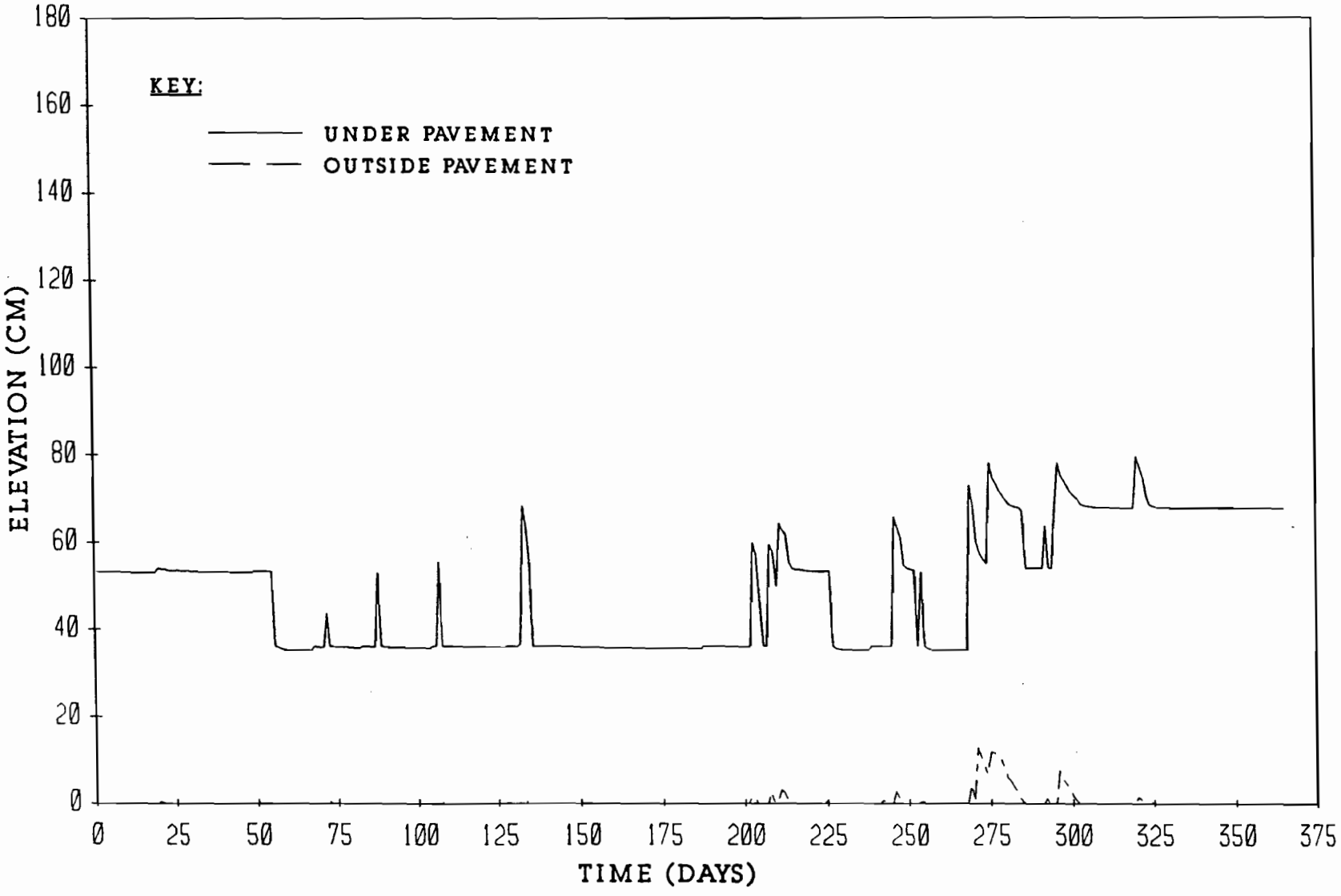

FIGURE D3.4 WATER LEVELS WITHIN THE CRACK FABRIC FOR FOURTH YEAR IN EL PASO

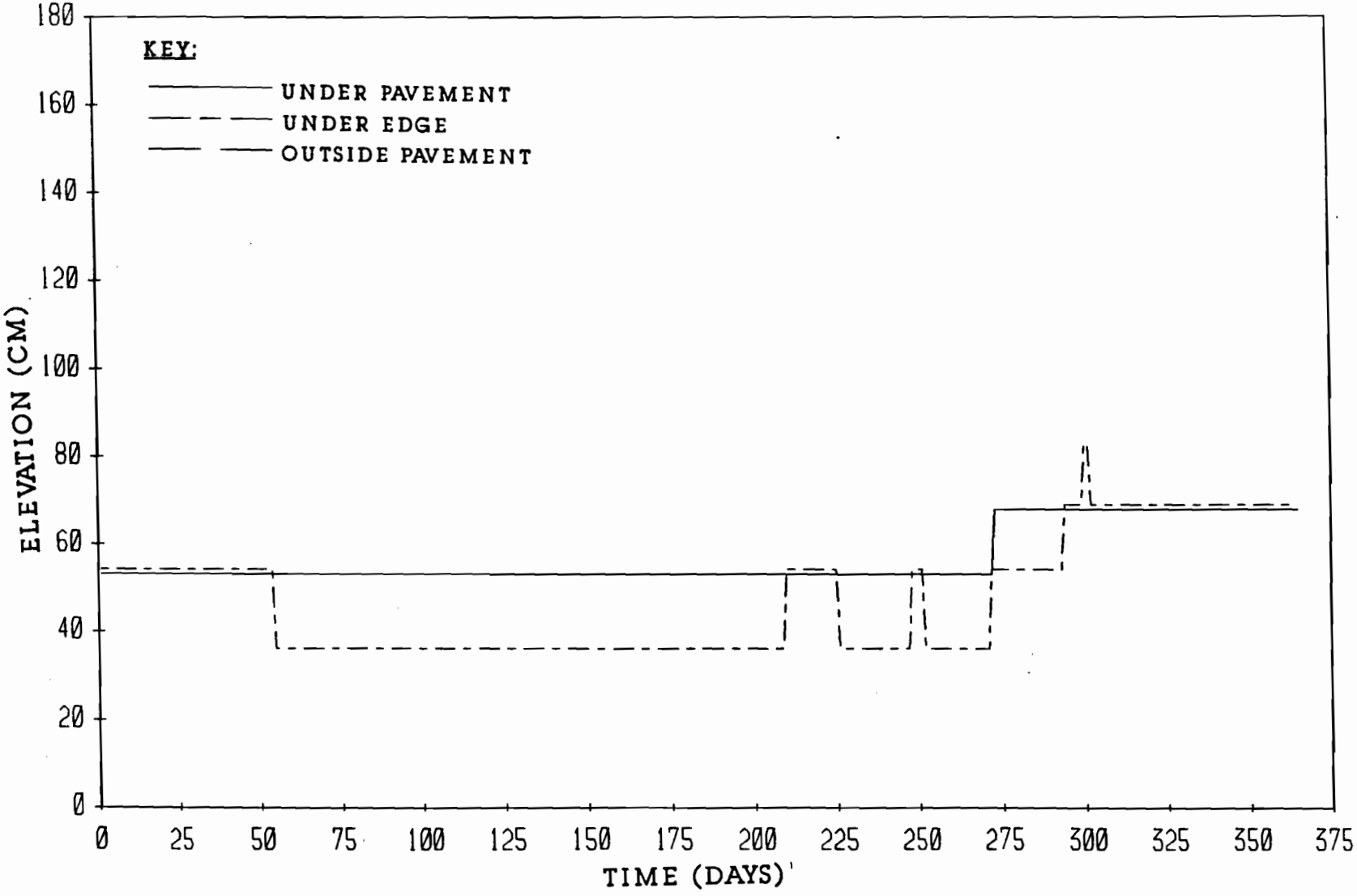

FIGURE D4.4 CRACK TIP ELEVATIONS FOR FOURTH YEAR IN EL PASO

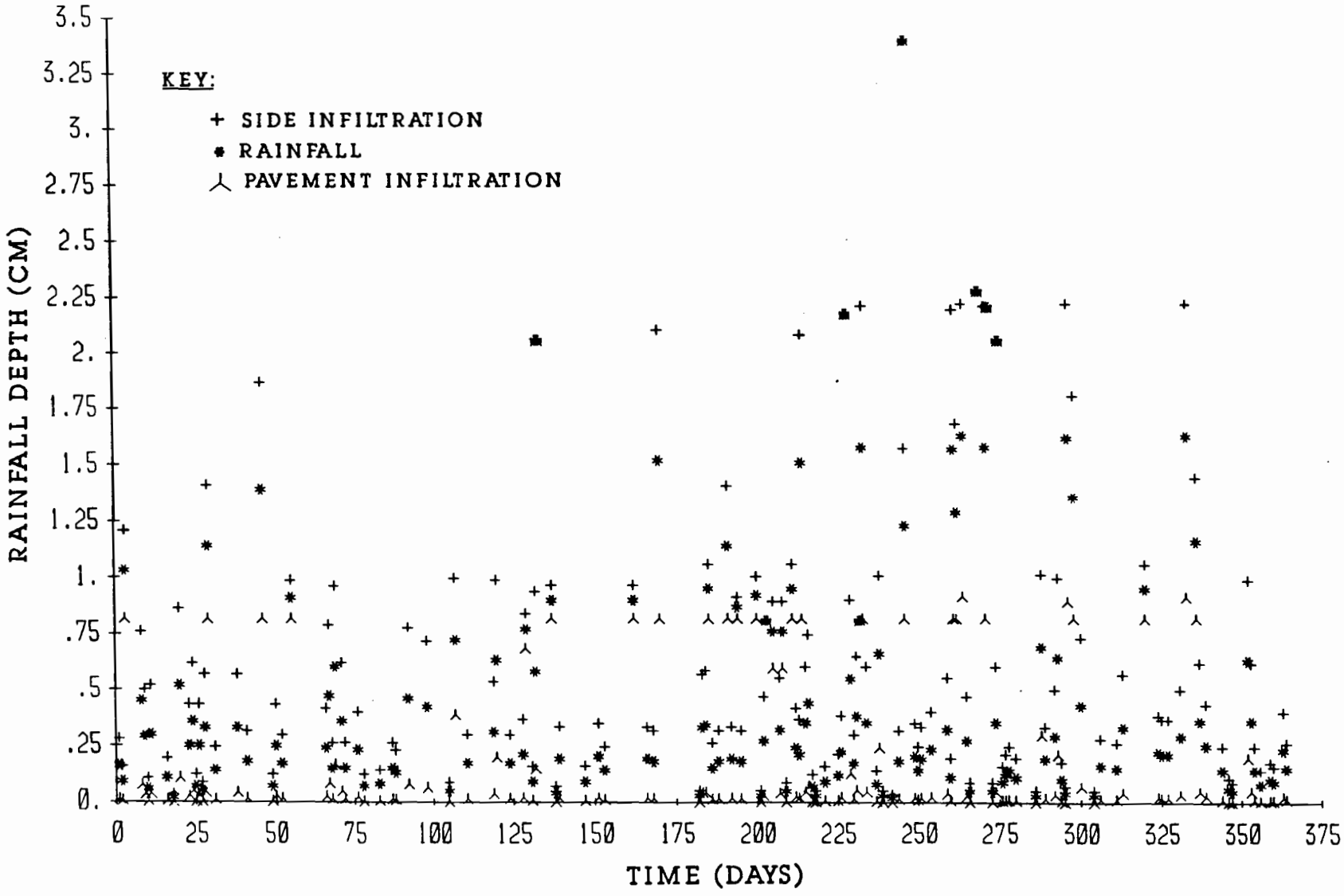

FIGURE D1.5 RAINFALL AND INFILTRATION DEPTHS FOR FIFTH YEAR

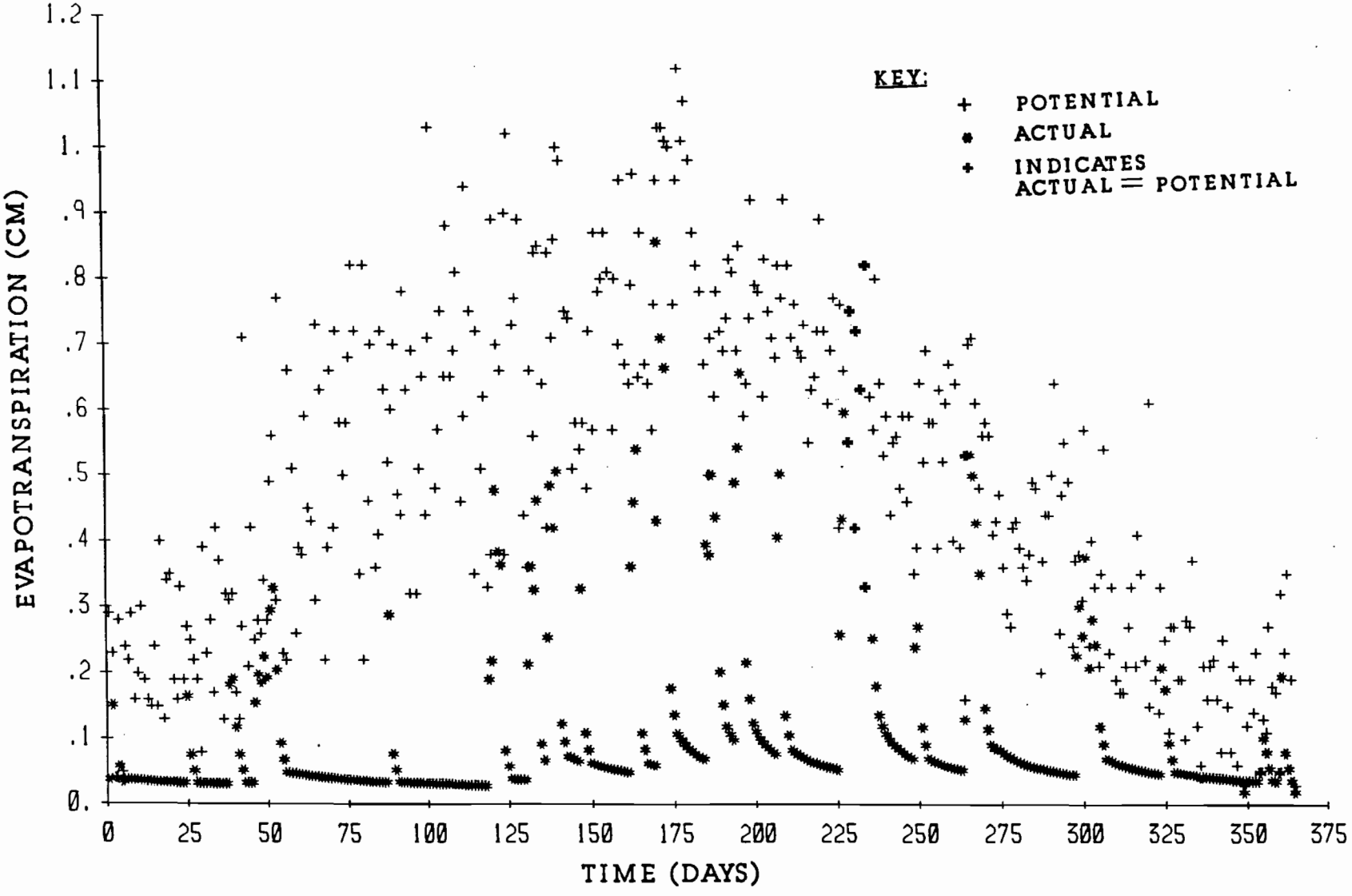

FIGURE D2.5 EVAPOTRANSPIRATION FOR FIFTH YEAR IN EL PASO

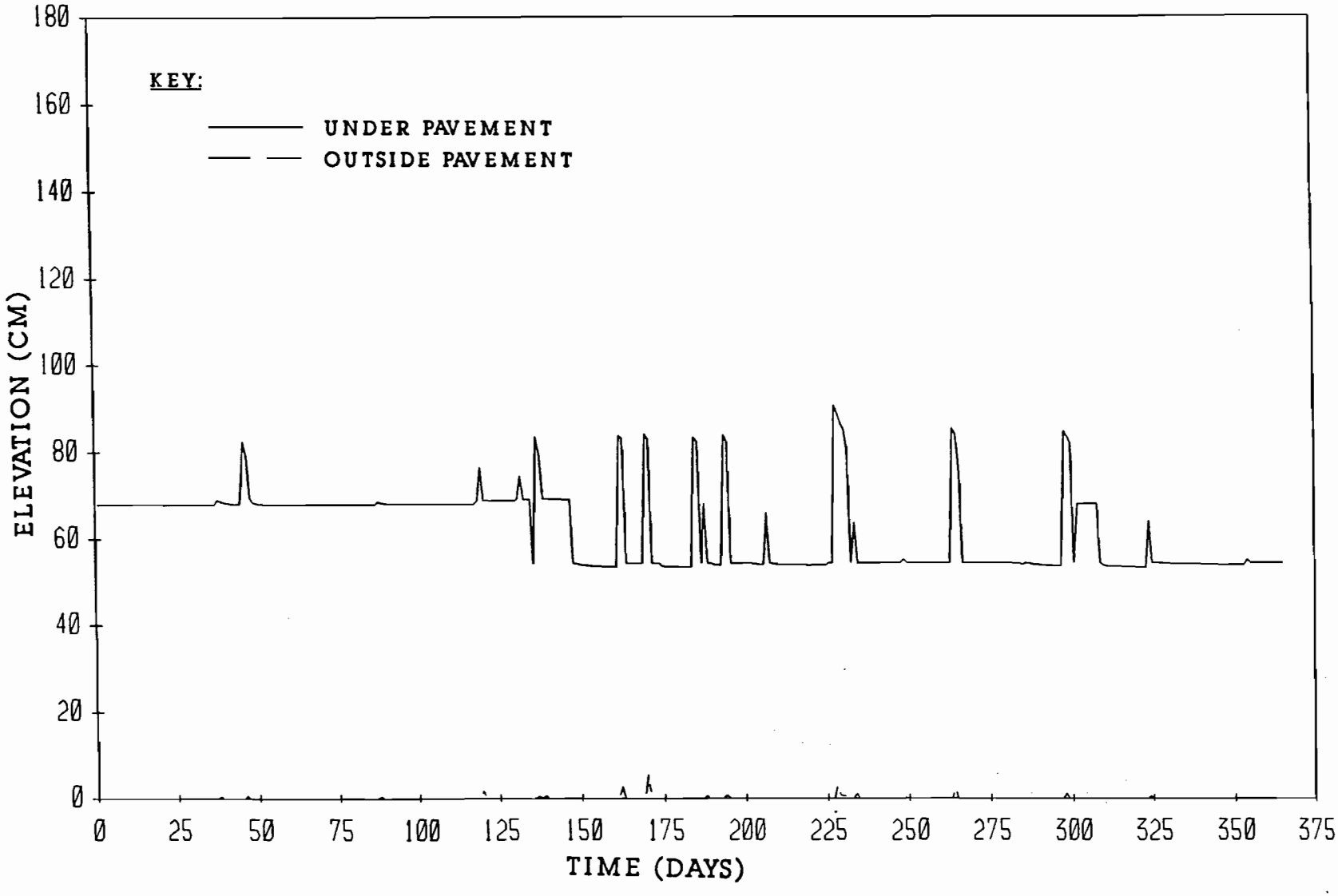

FIGURE D3.5 WATER LEVELS WITHIN THE CRACK FABRIC FOR FIFTH YEAR IN EL PASO

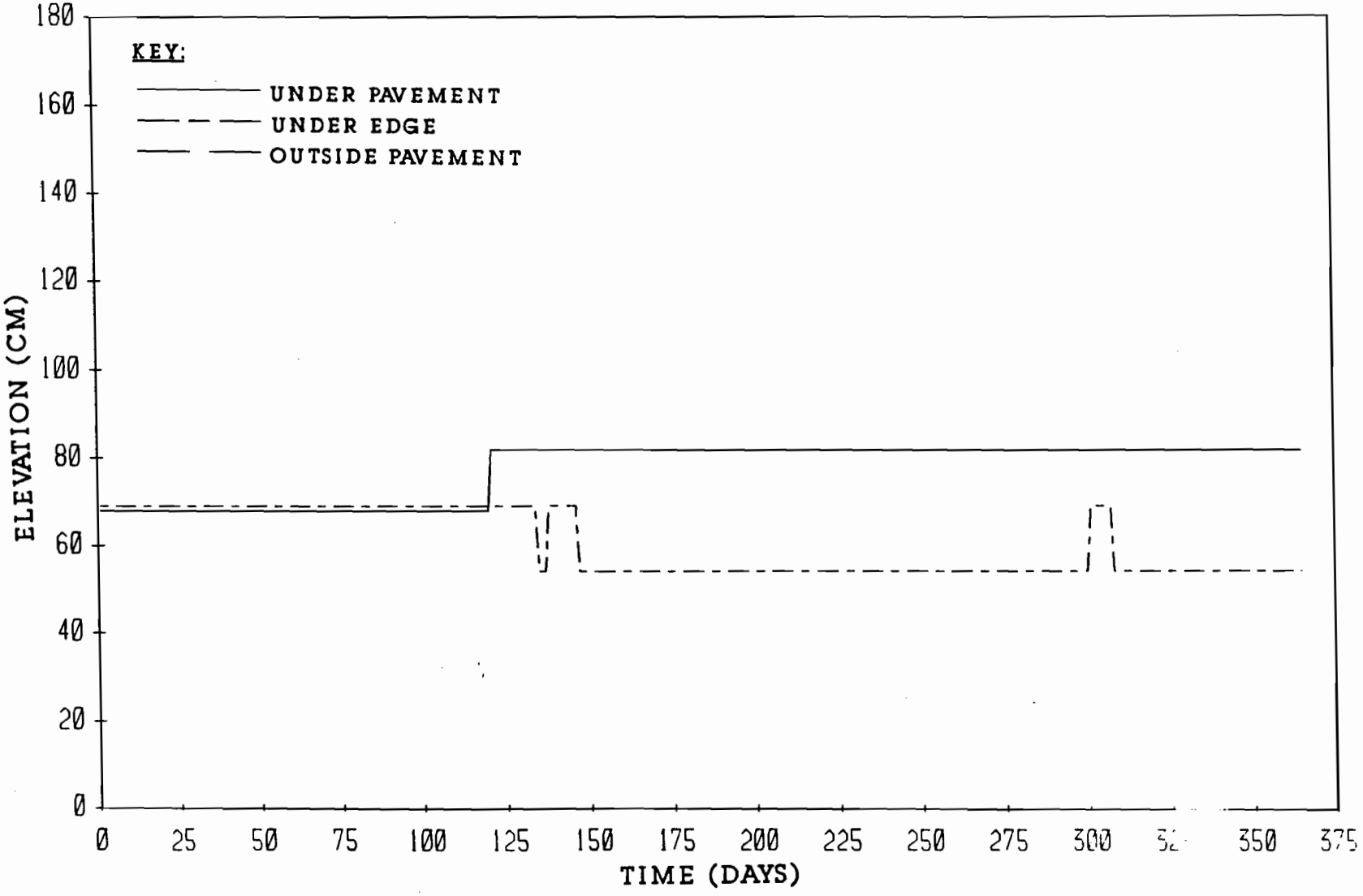

FIGURE D4.5 CRACK TIP ELEVATIONS FOR FIFTH YEAR IN EL PASO

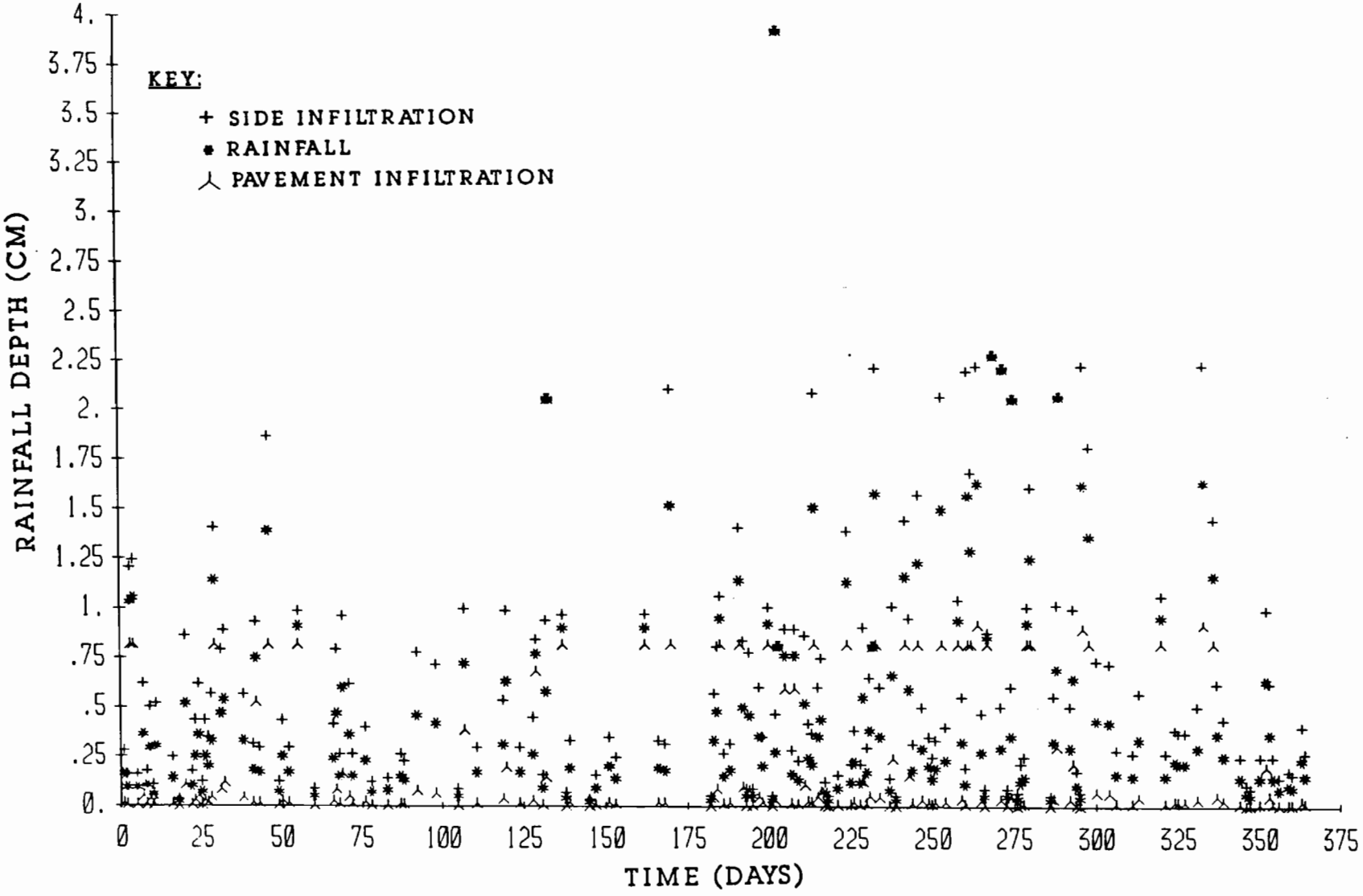

FIGURE D1.6 RAINFALL AND INFILTRATION DEPTHS FOR SIXTH YEAR IN EL PASO

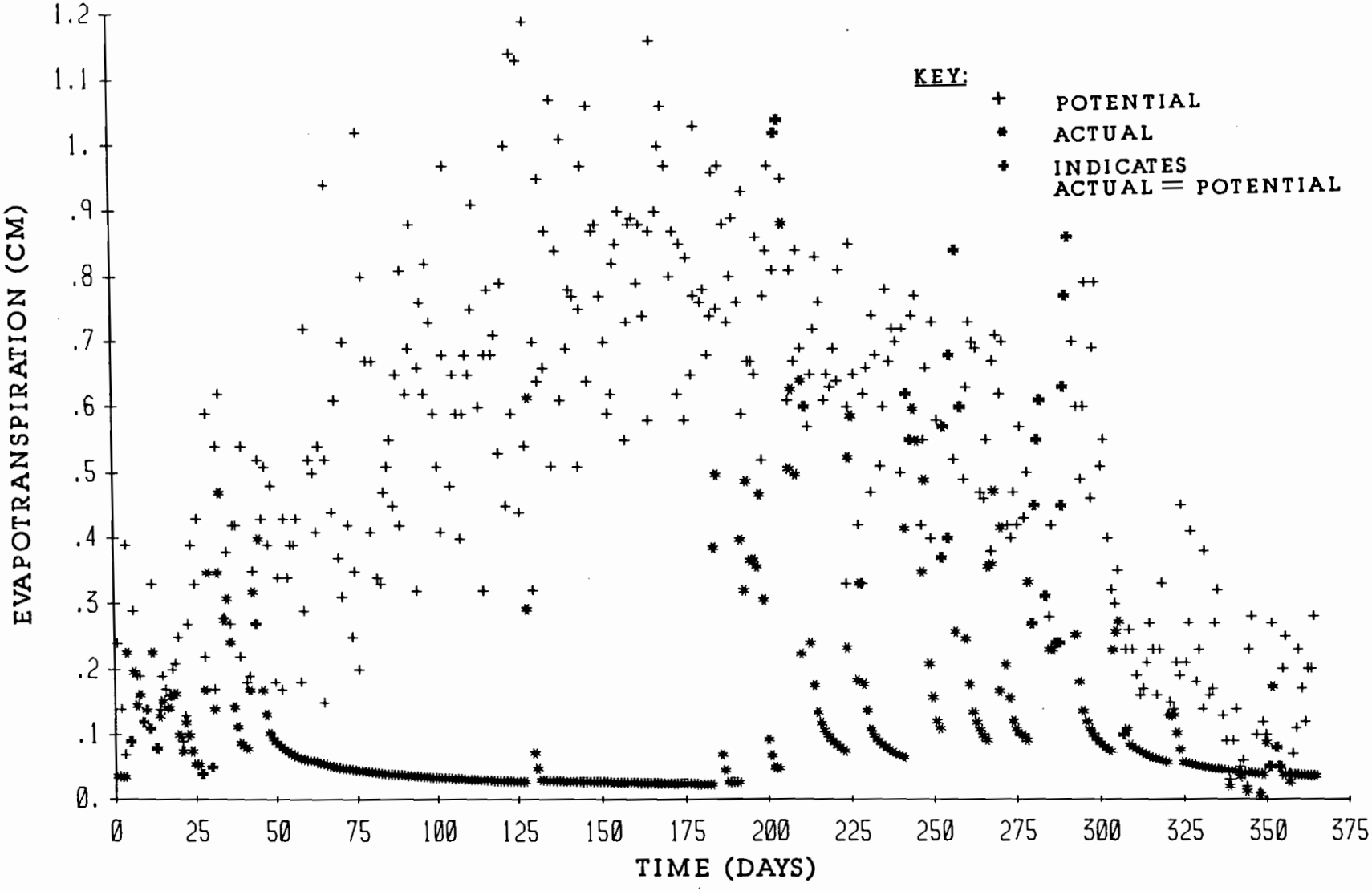

FIGURE D2.6 EVAPOTRANSPIRATION FOR SIXTH YEAR IN EL PASO

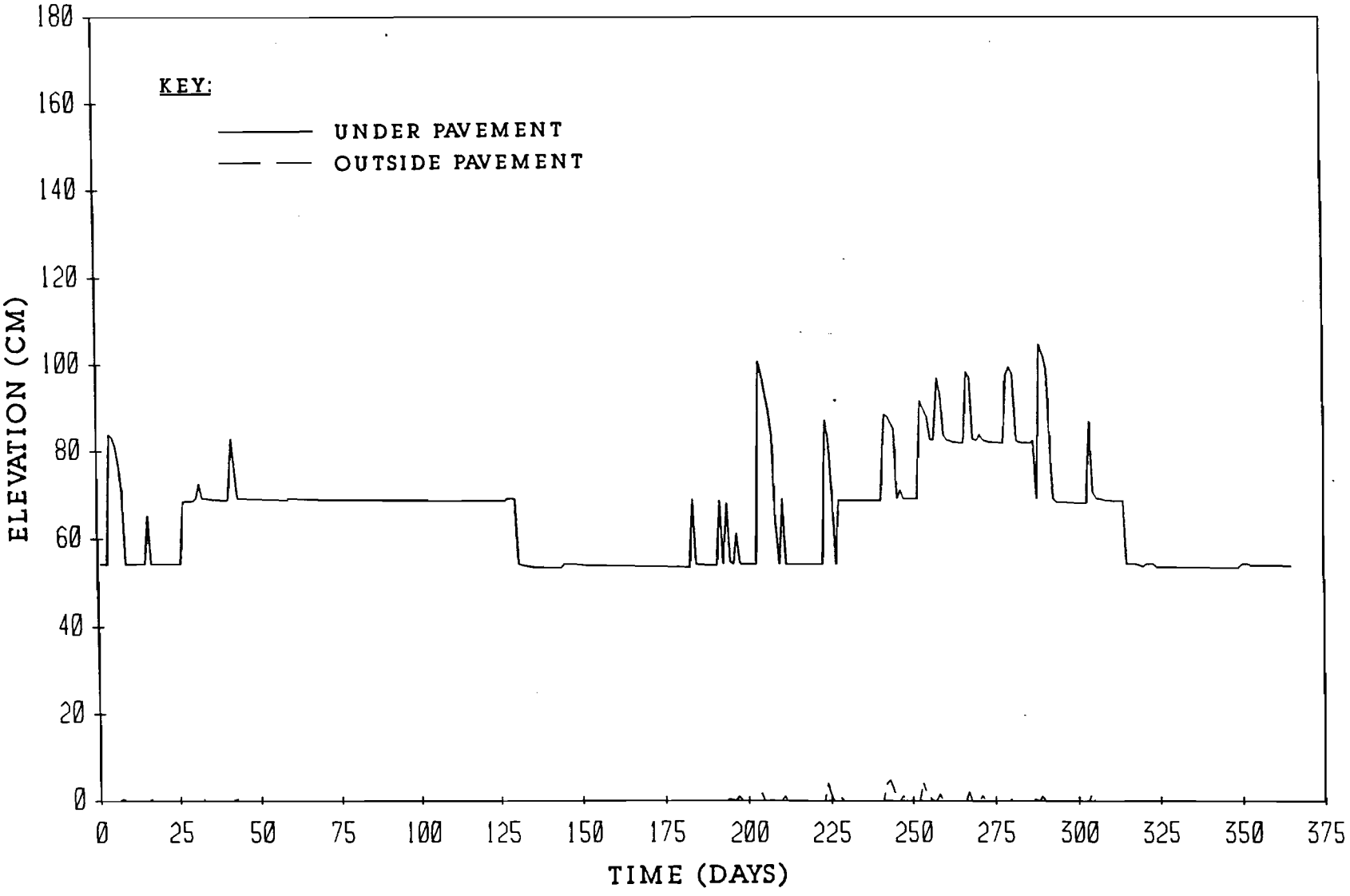

FIGURE D3.6 WATER LEVELS WITHIN THE CRACK FABRIC FOR SIXTH YEAR IN EL PASO

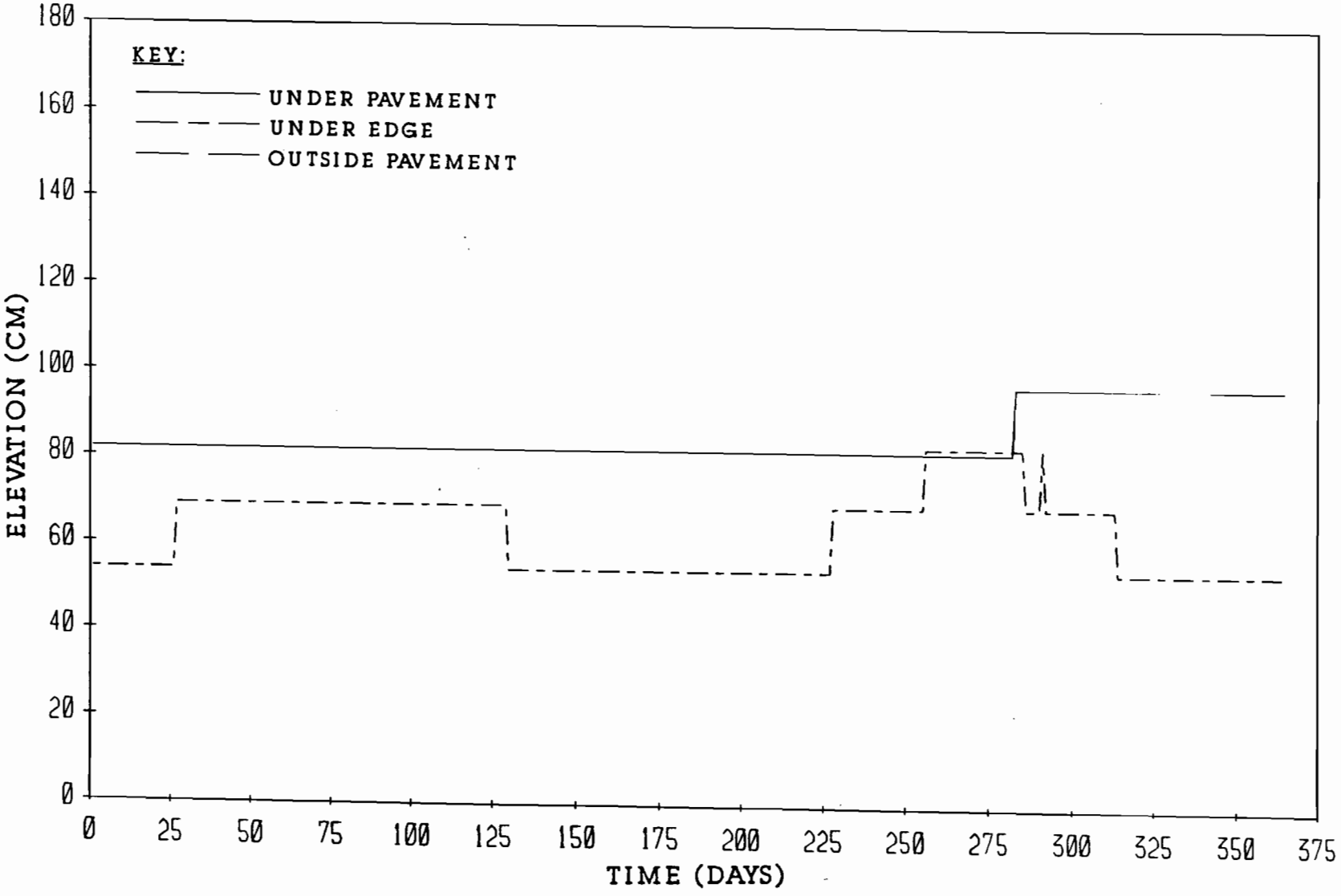

FIGURE D4.6 CRACK TIP ELEVATIONS FOR SIXTH YEAR IN EL PASO

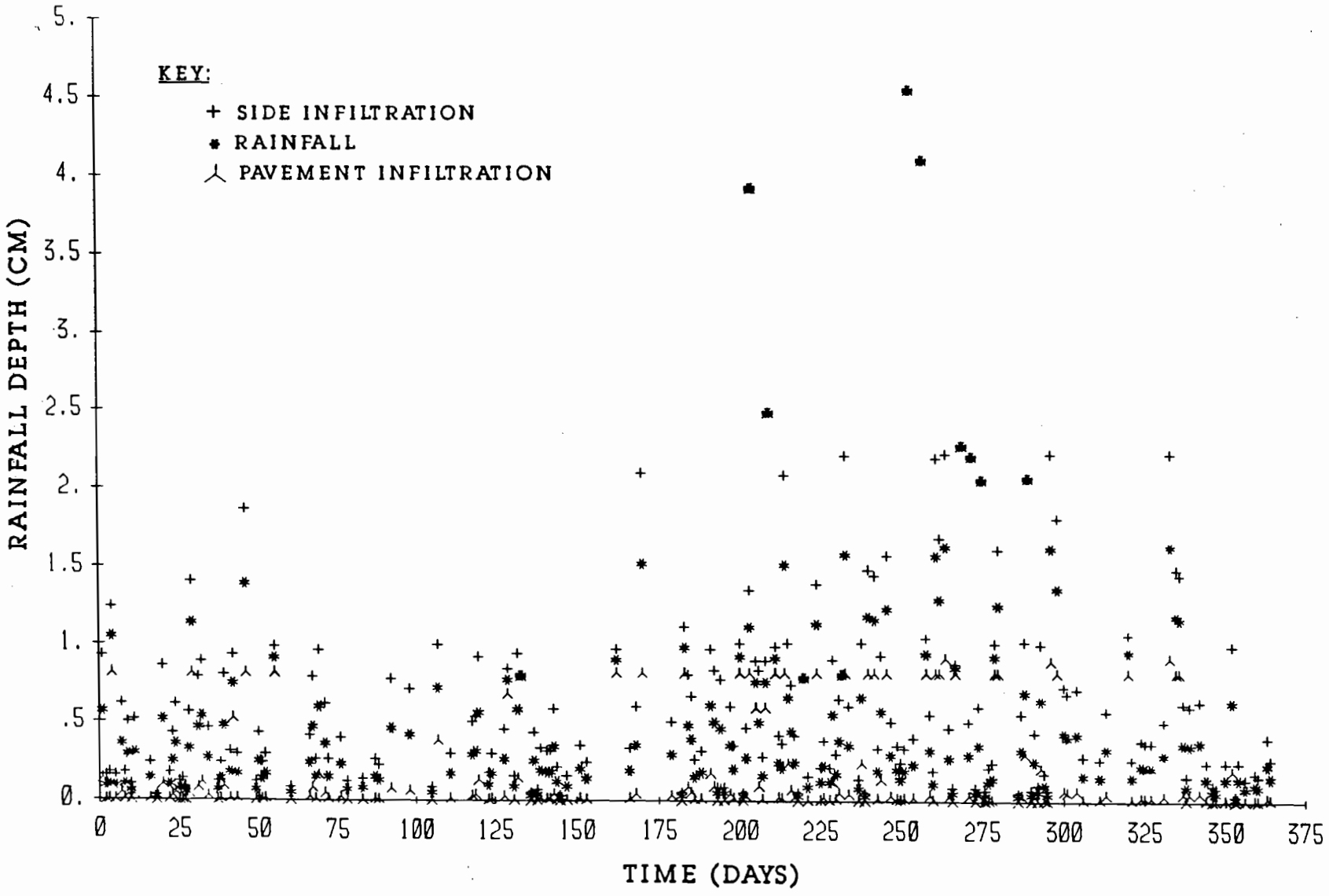

FIGURE D1.7 RAINFALL AND INFILTRATION DEPTHS FOR SEVENTH YEAR IN EL PASO

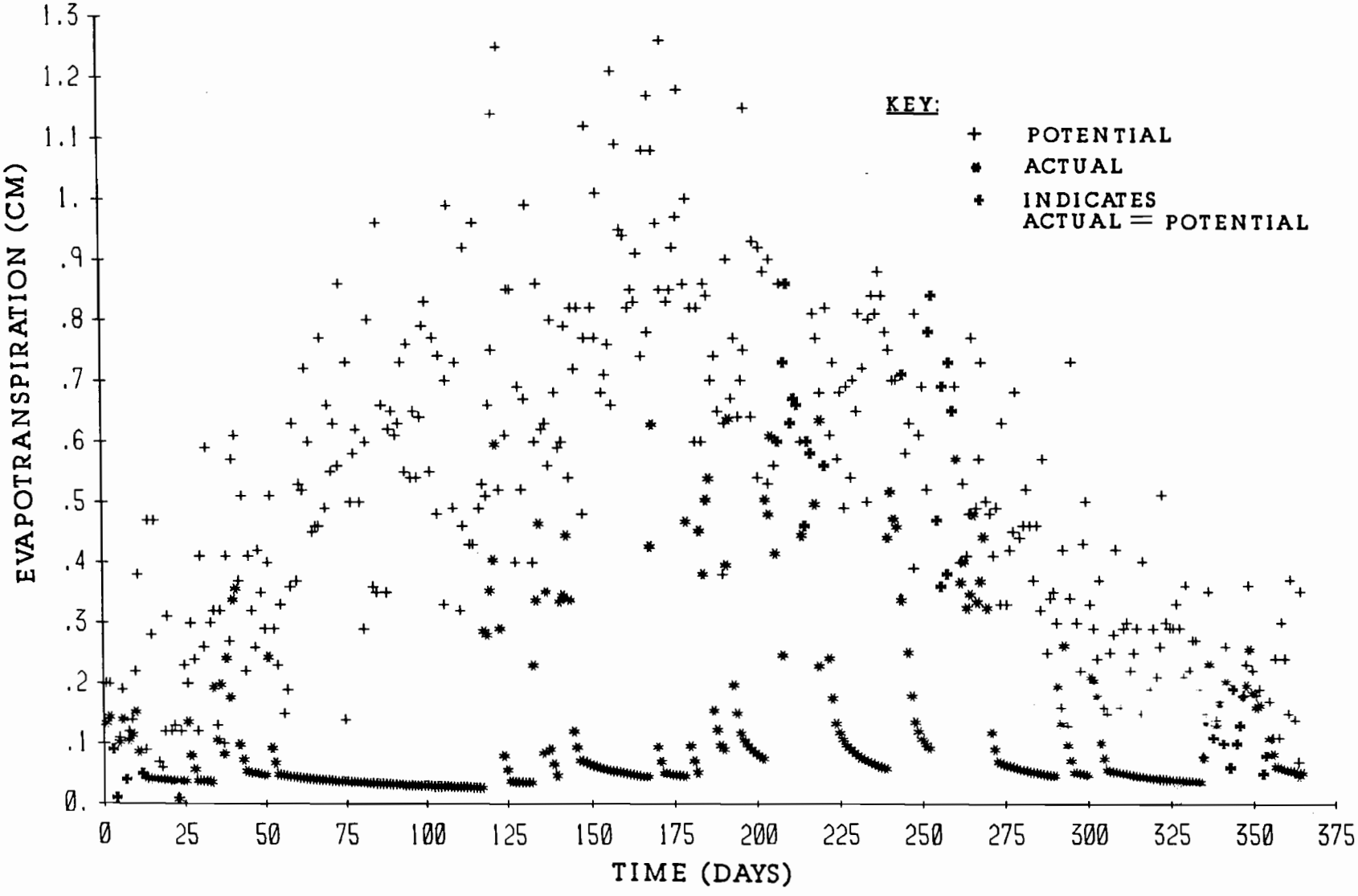

FIGURE D2.7 EVAPOTRANSPIRATION FOR SEVENTH YEAR IN EL PASO

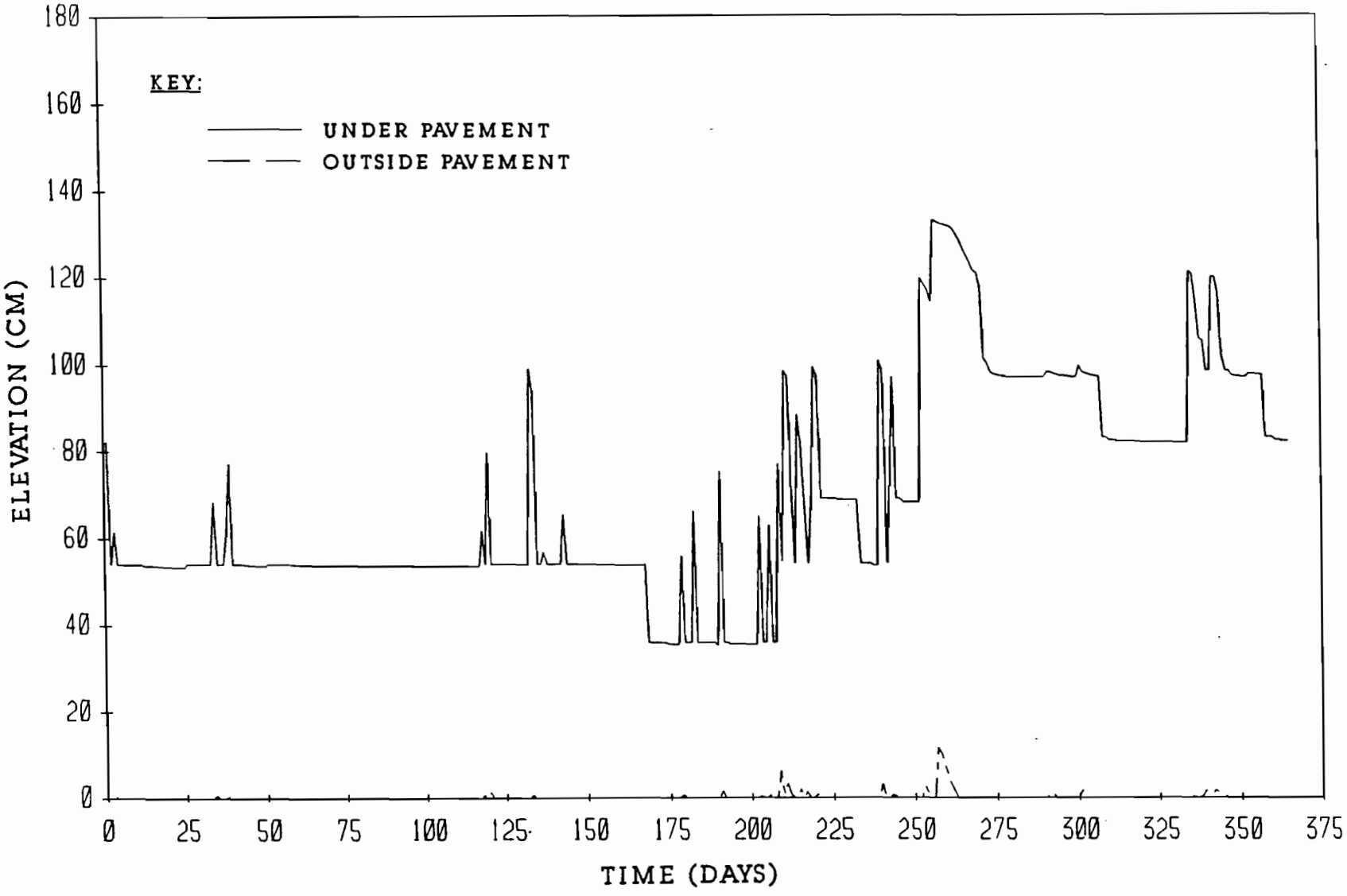

FIGURE D3.7 WATER LEVELS WITHIN THE CRACK FABRIC FOR SEVENTH YEAR IN EL PASO

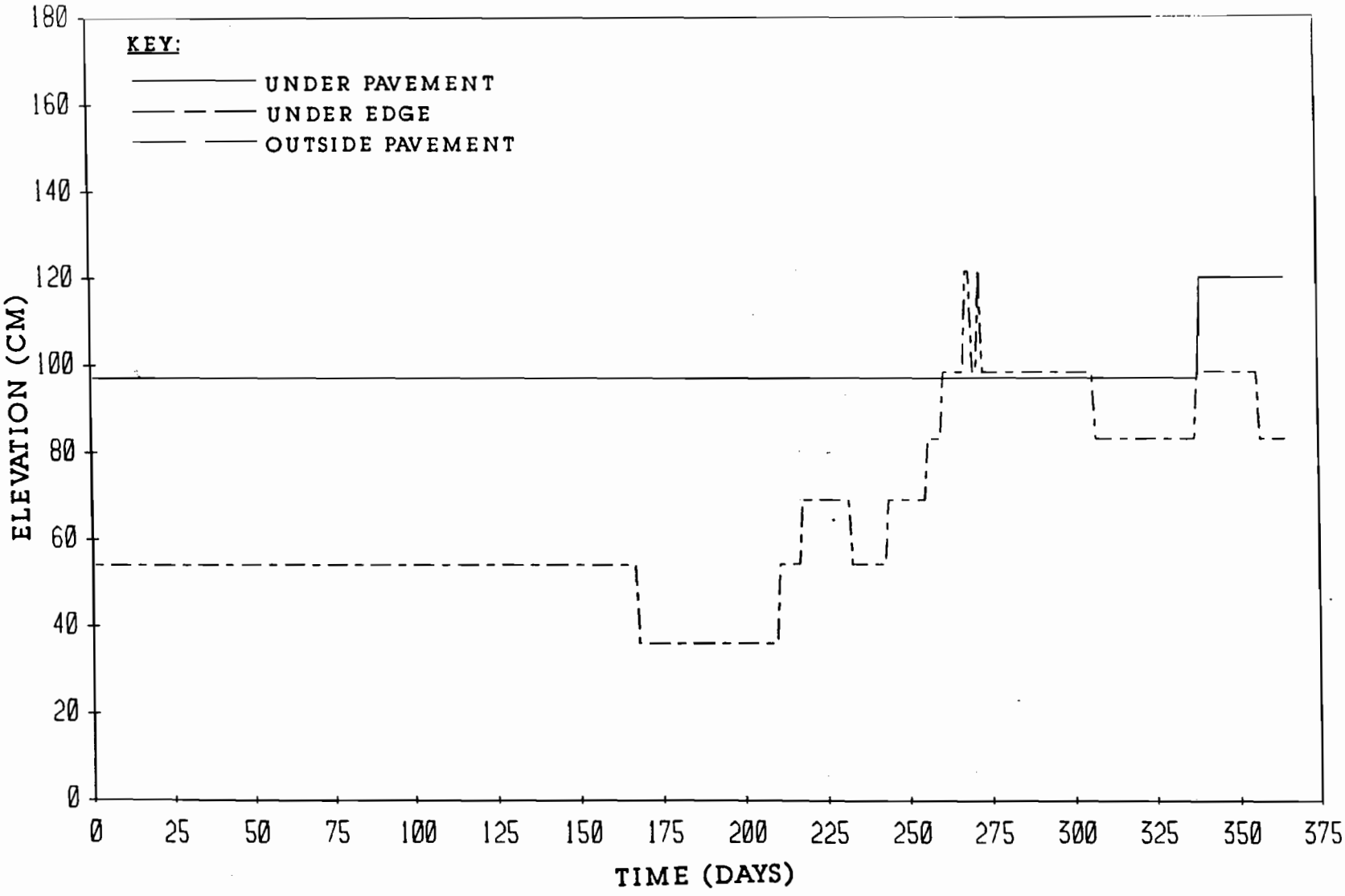

FIGURE D4.7 CRACK TIP ELEVATIONS FOR SEVENTH YEAR IN EL PASO

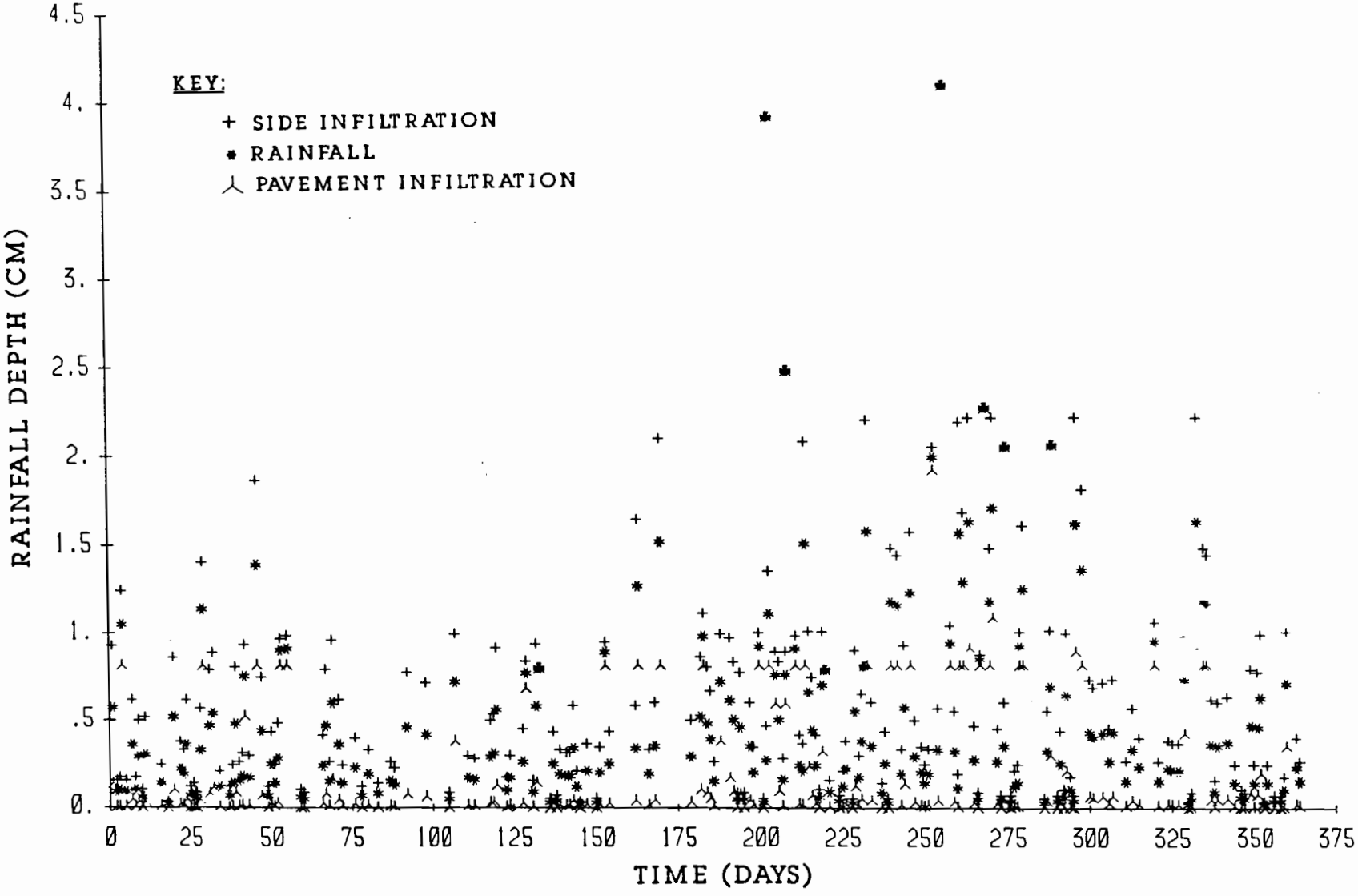

FIGURE D1.8 RAINFALL AND INFILTRATION DEPTHS FOR EIGHTH YEAR IN EL PASO

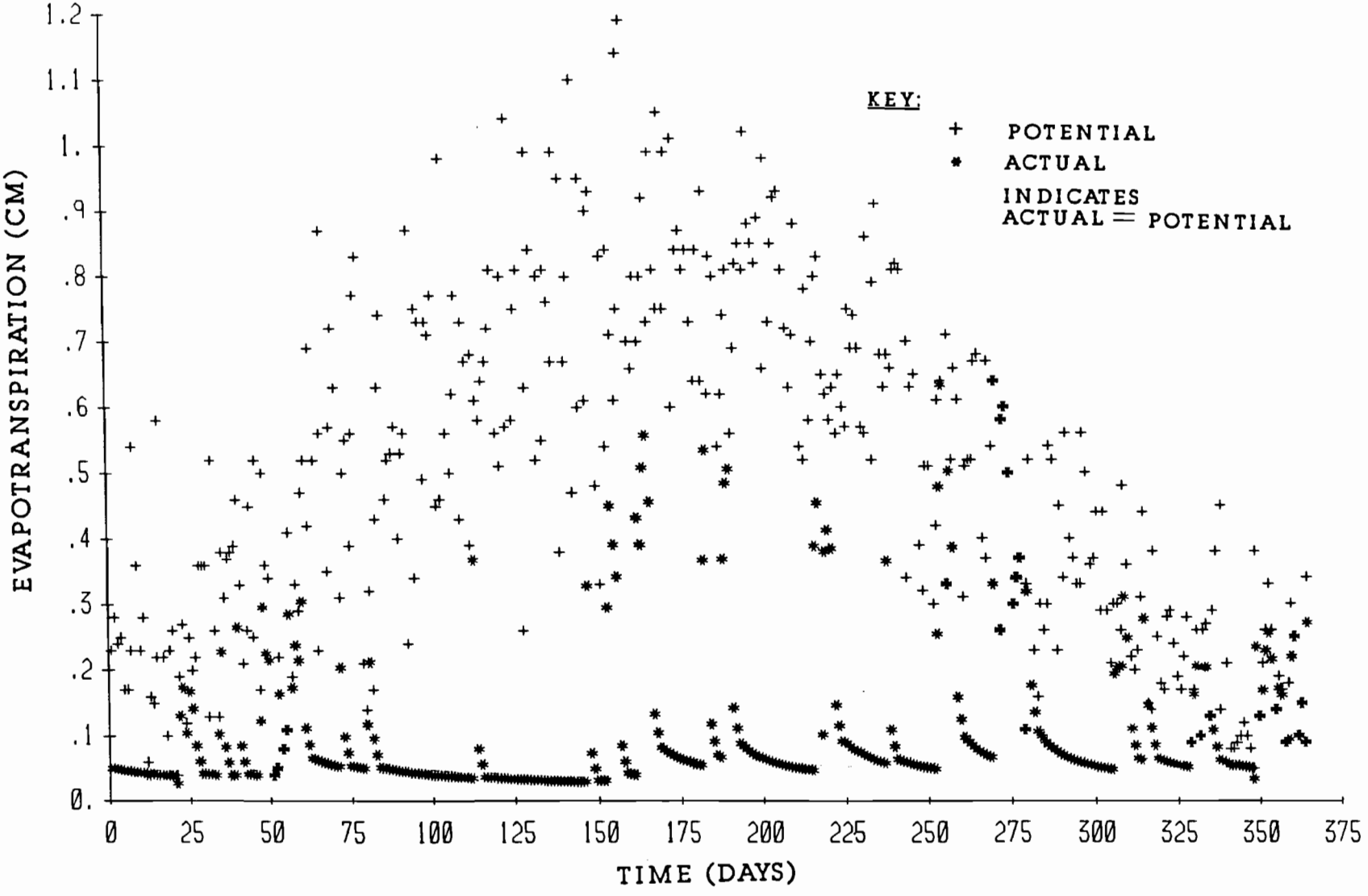

FIGURE D2.8 EVAPOTRANSPIRATION FOR EIGHTH YEAR IN EL PASO

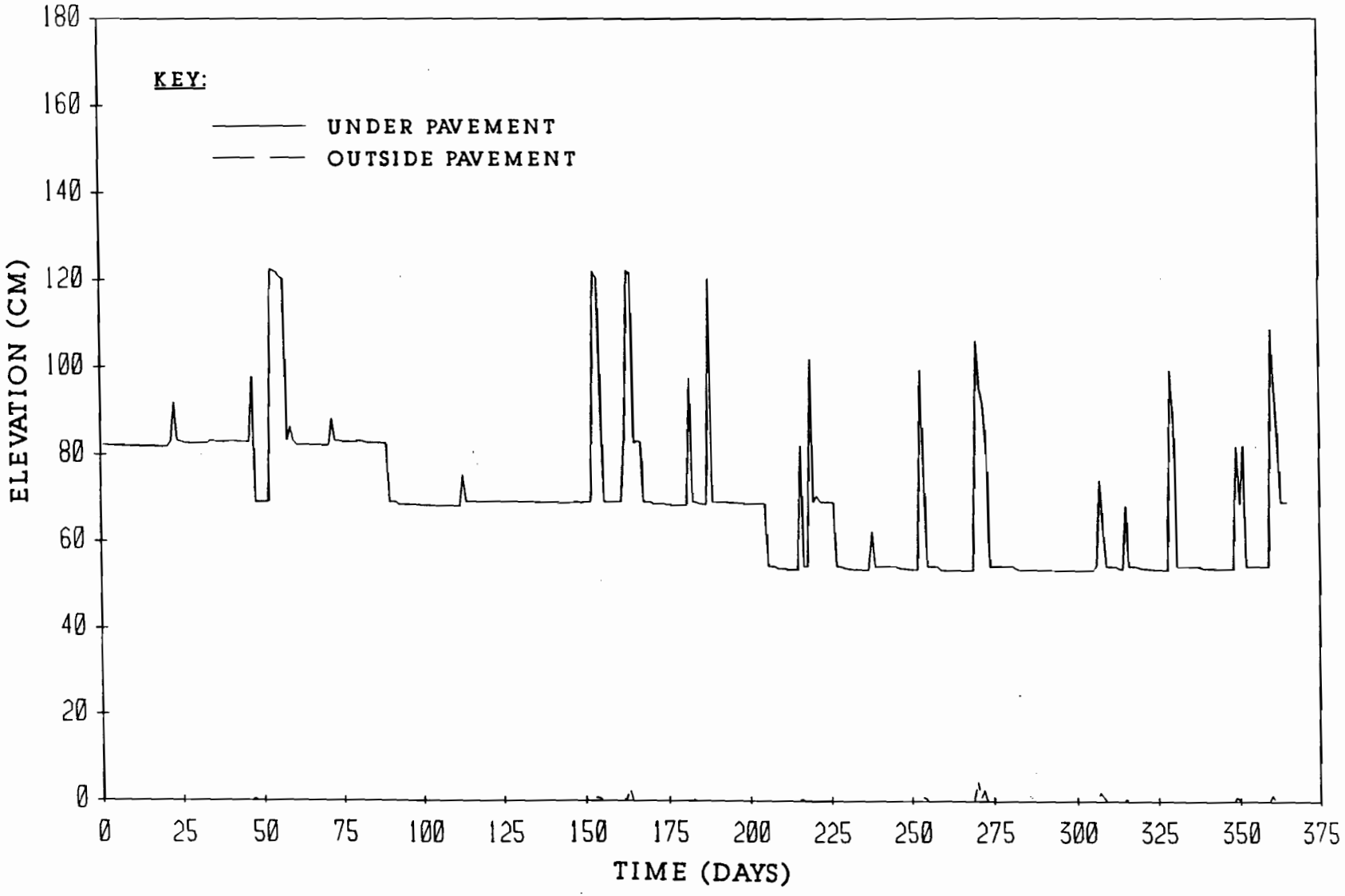

FIGURE D3.8 WATER LEVELS WITHIN THE CRACK FABRIC FOR EIGHTH YEAR IN EL PASO

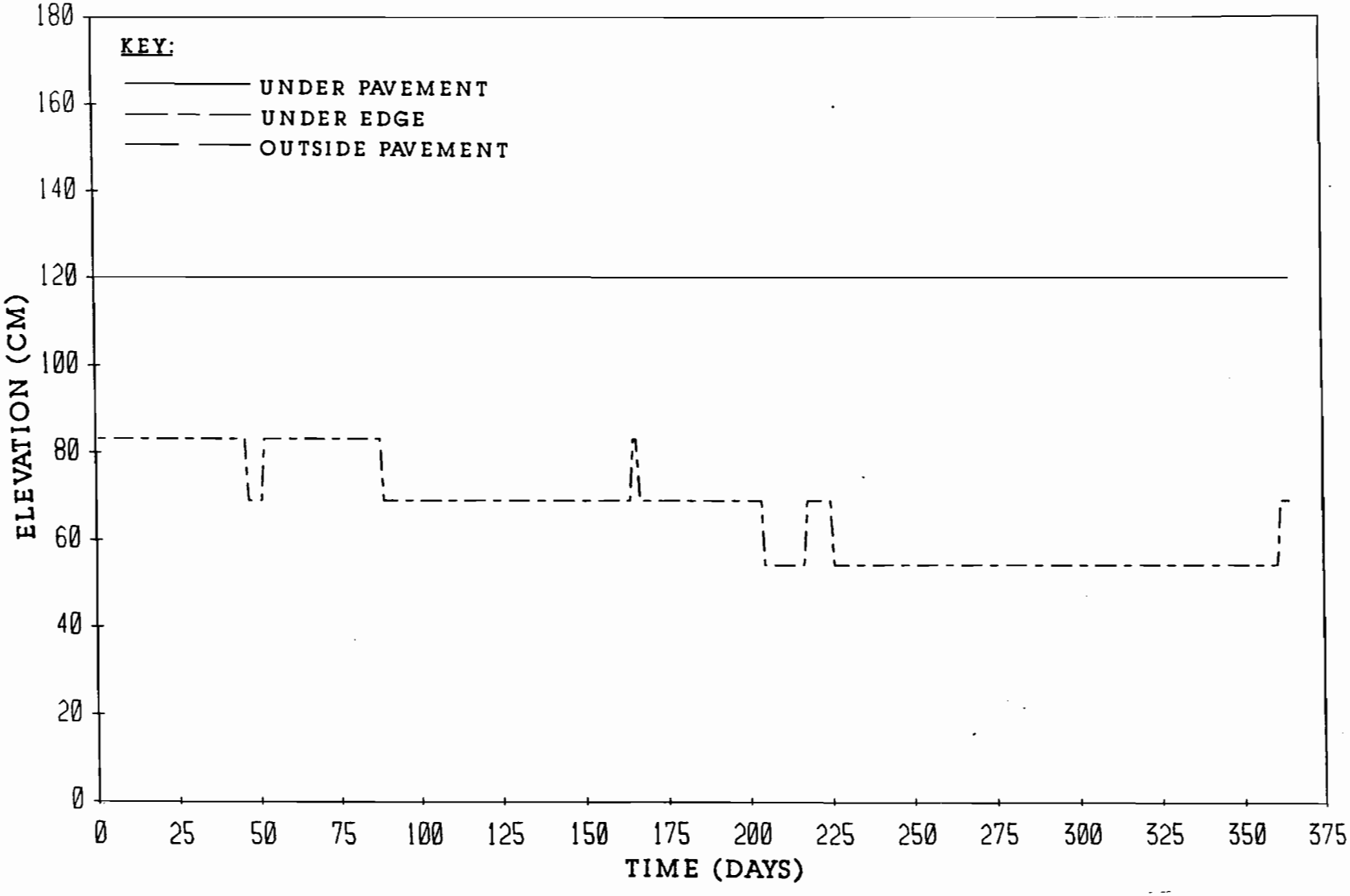

FIGURE D4.8 CRACK TIP ELEVATIONS FOR EIGHTH YEAR IN EL PASO

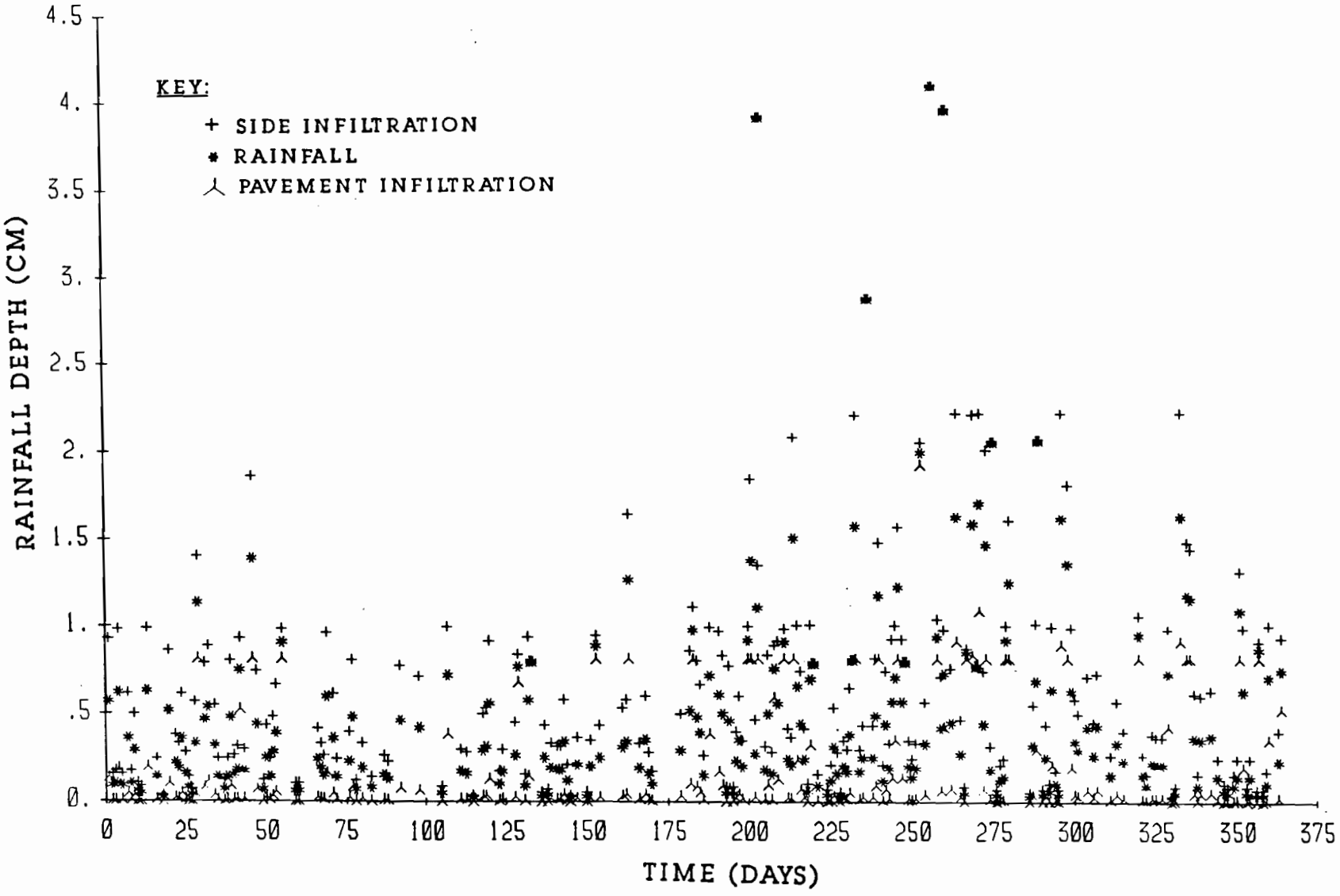

FIGURE D1.9 RAINFALL AND INFILTRATION DEPTHS FOR NINTH YEAR IN EL PASO

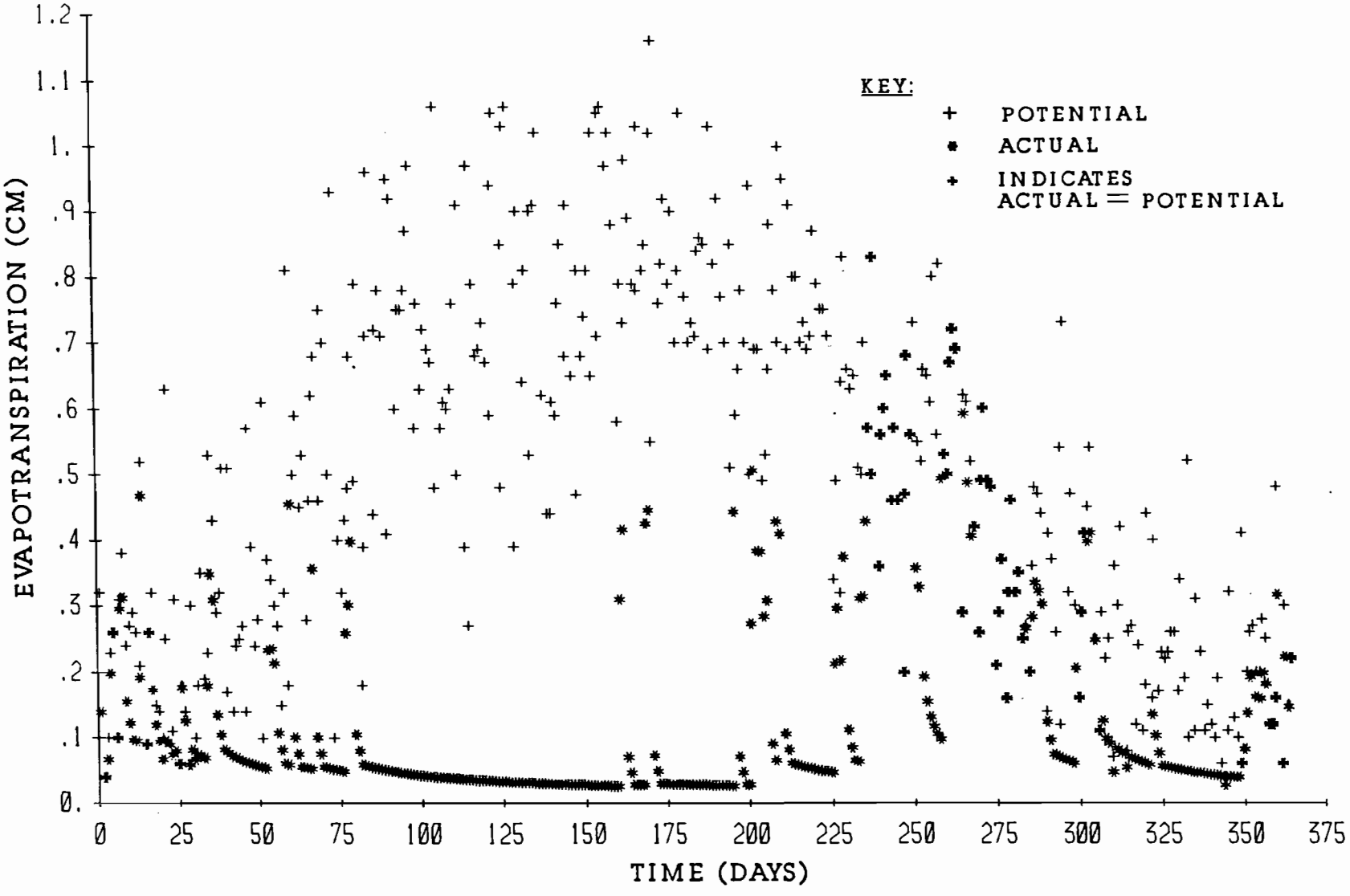

FIGURE D2.9 EVAPOTRANSPIRATION FOR NINTH YEAR IN EL PASO

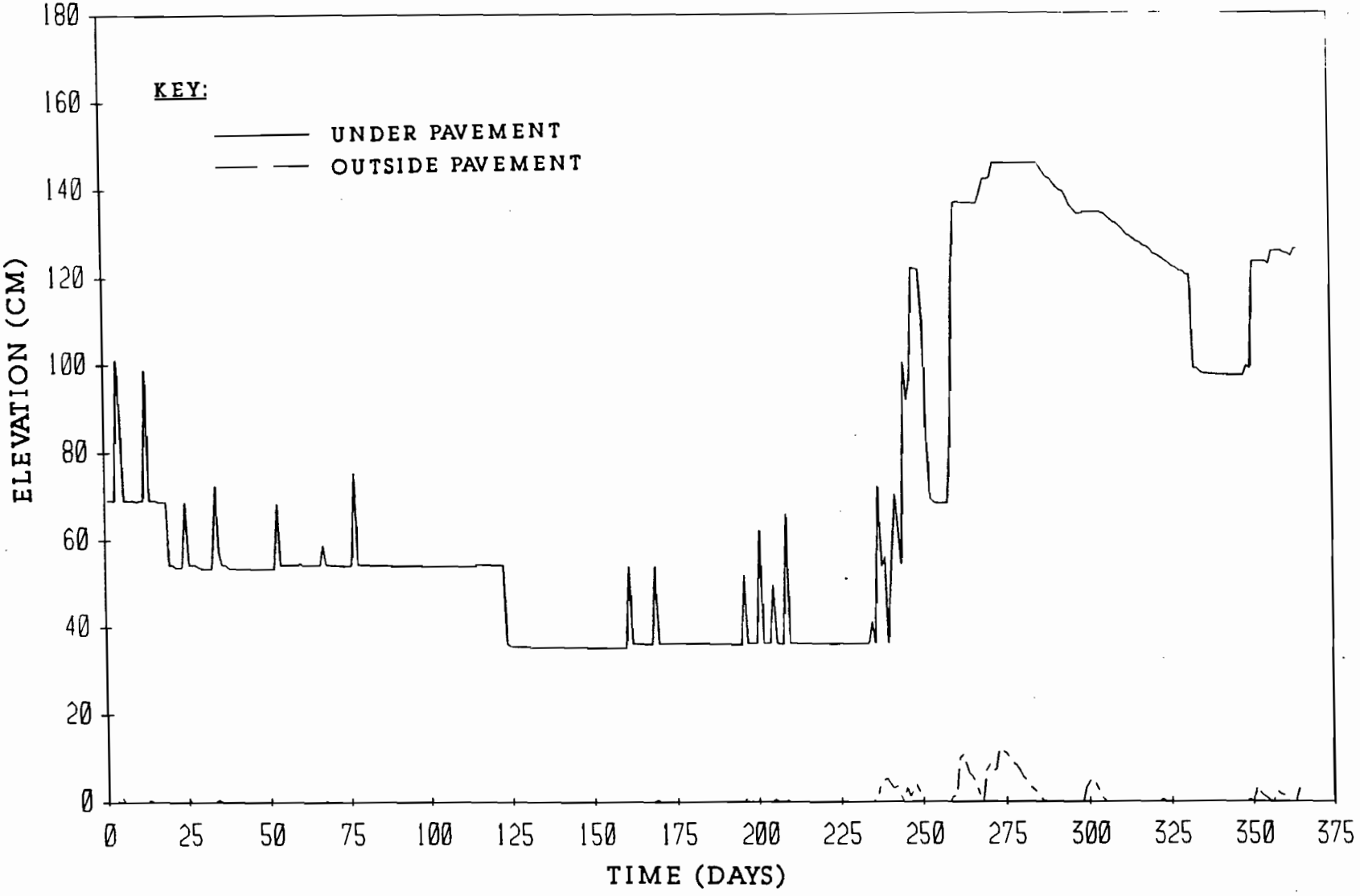

FIGURE D3.9 WATER LEVELS WITHIN THE CRACK FABRIC FOR NINTH YEAR IN EL PASO

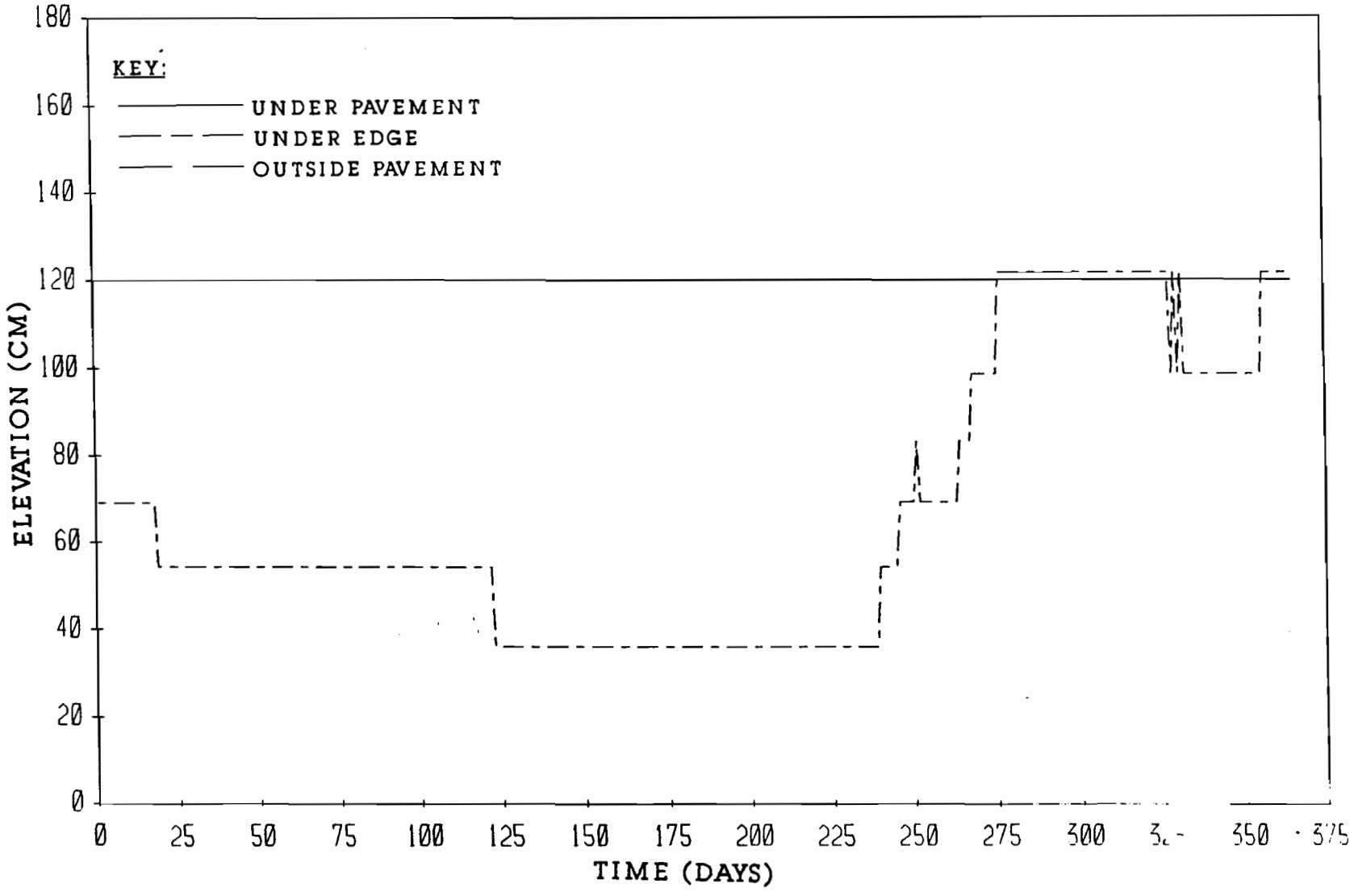

FIGURE D4.9 CRACK TIP ELEVATIONS FOR NINTH YEAR IN EL PASO

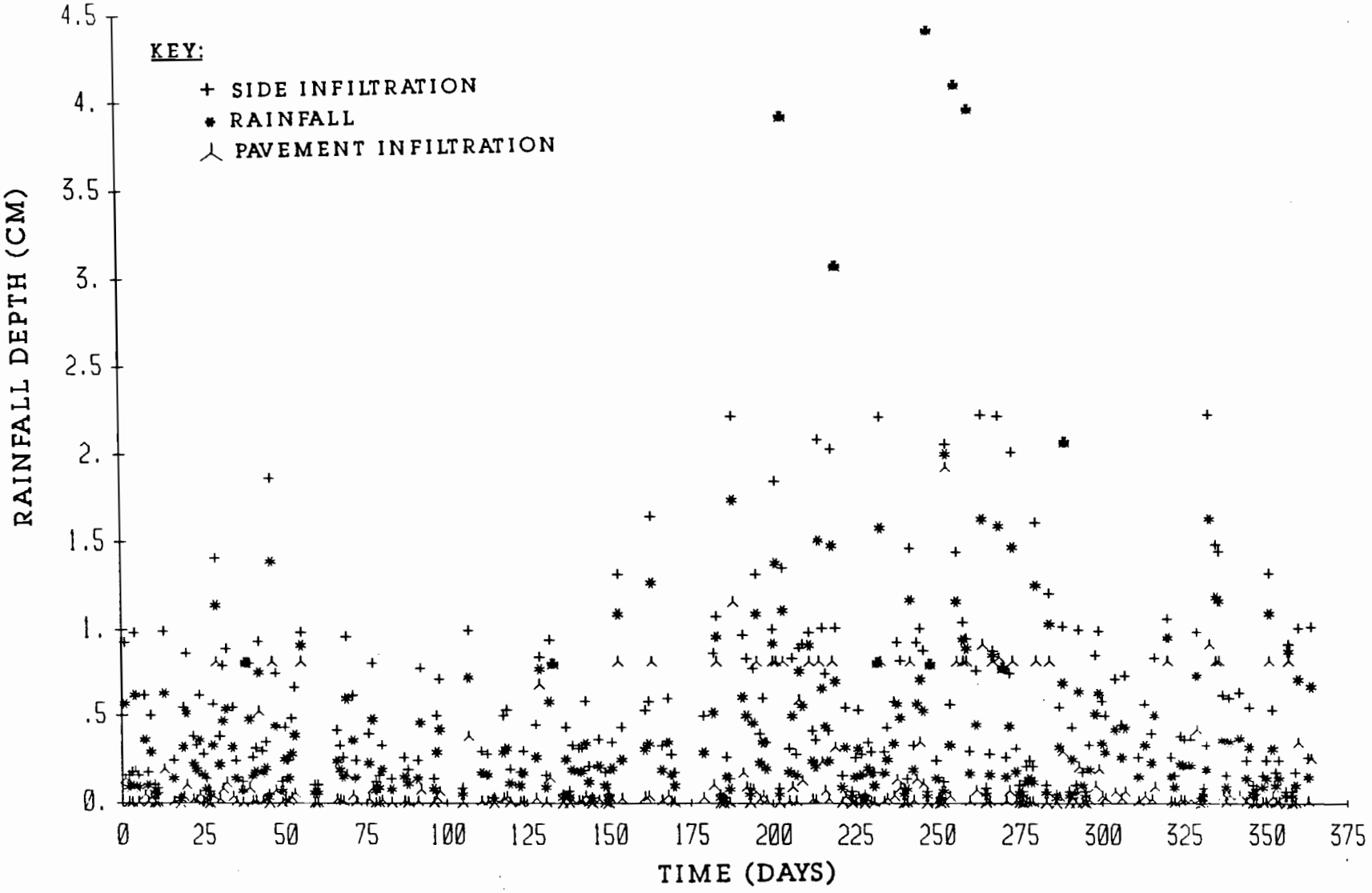

FIGURE D1.10 RAINFALL AND INFILTRATION DEPTHS FOR TENTH YEAR IN EL PASO

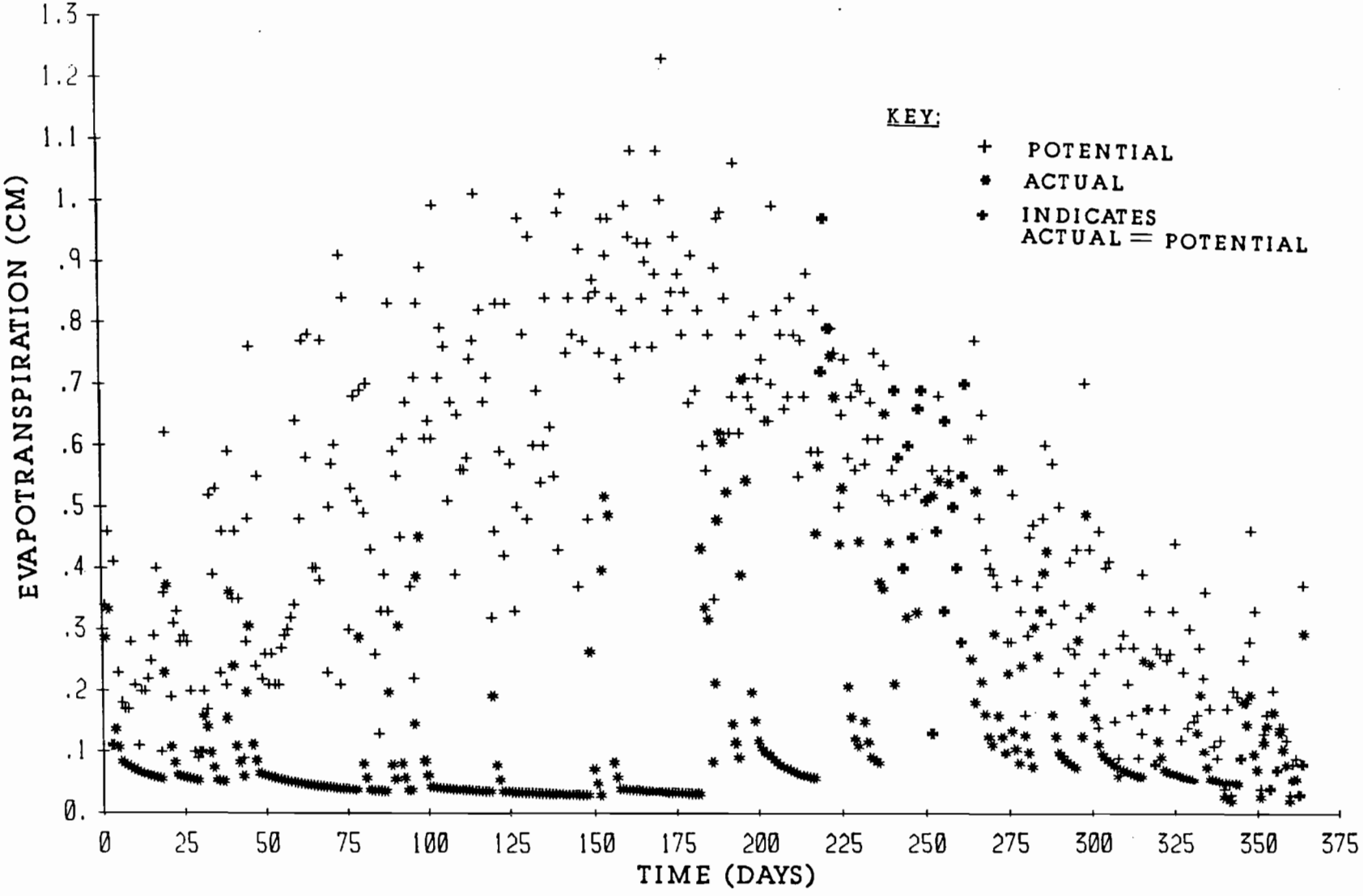

FIGURE D2.10 EVAPOTRANSPIRATION FOR TENTH YEAR IN EL PASO

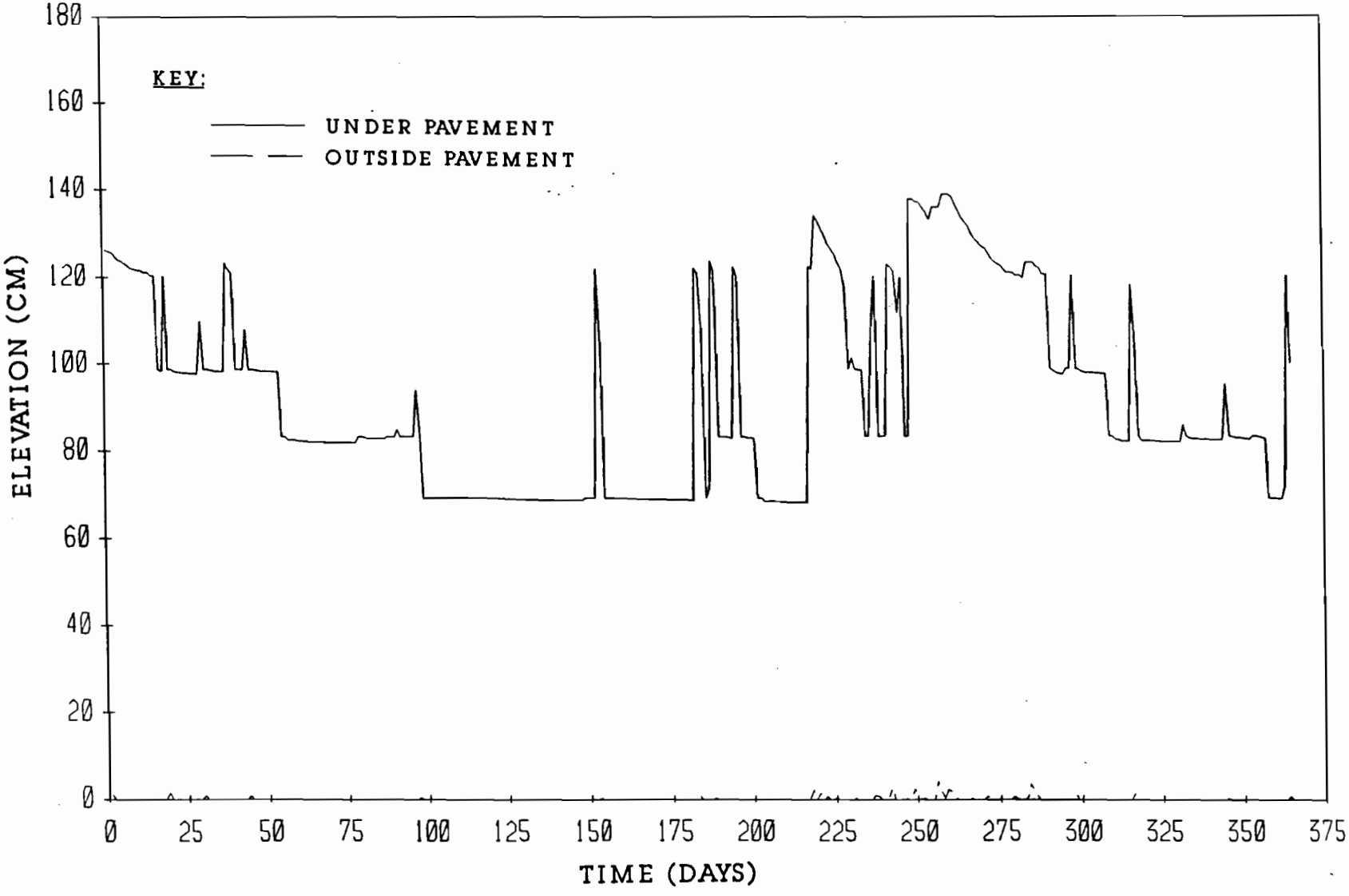

FIGURE D3.10 WATER LEVELS WITHIN THE CRACK FABRIC FOR TENTH YEAR IN EL PASO

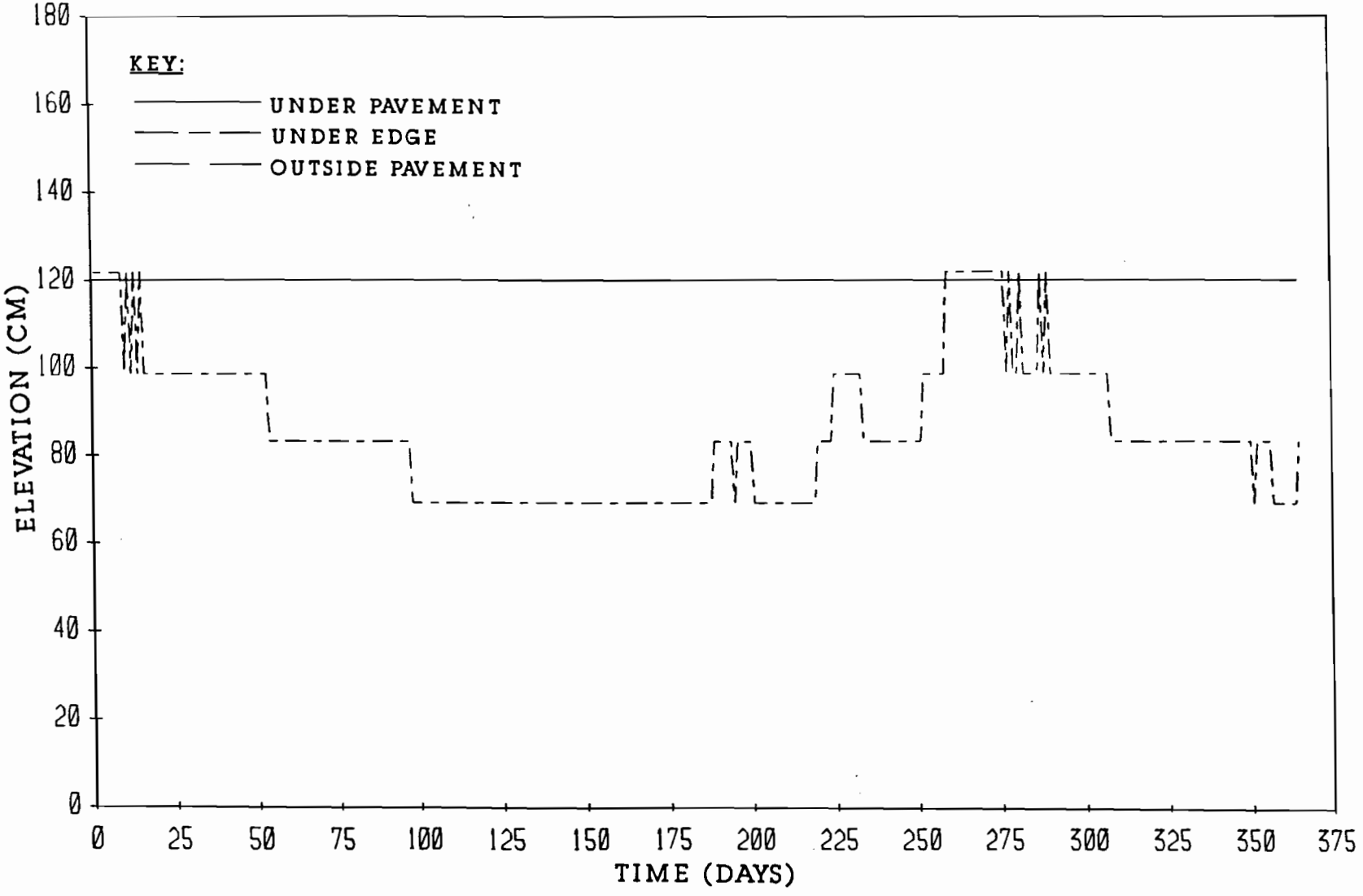

FIGURE D4.10 CRACK TIP ELEVATIONS FOR TENTH YEAR IN EL PASO

APPENDIX E

SIMULATION RESULT FOR SAN ANTONIO FOR MOISTURE BARRIER TIP AT ELEVATION 25 CM

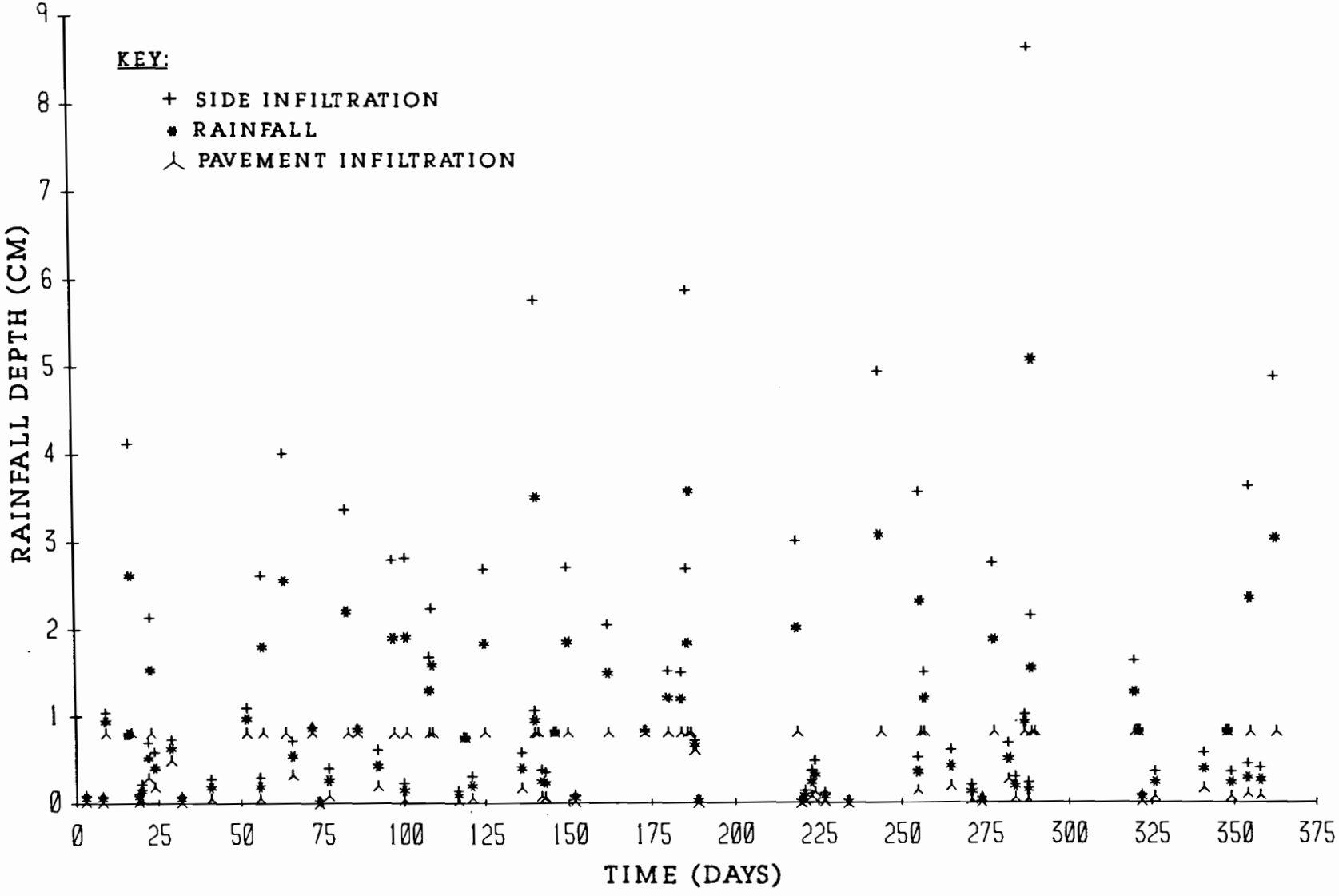

FIGURE E1.1 RAINFALL AND INFILTRATION DEPTHS FOR FIRST YEAR IN SAN ANTONIO FOR MOISTURE BARRIER TIP AT ELEVATION 25 CM

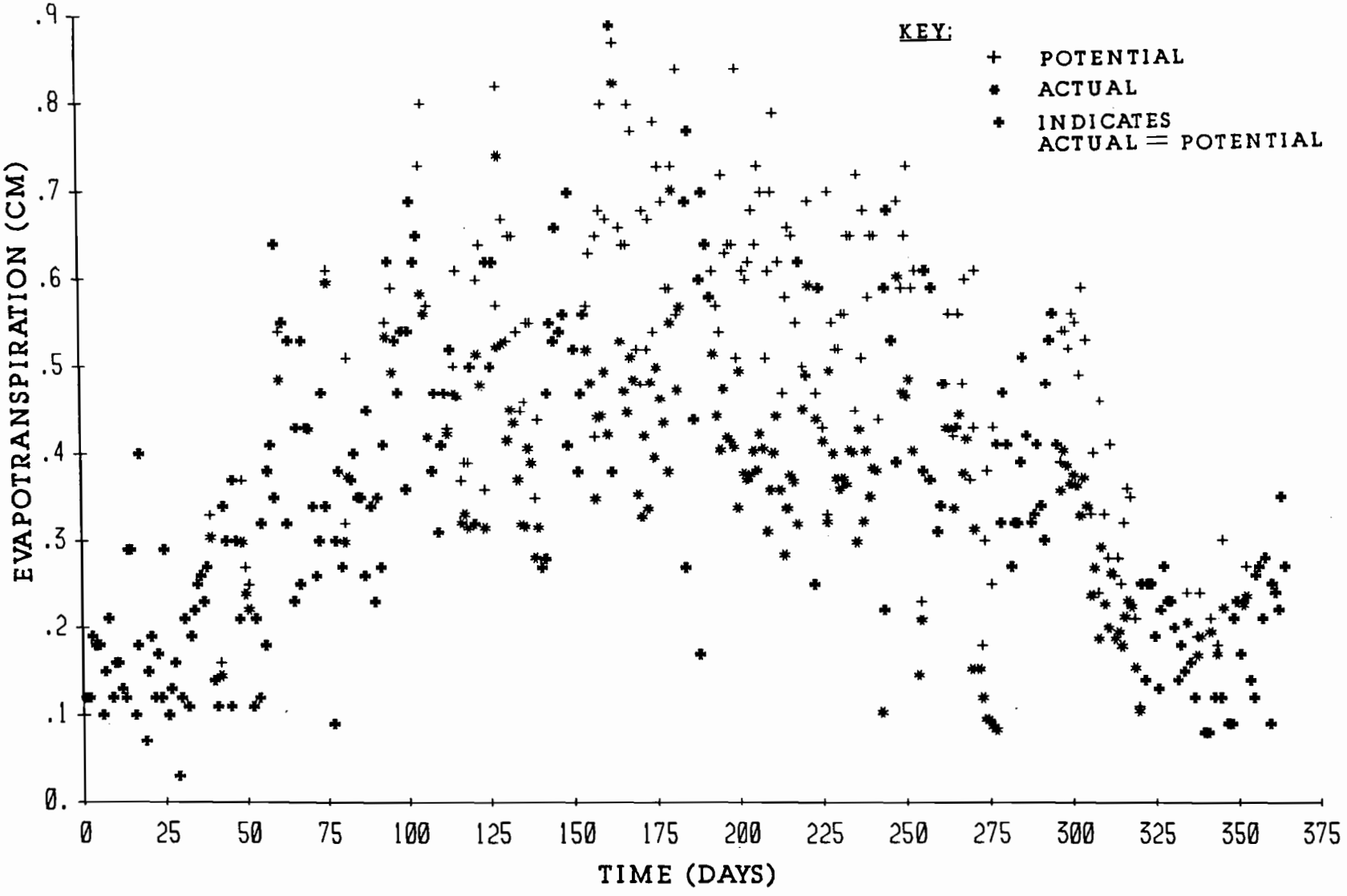

FIGURE E2.1 EVAPOTRANSPIRATION FOR FIRST YEAR IN SAN ANTONIO FOR MOISTURE BARRIER TIP AT ELEVATION 25 CM

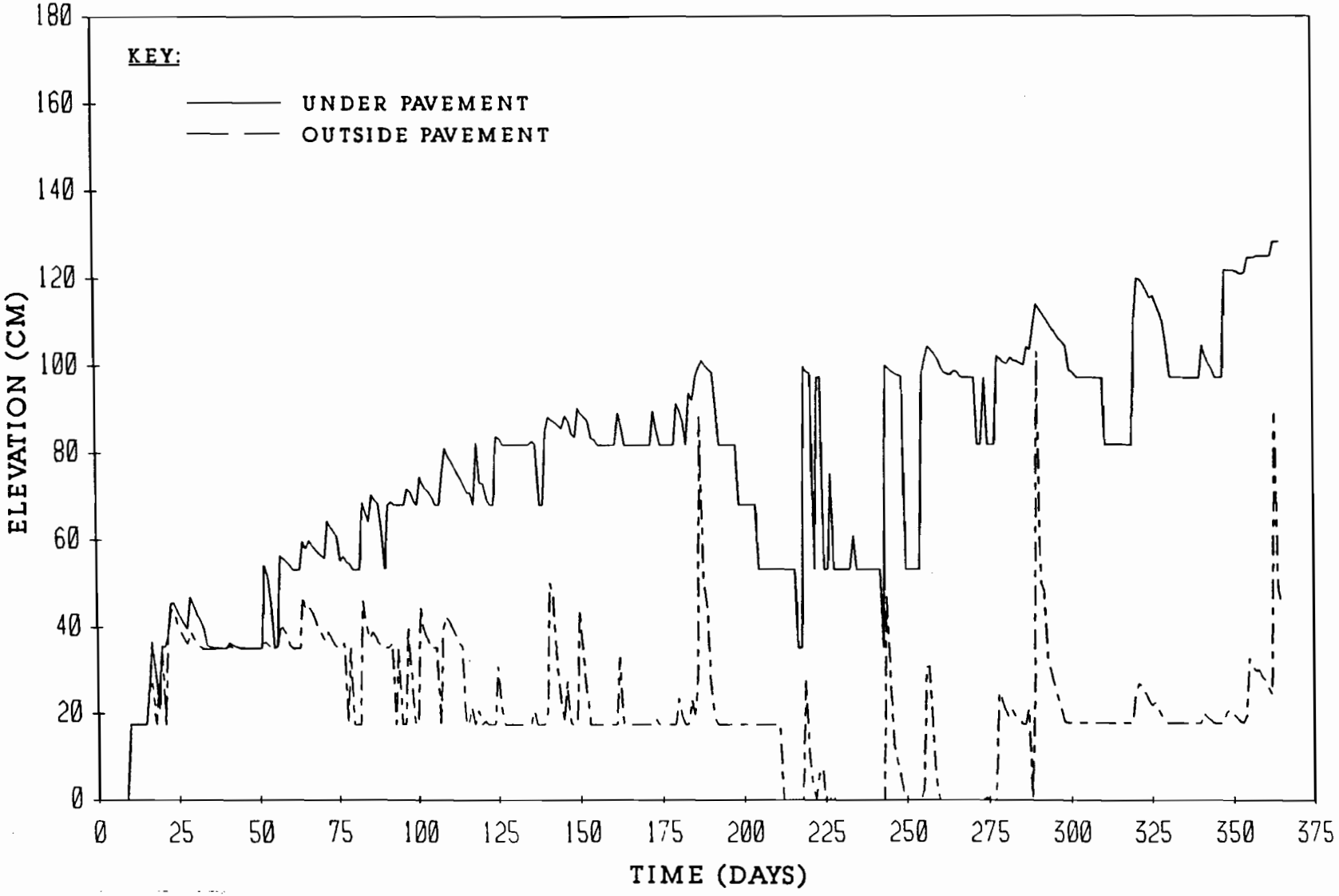

FIGURE E3.1 WATER LEVELS WITHIN THE CRACK FABRIC FOR FIRST YEAR IN SAN ANTONIO FOR MOISTURE BARRIER TIP AT ELEVATION 25 CM

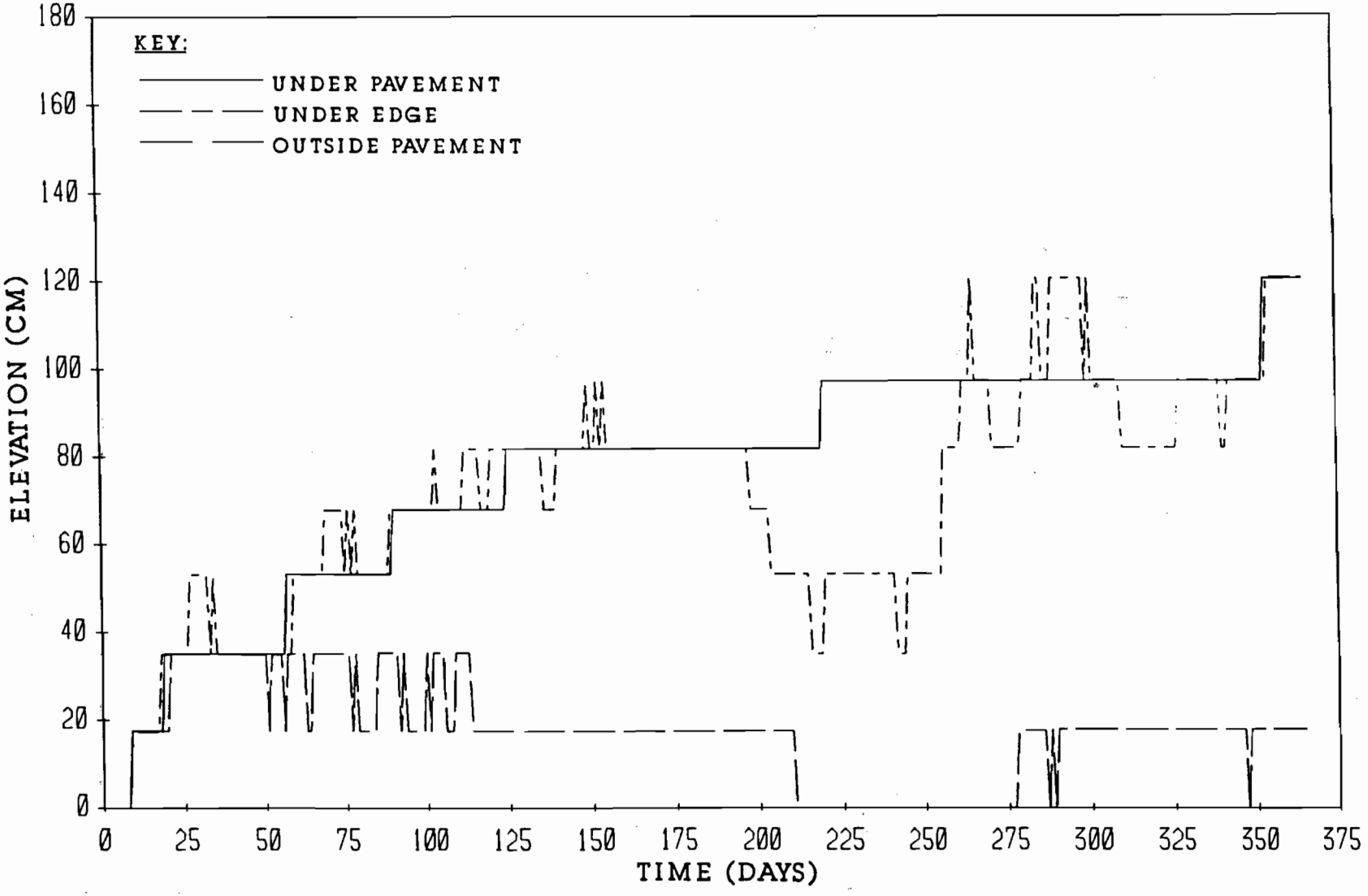

FIGURE E4.1 CRACK TIP ELEVATIONS FOR FIRST YEAR IN SAN ANTONIO FOR MOISTURE BARRIER TIP AT ELEVATION 25 CM

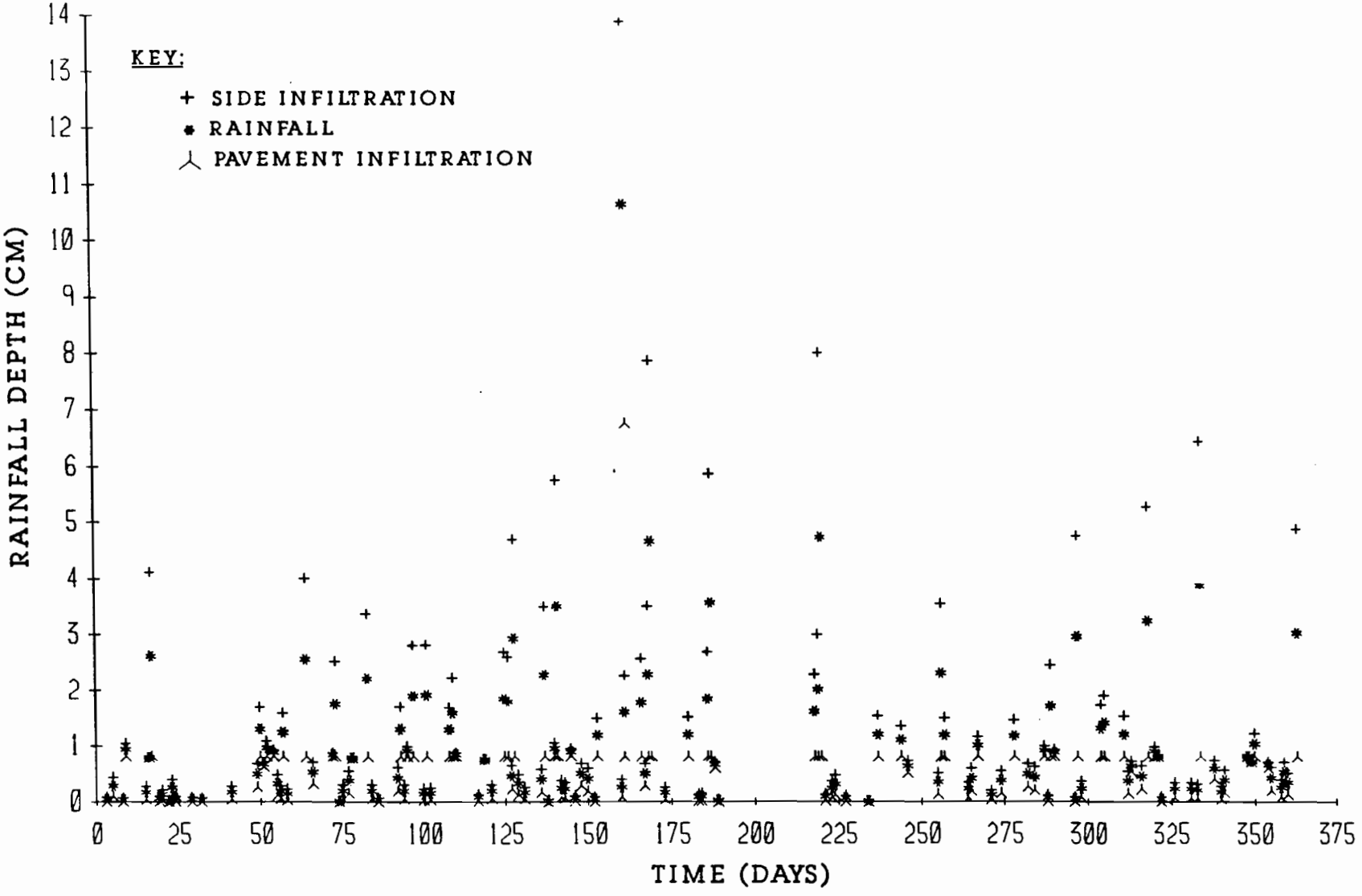

FIGURE E1.2 RAINFALL AND INFILTRATION DEPTHS FOR SECOND YEAR IN SAN ANTONIO FOR MOISTURE BARRIER TIP AT ELEVATION 25 CM

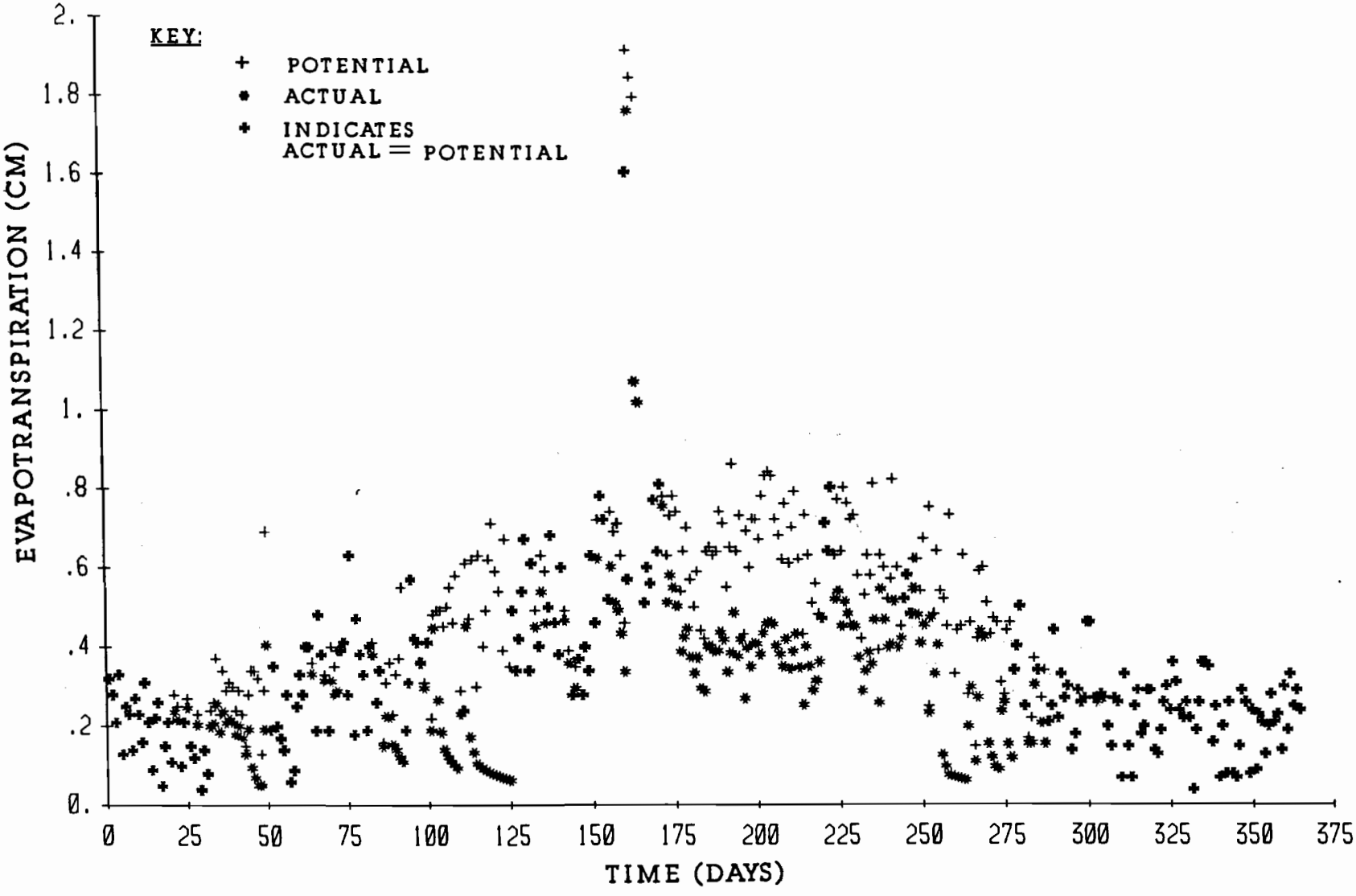

FIGURE E2.2 EVAPOTRANSPIRATION FOR SECOND YEAR IN SAN ANTONIO FOR MOISTURE BARRIER TIP AT ELEVATION 25 CM

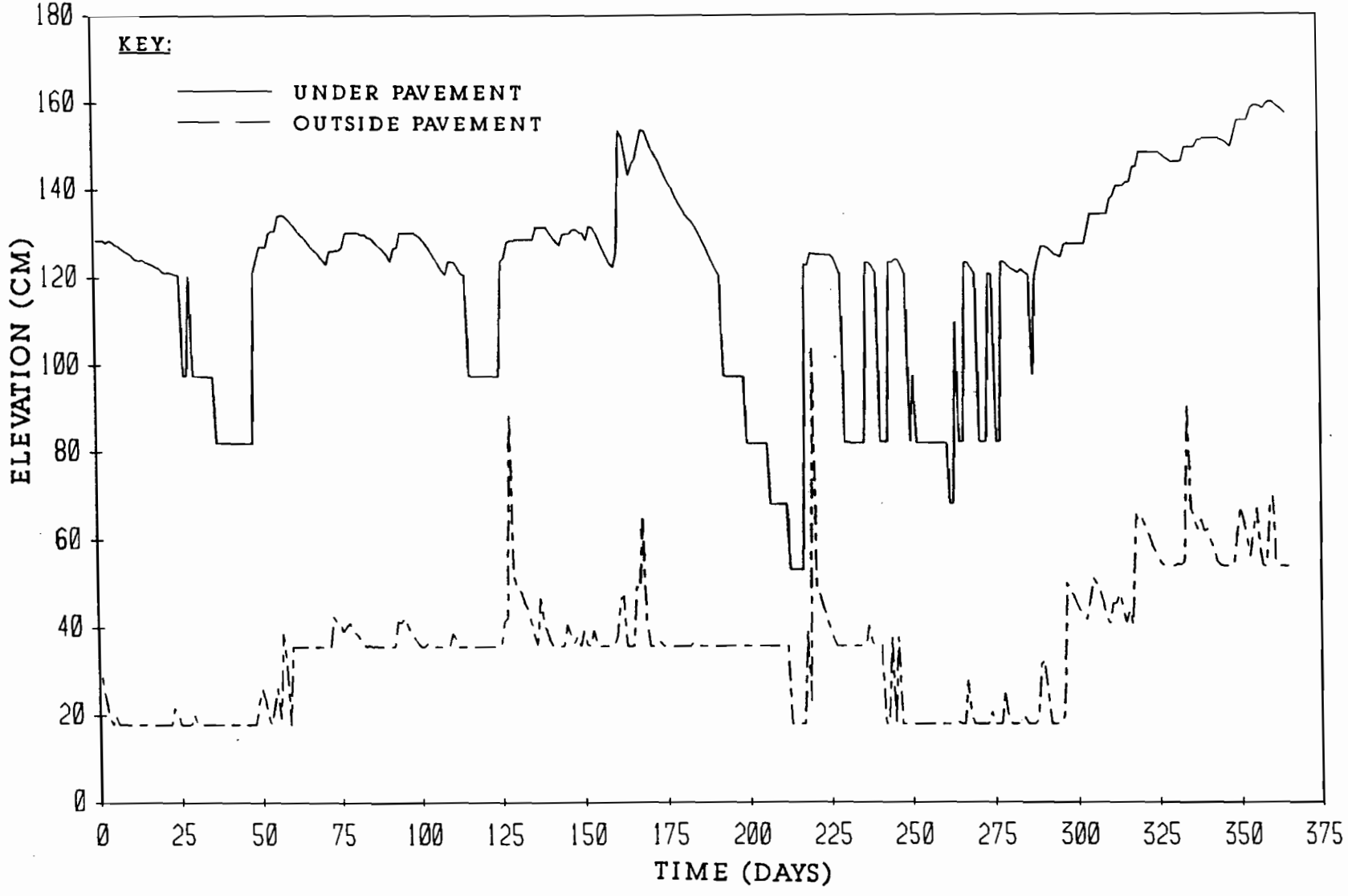

FIGURE E3.2 WATER LEVELS WITHIN THE CRACK FABRIC FOR SECOND YEAR IN SAN ANTONIO FOR MOISTURE BARRIER TIP AT ELEVATION 25 CM

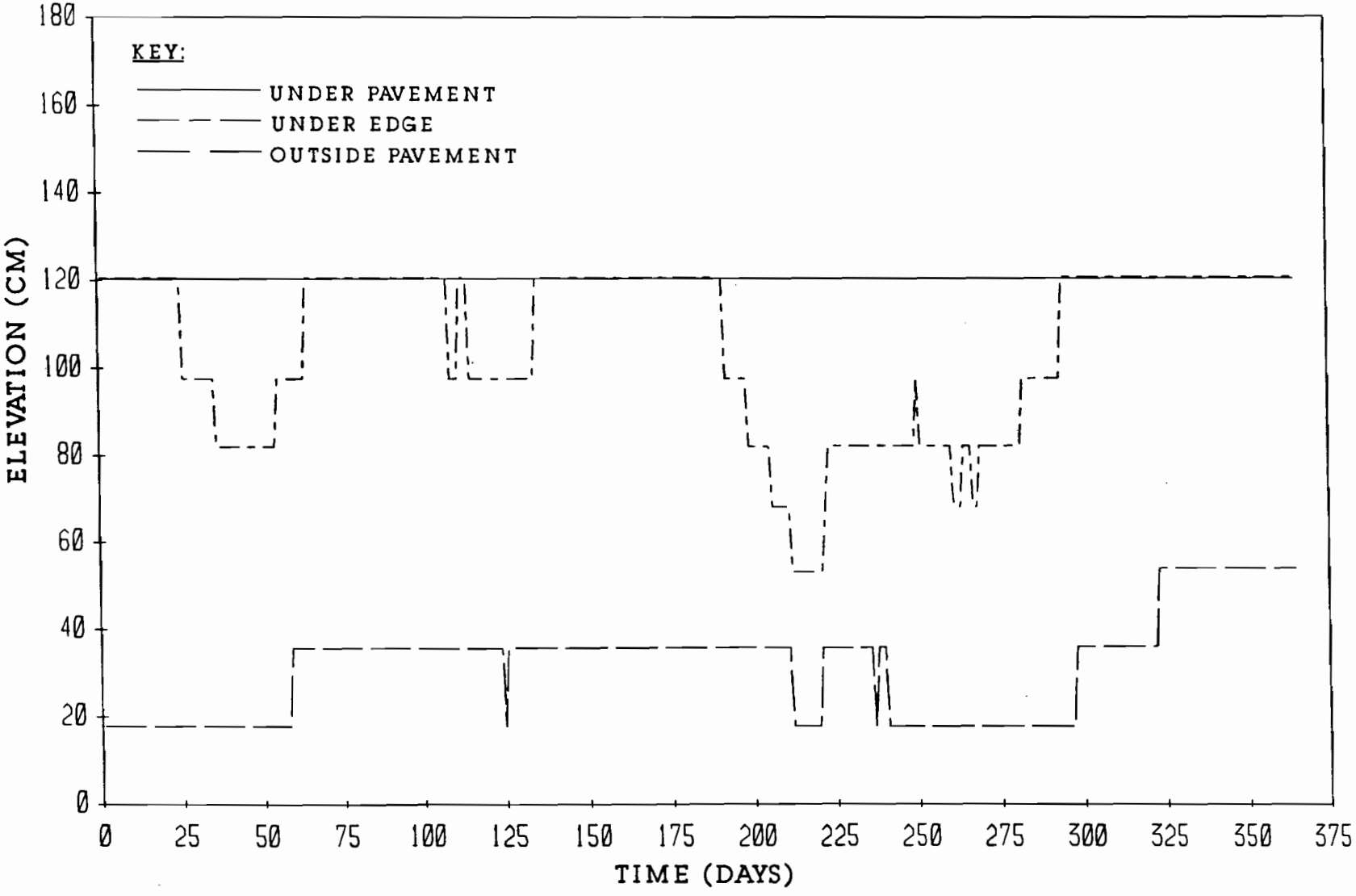

FIGURE E4.2 CRACK TIP ELEVATIONS FOR SECOND YEAR IN SAN ANTONIO FOR MOISTURE BARRIER TIP AT ELEVATION 25 CM

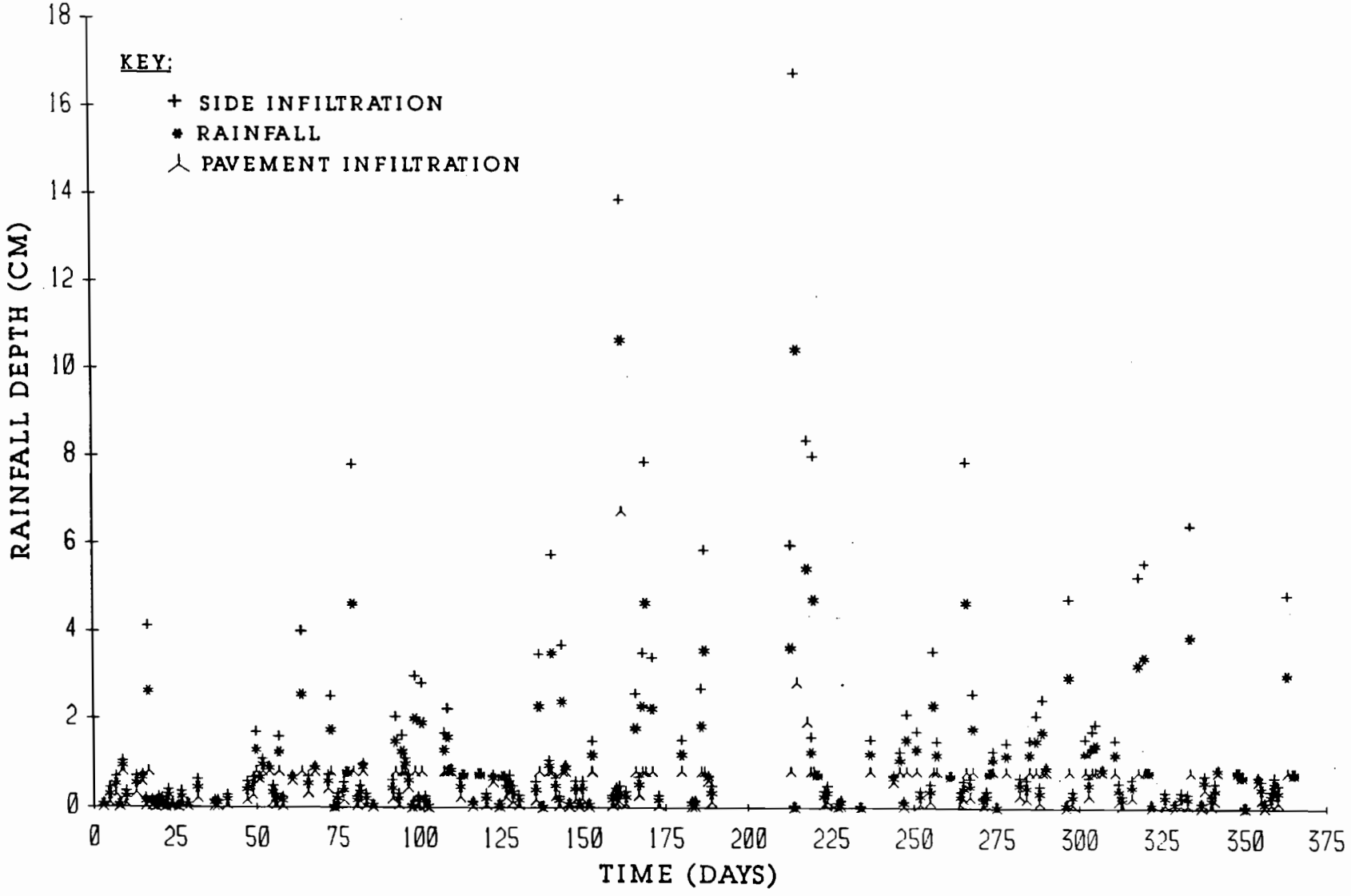

FIGURE E1.3 RAINFALL AND INFILTRATION DEPTHS FOR THIRD YEAR IN SAN ANTONIO FOR MOISTURE BARRIER TIP AT ELEVATION 25 CM

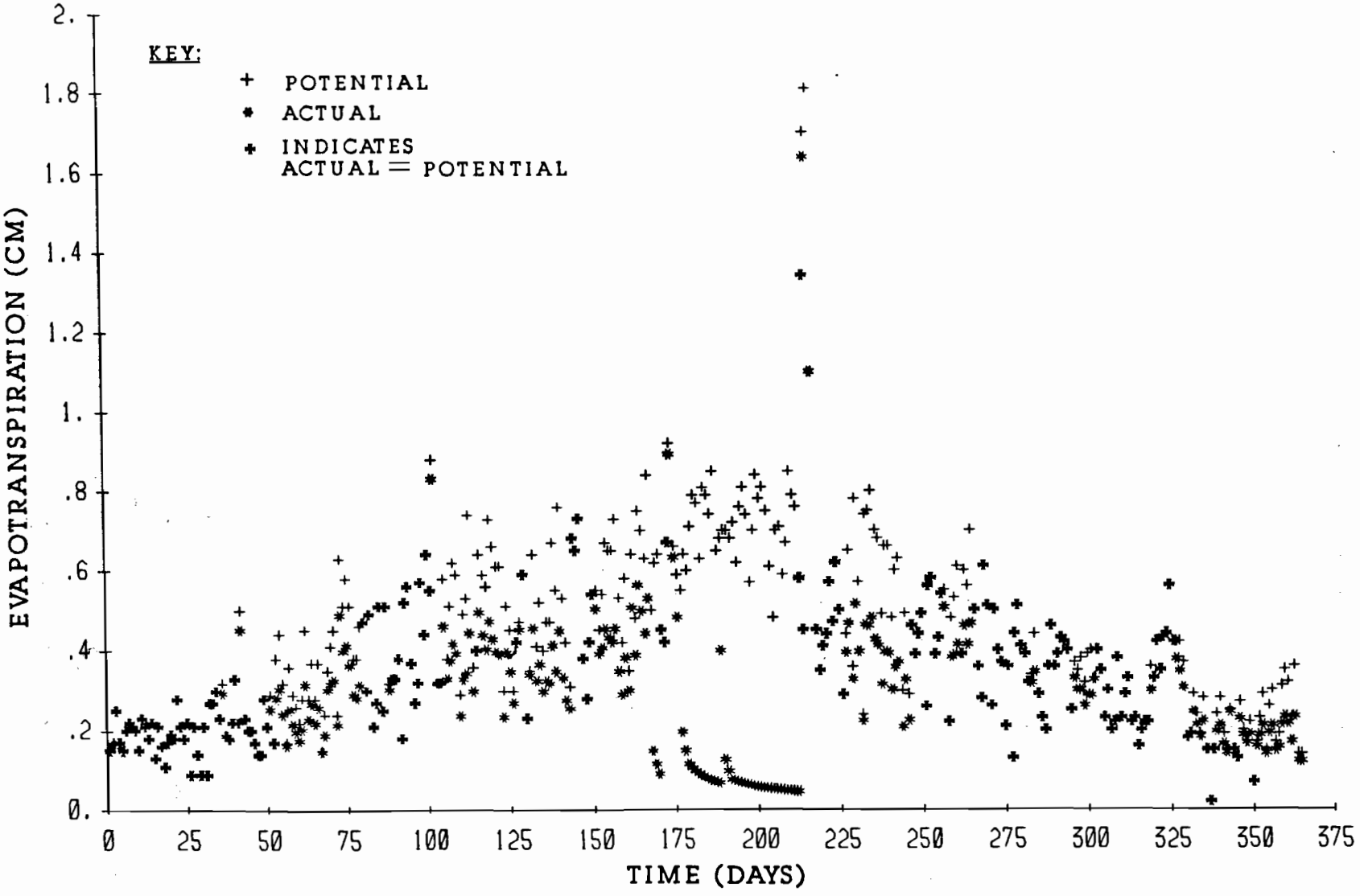

FIGURE E2.3 EVAPOTRANSPIRATION FOR THIRD YEAR IN SAN ANTONIO FOR MOISTURE BARRIER TIP AT ELEVATION 25 CM

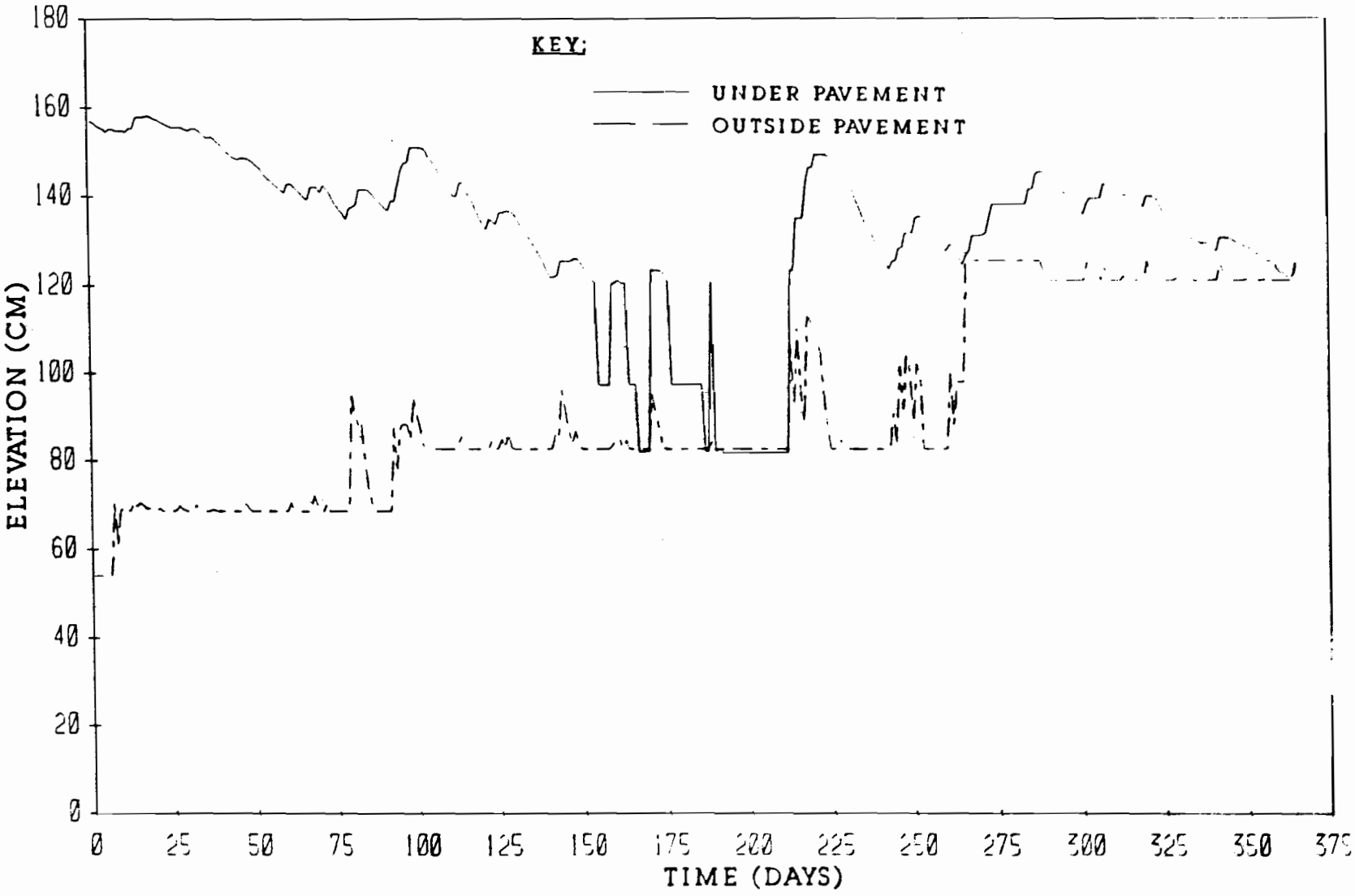

FIGURE B3.3 WATER LEVELS WITHIN THE CRACK FABRIC FOR THIRD YEAR IN SAN ANTONIO FOR MOISTURE BARRIER TIP AT ELEVATION 25 CM

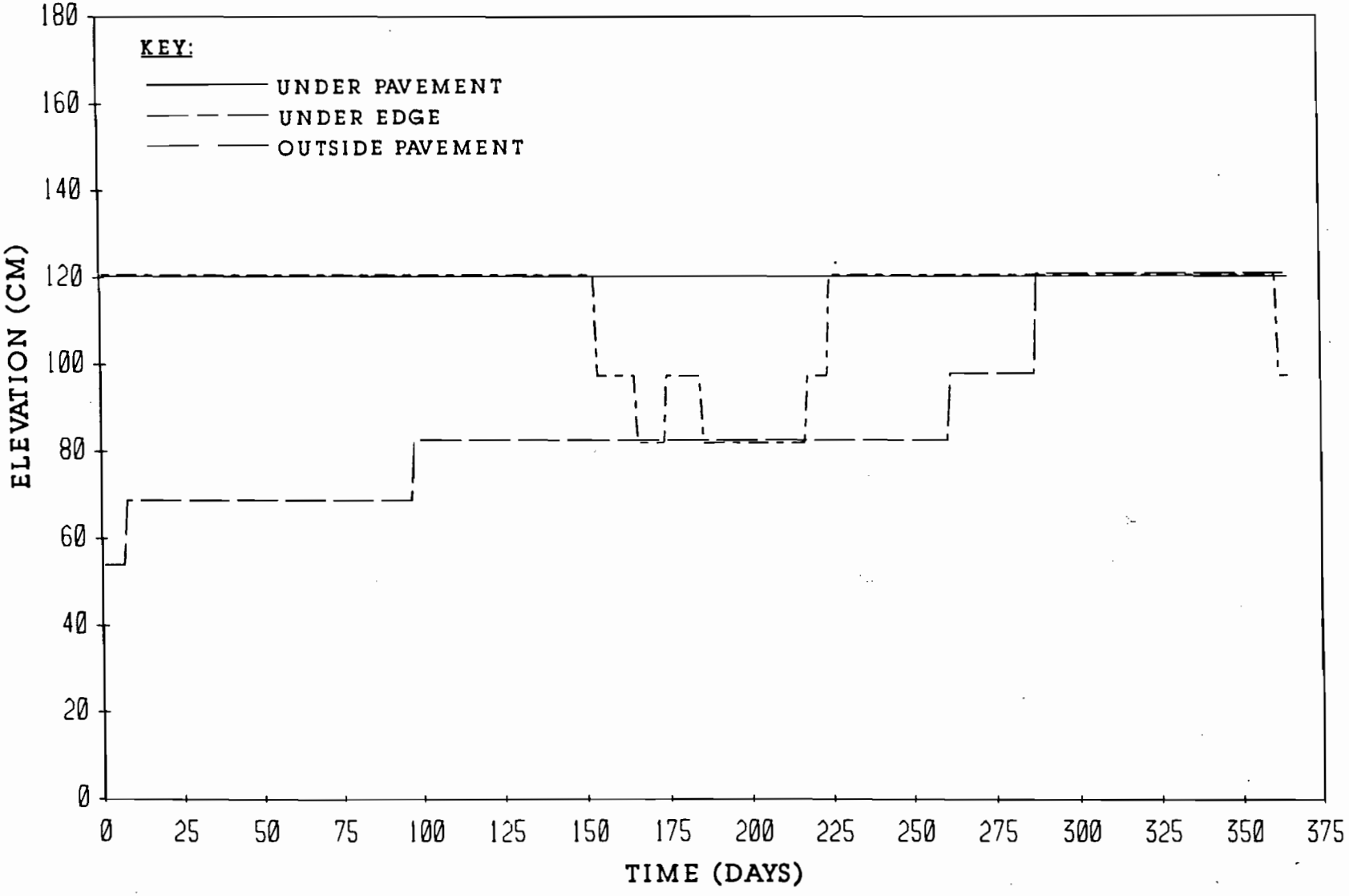

FIGURE E4.3 CRACK TIP ELEVATIONS FOR THIRD YEAR IN SAN ANTONIO FOR MOISTURE BARRIER TIP AT ELEVATION 25 CM

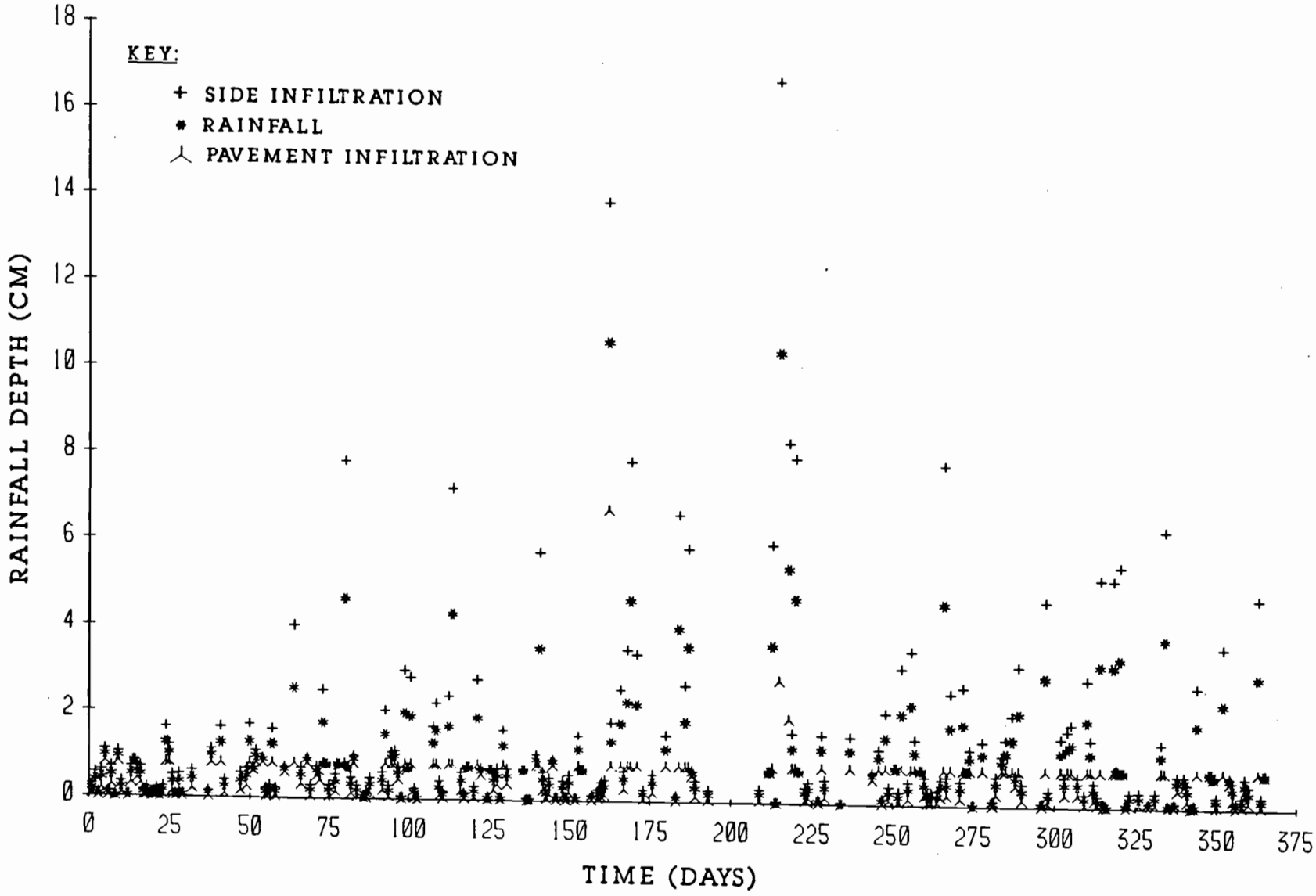

FIGURE E1.4 RAINFALL AND INFILTRATION DEPTHS FOR FOURTH YEAR IN SAN ANTONIO FOR MOISTURE BARRIER TIP AT ELEVATION 25 CM

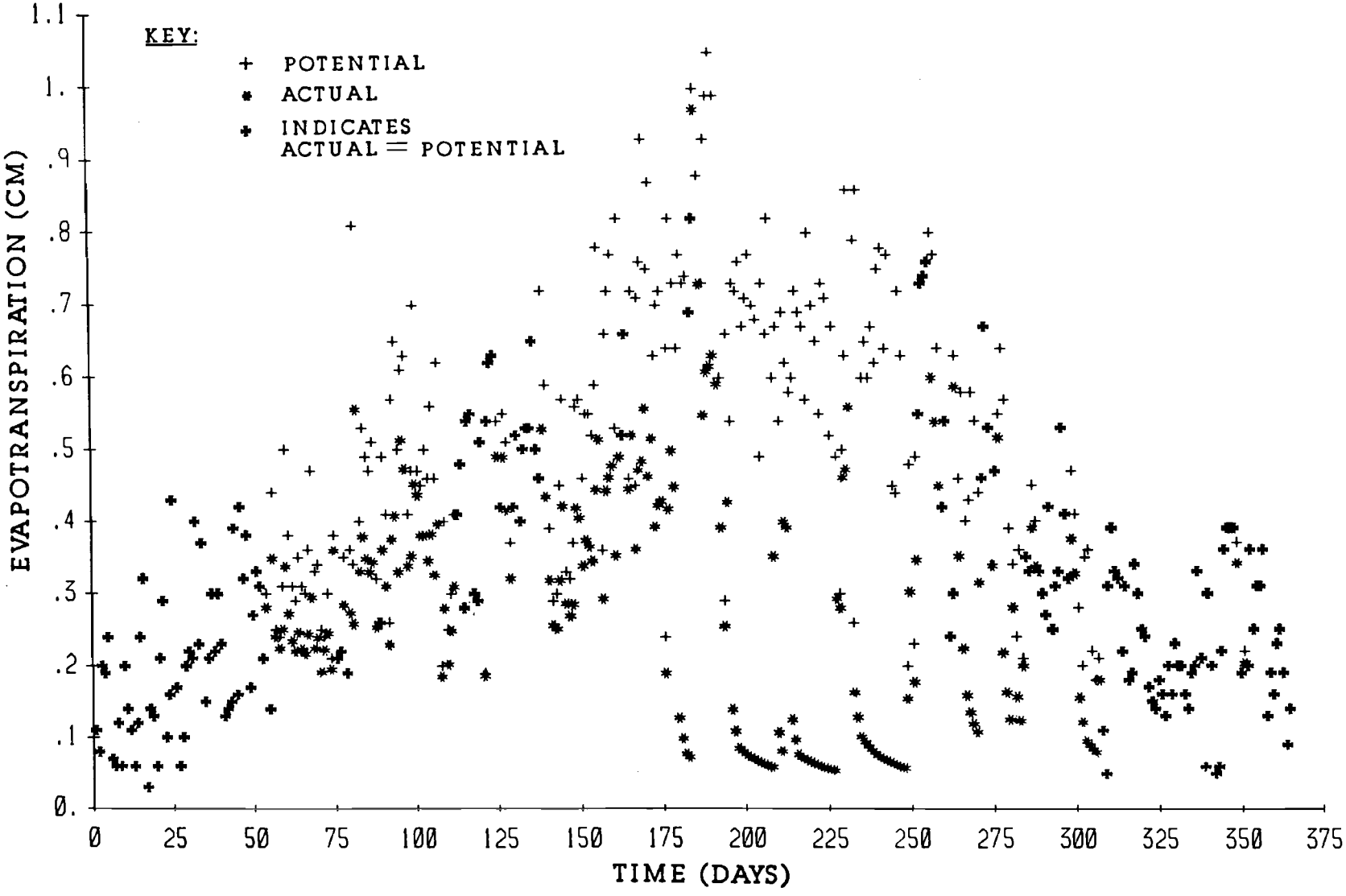

FIGURE E2.4 EVAPOTRANSPIRATION FOR FOURTH YEAR IN SAN ANTONIO FOR MOISTURE BARRIER TIP AT ELEVATION 25 CM

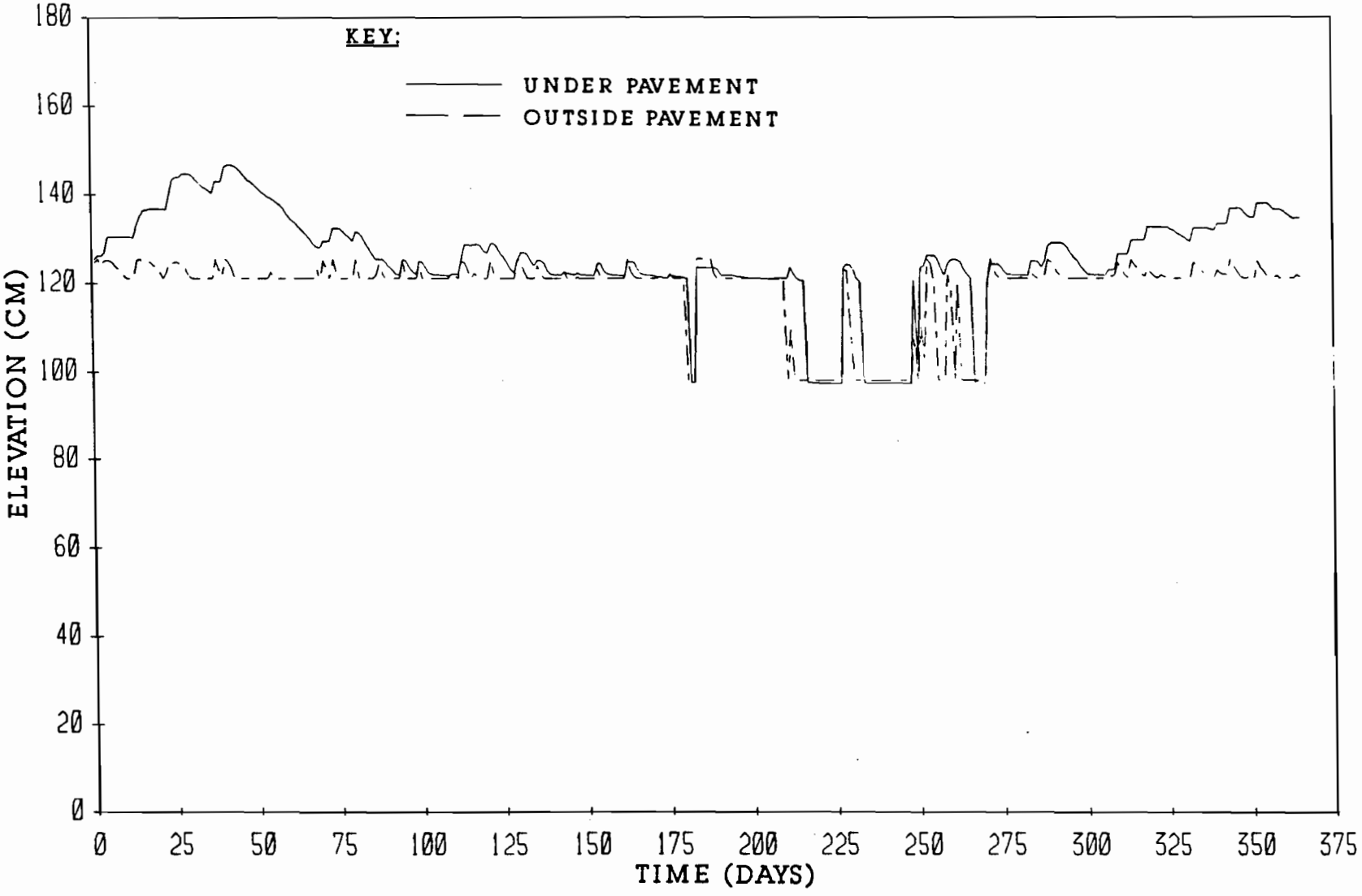

FIGURE E3.4 WATER LEVELS WITHIN THE CRACK FABRIC FOR FOURTH YEAR IN SAN ANTONIO FOR MOISTURE BARRIER TIP AT ELEVATION 25 CM

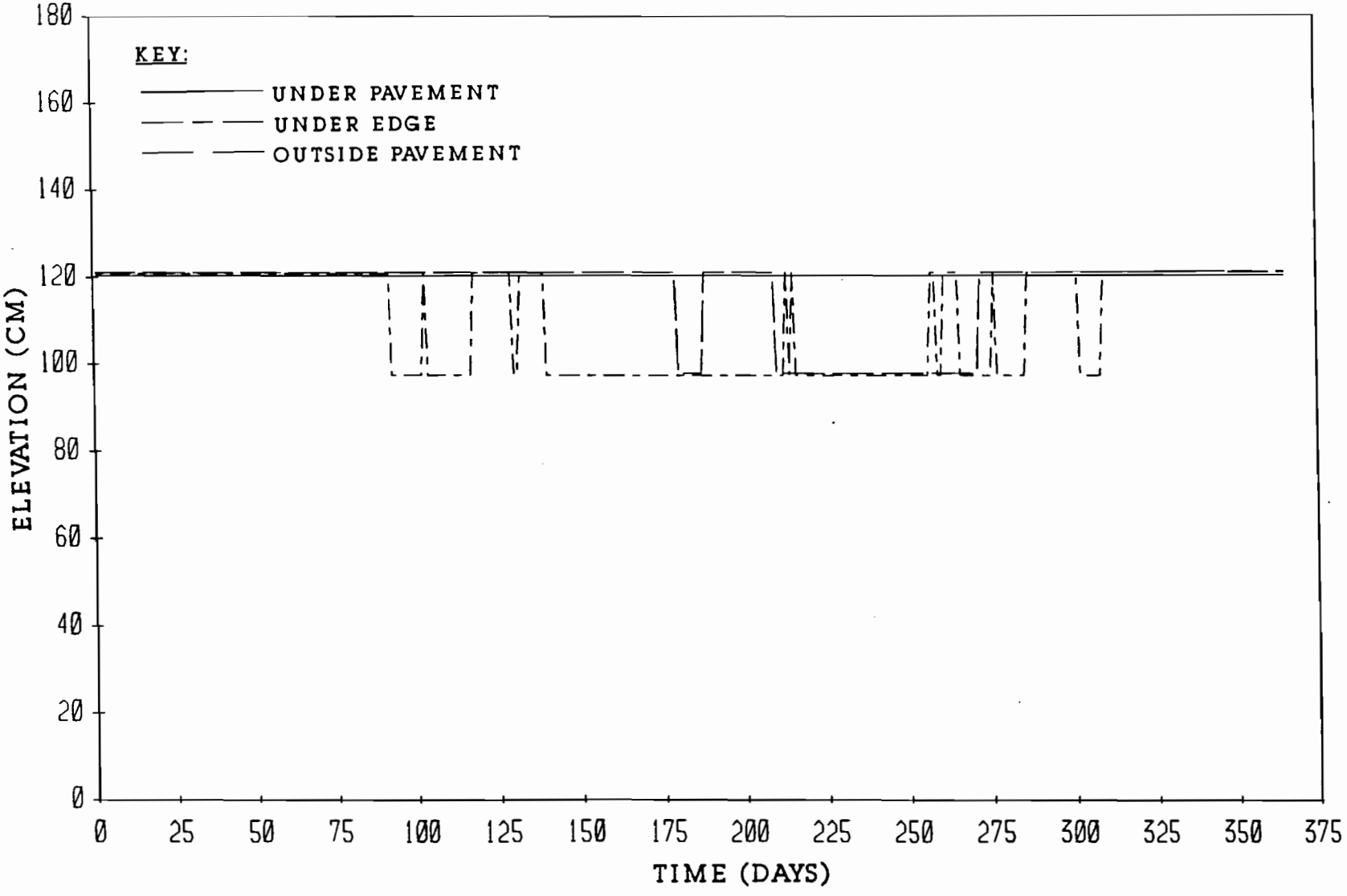

FIGURE E4.4 CRACK TIP ELEVATIONS FOR FOURTH YEAR IN SAN ANTONIO FOR MOISTURE BARRIER TIP AT ELEVATION 25 CM

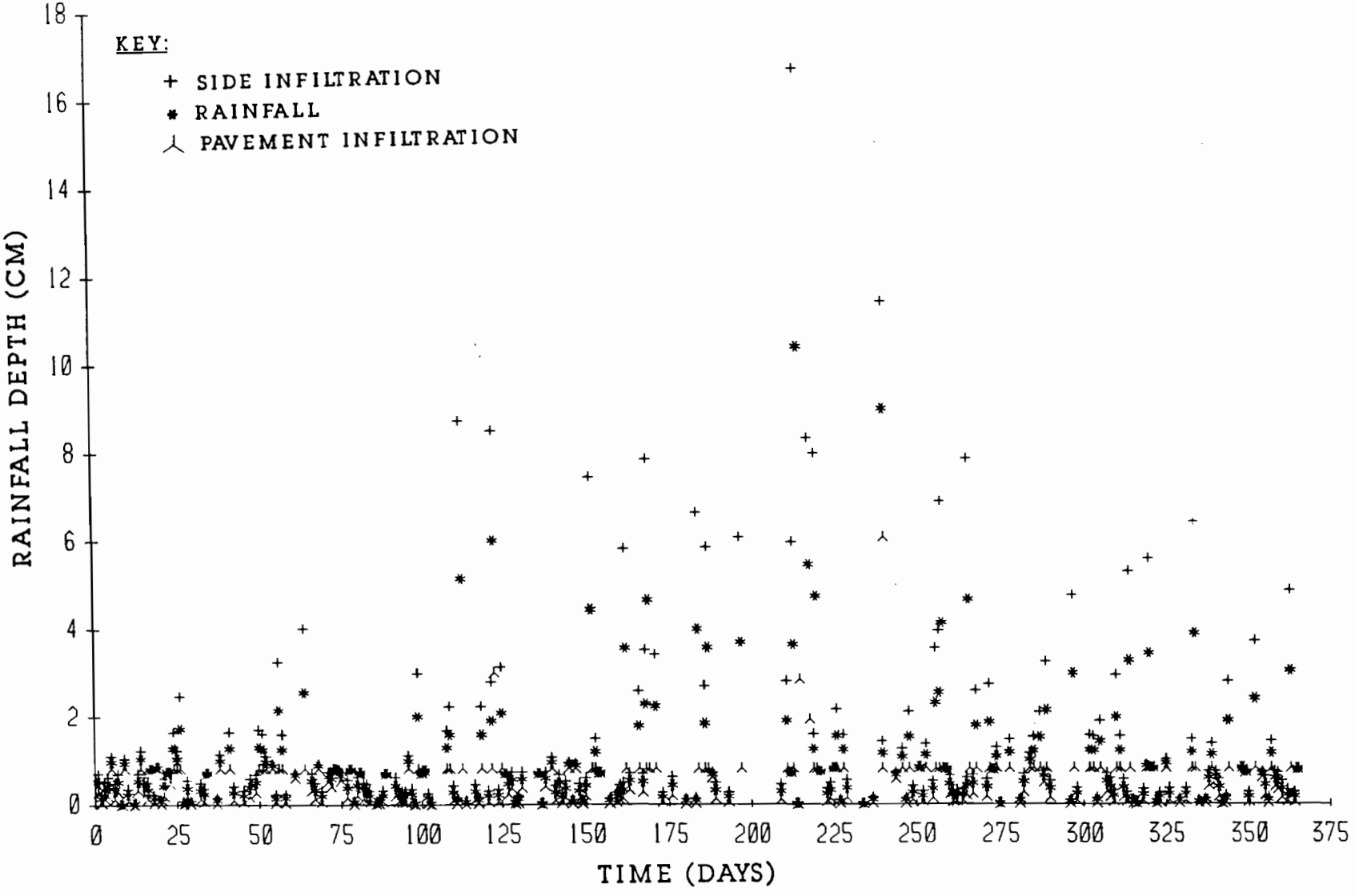

FIGURE E1.5 RAINFALL AND INFILTRATION DEPTHS FOR FIFTH YEAR IN SAN ANTONIO FOR MOISTURE BARRIER TIP AT ELEVATION 25 CM

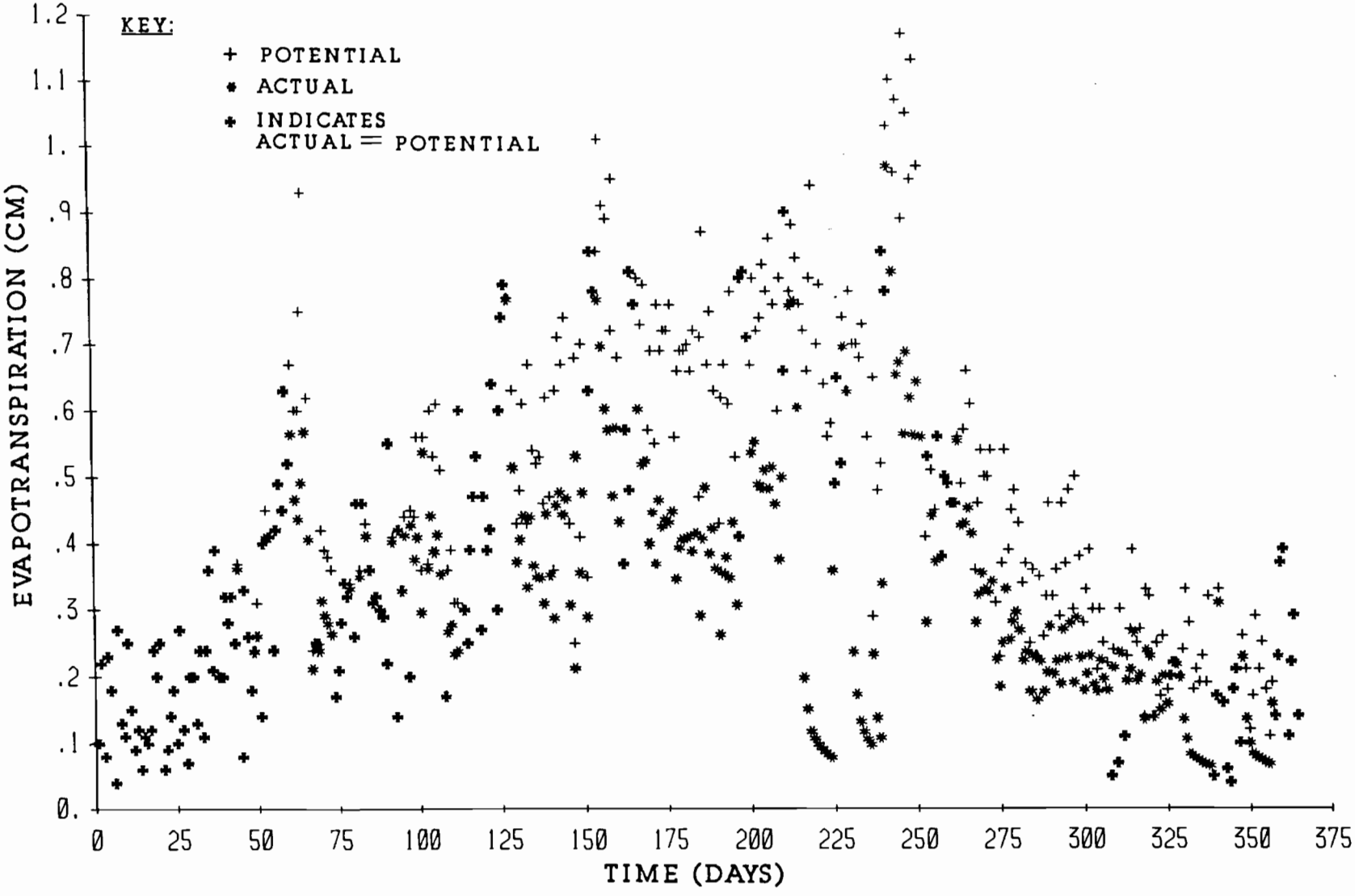

FIGURE E2.5 EVAPOTRANSPIRATION FOR FIFTH YEAR IN SAN ANTONIO FOR MOISTURE BARRIER TIP AT ELEVATION 25 CM

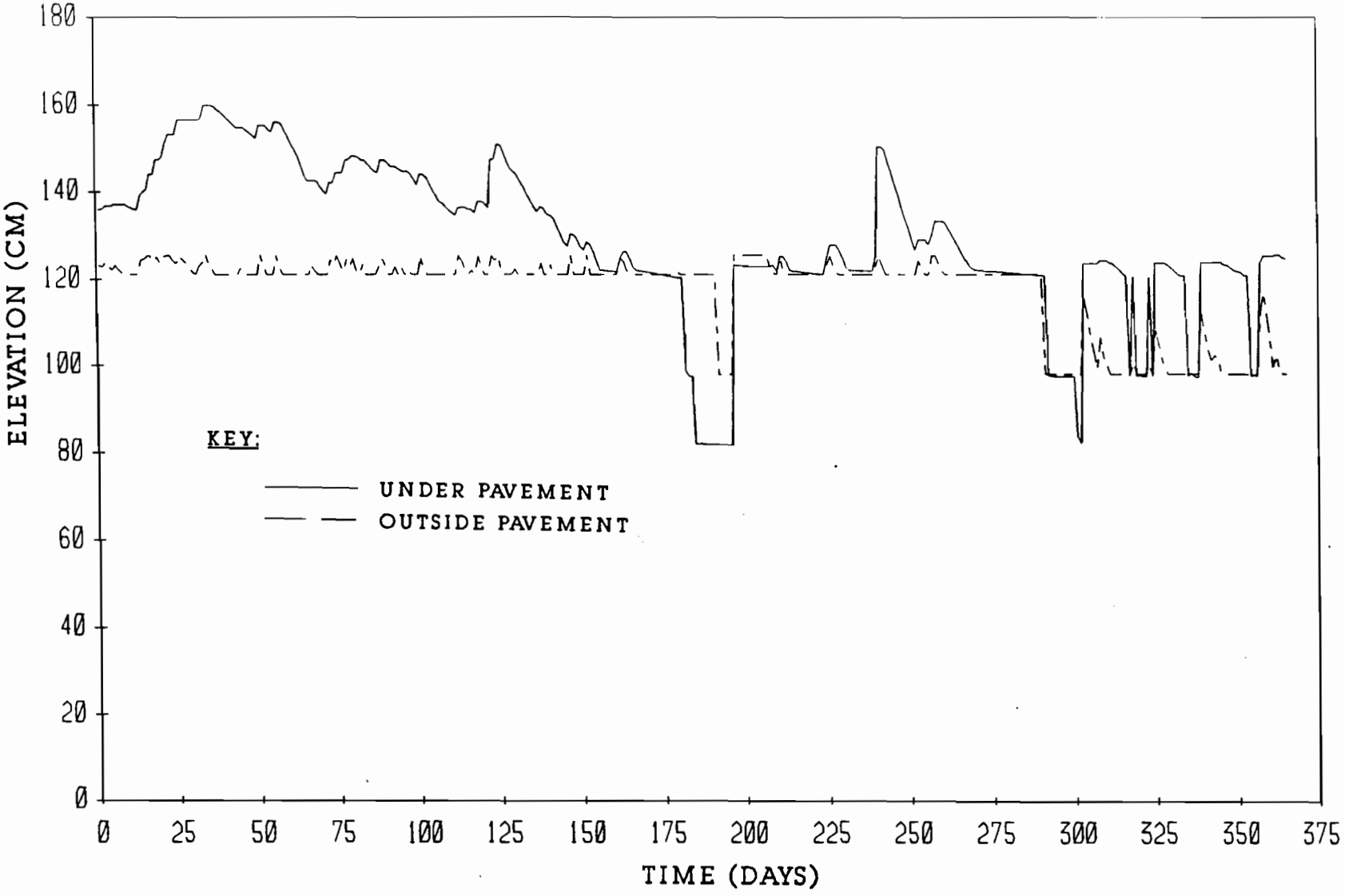

FIGURE E3.5 WATER LEVELS WITHIN THE CRACK FABRIC FOR FIFTH YEAR IN SAN ANTONIO FOR MOISTURE BARRIER TIP AT ELEVATION 25 CM

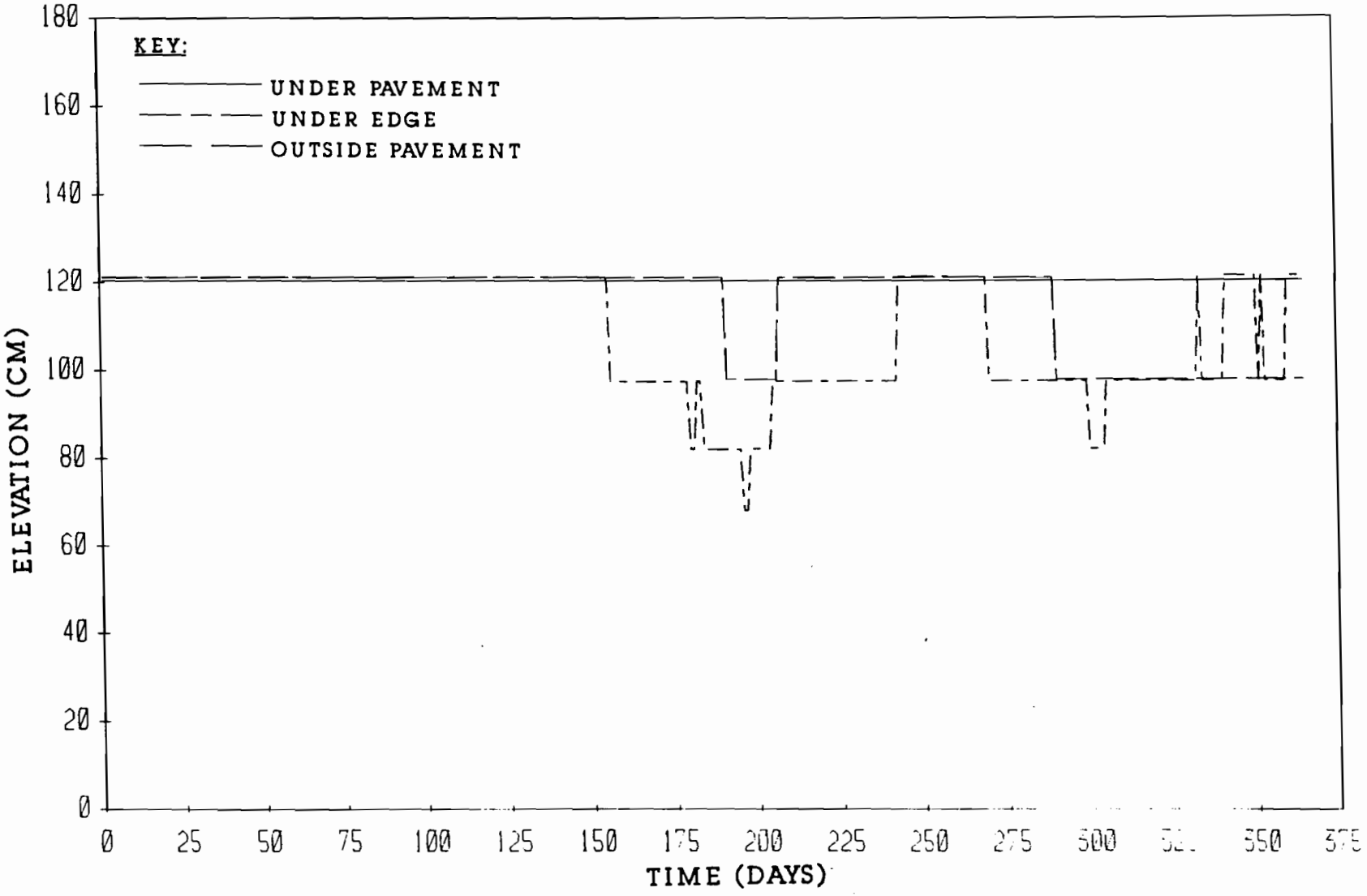

FIGURE E4.5 CRACK TIP ELEVATIONS FOR FIFTH YEAR IN SAN ANTONIO FOR MOISTURE BARRIER TIP AT ELEVATION 25 CM

APPENDIX F

SIMULATION RESULT FOR SAN ANTONIO FOR MOISTURE BARRIER TIP AT ELEVATION 0 CM

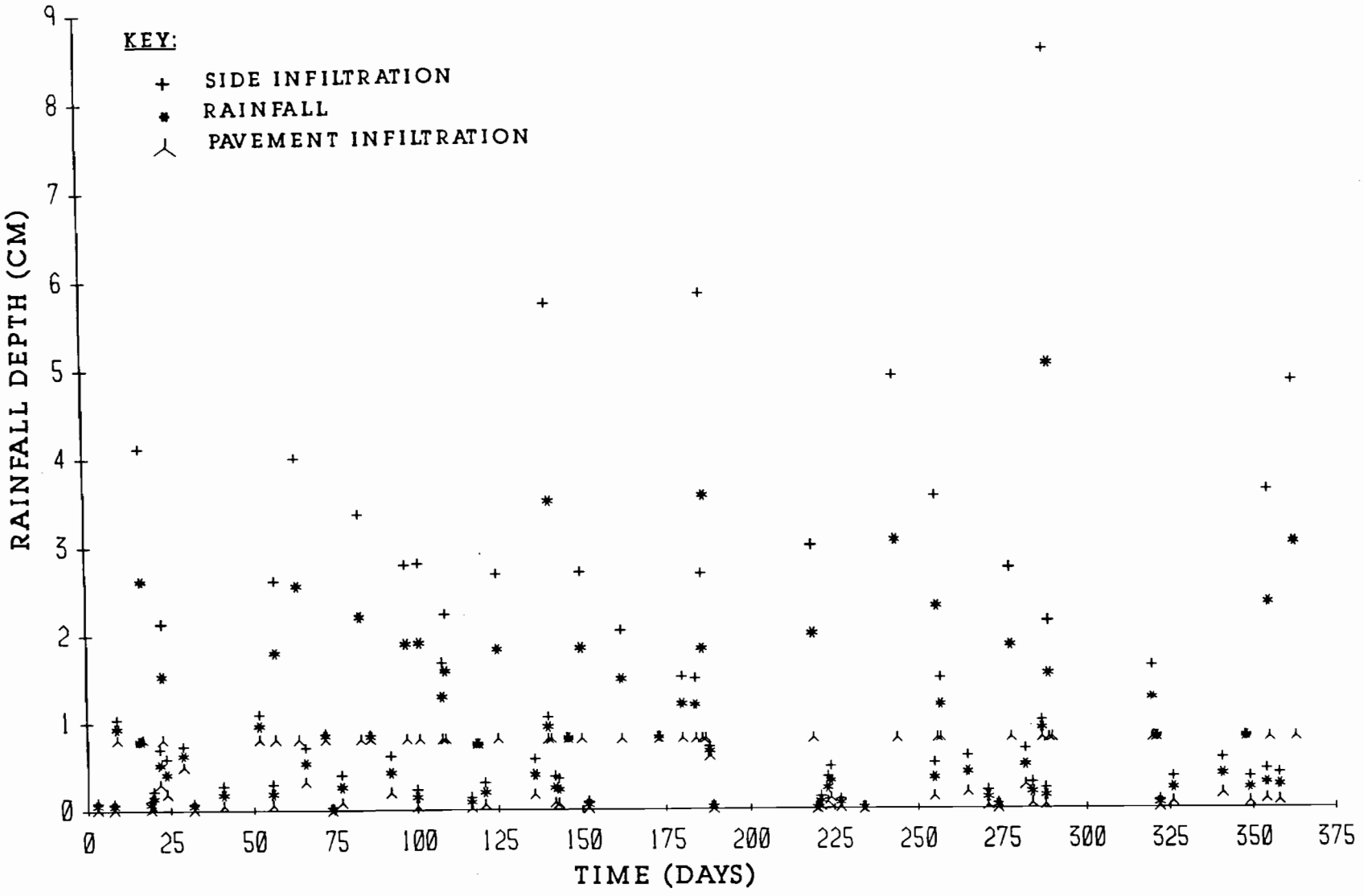

FIGURE F1.1 RAINFALL AND INFILTRATION DEPTHS FOR FIRST YEAR IN SAN ANTONIO FOR MOISTURE BARRIER TIP AT ELEVATION 0 CM

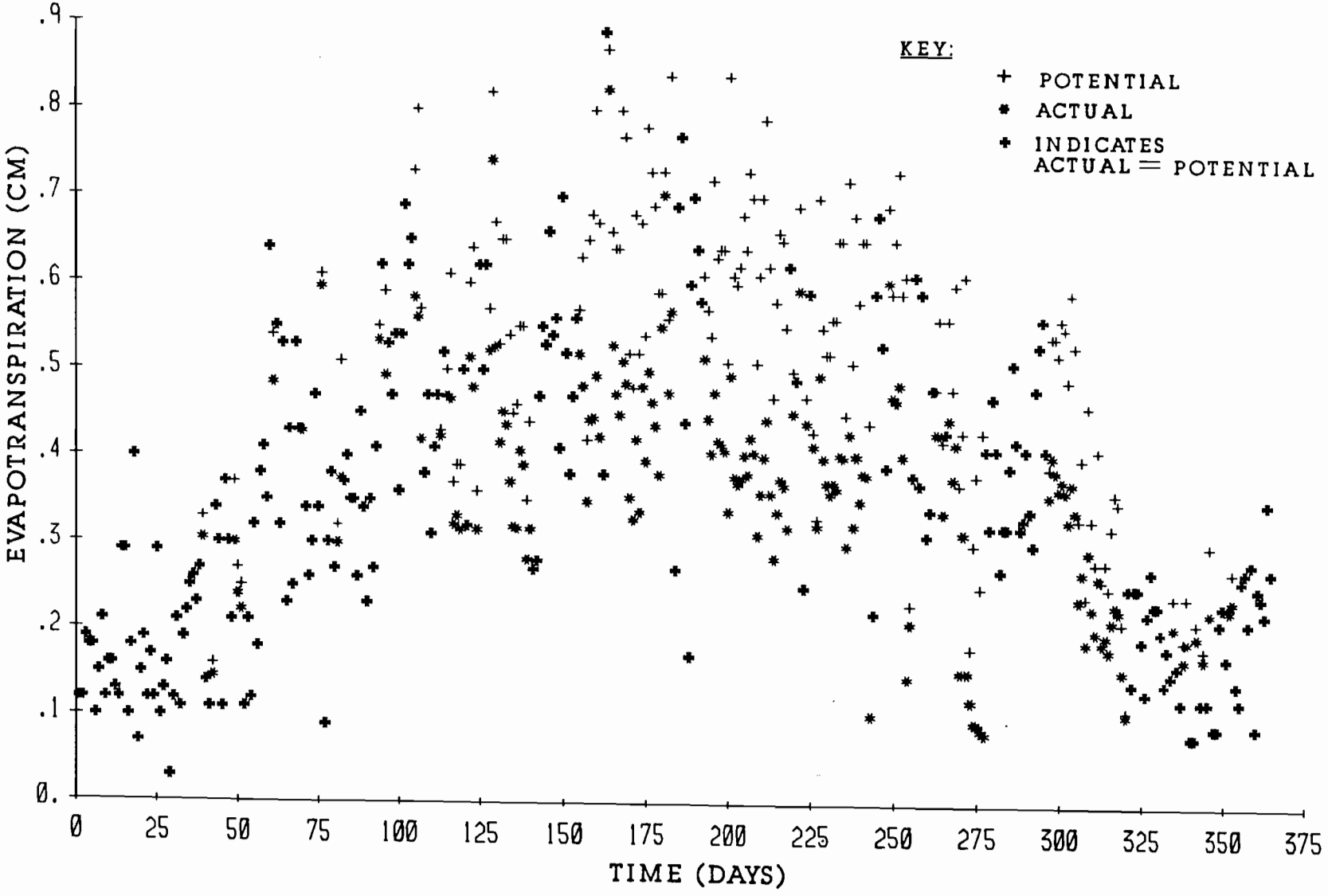

FIGURE F2.1 EVAPOTRANSPIRATION FOR FIRST YEAR IN SAN ANTONIO FOR MOISTURE BARRIER TIP AT ELEVATION 0 CM

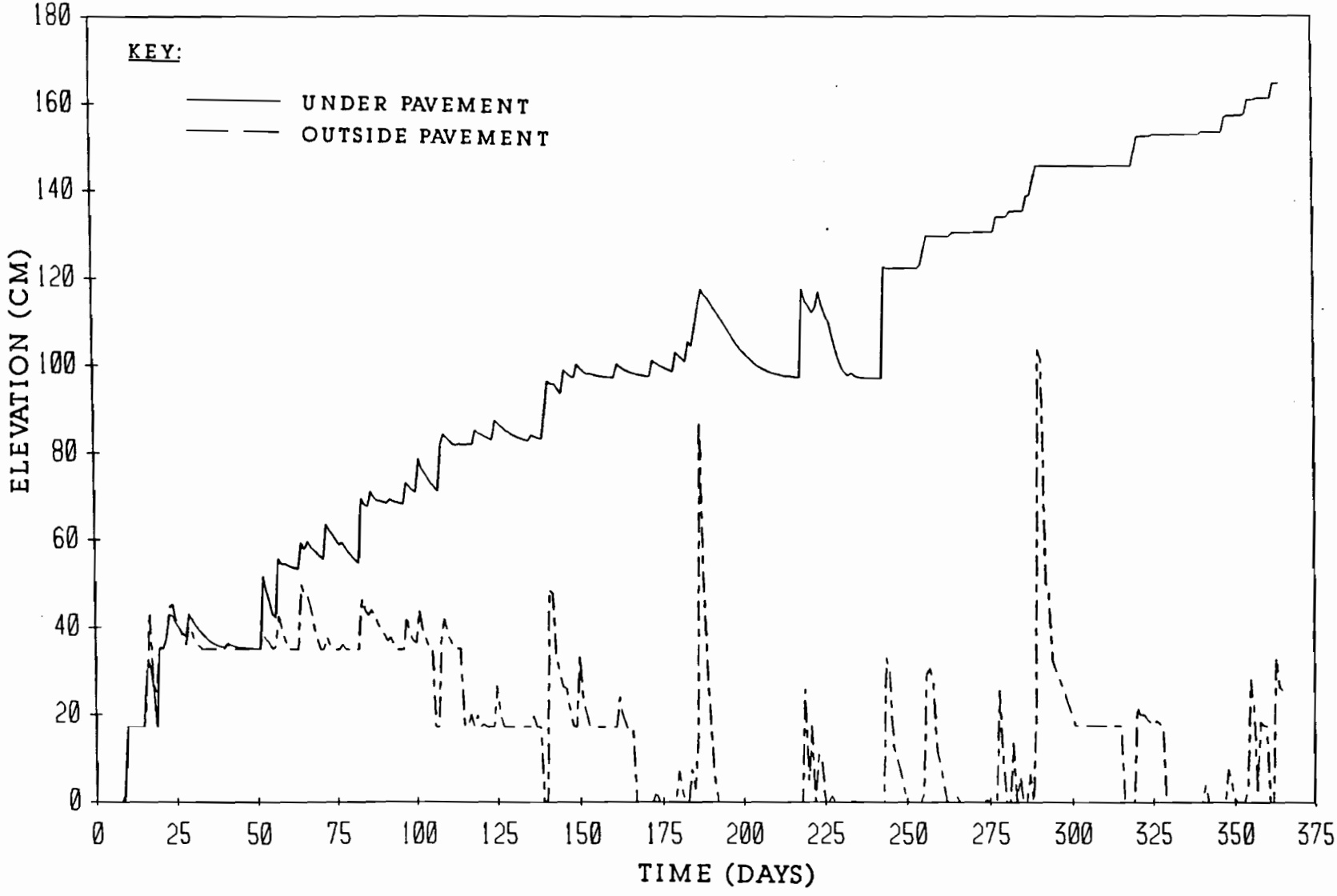

FIGURE F3.1 WATER LEVELS WITHIN THE CRACK FABRIC FOR FIRST YEAR IN SAN ANTONIO FOR MOISTURE BARRIER TIP AT ELEVATION 0 CM

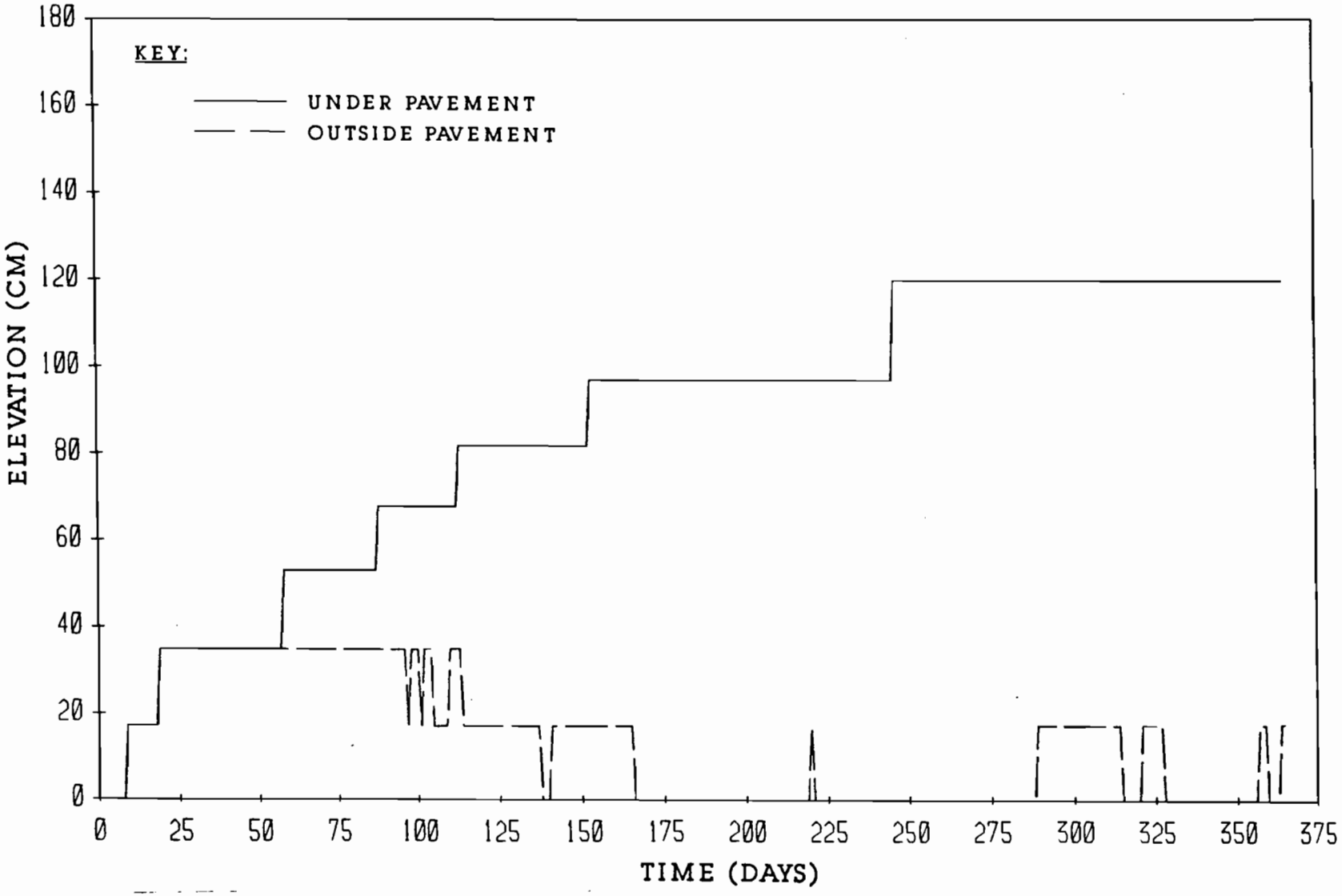

FIGURE F4.1 CRACK TIP ELEVATIONS FOR FIRST YEAR IN SAN ANTONIO FOR MOISTURE BARRIER TIP AT ELEVATION 0 CM

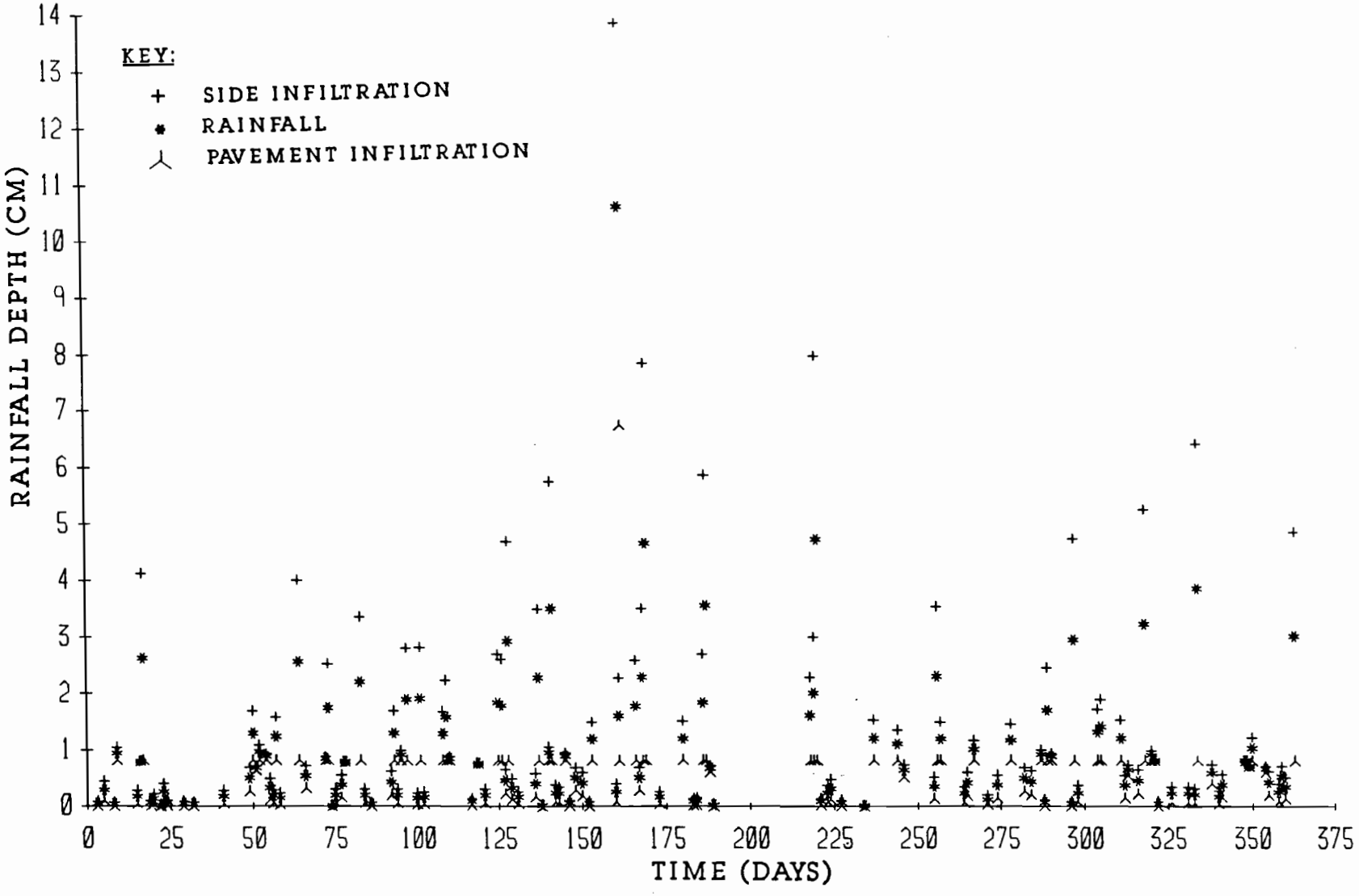

FIGURE F1.2 RAINFALL AND INFILTRATION DEPTHS FOR SECOND YEAR IN SAN ANTONIO FOR MOISTURE BARRIER TIP AT ELEVATION 0 CM

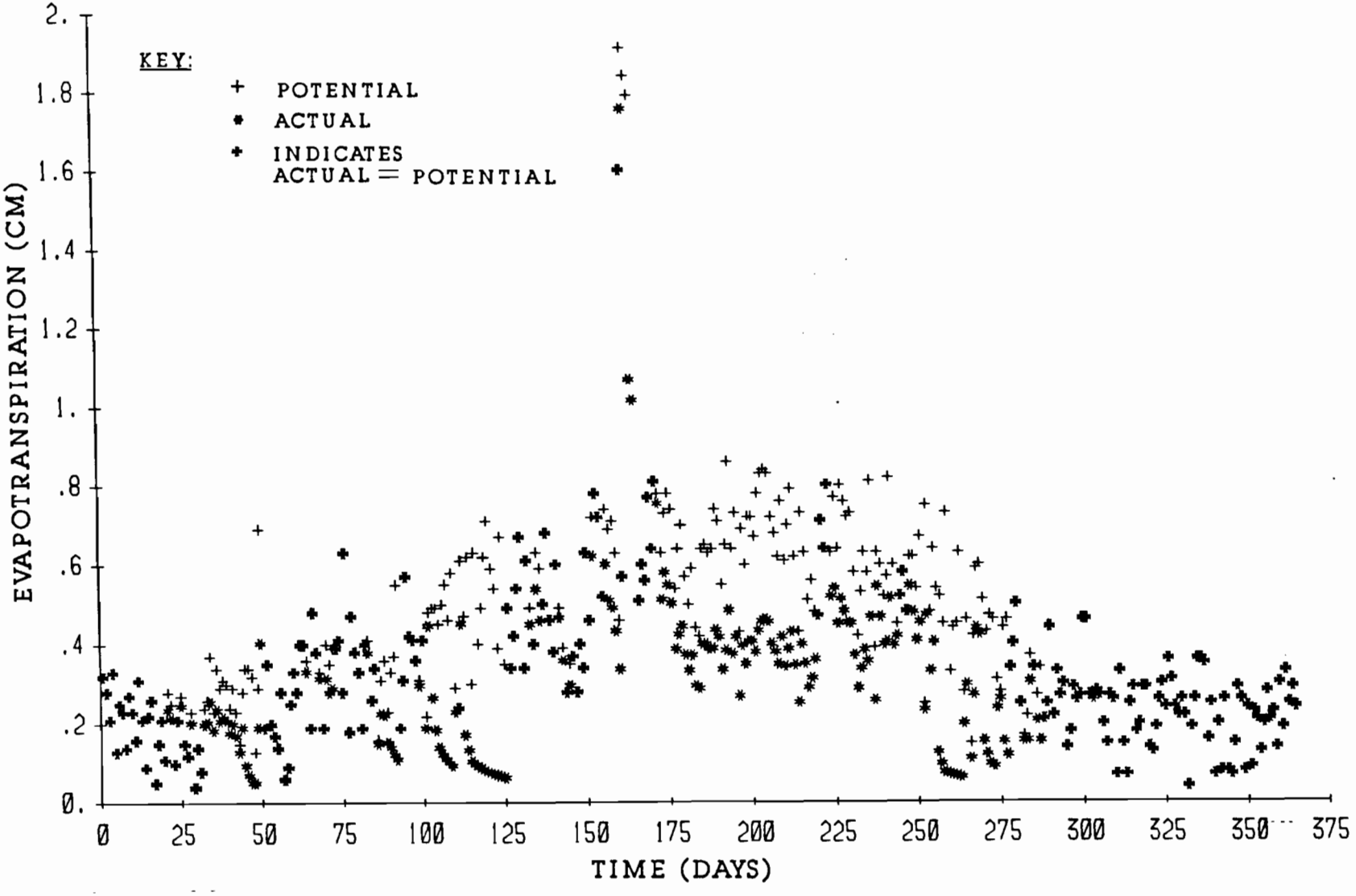

FIGURE F2.2 EVAPOTRANSPIRATION FOR SECOND YEAR IN SAN ANTONIO FOR MOISTURE BARRIER TIP AT ELEVATION 0 CM

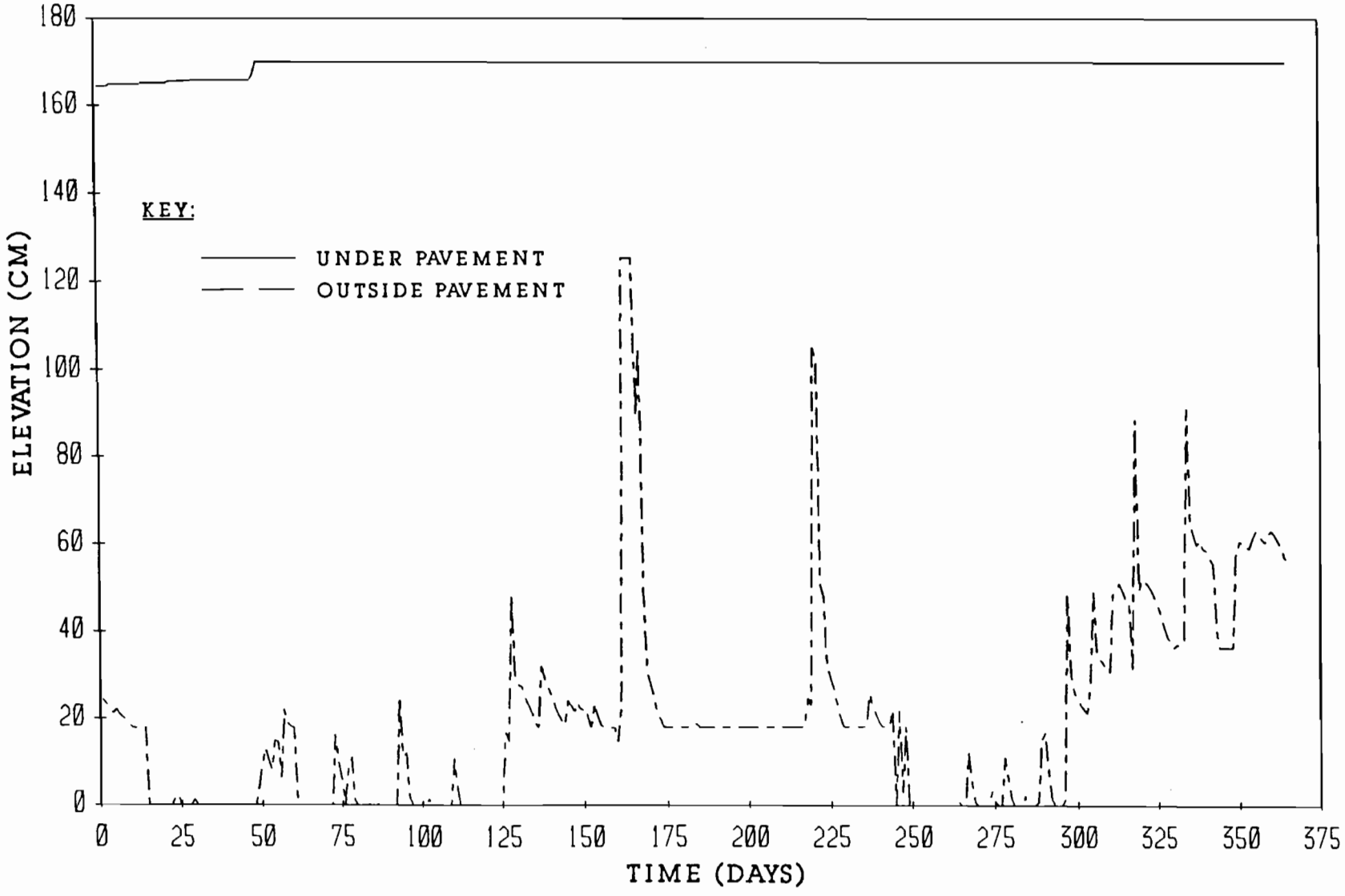

FIGURE F3.2 WATER LEVELS WITHIN THE CRACK FABRIC FOR SECOND YEAR IN SAN ANTONIO FOR MOISTURE BARRIER TIP AT ELEVATION 0 CM

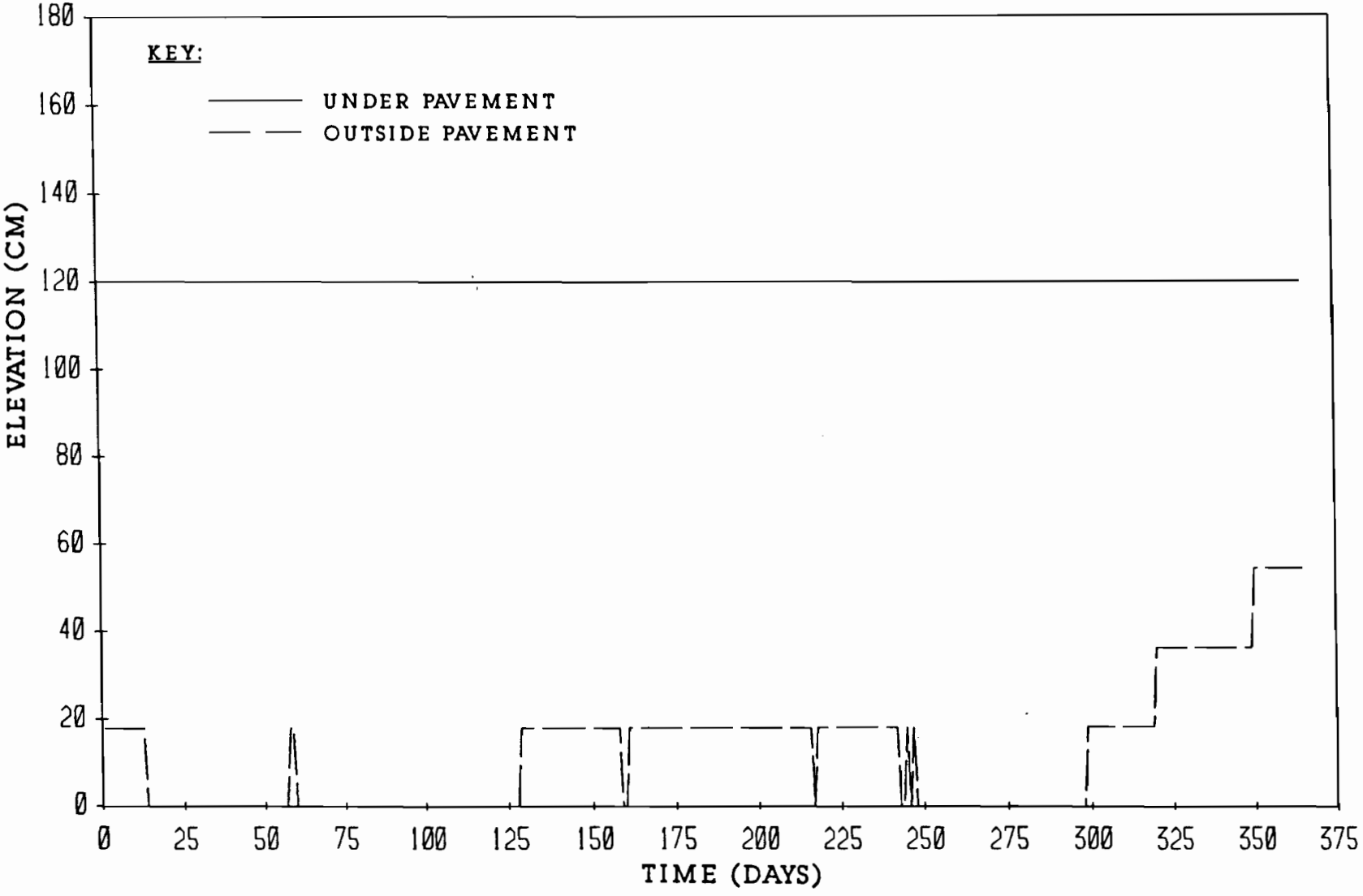

FIGURE F4.2 CRACK TIP ELEVATIONS FOR SECOND YEAR IN SAN ANTONIO FOR MOISTURE BARRIER TIP AT ELEVATION 0 CM

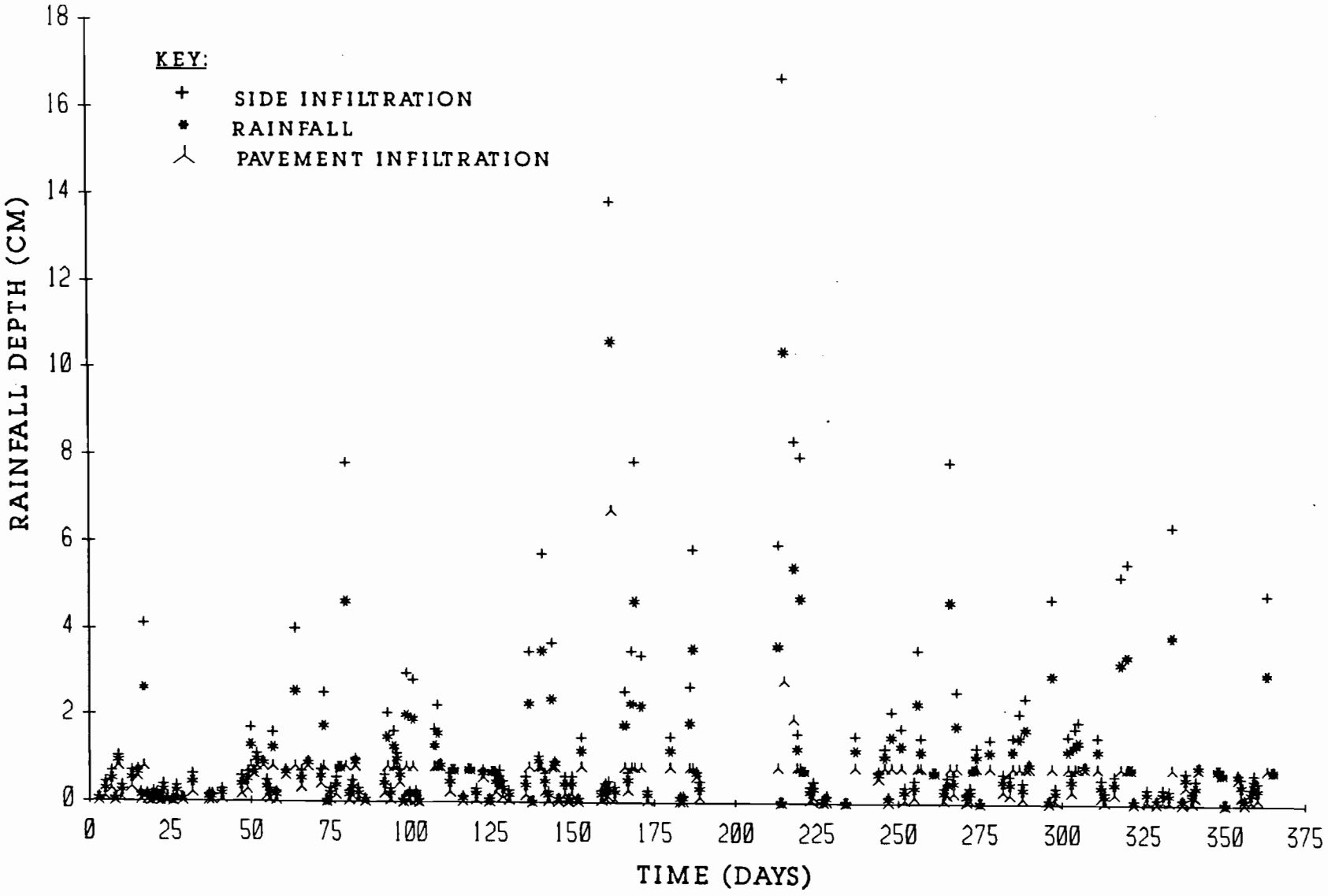

FIGURE F1.3 RAINFALL AND INFILTRATION DEPTHS FOR THIRD YEAR IN SAN ANTONIO FOR MOISTURE BARRIER TIP AT ELEVATION 0 CM

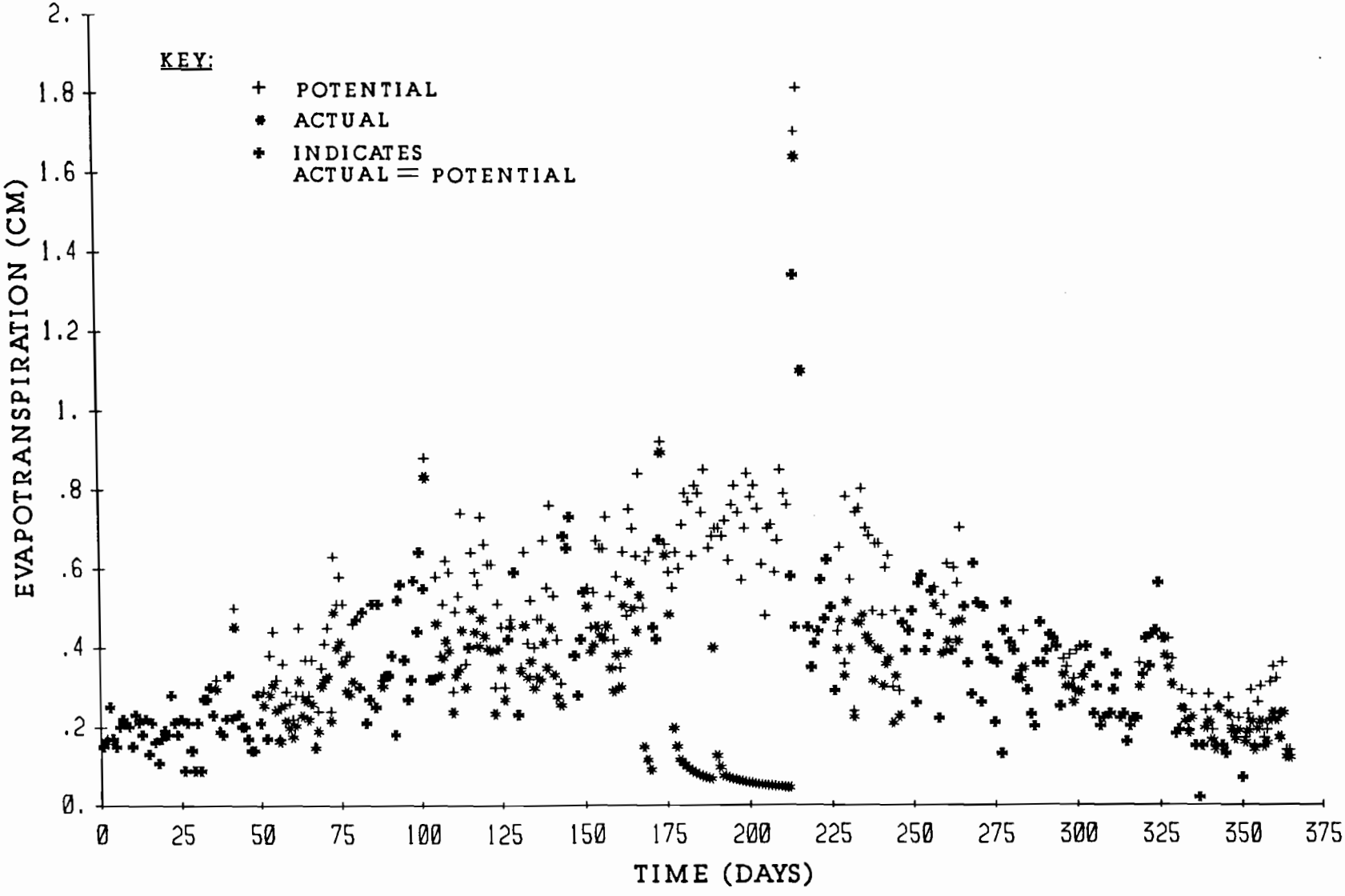

FIGURE F2.3 EVAPOTRANSPIRATION FOR THIRD YEAR IN SAN ANTONIO FOR MOISTURE BARRIER TIP AT ELEVATION 0 CM

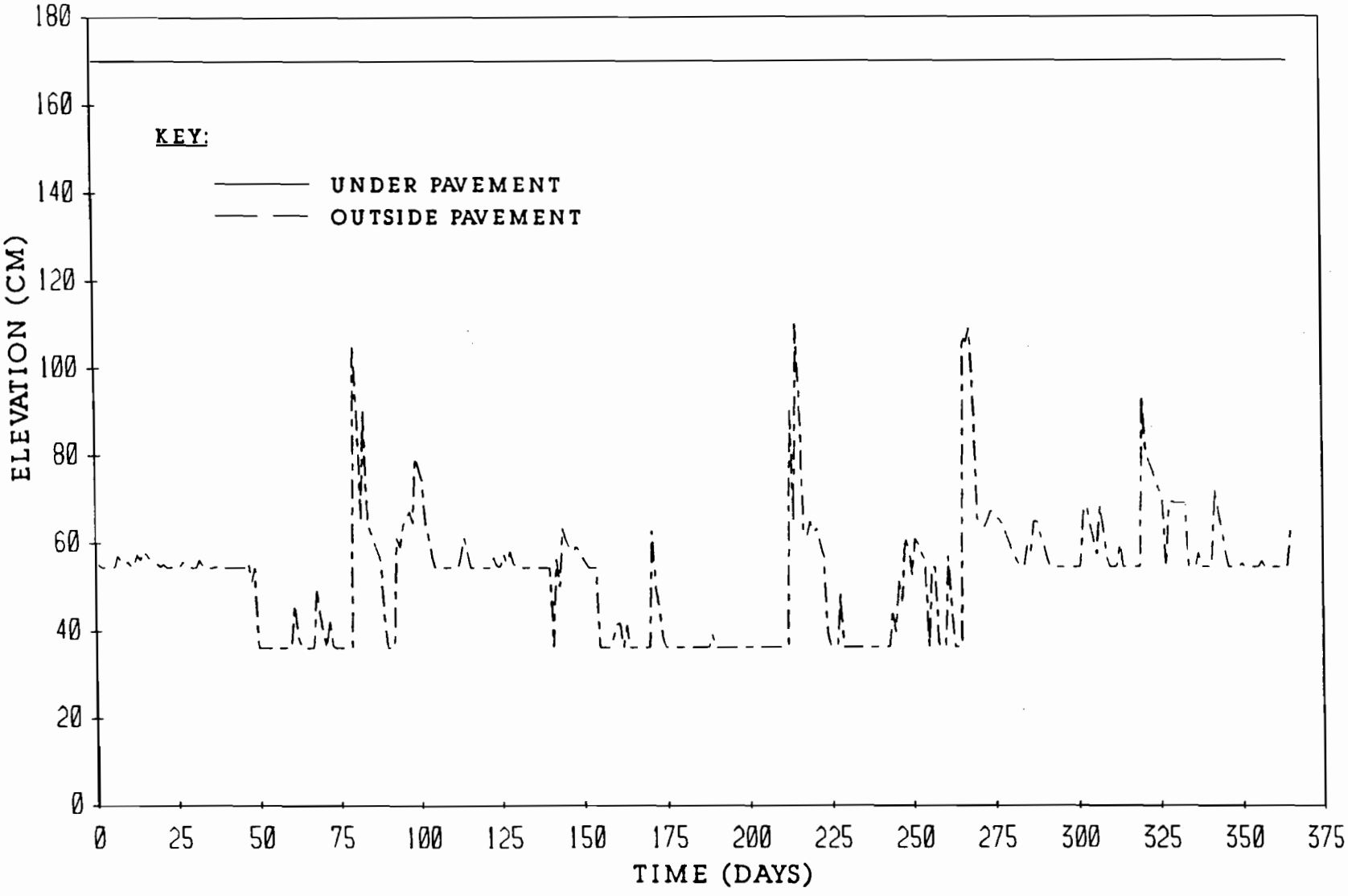

FIGURE F3.3 WATER LEVELS WITHIN THE CRACK FABRIC FOR THIRD YEAR IN SAN ANTONIO FOR MOISTURE BARRIER TIP AT ELEVATION 0 CM

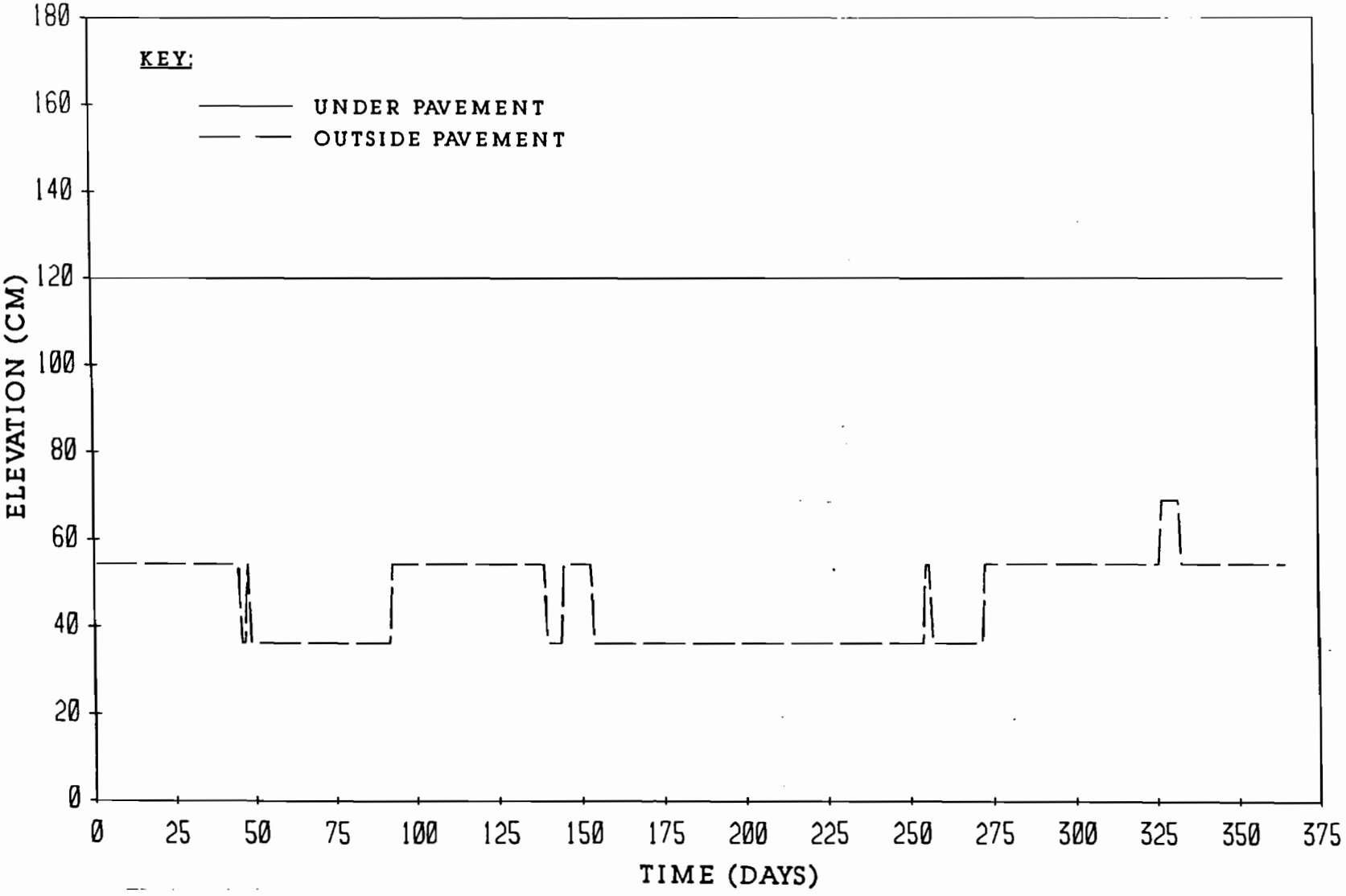

FIGURE F4.3 CRACK TIP ELEVATIONS FOR THIRD YEAR IN SAN ANTONIO FOR MOISTURE BARRIER TIP AT ELEVATION 0 CM

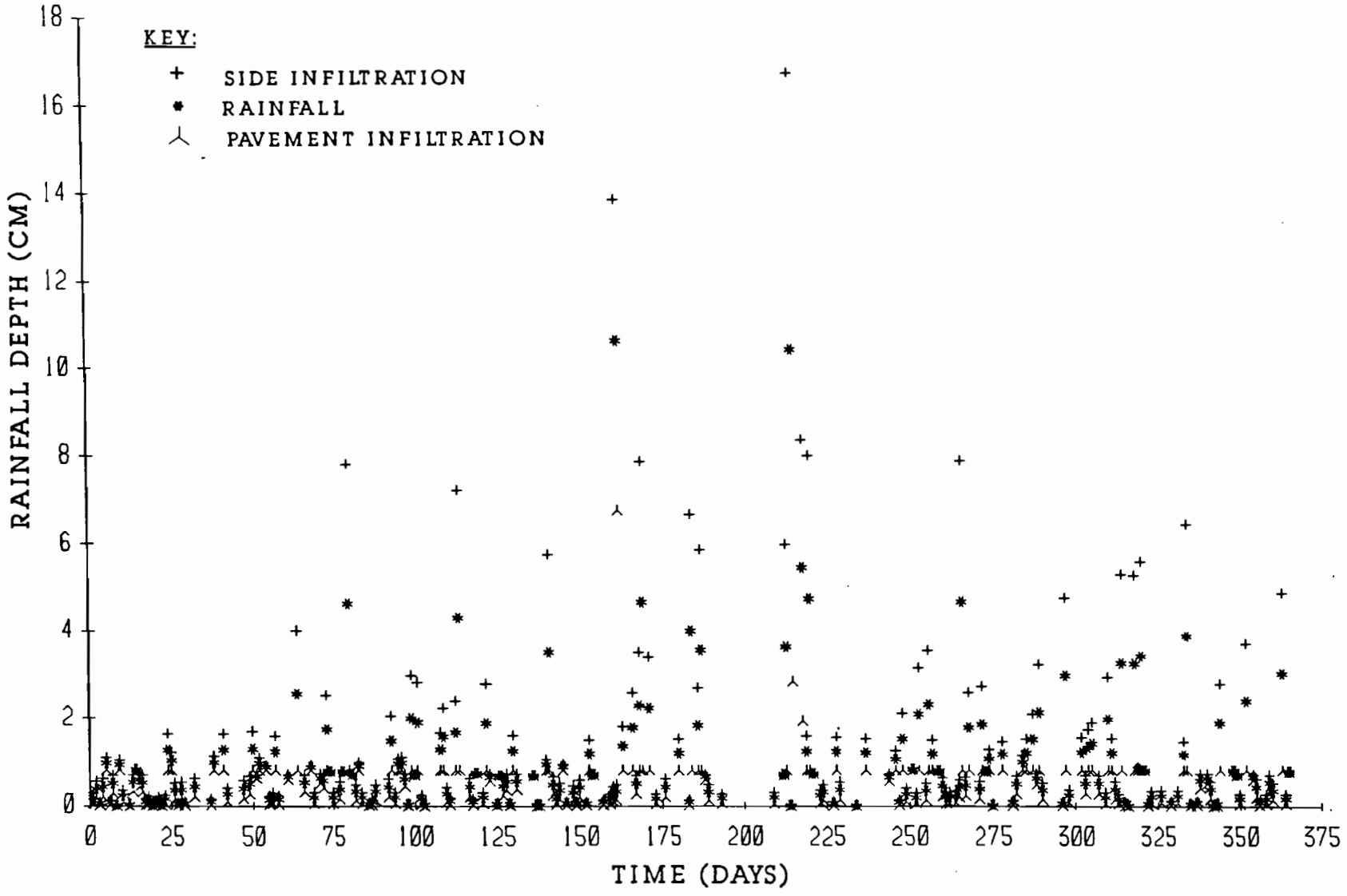

FIGURE F1.4 RAINFALL AND INFILTRATION DEPTHS FOR FOURTH YEAR IN SAN ANTONIO FOR MOISTURE BARRIER TIP AT ELEVATION 0 CM

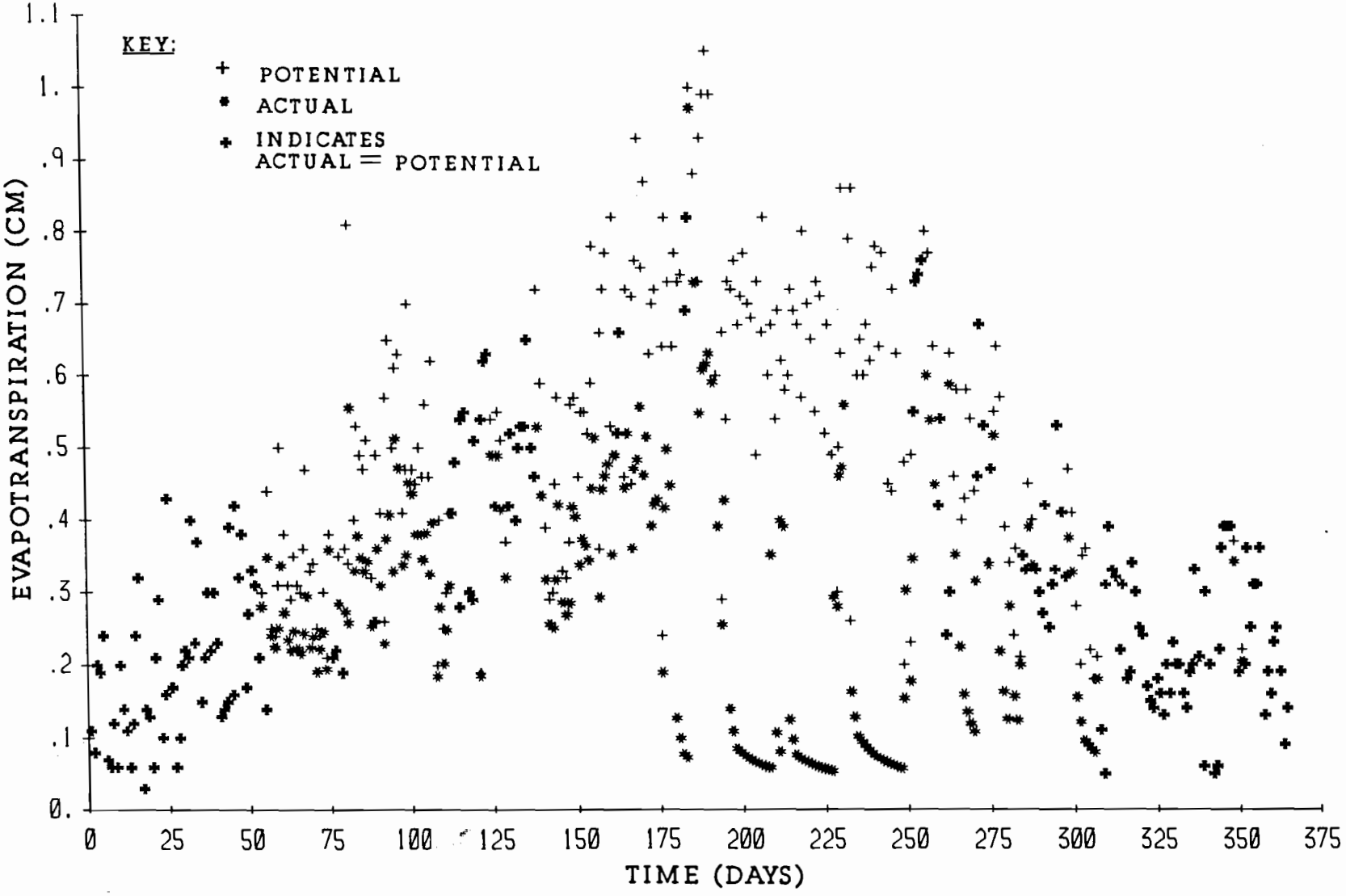

FIGURE F2.4 EVAPOTRANSPIRATION FOR FOURTH YEAR IN SAN ANTONIO FOR MOISTURE BARRIER TIP AT ELEVATION 0 CM

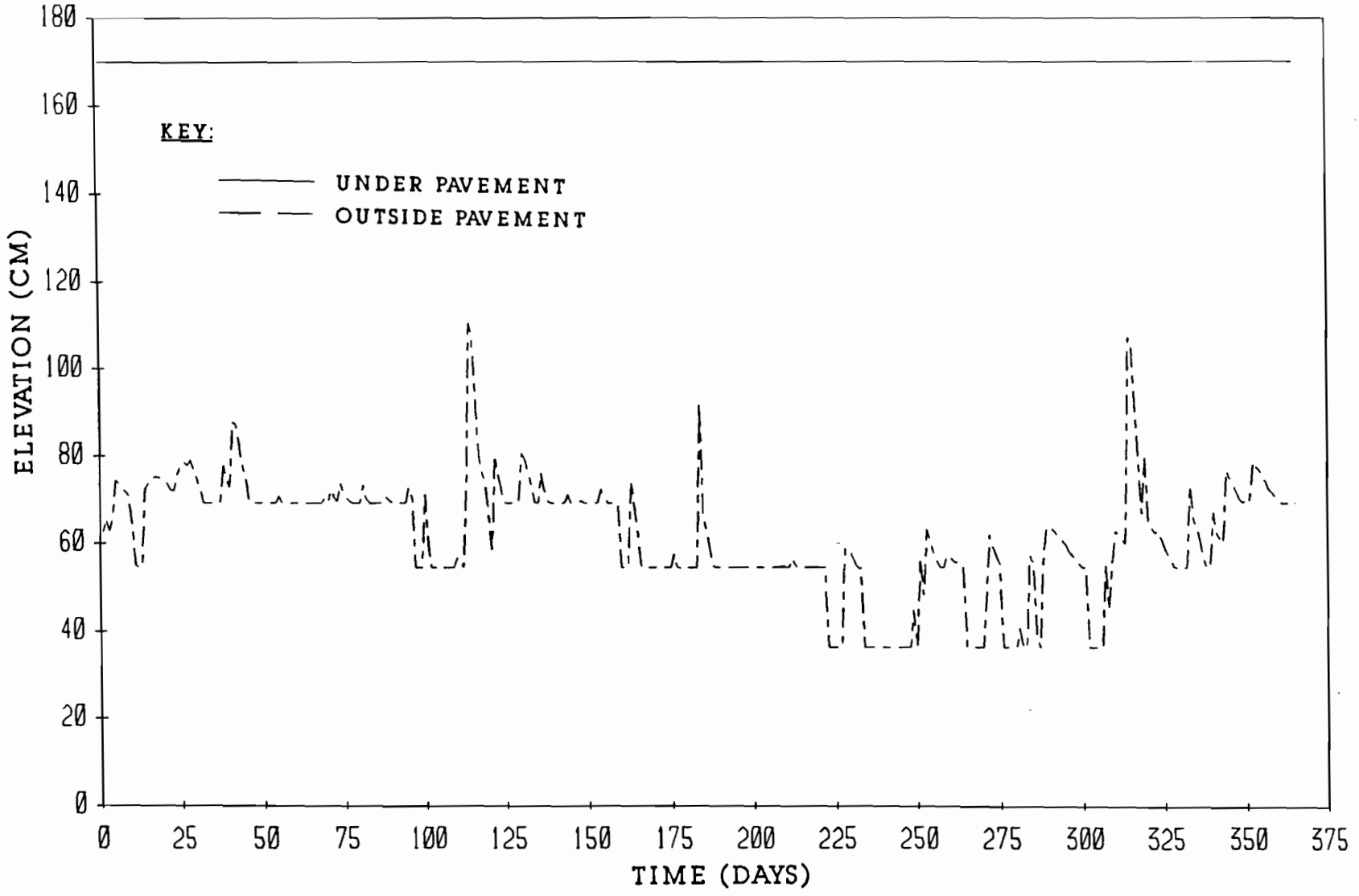

FIGURE F3.4 WATER LEVELS WITHIN THE CRACK FABRIC FOR FOURTH YEAR IN SAN ANTONIO FOR MOISTURE BARRIER TIP AT ELEVATION 0 CM

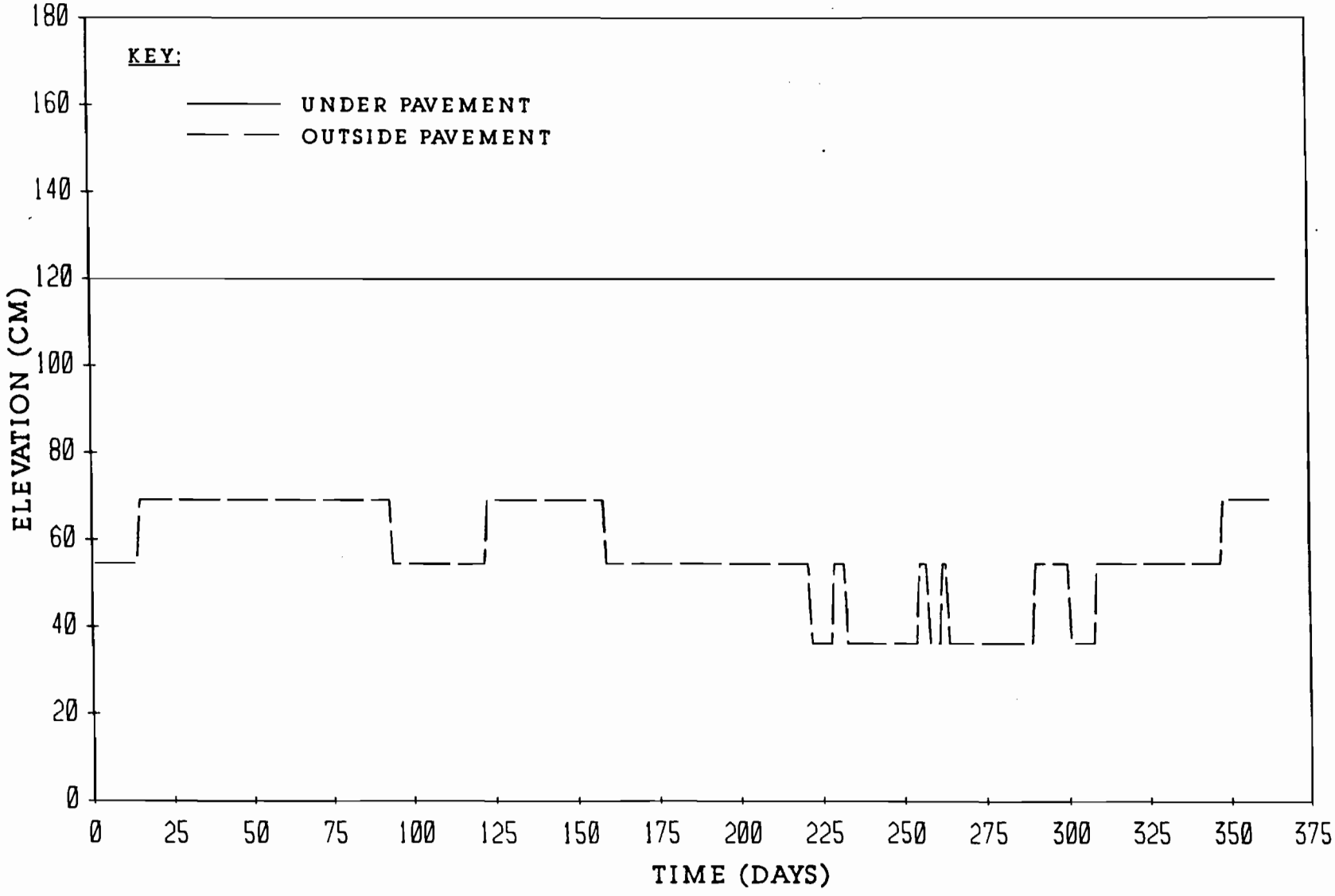

FIGURE F4.4 CRACK TIP ELEVATIONS FOR FOURTH YEAR IN SAN ANTONIO FOR MOISTURE BARRIER TIP AT ELEVATION 0 CM

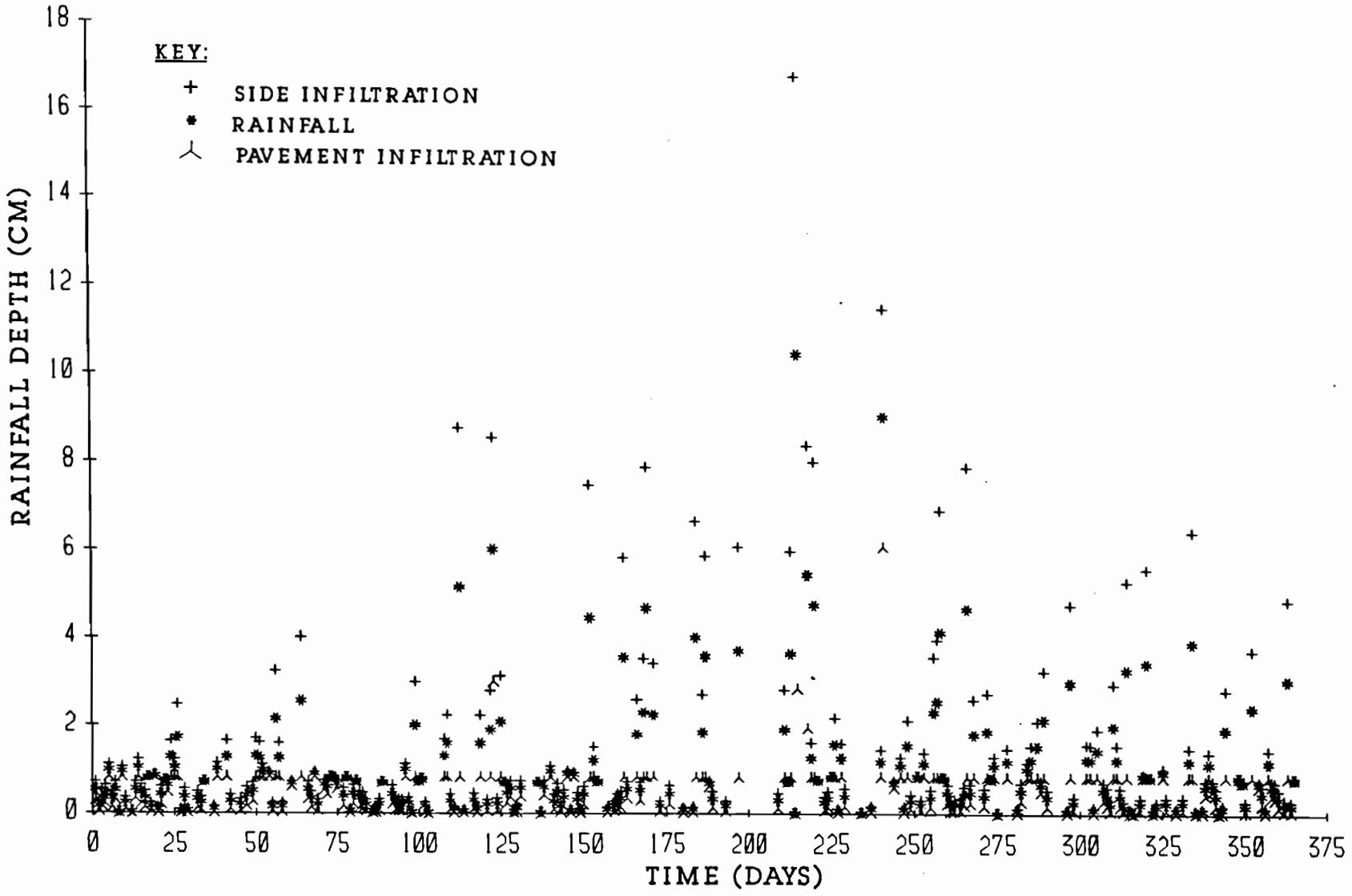

FIGURE F1.5 RAINFALL AND INFILTRATION DEPTHS FOR FIFTH YEAR IN SAN ANTONIO FOR MOISTURE BARRIER TIP AT ELEVATION 0 CM

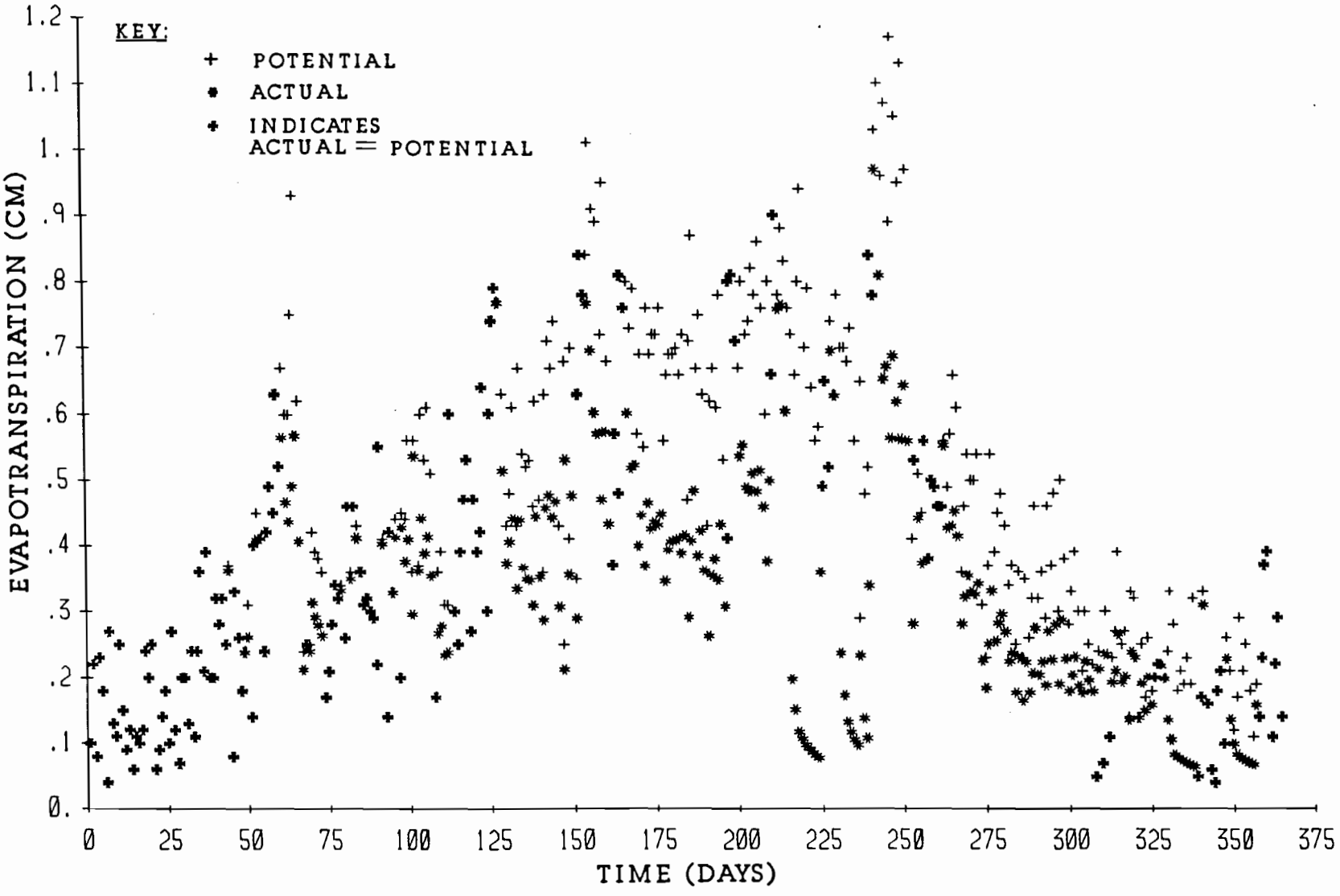

FIGURE F2.5 EVAPOTRANSPIRATION FOR FIFTH YEAR IN SAN ANTONIO FOR MOISTURE BARRIER TIP AT ELEVATION 0 CM

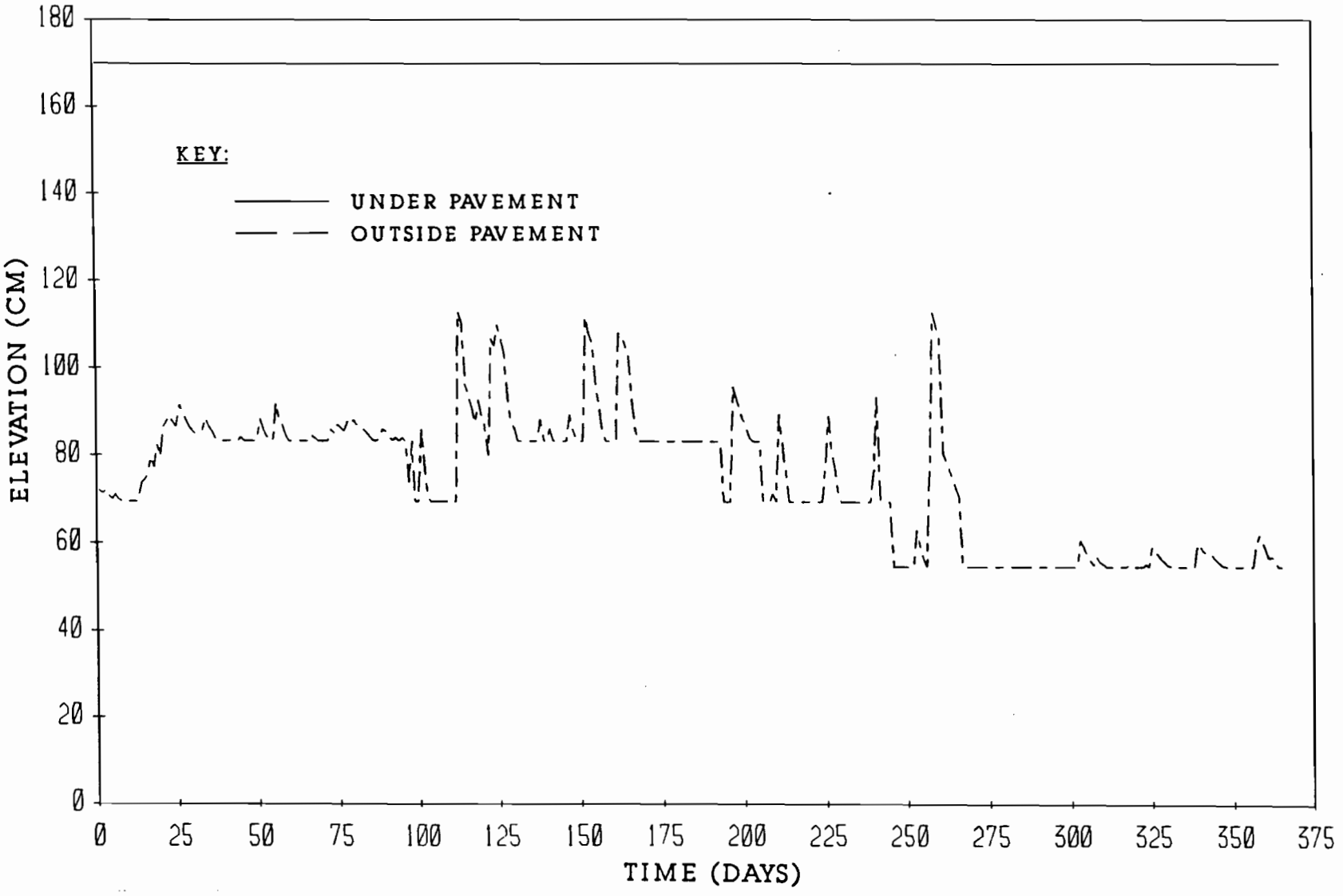

FIGURE F4.5 CRACK TIP ELEVATIONS FOR FIFTH YEAR IN SAN ANTONIO FOR MOISTURE BARRIER TIP AT ELEVATION 0 CM

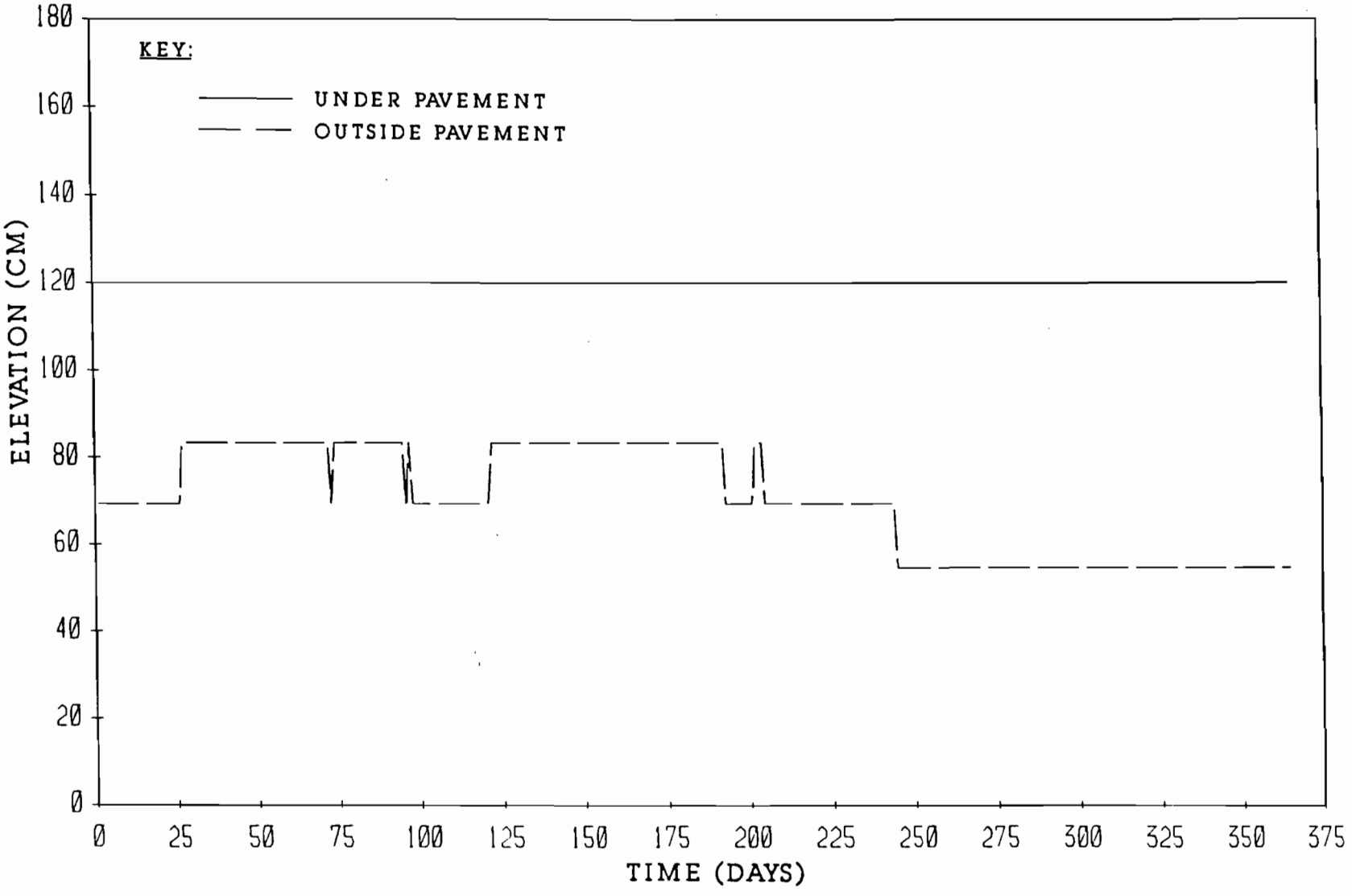

FIGURE F4.5 CRACK TIP ELEVATIONS FOR FIFTH YEAR IN SAN ANTONIO FOR MOISTURE BARRIER TIP AT ELEVATION 0 CM